The occurence and effects of short paths in scale-free geometric random graphs

Inaugural-Dissertation

zur

Erlangung des Doktorgrades

der Mathematisch-Naturwissenschaftlichen Fakultät

der Universität zu Köln

vorgelegt von

Arne Grauer

aus Düsseldorf

2022

Berichterstatter:

Prof. Dr. Peter Mörters, Universität zu Köln

Prof. Dr. Steffen Dereich, Westfälische Wilhelms-Universität Münster

Tag der mündlichen Prüfung: 14.12.2022

Abstract

In this thesis we investigate a large class of geometric random graphs defined on a Poisson point process on $\mathbb{R}^d$, where each vertex carries an independent random mark. On this vertex set edges are established at random, such that the class is only determined by upper and lower bounds on the connection probabilities between finitely many pairs of vertices, which depend crucially on the marks and the spatial distance of each pair of vertices. This class includes different geometric random graphs emerging from real-world network models, such as a version of spatial preferential attachment (where marks can be understood as birth times), and continuum percolation, such as the soft Boolean model, as well as a whole range of further graph models with scale-free degree distribution and edges between distant vertices.

For this class of geometric random graphs we study the occurence of short paths leading to ultrasmallness of the graphs, i.e. that the graph distance of a pair of distant vertices grows at most of doubly logarithmic order in the spatial distance of the pair. We give a sharp criterion for the absence of ultrasmallness of the graphs and in the ultrasmall regime establish a limit theorem for the chemical distance of two very distant vertices. Unlike in non-spatial scale-free network models and spatially embedded random graphs such as scale-free percolation the boundary of the ultrasmall regime and the limit theorem depend not only on the power-law exponent of the degree distribution but also on the rate of decay of the probability of an edge connecting two vertices with typical marks in terms of their Euclidean distance.

Furthermore, we study the effect of the short paths in the ultrasmall regime on the survival of the contact process on geometric random graphs in this class. We show that the non-extinction probability is positive for any positive choice of the infection rate and give precise asymptotics for it when the infection rate decays to zero. On finite spatial restrictions of the graphs we show that the extinction time is of exponential order of the size of the graphs.

Finally, we provide various examples of geometric random graphs from the class and discuss them with regard to the main result of this thesis.

Contents

CHAPTER 1

Introduction

1.1 Motivation

In 1967, 160 people in Nebraska got sent a folder by the University of Harvard. This folder included the name and address of a person in Boston, the target person, and a set of rules to follow. The following two rules were essential.

(i) If the recipient knows the target person on a first name basis, he or she should send the folder to the target person directly.

(ii) If this is not the case, the recipient should send the folder to the person he or she know on a first name basis, who is most likely to know the target person, and this person should proceed according to the same rules.

This process was part of a social experiment carried out by Milgram [82, 96] with the aim of empirically answering the question whether there exists a "chain of acquaintances" between two random people in USA connecting them and, should it exists, how long this chain is. The experiment led to surprising results. Although the folders needed to travel the large distance from sparsely populated Nebraska to Boston via acquaintances and there was no guarantee that the participants

would be willing to take part in this experiment, 44 of the 160 folders made it to the target person and the mean of the number of people through which the folder was sent by a successful chain was 5.5. Later experiments could increase the success rate of the received folders to 0.95 by giving more information about the target person and by pretending that the folder itself was valuable. The mean number of intermediaries to form a successful chain was confirmed to be between 5.5 to 6. This result led to the famous idea of "six degrees of separation" which states that two random people in the world are typically connected by a chain of at most 6 friends and friends of friends, which gained broad popularity in 1991 through the homonymous Broadway play by John Guare.

1.1.1 Real-World Networks and random graphs

The study of real-world networks has played an increasingly important role in science during the last several decades, such as with the internet and the world-wide web. Examples also include electrical power grids and telecommunication networks, (virtual) social networks as Twitter or Facebook or the friendship network, collaboration networks or even biochemical networks and neural networks. These networks are formed by a set of objects which will be called *vertices* and the connections between the objects, called *edges*. For example, in the friendship network the vertices are the people of the world and there exists an edge between two people if they are friends. As all these real-world networks are large, the main focus of the study of such networks does not lie in the analysis of the properties of individual vertices or edges but on the fundamental properties of the entire network. With the technological progress of the last decades, especially in terms of the storage and analysis of large datasets, the empirical study of large networks has become possible. In fact, many real-world networks share similar fundamental properties. In the following, three important properties will be depicted with the primary help of two examples for real-world networks. The first example is the internet on the level of autonoumous systems (AS from here on out). The second is the movie collaboration network, where the actors are the vertices and an edge is formed between two actors if both played a role in the same movie.

The small-world phenomenon The experiment of Milgram was the first demonstration of the *small-world phenomenon*. The observation that, although a network is very large, it is sufficiently well connected that most pairs of vertices are near to each other in the sense that they are connected via a short path of edges through the network, is intriguing and has been personally experienced by most when meeting a stranger who happens to have a friend in common. The closeness of two vertices can be measured by the *graph distance*, defined as the minimal amount of edges needed to be crossed to get from one vertex to the other and set to infinity if there exists no path between the two vertices. For networks with a finite amount of vertices, a good global measurement is given by the graph distance of two vertices taken uniformly at random, which is called the *typical distance* of the network. With this definition at hand, "six degrees of separation" implies that the expected typical distance in the friendship network with more than 7 billion vertices should be only around 7. This result has been confirmed in an experiment at a larger scale than Milgram's experiment in 2001 with more than 60.000 participants from 166 countries, where the packages have been sent by e-mail. See [40] for a detailed analysis of the experiment. In fact, such a small-world phenomen can be seen in other real-world networks as well. In 2012, the expected typical distance of Facebook with more than 700 million active users has been estimated to be 4.7 in [4]. Although Facebook has grown over time the typical distance has been stable and actually decreased a bit, see [11] for the analysis of Facebook done in 2016. In the movie collaboration network with more than 200000 actors, the typical distance is estimated to be around 3.6, see [97]. As a final example, the internet actually needs to have short paths such that information packages can be sent across the world in as short a time as possible. Indeed this is the case, as the internet on AS-level has an estimated typical distance of 4.2 with more than 25000 autonoumous systems. More impressively, this has been shown to be stable over a period of ten years although the size of the network increased, see [38]. Such a sequence of growing networks is *small world* if the typical distance growth is at most of logarithmic order of the number of vertices. In fact, the analysis of real-world networks indicate, that the typical distance may grow even slower in doubly-logarithmic order of the number of vertices, leading to a so-called *ultrasmall world*.

The scale-free degree distribution The small-world phenomenon is often linked to another fundamental property of real-world networks. The shortest paths between two vertices chosen uniformly at random mostly consist of powerful vertices with a large number of neighbours, i.e. vertices connected by an edge to them. The number of a vertex' neighbours is called the *degree* of the vertex. Thus, to ensure short paths in a network, the degrees of the vertices in the network must vary sufficiently, such that the proportion of vertices with a large number of neighbours only decays slowly in the number of neighbours. For real-world networks this is often the case, as the proportion of vertices with degree k often decays polynomially as $k^{-\tau}$ for some $\tau > 0$ when k becomes large. Then, although the average degree can be relatively small, there still exist vertices with very large degree. For the movie collaboration network Barabási and Albert estimated the *power-law exponent* τ to be 2.3, see [5]. The internet on the AS-level also exhibits polynomial decay of the empirical degree distribution and the *power-law exponent* τ has been first estimated as $2.15-2.2$ in [47] and in 2012 the estimate was refined to 2.1, see [75]. An empirical degree distribution with such a behaviour is called *scale-free degree distribution*, as for any real numbers $c_1, c_2 > 0$, the proportion of vertices with degree $c_1 k$ and the proportion of the ones with degree $c_2 k$ decay with the same speed as k goes to infinity.

Clustering Are two random friends of yours more likely to be friends with each other than two random inhabitants of the world? This question leads to another property of many real-world networks called *clustering*, where the information that two vertices share a common neighbour increases the probability that there exists an edge between these two vertices. By its definition this property is linked to the number of triangles apparent in the network compared to the number of *wedges*, i.e. the pairs of edges which share one of their endvertices. Two measures for this effect of clustering are well established. The first one is the so-called *global clustering coefficient* c^{glob}, which is proportional to the proportion of triangles to wedges in the network. More precisely, it is given by $c^{\text{glob}} := 3\frac{\text{Number of triangles}}{\text{Number of wedges}}$, as the existence of each triangle implies the existence of three wedges. Alternatively one can look more locally for each vertex at the proportion of triangles containing the vertex to the wedges which share the vertex as an endpoint, which is called the *local clustering coefficient*. The second measure is then given by the *average clustering coefficient* c^{avg}, which is the average over

the local clustering coefficients of all vertices in the network. This measure describes the probability that two random neighbours of a typical vertex, i.e. a vertex drawn uniformly at random, are connected by an edge, whereas the global clustering coefficient puts more weight on powerful vertices with large degrees. Positive clustering coefficients have been estimated for many real-world networks, see [89]. For the internet on AS-level the global clustering coefficient has been estimated to be around $0.02 - 0.03$ and the average clustering coefficient to be 0.3, see [79]. For the movie collaboration network the proportion of triangles to wedges is much higher as the average clustering coefficient has been estimated to be 0.79 in [97].

With these properties in mind, the modelling of such real-world networks becomes an interesting field, as real-world networks are typically large and complex such that the complete analysis of such networks remains difficult. A good choice for models of such networks have become random graphs, where vertices are connected by probabilistic rules which may depend on local properties of the vertices. The advantage of random graphs compared to deterministic models is that the random occurence of edges by given local rules can model the complexity of connections in real-world networks, whereas deterministic models are either not defined by local rules or lead to networks which do not represent the structure of real-world networks. The aim of these models is not to describe real-world networks precisely, but to understand the influence of the given random connection rules on the fundamental properties of the graph, as these rules could be used to explain the empirically measured properties of real-world networks.

Graph metrics Before giving a short overview of well-known random graphs and their properties, we define the previously outlined metrics and properties of real-world networks on graphs. For an undirected graph $G = (V, E)$ we write $x \sim y$ if the vertices $x, y \in G$ are connected by an edge, i.e. if $\{x, y\} \in E$. The *degree* of a vertex x is then given by $\deg(x) := \big|\{y \in G : x \sim y\}\big|$ as the number of neighbours of x in G. When G is finite, the *empirical degree distribution* μ_G of G is defined as

$$\mu_G(k) := \frac{1}{|V|} \sum_{x \in G} \mathbf{1}_{\{\deg(x)=k\}}, \quad \text{for } k \in \mathbb{N}_0.$$

It is easy to see that $\mu_G(k)$ is also the probability that a vertex taken uniformly at random from G has degree k. Thus, we can think of the empirical degree distribution as the degree distribution of a *typical vertex*, in the sense that it is uniformly drawn from G. A path of length n exists between two vertices x and y in G, if there exists a sequence of vertices $x_1, \ldots, x_{n-1} \in G$ such that $x \sim x_1 \sim \ldots \sim x_{n-1} \sim y$. We write $x \overset{n}{\leftrightarrow} y$ if there exists a path of length n between x and y in G and denote by $x \leftrightarrow y$ if there exists a path of any length between the two vertices, implying that both vertices belong to the same connected component in G. The *graph distance* of two vertices $x, y \in G$ is given by

$$d(x, y) = \min\{n \in \mathbb{N} : x \overset{n}{\leftrightarrow} y\}$$

and we set $d(x, y) = \infty$ when the vertices are not connected by a path of any length. Similarly to the degree, we can observe the typical behaviour of the distance of two vertices in a finite graph by taking a pair of vertices (X_1, X_2) uniformly from all pairs of vertices with $x \leftrightarrow y$. We denote the graph distance $D_G := d(X_1, X_2)$ between these two vertices as the *typical distance* of G.

As mentioned previously, we call a pair of edges in G a *wedge*, if they share an endvertex (called the *tip*). We now give the exact definitions of the previously mentioned clustering coefficients. The *global clustering coefficient* or *transitivity* of a finite graph G is then given by

$$c^{\text{glob}}(G) := 3\frac{\text{Number of triangles in } G}{\text{Number of wedges in } G},$$

if there is at least one wedge in G and $c^{\text{glob}}(G) := 0$ otherwise. By definition, $c^{\text{glob}}(G) \in [0, 1]$. Another way to study clustering is to count only the triangles and wedges containing a fixed vertex x. For a vertex x with at least two neighbours, define the *local clustering coefficient* by

$$c_x^{\text{loc}}(G) := \frac{\text{Number of triangles in } G \text{ containing vertex } x}{\text{Number of wedges with tip } x \text{ in } G},$$

which is also an element of $[0, 1]$. Let $V_2(G) \subseteq G$ be the set of vertices in G with

degree at least two, and define the *average clustering coefficient* by

$$c^{\mathrm{av}}(G) := \frac{1}{|V_2(G)|} \sum_{x \in V_2(G)} c_x^{\mathrm{loc}}(G),$$

if $V_2(G)$ is not empty and as $c^{\mathrm{av}}(G) := 0$ otherwise.

In terms of modelling the behaviour of large real-world networks, one way is to consider a growing graph sequence $(G_n)_{n\in\mathbb{N}}$, where n denotes the number of vertices in G_n. We say such a graph sequence is *sparse* when the sequence of empirical degree distributions $(\mu_{G_n})_{n\in\mathbb{N}}$ converges to a probability measure μ on $\mathbb{N}_0$. We say a graph (sequence) has a *scale-free degree distribution* if it is sparse and the measure μ satisfies

$$\mu(k) = k^{-\tau+o(1)} \quad \text{as } k \to \infty \tag{1.1}$$

for some *power-law exponent* $\tau > 0$. A graph (sequence) is *small world* if with high probability the typical distance grows at most of logarithmic order in the number of vertices, i.e. if there exists a constant $c > 0$ such that it holds $\lim_{n\to\infty} \mathbb{P}(D_{G_n} \leq c \log n) = 1$, and *ultrasmall* if there exists a constant $c > 0$ such that

$$\lim_{n\to\infty} \mathbb{P}(D_{G_n} \leq c \log\log n) = 1.$$

Random graphs The simplest probabilistic connection rule is to connect each pair of vertices with the same probability independently of each other. Thus, for a given set of n vertices, an edge is formed between each pair of vertices with a fixed probability p. This graph was introduced in [52] and is called the Erdös-Rényi graph, due to the extensive analysis done by Erdös and Rényi in various papers, see [44, 45, 46]. It is easy to see that the degree of a vertex in this graph is binomially distributed with parameters $n-1$ and p. As we are interested in large sparse graphs, the edge probability p should decay with the amount of vertices n as n becomes large, since otherwise the structure of the graph becomes dense as then the expected degree of each vertex is not finite. But, by taking $p = \lambda/n$ for some $\lambda > 0$ the degree distribution of a vertex converges to a Poisson distribution with parameter λ as $n \to \infty$. Thus, the Erdös-Rényi graph does not have a scale-free degree distribution contrary to many real-world networks

as discussed beforehand.

One simple way to ensure a graph with scale-free degree distribution is to set the degree of each vertex in advance. This idea leads to the *configuration model* introduced in [15, 83], where an independent (possibly random) number of half-edges is assigned to each vertex. Given theses half-edges, all half-edges are paired uniformly. Note that this procedure allows the graph to have self-loops and multiedges, but the number of both is sufficiently small, that the erasure of self-loops and the merging of multiedges to one does not have any influence on the degree distribution of a typical vertex when the number of vertices is large, see [65]. Thus, a suitable choice for the number of half-edges for each vertex yields a graph with scale-free degree distribution. An alternative way to enforce a scale-free degree distribution is to assign to each vertex an independent identically distributed random weight and form edges independently with a probability proportional to the product of both end vertices' weights. This leads to random graphs such as the Chung-Lu random graph discussed in [28, 29], where the edge between two vertices occurs with a probability given by the product of the two weights normalised by the sum over all weights, or the Norros-Reittu random graph introduced in [91]. Here, if the random weights have a power-law distribution, these graphs have a scale-free degree distribution, see [29] and [91].

Whereas these models are mostly static in their construction, the idea of preferential attachment by Barabási and Albert [5] gives a potential description of the growth of real-world networks leading to a scale-free degree distribution. The main idea of such models is that vertices are added to the graph one after the other and new vertices are more likely to form an edge to already present vertices with high degrees. First formally introduced in [17], where a fixed number of new edges is formed when a new vertex is added to the graph and the probability to connect to an already present vertex is proportional to its degree, the idea of preferential attachment has been discussed in many different variants. See [42, 65] for general models with linear influence of the already present vertices' degrees and [36, 37] for preferential attachment models, where newly added vertices connect to a random number of already present vertices with a sublinear influence of the vertices' degrees. As heuristically predicted in [6] for the first ideas of random graphs with preferential attachment, the empirical degree distribution of these variants converge to a scale-free degree distribution, see [18, 65, 85] for

classical models with fixed number of edges added for each newly added vertex and [36] for models with random number of new edges.

Beside having a scale-free degree distribution, such random networks also exhibit the small-world phenomenon. In fact, the graphs are even *ultrasmall*, i.e. the typical distance is of at most doubly-logarithmic order of the number of vertices, when the power-law exponent τ of the degree distribution is between 2 and 3. See [28, 67, 91] for the existence of an ultrasmall phase in the configuration model, Chung-Lu random graph and Norros-Reitu random graph and [41, 84] for preferential attachment models. In [35] corresponding asymptotic lower bounds on the typical distance are shown which lead to limit theorems in the ultrasmall phase. Unlike the first two propertiers, clustering is not exhibit by these models. Such random graphs tend to be locally tree-like, which is a useful property for their global analysis, but leads to the clustering coefficients becoming zero when these models get large, see [2, 19] for corresponding results on classical preferential attachment models. This might be explained as the introduced random graphs not capture the possible similarities of vertices in real-world networks, such as location, age or mutual interests in social networks. Thus, several geometric variants of the models have been introduced, where the added spatial features of the vertices do not necessarily describe locations in real-world networks but rather the properties of vertices, such that vertices being near to each other indicates that they are similar in some sense. Various geometric variants of preferential attachment models have been studied in recent years. Flaxman, Frieze and Vera [48] introduced a model where new vertices get a spatial position leading to a set of candidate vertices which are sufficiently near to the new one. Then, by classical preferential attachment a fixed number of edges is formed between the new vertex and the candidates. This model was generalised and studied further in [72, 73, 74]. An alternative model was introduced by Aiello et al. in [1] and studied further in [30, 71]. In this model, each vertex has an influence region, whose size grows linearly with the degree of the vertex. New vertices connect to already existing vertices with a fixed probability if they fall into their influence regions. A significantly generalization of this model is the spatial preferential attachment network introduced and discussed by Jacob and Mörters in [69, 70]. In this model new vertices are added at the rate of a Poisson process of unit intensity and placed uniformly on the torus $\mathbb{T}_1^d$ of width one. A new vertex x

forms an edge to each already present vertex y independently with probability

$$\varphi\left(\frac{t d_{\mathbb{T}_1^d}(x,y)}{f(\texttt{indeg})}\right),$$

where

- t is the arrival time of the new vertex and $d_{\mathbb{T}_1^d}(x,y)$ the distance of the two vertices with respect to the torus metric,
- `indeg` the number of neighbours of y which arrived to the network after y,
- $f : \mathbb{N} \to \mathbb{R}_+$ an asymptotic linear function with slope $\gamma \in (0,1)$ and $\varphi : [0,\infty) \to [0,1]$ a non-increasing integrable function.

This model preserves the mechanism of preferential attachment such that the empirical degree distribution converges to a scale-free degree distribution with power-law exponent $\tau = 1 + \frac{1}{\gamma}$, but due to the induced spatial correlations the model also exhibits a positive average clustering coefficient, see [69]. A key technique of the analysis of this model is a rescaling argument which changes the analysis to a model where the arrival times of the vertices are uniform in the interval $(0,1]$ but the width of the torus grows. This type of spatial preferential attachment model ends up being too complicated to fully characterize ultrasmallness. The existence of an ultrasmall phase in the rescaled model has been shown by Hirsch and Mönch in [64], but a sharp phase transition and a limit theorem in the ultrasmall phase remain an open problem.

1.1.2 Percolation

Beside the observation of the small-world phenomenon, the introductory example of Milgram's experiment offers an empirical view to another question. Given a person with a folder as described in Milgram's experiment, what is the probability that the folder reaches an arbitrary person by the defined process and in particular do not get lost at some point? Such questions also arises for various phenomena in nature. How does water flow through a porous medium? How does a fire spread through a tree farm? These questions gave rise to the field of discrete percolation, where such phenomena are modelled by geometric random graphs defined on $\mathbb{Z}^d$. The edges in these models then represent the inner pas-

sageways of the porous medium, the paths of aquantainces, or the neighbouring trees of a tree on fire. The easiest model of discrete percolation is Bernoulli percolation and was introduced in [23]. Starting with the lattice $\mathbb{Z}^d$, each edge between neighbouring points on the lattice is declared to be *open* independently with probability p and *closed* with probability $1-p$. Then, removing all closed edges leads to a random graph with vertex set $\mathbb{Z}^d$, where an edge exists between two nearest-neighbour vertices independently with probability p. Looking at the original questions of having fire spreading between neighbours or water flowing along open passages, one interesting aspect is to look at the size of the *connected component* of the vertex 0, i.e. the set of vertices which are connected to 0 via a path. In many cases, the main focus lies on whether the connected component of 0 is infinite, i.e. when information or fire can spread indefinitely. The probability of this event is denoted as the *percolation probability*. It is easy to see that this percolation probability is non-decreasing in p, the probability of an edge of the lattice to be open. Thus, the *critical percolation probability* can be defined as the infimum of all p for which the percolation probability remains positive. For all p larger than the critical percolation probability the model *percolates*, which means that there exists an infinite connected component in the random graph with positive probability. These properties are well understood for Bernoulli percolation. For dimension two or larger, the critical percolation probability is positive and the infinite component is unique if it exists. See [60] for a discussion of various properties of Bernoulli percolation on the lattice. Beside the existence of an infinite component, another interesting topic is the comparison of Euclidean distances of two points with their graph distance, often in this field referred to as *chemical distance*. This can be linked to the speed of the spread in the introducing examples, when it is assumed that, for example the water needs a constant time to cross one edge. Then, the time the water takes to get from the origin to an arbitrary vertex is proportional to the chemical distance between the vertex and the origin. Thus, a small chemical distance in comparison to the Euclidean distance indicates a quick spread of water through a porous media for example. In analogy to a sequence of finite random graphs, a geometric random graph is *ultrasmall* when the chemical distance of two vertices of the infinite component that are far apart in Euclidean distance is at most of doubly-logarithmic order in their Euclidean distance with high probability. The idea of Bernoulli percolation can be extended to other discrete percolation models such as inhomogeneous

models, where edges have different probabilities to be open, or long-range models, in which open connections between pairs of vertices with large distance to each other are possible, see for example [60, Chapter 12] for different variants of discrete percolation.

As in the experiment of Milgram, typically the geometric foundation of real-world problems does not coincide with a lattice but more with a random set of vertices in $\mathbb{R}^d$. Thus, beside discrete percolation models, the field of continuum percolation has emerged. Here, the vertices are not given by $\mathbb{Z}^d$, but typically by a homogenous Poisson point process on $\mathbb{R}^d$. A major example is the Boolean model introduced by Gilbert [53], where each vertex of the Poisson point process represents the center of a ball with (random) radius, where the radii are drawn independently from each other and from the Poisson point process itself. The region covered by the balls is conventionally called the *occupied* region and the complement the *vacant* region. From the Boolean model one can easily derive a geometric random graph by taking the centers of the balls as the vertex set and forming an edge between two vertices if their corresponding balls intersect. This can be seen as a simplified model for a telecommunication system where each cellphone tower has a random range. In order for the system to be functional, although there might not necessarily exist a direct connection between two towers, each pair of towers must be connected by a chain of towers. Furthermore, if the chains are required to be short, this leads to the familiar areas of interest seen already in discrete percolation, such as the existence of an infinite connected component and the behaviour of the chemical distance in comparison to the Euclidean distance, in particular the occurence of *ultrasmallness*. A second example is the *random connection model*, where the vertices are again given by a Poisson point process and edges between vertices are formed independently from each other with probability given by a non-increasing function of the Euclidean distance of the pair. The flexible choice of the connection function allows continuum versions of Bernoulli percolation but also allows the appearance of edges spanning large distances in the random graph. For a detailed discussion of both models, we refer to [80].

1.2 Aim and structure of the thesis

In this thesis a large class of geometric random graphs is discussed with examples motivated either by random models for real-world networks or as an extension of continuum percolation models. These graphs are defined on a Poisson point process on $\mathbb{R}^d$ of unit intensity, where each vertex carries an independent uniform mark in $(0,1)$. Given the Poisson point process and the marks of each vertex, the discussed class of geometric random graphs is characterized by upper and lower bounds on the connection probabilities between finitely many pairs of vertices, which crucially depends on the Euclidean distance and the marks of each pair of vertices. This characterization includes a whole range of graph models with long edges and scale-free degree distributions. In analogy to random networks, the latter is defined as a typical vertex of the Poisson point process having a degree distribution which satisfies (1.1) for some $\tau > 0$, where we understand a typical vertex as a vertex with fixed location and uniform mark in $(0,1)$, see Section 1.2.2. In particular, the characterization includes two important main examples, where it is helpful for the reader to think of them in terms of the results of this thesis.

1.2.1 Main examples

The soft Boolean model The first example we consider is the *soft Boolean model*. In this model the vertex set is given by a Poisson point process on $\mathbb{R}^d \times (0,1)$ of unit intensity. For a vertex $\mathbf{x} = (x,t)$, the first entry $x \in \mathbb{R}^d$ describes the center of a ball and the second entry $t \in (0,1)$ determines the radius by $t^{-\gamma/d}$ of the corresponding ball, where $\gamma \in [0,1)$. This leads to a heavy-tailed distribution of the radii, since a uniform random variable T on $(0,1)$ and s large enough lead to $\mathbb{P}(T^{-\gamma/d} > s) = s^{-d/\gamma}$. As described in the previous section, a graph can be derived by taking the centers of the balls as the vertex set and by drawing an edge between two vertices if the two corresponding balls intersect. This yields that an edge is drawn between two vertices $(x,t),(y,s)$ if and only if $|x-y| < s^{-\gamma/d} + t^{-\gamma/d}$. For the soft Boolean model this condition is relaxed. Instead, independent identically distributed random variables $X = X(\mathbf{x},\mathbf{y})$ are associated with every unordered pair of vertices $\{\mathbf{x},\mathbf{y}\}$ and an edge is drawn if

and only if

$$|x - y| \leq X \cdot (s^{-\gamma/d} + t^{-\gamma/d}), \tag{1.2}$$

where x, y are the locations and t, s the marks of the vertices. This new condition can be interpreted in the following way. For each unordered pair of balls, consider copies of them for which the radii are multiplied by X. Then, an edge is drawn between the centers of the balls if the modified copies intersect. This mechanism keeps the idea of the classical Boolean model to draw an edge when two balls intersect but soften it by enlarging the corresponding balls. To fit this model in the class of geometric random graphs discussed in this thesis, the random variable X is chosen to be heavy-tailed with decay

$$\mathbb{P}(X > r) \asymp r^{-\delta d} \text{ as } r \to \infty,$$

for some $\delta > 1$. This choice allows the appearence of long edges in the graph, in fact taking $\gamma = 0$ in (1.2) yields the continuous long-range percolation model. Whereas the soft condition on the connection of two vertices has no influence on the scale-free degree distribution of the graph, see Proposition 4.14, an important result of this thesis shows that the appearence of long edges crucially changes the behaviour of the chemical distance and thus enables the occurence of ultrasmallness. For a formal introduction of the model and a detailed discussion with regard to the main results, see Section 4.2.

The age-dependent random connection model The second major example is the *age-dependent random connection model*, which will be introduced and discussed in detail in Section 4.1. This model is motivated as the limiting graph of a rescaled version of the following model. The *age-based spatial preferential attachment model* is a simplified version of the spatial preferential attachment model introduced by Jacob and Mörters and discussed in the previous section. In both models vertices are added at the rate of a Poisson process with unit intensity and placed uniformly on the torus $\mathbb{T}_1^d$. This time however, a new vertex x forms an edge to each existing vertex y independently with probability

$$\varphi\left(\frac{t d_{\mathbb{T}_1^d}(x,y)}{\beta(t/s)^\gamma}\right),$$

where t resp. s are the arrival times of x resp. y, $\gamma \in (0,1)$, $\beta > 0$ is a edge density parameter and $\varphi : [0,\infty) \to [0,1]$ is a non-increasing profile function. This choice for the probability function simplifies the model as it removes the complicated but on large scale inessential correlations between the edges and allows to focus on the crucial correlations coming from the spatial embedding. This is achieved by replacing the influence of the degree with its asymptotic expectation, as for $s < t$, the expected number of neighbours of a vertex added at time s, which are added between time s and t, is of order $(t/s)^\gamma$. This simplification still preserves the properties of the spatial preferential attachment model as introduced by Jacob and Mörters. It has a scale-free degree distribution with power-law exponent $\tau = 1 + \frac{1}{\gamma}$, see Section 4.1.3, and it exhibits positive clustering coefficients, see Theorem 4.9(a) for the average clustering coefficient and Theorem 4.9(b) for the global clustering coefficient. These results are proven in Section 4.1 through the analysis of the limiting age-dependent random connection model. Here, the vertex set is given by a Poisson point process on $\mathbb{R}^d \times (0,1)$ of unit intensity. We denote by the first entry of a vertex $\mathbf{x} = (x,t)$ its location in $\mathbb{R}^d$ and by the second entry the vertex' *birth time*. Hence, vertices with small birth time are considered *old* and vertices with birth time near to one are *young*. Given the vertex set, edges are drawn independently between two vertices $\mathbf{x} = (x,t)$ and $\mathbf{y} = (y,s)$ with probability

$$\varphi\big(\beta^{-1}(t \wedge s)^\gamma (t \vee s)^{1-\gamma} |x-y|\big), \tag{1.3}$$

where $|x-y|$ is the Euclidean distance of the vertices. Note that by definition the probability to form an edge between a vertex and an older vertex is similar to the probability given in the definition of the age-based spatial preferential attachment model, which allows to derive results from this model to the age-based spatial preferential attachment model by rescaling arguments. This key technique and the proofs of the stated results will be given in Section 4.1, introduced by a discussion of the application of this thesis main results to the age-dependent random connection model.

1.2.2 Characterization of geometric random graphs

As mentioned previously the class of geometric random graphs which we are interested in is characterized by upper and lower bounds on the connection probabilities between finitely many pairs of vertices. All main results stated in this thesis hold for geometric random graphs satisfying the following assumptions. Let the vertex set of the geometric random graph $\mathscr{G}$ be given by a Poisson point process $\mathcal{X}$ on $\mathbb{R}^d \times (0,1)$, and fix the parameters $\delta > 1$ and $0 \leq \gamma < 1$. We write the vertices of $\mathscr{G}$ as $\mathbf{x} = (x,t)$ and refer to x as the location and t as the mark of the vertex $\mathbf{x}$.

Assumption UBA*: Upper bound assumption

Given $\mathcal{X}$, let edges be drawn independently of each other and there exists $\kappa > 0$ such that for every pair of vertices $\mathbf{x} = (x,t) \in \mathcal{X}$ and $\mathbf{y} = (y,s) \in \mathcal{X}$, the probability that there exists an edge between them is smaller than

$$\kappa(t \wedge s)^{-\delta\gamma}(t \vee s)^{\delta(\gamma-1)} |x-y|^{-\delta d}.$$

Assumption LBA: Lower bound assumption

Given $\mathcal{X}$, let edges be drawn independently of each other and there exists $\alpha, \kappa > 0$ such that for every pair of vertices $\mathbf{x} = (x,t) \in \mathcal{X}$ and $\mathbf{y} = (y,s) \in \mathcal{X}$, the probability that there exists an edge between them is larger than

$$\alpha\big(1 \wedge \kappa(t \wedge s)^{-\delta\gamma} |x-y|^{-\delta d}\big).$$

The choice of the parameter γ in these assumptions controls the influence of the marks on the connection probability, where larger values of γ imply a stronger dependence of the connection probability on the vertex with the smaller mark, i.e. the vertex with the larger ball in the soft Boolean model and the older vertex in the age-dependent random connection model. In fact, since the assumptions imply that given the Poisson point process $\mathcal{X}$ edges occur independently, the degree of vertex with mark t is bounded from above and below by Poisson-distributed random variables with parameter of order $t^{-\gamma}$, see Proposition 4.5 and 4.14. Consequently, under Assumption UBA* and LBA the random graph has a scale-free degree distribution with parameter $\tau = 1 + \frac{1}{\gamma}$, see Section 4.1.3 for

the proof in the case of the age-dependent random connection model. However, the parameter δ is a geometric quantity which influences the occurence of long edges between vertices with typical marks by controlling the influence of the Euclidean distance on the connection probability.

Remark 1.2.1. Although all main results of this thesis hold for this class of geometric random graphs, it is worth mentioning that for some significant results the assumptions can be relaxed, which leads to an even larger class with examples discussed in Sections 4.5 and 4.6.

Throughout this thesis it is necessary to be able to distinguish between multiple different vertices of the Poisson point process $\mathcal{X}$. Thus, for $\mathbf{x}_1, \dots, \mathbf{x}_n \in \mathbb{R}^d \times (0,1)$, we denote by $\mathbb{P}_{\mathbf{x}_1,\dots,\mathbf{x}_n}$ the law of the graph $\mathscr{G}$ when the vertex set is given by $\mathcal{X} \cup \{\mathbf{x}_1, \dots, \mathbf{x}_n\}$ and the connection rules remains as before. Since $\mathcal{X}$ is a Poisson point process, Mecke's equation [76, Theorem 4.1] and its multivariate variant [76, Theorem 4.4] holds and we can think of $\mathbb{P}_{\mathbf{x}_1,\dots,\mathbf{x}_n}$ as the law of $\mathscr{G}$ conditioned on the event that $\mathbf{x}_1, \dots, \mathbf{x}_n$ are points of $\mathcal{X}$; we will refer to this measure with this interpretation in mind throughout this thesis. At some points in this thesis we will consider the *Palm*-version of $\mathscr{G}$. More precisely, we add to $\mathcal{X}$ a vertex $(0, T_0)$, where T_0 is an independent on the interval $(0,1)$ uniformly distributed random variable. We denote the resulting graph by $\mathscr{G}_{(0,T_0)}$ and refer to the vertex $(0, T_0)$ as the *origin* of the Palm-version. We denote the law of $\mathscr{G}_{(0,T_0)}$ by $\mathbb{P}_{(0,T_0)}$ and since T_0 is independent of the underlying Poisson point process $\mathcal{X}$ and by Assumption UBA* and Assumption LBA edges are drawn independently given the vertex set, it holds $\mathbb{P}_{(0,T_0)} = \mathbb{P}_{(0,t_0)}\mathrm{d}t_0$. We can roughly think of the Palm-version as the random graph with a *typical vertex* at the origin.

1.2.3 Chemical distance

The main focus of this thesis is to analyse the behaviour of the chemical distance of two vertices with large Euclidean distance. In particular, the focus lies on the occurence of *ultrasmallness* in the graphs, i.e. that with high probability the chemical distance of two vertices grows at most doubly-logarithmically in their Euclidean distance.

In Chapter 2 a sharp criterion for the occurence and absence of ultrasmallness in

geometric random graphs is given and in the ultrasmall regime a limit theorem for the chemical distance of two vertices is established, both of which crucially depend on the upper and lower bounds of the connection probabilities. In fact, the occurence of ultrasmallness highly depends on both parameters γ and δ, which control the influence of the marks and the Euclidean distance of two vertices on their connection probability. A consequence of the main Theorems 2.1 and 2.2 of Chapter 2 is the following.

Theorem 1.1

Let $\mathscr{G}$ be a geometric random graph as characterized in Section 1.2.2 which satisfies Assumption UBA* and Assumption LBA for some $\gamma \in [0, 1)$ and $\delta > 1$. Then,

- if $\gamma < \frac{\delta}{\delta+1}$, the graph is **not ultrasmall** and
- if $\gamma > \frac{\delta}{\delta+1}$, the graph is **ultrasmall** and it holds

$$\frac{\mathrm{d}(\mathbf{x}, \mathbf{y})}{\log\log(|x-y|)} \to \frac{4}{\log\left(\frac{\gamma}{\delta(1-\gamma)}\right)} \text{ with high probability as } |x-y| \to \infty,$$

where $\mathrm{d}(\mathbf{x}, \mathbf{y})$ is the chemical distance of two vertices $\mathbf{x}$ and $\mathbf{y}$ and $|x-y|$ their Euclidean distance.

These results indicate a new universal behaviour of geometric random graphs which differs markedly from the behaviour of the well-understood non-spatial scale-free models discussed in Section 1.1.1 and spatial scale-free random graphs, such as the ones investigated in [21]. For these models the occurence of ultrasmallness depends solely on the finiteness of the variance of the degree distribution and therefore on the power-law exponent τ, whereas this new universal behaviour exhibits a strong dependence on both, the power-law exponent τ and the parameter δ. See Section 2.1 for a further discussion and a comparison to other well-studied models.

In Chapter 2 the proofs of Theorem 1.1 are given and the application of the theorem to various examples of geometric random graphs is discussed in Chapter 4. It is worth noting at this point that the main result can be broken into results on asymptotic lower and upper bounds for the chemical distance (see Theorem

2.1 and Proposition 2.13), where the upper bounds on the chemical distance are a consequence of the lower bound assumptions and the lower bounds on the chemical distance a consequence of the upper bound assumptions. The proof of the upper bounds is a constructive proof, where a strategy is given to ensure that two given vertices $\mathbf{x}$ and $\mathbf{y}$ are connected to the same vertex with very small mark in a number of steps of order $\frac{2\log\log(|x-y|)}{\log(\frac{\gamma}{\delta(1-\gamma)})}$, leading to the existence of a path of length of order $\frac{4\log\log(|x-y|)}{\log(\frac{\gamma}{\delta(1-\gamma)})}$ between the two vertices. For the lower bounds it is necessary to show that this strategy is actually the optimal one, i.e. it connects two vertices with high probability in the shortest way possible. To do so, new techniques are developed in Chapter 2 capturing not only the influence of the degree distribution but also the subtle yet crucial influence of the spatial embedding in terms of δ to the occurence of short paths in the graph, leading to the given lower bounds in Theorem 2.1.

As mentioned earlier for the results on asymptotic lower bounds of the chemical distance the upper bound assumption UBA* can be relaxed by replacing it with the following more general assumption, as stated in Remark 1.2.1.

Assumption UBA: Upper bound assumption

Given $\mathcal{X}$, there exists $\kappa > 0$ such that, for every finite set of pairs of vertices $I \subset \mathcal{X}^2$, where each vertex is part of at most two pairs, the probability that an edge exists between each pair of I is smaller than

$$\prod_{(\mathbf{x}_i,\mathbf{y}_i)\in I} \kappa(t_i \wedge s_i)^{-\delta\gamma}(t_i \vee s_i)^{\delta(\gamma-1)} |x_i - y_i|^{-\delta d},$$

where $\mathbf{x}_i = (x_i, t_i)$, $\mathbf{y}_i = (y_i, s_i)$.

This assumption does not include conditional independence of the occurence of edges in the graph, which makes it much more difficult to track the behavior of the graphs appropriately. Examples satisfying Assumption UBA but not Assumption UBA* are given in Section 4.5 and 4.6.

1.2.4 Contact process

In the second part of the thesis covered in Chapter 3 we shift the focus to the analysis of the contact process on geometric random graphs, as a model for the spread of infection on a population or a network. Here, each vertex is either healthy or infected at any point in time. Infected vertices recover at a constant rate and are able to transmit the infection to each of its healthy neighbours with a given rate $\lambda > 0$, see Section 3.1.1 for a precise introduction of the contact process. In epidemics literature this process is also known as the SIS-model, as at any time each vertex is either infectious or susceptible for the infection, even if the vertex has already recovered from the infection beforehand. This is a significant difference to the SIR-model, where vertices are assumed to be able to develop an immunity to the infection such that once they recovered from the infection they are not susceptible to it any more.

The main interest in Chapter 3 lies in the time at which the infection reaches its only absorbing state, which is given by the configuration where all vertices are healthy. We denote this time as the *extinction time* of the process and look at its behaviour, when the underlying geometric random graph exhibits sufficiently short paths such that it is ultrasmall, i.e. when $\gamma > \frac{\delta}{\delta+1}$. In this regime we show that the graph is so well-connected that for any choice of λ the contact process starting only in one vertex of the graph does not go extinct with positive probability. Put differently, the extinction time of the process is infinite with positive probability, and as a main result we give precise asymptotics of this non-extinction probability in terms of λ when λ is small, see Theorem 3.1.

Theorem 1.2

Let $\mathscr{G}$ be a geometric random graph as characterized in Section 1.2.2 which satisfies Assumptions UBA* and LBA for $\gamma > \frac{\delta}{\delta+1}$ and denote by $\Gamma(\lambda)$ the probability that the contact process with rate λ starting in the origin of the Palm-version of $\mathscr{G}$ does not go extinct. Then, there exist constants $c, C > 0$ such that

$$c\frac{\lambda^{2/\gamma-1}}{\log(1/\lambda)^{(1-\gamma)/\gamma}} \leq \Gamma(\lambda) \leq C\frac{\lambda^{2/\gamma-1}}{\log(1/\lambda)^{(1-\gamma)/\gamma}}$$

for λ sufficiently small.

A positive probability $\Gamma(\lambda)$ for any choice of λ has been shown for the contact process on various scale-free random graphs. This is unlike the behaviour of the contact process on the lattice or regular trees, where there exists a critical value λ_c such that the contact process almost surely dies out if and only if $\lambda \leq \lambda_c$. The result of Theorem 1.2 shows a remarkably different behaviour to the contact process on other well-understood (spatial) scale-free random graphs such as the configuration model or hyperbolic random graphs, since for those graphs $\Gamma(\lambda)$ exhibits multiple different rates of decay depending on the power-law exponent τ, especially when τ is near to 2. For a further discussion and comparison to recent other results see Section 3.1 and Section 3.2.

Furthermore, we look at the behaviour of the extinction time of the contact process on finite versions of the geometric random graphs, where, for $n \in \mathbb{N}$, the graph is spatially restricted to a box $B_n := [-\frac{n^{1/d}}{2}, \frac{n^{1/d}}{2}]^d$. In this case the extinction time is almost surely finite. However, we show in Theorem 3.14 that with high probability the extinction time is of exponential order of the volume in the box leading to the following result.

Theorem 1.3

Let $(\mathscr{G}_n)_{n\in\mathbb{N}}$ be the spatially on B_n restricted finite graph sequence of a general geometric random graph $\mathscr{G}$ which satisfies Assumption LBA for $\gamma > \frac{\delta}{\delta+1}$ and denote by τ_n the extinction time of the initially fully infected contact process on $\mathscr{G}_n$. For any $\lambda > 0$, there exists $c > 0$ such that

$$\lim_{n\to\infty} \mathbb{P}\{\tau_n \geq e^{cn}\} = 1.$$

This result agrees with well-known results on the lattice, where the range of values of λ for which with positive probability the contact process does not extinct coincides with the range that has an exponential extinction time on its finite restriction. It is worth to note, as the main contribution to the proof of this result, in Proposition 3.15 an explicit construction of a connected component containing a positive proportion of vertices of $\mathscr{G}_n$ is given for n sufficiently large.

1.2.5 Structure

We now give a quick overview of the thesis' structure. In Chapter 2 the occurence and absence of ultrasmallness of geometric random graphs is discussed and the sharp criterion for the absence of ultrasmallness as well the limit theorem in the ultrasmall regime stated in Theorem 1.1 is proven. Section 2.1 provides a short overview and a discussion of the results of the chapter in comparison to the behaviour of other well-known random graphs from the literature. In Section 2.2 the main results of this section are stated and the precise lower and upper bound assumptions for the geometric random graphs are given. Section 2.3 is dedicated to the proof of the asymptotic lower bounds for the chemical distance of two distant vertices, where we start in Section 2.3.1 with an introduction of a truncated first moment bound used in the following parts and simple applications of the truncated first moment bound to geometric random graph models which do not fit in the introduced class in Section 1.2.2. Section 2.3.2 provides a short overview of the proof structure and its heuristic leading to the stated results. The full proofs are carried out in Section 2.3.3 for the ultrasmall regime and Section 2.3.4 for the non-ultrasmall regime. In Section 2.4 we complete the proof by showing the corresponding upper bound on the chemical distance in the ultrasmall regime.

Chapter 3 is dedicated to the behaviour of the contact process on geometric random graphs in the ultrasmall regime. We give an introduction to the contact process and an overview of its behaviour and extinction time on well-known (random) graphs in Section 3.1. In Section 3.2 we discuss the non-extinction probability of the contact process and prove the stated sharp asymptotics when λ is small. This proof is divided into a proof of an asymptotic lower bound, carried out in Section 3.2.1, and the corresponding upper bound in Section 3.2.2. Finally, the proof of the exponential extinction time on finite restrictions of the graph can be found in Section 3.2.

In Chapter 4 we provide various examples of the class of geometric random graphs characterized in 1.2.2 and two examples of geometric random graphs which do not fit this class but still satisfy upper bound assumptions on their connection probability. Simpler applications of the truncated first moment bound are carried out for them in Section 2.3.1. The first two sections are especially important, as

in Section 4.1 we introduce the age-based preferential-attachment network and the age-dependent random connection model and discuss various properties of it, such as the degree distribution of a typical vertex, the global and local clustering coefficients and the typical edge length. In Section 4.2 we introduce the soft Boolean model and discuss it with regard to the main results of this thesis.

In the last Chapter 5 we conclude the thesis with a brief summary of the results obtained and a discussion of possible open research possibilities.

This thesis includes the work of three papers or preprints. Namely,

[56] **Chemical distance in geometric random graphs with long edges and scale-free degree distribution** with Peter Gracar and Peter Mörters, *Communications in Mathematical Physics (2022)*, DOI: 10.1007/s00220-022-04445-3

[55] **The age-dependent random connection model** with Peter Gracar, Lukas Lüchtrath and Peter Mörters, *Queueing Systems. Theory and Applications (2019)*, DOI: 10.1007/s11134-019-09625- y

[54] **The contact process on scale-free geometric random graphs** with Peter Gracar, *ArXiv Preprint (2022)* arXiv: 2208.08346

We now describe for each of the three works their inclusion in the thesis and give a short description of the thesis' author contribution to each. In the following paragraphs of this section the thesis' author is referred to in first person singular.

Chapter 2 contains the work of [56], namely the framework and the main results of the chapter stated in Section 2.2 as well the corresponding proofs given in Section 2.3 and Section 2.4. Furthermore parts of Section 4.5 and Section 4.6 are part of [56]. Slight changes to the text and notation have been made to improve the readability of the thesis. Figures in the mentioned sections have been taken out of [56].
My contribution to the work in [56] was essential, as under joint discussions with my colleagues I was responsible for the development of the key ideas and formulations and carried out the technical part of proving the main results in this work. I also contributed significantly to the writing process of this work and its revision.

The work of [55] is contained in Section 4.1, more precisely Sections 4.1.1-4.1.5. For the readability of the thesis the notation has been adapted to the notation used throughout this thesis. Figures in the mentioned sections have also been taken out of [55].
I contributed significantly in this joint work, as I participated and contributed in all group discussions leading to the new techniques and ideas and coauthored the proofs together with Lukas Lüchtrath. Together with Peter Gracar, I developed the code which provides the simulation results, see Section A.3.

Chapter 3 corresponds to the work in [54]. Slight changes have been made in Section 3.1 due to the structure of the thesis and with regard to [54, Remark 1.1] the propositions and theorems in this chapter have been made stronger by assuming only the relevant bound given by Assumption UBA* or Assumption LBA. Figures in this chapter have been taken out of [54].
I was the primary contributor to the work in [54], as I proved the results in Section 3.2 independently and for the results in Section 3.3 I carried out the proof under joint discussion with my colleague. I also did the majority of writing.

This thesis is written in Texmaker (Version 4.4.1) with LaTeX(TeXLive 2022). Figures which have not been taking out of the previous mentioned works were created by the author using Jupyter Notebook (Version 6.0.3) with Python (Version 3.7.7).

CHAPTER 2

Ultrasmallness in scale-free geometric random graphs

In this chapter we discuss the occurence and absence of ultrasmallness in geometric random graphs. For the main result of this chapter we state and prove a sharp criterion for the absence of ultrasmallness and in the ultrasmall regime we give a precise description of the asymptotic behaviour of the chemical distance of two vertices with large Euclidean distance by deriving a limit theorem in Theorem 2.1 and 2.2. As mentioned in Section 1.2.5, this chapter contains the work done in [56], as Sections 2.2 - 2.4 can be found in [56]. For a detailed discussions of the parts coinciding with [56] and the thesis' author's contribution to this work, see Section 1.2.5.

2.1 Literature review and discussion

First, we briefly review what is known for the comparison of the Euclidean distance of two vertices with their chemical distance for geometrically embedded random graphs.

Starting with the work of Grimmett and Marstrand [59], this problem has been extensively studied for Bernoulli percolation on the lattice $\mathbb{Z}^d$, as introduced

in Section 1.1.2, where an edge is open between two nearest-neighbour vertices independently with probability p and closed with probability $1-p$. In the supercritical phase the Euclidean and the chemical distance of two vertices on the unbounded connected component are typically of comparable order when the vertices are distant, see [59] and [51]. Further analysis of the chemical distance for Bernoulli percolation has been done by Antal and Pistora [3] and Garet and Marchand [49, 50] by deriving large deviation estimates for the chemical distance [3, 50] and an asymptotic shape theorem [49]. The Euclidean distance and the chemical distance of two distant vertices are also typically comparable in models with long range interactions, such as random interlacements (see Černý and Popov [26]), its vacant set and the Gaussian free field, see Drewitz et al. [43]. In [43] the authors provide general conditions for percolation models on $\mathbb{Z}^d$ to share this behaviour and give large deviation estimates as well as an asymptotic shape theorem for the chemical distance. This behaviour is also apparent in continuum percolation for the Boolean model where each ball has a fixed radius, see [98].

The behaviour of the chemical distance in comparison to the Euclidean distance can change by the introduction of additional long edges to the graph. A classical example is *long-range percolation*. Here, vertices x, y of a Poisson point process in $\mathbb{R}^d$ or on the lattice $\mathbb{Z}^d$ are connected independently with probability

$$p(x,y) = 1 \wedge |x-y|^{-\delta d + o(1)},$$

for some $\delta > 1$. Biskup et al. [13, 14] has shown that if $1 < \delta < 2$ then the chemical distance for two vertices x, y of the infinite component is

$$d(x,y) = (\log|x-y|)^{\Delta + o(1)},$$

with high probability as $|x-y| \to \infty$, where $\Delta = \frac{\log 2}{\log(2/\delta)}$. For $\delta < 1$ the number of long edges added to the graph is so high that the diameter of the graph is finite, as shown in [8]. Benjamini et al. show that between all pairs of vertices x and y the chemical distance is bounded by a constant term not depending on the Euclidean distance. If $\delta > 2$, not sufficiently many long edges are added to the graph such that a change in the behaviour of the chemical distance in comparison to Bernoulli percolation is not expected. It was shown by Benjamini and Berger [7] that the diameter of one-dimensional long-range percolation restricted to finite

intervals is at least linear in the size of the intervals. The boundary cases $\delta = 1$ and $\delta = 2$ have been discussed by Coppersmith et al. [31] and Ding and Sly [39], but in general, ultrasmallness cannot occur in long-range percolation models.

Non-spatial scale-free networks

Ultrasmallness is however a well established phenomenon in scale-free networks, such as the Chung-Lu random graph [28, 29], the Norros-Reittu random graph [91], the configuration model [15, 83] or preferential attachment models [36, 37, 42, 65] discussed in Section 1.1.1. Since these networks are typically not modelled as geometrically embedded graphs, in order to compare these models to the class of geometric random graphs discussed in this thesis, we introduce a geometrically embedded *toy model* which mimics the behaviour of the well-studied non-spatial scale-free networks. Let the vertex set be given by the lattice or a Poisson point process on $\mathbb{R}^d$ and restrict the graph to the vertices inside a ball of radius R. Thus, the ball contains N lattice or Poisson points, where N is of order R^d. The mean-field nature of these models is reflected in the fact that connection probabilities do not depend on the location of these points. Instead, each point carries independent uniform marks and connections between vertices are established independently given the marks, with a probability $1 \wedge \frac{g(s,t)}{N}$ depending on the marks s, t of the endvertices of a potential edge. Potential dependencies $g : (0,1) \times (0,1) \to \mathbb{R}_+$ are given by

$$g^{prod}(s,t) := s^{-\gamma} t^{-\gamma} \text{ or}$$
$$g^{pa}(s,t) := (s \wedge t)^{-\gamma} (s \vee t)^{\gamma - 1}.$$

In both cases this leads to a random graph with scale-free degree distribution with power-law exponent $\tau = 1 + \frac{1}{\gamma}$ as $R \to \infty$. As mentioned beforehand, one can think of these models as simplified versions of well-studied scale-free networks showing the same behaviour in terms of degree distribution and the occurence of ultrasmallness. Here, the toy model with $g := g^{prod}$ behaves like scale-free networks where the connection probability is proportional to the product of weights assigned to each vertex, such as the Chung-Lu random graph, the Norros-Reittu random graph or the configuration model. The toy model with $g := g^{pa}$ behaves like classical non-spatial preferential attachment models.

Why are these models ultrasmall when the power-law exponent τ is between 2 and 3 as mentioned in Section 1.1.1? Thinking about the scale-free networks associated to the toy model with g^{prod}, one can give a heuristic explanation of this by using the fact that these models have a locally tree-like structure, see [66, Theorem 4.1] in case of the configuration model and [66, Theorem 3.18] for the Chung-Lu random graph and the Norros-Reittu random graph. Thus, the neighbourhood of a vertex can be compared to a branching process with infinite mean if $\tau \in (2,3)$ and therefore the variance of the degree distribution does not exist. In this case the branching process grows at a superexponential rate and therefore the k-th neighbourhood of a vertex, i.e. all vertices which can be reached from the vertex in k steps, also grows super exponentially at rate $e^{(\tau-2)^{-k}}$, see [66, Theorem 7.17]. Hence, for two given vertices, both neighbourhoods given by vertices reached in a number of steps of order $\log\log N$ are so large that they need to share at least one vertex and thus a path with length of doubly logarithmic order of the amount of vertices N exists between the two given vertices. This heuristic argument does not work for geometrically embedded random graphs as these graphs tend to not be locally tree-like, but it still gives valuable insight to the typical structure of a path connecting two vertices in such models. For the size of the k-th neighbourhood of a vertex x to grow super exponentially in k, x needs to be connected via a path to vertices which have an increasing number of neighbours. For the toy model this means that x is connected by a path to vertices with increasingly small marks such that longer paths starting in x reach vertices with arbitrarily small marks. Thus, a typical short path between two vertices x and y which minimizes their chemical distance is formed by two subpaths starting in x, resp. y, which steadily lead to more powerful vertices until both subpath reach the same powerful vertex, i.e. a vertex with a very small mark. More precisely for the toy model with $g := g^{prod}$, the probability that a vertex with mark t has no neighbour with mark smaller than $\ell < t$ is close to $\exp(-ct^{-\gamma}\ell^{\gamma-1})$ for some constant $c > 0$. This holds since each of the other $N-1$ vertices is a neighbour with smaller mark with probability

$$\int_0^\ell \mathrm{d}s 1 \wedge \frac{s^{-\gamma}t^{-\gamma}}{N} = \frac{1}{1-\gamma}\frac{t^{-\gamma}\ell^{1-\gamma}}{N} - \frac{\gamma}{1-\gamma}\left(\frac{\ell^{-\gamma}}{N}\right)^{1/\gamma}$$

and the second term on the right hand side becomes negligible as the number of vertices N is made large. Thus, with high probability the vertex is connected by

an edge to at least one vertex with mark of order $t^{\gamma/(1-\gamma)}$ or smaller. Repeating this argument and using that $\tau - 2 = \frac{1-\gamma}{\gamma}$ leads to the heuristic observation that after $(1 + o(1))\frac{\log\log N}{|\log(\tau-2)|}$ steps the vertices x and y can reach vertices with mark smaller than $N^{1/2}$ with high probability which are then connected by a direct edge in the toy model and by at most two edges in the Chung-Lu random graph, the Norros-Reittu random graph or the configuration model, see [66]. Thus, if $2 < \tau < 3$ these graphs are ultrasmall and for two randomly chosen vertices x, y it holds

$$\frac{d(x,y)}{\log\log(N)} \longrightarrow \frac{2}{|\log\tau - 2|}, \tag{2.1}$$

with high probability as the number of vertices N goes to infinity.

In the case $g = g^{pa}$ this heuristic no longer works. Here, we cannot guarantee with high probability that a vertex with a small mark is connected by an edge to a vertex with even smaller mark, since for a vertex with mark t the expected number of neighbours with mark smaller than t does not increase as t is made smaller. This fits with the behaviour of non-spatial preferential attachment models where old vertices, i.e. vertices which have been added early to the graph, are not connected to other significantly older vertices with sufficiently high probability. This is a consequence of the fact that vertices with high degree do not have an increased probability to form an edge to every vertex of the graph but only to those that have been added to the graph towards the end, since it takes time for these vertices to achieve a high degree. On the other hand, although old vertices are not connected by an edge to older vertices with high enough probability, they have plenty of neighbours which have been added to the graph after their own appearance. Thus, for non-spatial preferential attachment models, a vertex with high degree can reach a vertex with significantly higher degree not through an direct edge but via a path of length two, where the intermediate vertex is a young vertex, i.e. a vertex which has been added to the random graph towards the end. Consequently, it takes twice as many steps to connect two vertices and, if $2 < \tau < 3$, for two randomly chosen vertices x, y, satisfy

$$\frac{d(x,y)}{\log\log(N)} \longrightarrow \frac{4}{|\log\tau - 2|}, \text{ with high probability as } N \to \infty. \tag{2.2}$$

To compare these results to geometrically embedded random graphs, note that two randomly chosen vertices x, y in the toy model typically have Euclidean

distance of order R. As N is of order R^d we can replace N in the preceding statements by the Euclidean distance such that if $2 < \tau < 3$, for two randomly chosen vertices x, y, it holds

$$\frac{d(x,y)}{\log\log(|x-y|)} \longrightarrow \frac{c}{|\log\tau - 2|}, \text{ with high probability as } R \to \infty, \tag{2.3}$$

where $c = 2$ for $g = g^{prod}$ and $c = 4$ for $g = g^{pa}$. When $\tau > 3$ (or, equivalently, $\gamma < \frac{1}{2}$) the chemical distance of two randomly chosen vertices x, y in the largest connected component is of order $\log N$ or, equivalently, $\log|x-y|$, see Bollobas et al. [16].

Well-studied scale-free spatial models

Looking at geometrically embedded random graphs with scale-free degree distribution, a well-studied range of spatial models are geometric random graphs, where vertices are endowed with weights which are independent sampled from some heavy-tailed distribution. In these models an edge is formed between two vertices with a connection probability depending on the *product* of the weights and the spatial distance of the vertices. Popular examples are *scale-free percolation* introduced and studied for the lattice by Deijfen et al. [33] and extended to a continuum version on a Poisson point process by Deprez et al. [34] and *geometric inhomogeneous random graphs* introduced by Bringmann et al. [20] which include *hyperbolic random graphs* as a special case. As the heavy-tailed weights of the vertices correspond loosely to negative powers of uniformly distributed marks t, the following model shares the same properties as the previously introduced examples. Let the vertex set be given by the lattice or a Poisson point process of unit intensity on $\mathbb{R}^d$ and let each vertex carry an independent uniform mark. Then, given the vertex set and the marks an edge is formed between two vertices independently with probability

$$\varphi\big(\beta^{-1}t^{\gamma}s^{\gamma}|x-y|^d\big),$$

where $\varphi : (0,\infty) \to [0,1]$ is a non-increasing integrable function,the parameter β controls the edge density and t, resp. s, are the marks of x, resp. y. These models are all scale-free with power-law exponent $\tau = 1 + \frac{1}{\gamma}$, independent of the spatial embedding of the models, see [33], [21] and Section 4.3. Interestingly,

the influence of the product of the weights on the connection probability is so strong that the spatial embedding does not play a significant enough role and the behaviour of the chemical distance does not deviate from the non-spatial models. Namely, the transition between ultrasmall and small world behaviour occurs at $\gamma = \frac{1}{2}$ (equivalently, $\tau = 3$) and in the former case a limit theorem as in 2.3 with $c = 2$ holds. See [33] and [34] for details in the case of scale-free percolation and its continuous version, and [21] for a large class of geometric variants of the Chung-Lu random graph, which includes geometric inhomogeneous random graphs. Additionally, an interesting algorthmic view on this problem is given by Bringmann et al. in [22]. In this work they look at the strategy of Milgram's experiment described in the beginning of this thesis and show that this strategy actually works in geometric inhomogeneous random graphs and leads to a shortest path between the starting vertex and the target.

In summary, for these models, there is no influence of the spatial embedding on the absence and occurence of ultrasmallness and the results of [33], [34] and [21] hold for models with induced long edges such as scale-free percolation as well as for models like hyperbolic random graphs without long edges. We will see now how not only the proof techniques but also the results themselves depend crucially on the structure of the connection probability. Namely, the probability depends on taking the product of the heavy-tailed weights of the vertices. In fact, the situation changes drastically when other, equally natural forms of the connection probability are considered, such as the two main examples introduced in Section 1.2.1. We will see that the novel behaviour of these examples is also of a universal nature, as it appears for a whole class of geometric random graphs characterized in Section 1.2.2.

Novel universal behaviour of geometric random graphs

Recall the *soft Boolean model* introduced in Section 1.2.1. When the random variable X in the connection rule (1.2) is heavy-tailed with decay $\mathbb{P}(X > r) \asymp r^{-\delta d}$ as $r \to \infty$ for $\delta > 1$ the results of this chapter yield, as stated in Theorem 1.1,

- *no ultrasmallness* if $\gamma < \frac{\delta}{\delta+1}$ but,
- *ultrasmallness* if $\gamma > \frac{\delta}{\delta+1}$.

In the *age-dependent random connection model*, the marks of the vertices correspond to birth times and an edge is drawn independently with probability

$$\varphi\big(\beta^{-1}(t \wedge s)^{\gamma}(t \vee s)^{1-\gamma}\,|x-y|^{d}\big)$$

where $\gamma \in (0,1)$. The behaviour is similar to the soft Boolean model when the profile function $\varphi : (0,\infty) \to [0,1]$ determining the connection probability in (1.3) decays polynomially at rate $\delta > 1$, i.e. $\varphi(r) \asymp r^{-\delta}$ as $r \to \infty$. Our results show that in the age-dependent random connection model ultrasmallness fails if $\gamma < \frac{\delta}{\delta+1}$ and if $\gamma > \frac{\delta}{\delta+1}$, the model is ultrasmall.

Note that this boundary depends not only on the power-law exponent $\tau = 1 + \frac{1}{\gamma}$ of the degree distribution, but also on the parameter δ, which is a geometric quantity controlling the presence of long edges between vertices with typical marks as described in Section 1.2.2. We will see that this behaviour holds not only for the two main examples but for the whole class of geometric random graphs satisfying Assumptions UBA* and Assumptions LBA and even further examples. In particular ultrasmallness does not occur in these models when the variance of the degree distribution becomes infinite, but at a threshold that depends on spatial correlations influencing the graph topology beyond the degree distribution, which is a new feature not seen in other well-studied models such as scale-free percolation and hyperbolic random graph models. As a consequence, the results cover many random graph models whose variance of the degree distribution is infinite but where the graphs are not ultrasmall. An extreme example is the age-dependent random connection model, when the function φ is an indicator function on the interval $[0,1]$. Our results show that this model is never ultrasmall for any power-law exponent $\tau > 2$, a behaviour remarkably different from models such as hyperbolic random graph models.

In the ultrasmall phase of the soft Boolean model and the age-dependent random connection model, as well as all models satisfying Assumptions UBA* and Assumptions LBA we also get a new form of the limit theorem for the chemical distance, namely

$$\frac{\mathrm{d}(\mathbf{x},\mathbf{y})}{\log\log(|x-y|)} \to \frac{4}{\log\left(\frac{\gamma}{\delta(1-\gamma)}\right)} \text{ with high probability as } |x-y| \to \infty, \quad (2.4)$$

as stated in Theorem 1.1. Here, the dependence of the limiting constant on δ is another novel feature. Note that consequently the chemical distance in the ultrasmall phase is larger than in non-spatial preferential attachment models discussed in the beginning of this section, even when the power-law exponent is kept the same. This effect vanishes if we allow very long edges in the models, i.e. δ is near to one. In this case the behaviour once again is approximately the same as for non-spatial preferential attachment models.

2.2 Framework and main result

2.2.1 Framework

As described in Section 1.2.2, we consider a geometric random graph $\mathscr{G}$ with vertex set given by the points of a Poisson point process $\mathcal{X}$ of unit intensity on $\mathbb{R}^d \times (0,1)$. Recall, that we write the vertices of $\mathscr{G}$ as $\mathbf{x} = (x,t)$ and refer to x as the location and t as the mark of the vertex $\mathbf{x}$ and note that small marks indicate powerful vertices, i.e. vertices with large neighbourhoods.

Recall that we write $\mathbf{x} \sim \mathbf{y}$ if the vertices $\mathbf{x}$, $\mathbf{y}$ are connected by an edge in $\mathscr{G}$ and by $\mathbb{P}_{\mathbf{x_1},\dots,\mathbf{x_n}}$ the law of $\mathscr{G}$ conditioned on the event that $\mathbf{x_1},\dots,\mathbf{x_n}$ are points of the Poisson point process $\mathcal{X}$. By $\mathbb{P}_{\mathcal{X}}$ we denote the law of $\mathscr{G}$ conditioned on the Poisson point process $\mathcal{X}$.

We now state the assumptions in their full generality. The first leads to *lower bounds* on chemical distances in the graph. As in Section 1.2.2 the assumption depends on the parameters $\delta > 1$ and $0 \le \gamma < 1$.

Assumption UBA

There exists $\kappa > 0$ such that, for every finite set of pairs of vertices $I \subset \mathcal{X}^2$ in which each vertex appears at most twice, we have

$$\mathbb{P}_{\mathcal{X}}\Big(\bigcap_{(\mathbf{x}_i,\mathbf{y}_i)\in I} \{\mathbf{x}_i \sim \mathbf{y}_i\}\Big) \le \prod_{(\mathbf{x}_i,\mathbf{y}_i)\in I} \kappa\,(t_i \wedge s_i)^{-\delta\gamma}(t_i \vee s_i)^{\delta(\gamma-1)}\,|x_i - y_i|^{-\delta d}$$

where $\mathbf{x}_i = (x_i,t_i)$, $\mathbf{y}_i = (y_i,s_i)$.

This assumption is a relaxed version of the upper bound assumption UBA*. In Chapter 4 we shall see several natural examples of geometric random graphs which satisfy Assumption UBA and in Section 4.6 and 4.5 natural examples which satisfy this assumption but not Assumption UBA*. Note that unlike Assumption UBA* this assumption does not include conditional independence of the events $\{\mathbf{x}_i \sim \mathbf{y}_i\}$, which makes several classical tools, such as the BK-inequality, unavailable in our proofs. Without the conditional independence one cannot give a precise description for the degree distribution, as done in Section 1.2.2. However, it is worth noting that Assumption UBA still implies the existence of a constant $C > 0$ for which the *expected* degree of a vertex with mark t is smaller than $Ct^{-\gamma}$. The next assumption agrees with Assumption LBA and is used to give matching *upper bounds* on chemical distances in the ultrasmall regime. Unlike Assumption UBA, it does contain a conditional independence assumption.

Assumption LBA

Given $\mathcal{X}$, edges are drawn independently of each other and there exists $\alpha, \kappa > 0$ such that, for every pair of vertices $\mathbf{x} = (x, t), \mathbf{y} = (y, s) \in \mathcal{X}$,

$$\mathbb{P}_{\mathbf{x},\mathbf{y}}\{\mathbf{x} \sim \mathbf{y}\} \geq \alpha \left(1 \wedge \kappa \left(t \wedge s\right)^{-\delta\gamma} |x - y|^{-\delta d}\right).$$

As we will see in Section 4.7 many but not all of our examples of geometric random graphs are incorporated in a general framework of geometric random graphs, the weight dependent random connection model introduced in [57, 58]. In that context our assumptions can be interpreted to say that the random graphs are stochastically dominated by the weight random connection model with preferential attachment kernel (Assumption UBA) and they themselves dominate the random connection model with min kernel (Assumption LBA). As discussed in Section 1.2.2, these models have a scale-free degree distribution with power-law exponent $\tau = 1 + \frac{1}{\gamma}$. Hence, as previously mentioned these examples deviate from the behaviour of non-spatial models and scale-free percolation in that the emergence of ultrasmallness does not depend only on the power-law exponent.

2.2.2 Statement of the main results

Recall, that we write $\mathbf{x} \overset{n}{\leftrightarrow} \mathbf{y}$ if there exists a path of length n from $\mathbf{x}$ to $\mathbf{y}$ in $\mathscr{G}$ and we denote by $\mathbf{x} \leftrightarrow \mathbf{y}$ if $\mathbf{x} \overset{n}{\leftrightarrow} \mathbf{y}$ holds for some n, i.e. if $\mathbf{x}$ and $\mathbf{y}$ are in the same connected component in $\mathscr{G}$. The graph distance, or chemical distance, is given by

$$\mathrm{d}(\mathbf{x}, \mathbf{y}) = \min\{n \in \mathbb{N} \colon \mathbf{x} \overset{n}{\leftrightarrow} \mathbf{y}\}.$$

Our main results in this chapter identify the regime where $\mathscr{G}$ is ultrasmall, i.e. where the graph distance behaves like an iterated logarithm of the Euclidean distance. Moreover in this regime we provide a precise limit theorem for the behaviour of the graph distance of remote vertices. The first and foremost result in this context are lower bounds for the chemical distance of two points at large Euclidean distance using only Assumption UBA.

Theorem 2.1

Let $\mathscr{G}$ be a general geometric random graph which satisfies Assumption UBA for some $\gamma \in [0, 1)$ and $\delta > 1$.

(a) If $\gamma < \frac{\delta}{\delta+1}$, then $\mathscr{G}$ is **not ultrasmall**, i.e. for $\mathbf{x}, \mathbf{y} \in \mathbb{R}^d \times (0, 1)$, under $\mathbb{P}_{\mathbf{x},\mathbf{y}}$, the distance $\mathrm{d}(\mathbf{x}, \mathbf{y})$ is of larger order than $\log\log|x - y|$ with high probability as $|x - y| \to \infty$.

(b) If $\gamma > \frac{\delta}{\delta+1}$, then for $\mathbf{x}, \mathbf{y} \in \mathbb{R}^d \times (0, 1)$ we have

$$\mathrm{d}(\mathbf{x}, \mathbf{y}) \geq (4 + o(1)) \frac{\log\log|x - y|}{\log\left(\frac{\gamma}{\delta(1-\gamma)}\right)}$$

under $\mathbb{P}_{\mathbf{x},\mathbf{y}}$ with high probability as $|x - y| \to \infty$.

The second result provides a matching upper bound for the chemical distance in the ultrasmall regime under Assumption LBA. Putting both results together we get the following limit theorem for the chemical distance under Assumptions UBA and LBA in the ultrasmall regime.

Theorem 2.2

Let $\mathscr{G}$ be a general geometric random graph which satisfies Assumption UBA and Assumption LBA for some $\gamma > \frac{\delta}{\delta+1}$. Then $\mathscr{G}$ is **ultrasmall** and, for $\mathbf{x}, \mathbf{y} \in \mathbb{R}^d \times (0,1)$, we have

$$\mathrm{d}(\mathbf{x}, \mathbf{y}) = (4 + o(1)) \frac{\log\log|x-y|}{\log\left(\frac{\gamma}{\delta(1-\gamma)}\right)} \tag{2.5}$$

under $\mathbb{P}_{\mathbf{x},\mathbf{y}}(\ \cdot\ \mid \mathbf{x} \leftrightarrow \mathbf{y})$ with high probability as $|x-y| \to \infty$.

Remark 2.2.1.

- An explicit lower bound on $\mathrm{d}(\mathbf{x}, \mathbf{y})$ under Assumption UBA when $\mathscr{G}$ is not ultrasmall is formulated in Proposition 2.10. Likewise the upper bound on $\mathrm{d}(\mathbf{x}, \mathbf{y})$ in the ultrasmall phase under Assumption LBA which matches the lower bound in Theorem 2.1(b) is formulated in Proposition 2.13.
- For the convergence in Theorem 2.2 we fix marks $s, t \in (0,1)$ and add points $\mathbf{x} = (x, s)$ and $\mathbf{y} = (y, t)$ to the Poisson process. Then we show that

  $$\mathbb{P}_{\mathbf{x},\mathbf{y}}\Big(\Big|\frac{\mathrm{d}(\mathbf{x}, \mathbf{y})}{\log\log|x-y|} - \frac{4}{\log\left(\frac{\gamma}{\delta(1-\gamma)}\right)}\Big| > \epsilon \,\Big|\, \mathbf{x} \leftrightarrow \mathbf{y}\Big)$$

  converges to zero if $|x-y| \to \infty$, as a consequence of Theorem 2.1 and Proposition 2.13.
- The results continue to hold *mutatis mutandis* when the underlying Poisson process is replaced by the points of the (percolated) lattice $\mathbb{Z}^d$ endowed with independent uniformly distributed marks.
- In Section 2.3.1 we show lower bounds on $\mathrm{d}(\mathbf{x}, \mathbf{y})$ under alternative assumptions which arise from other natural examples such as *scale-free percolation* and the *ultra-small scale-free geometric networks*. It turns out that in geometric random graphs under these assumptions $\mathrm{d}(\mathbf{x}, \mathbf{y})$ is much more tractable, as there is no significant influence of the spatial distance on the chemical distance.

2.3 Proof of the lower bounds for the chemical distance

2.3.1 The truncated first moment method

To prove the lower bounds of Theorem 2.1 we find an upper bound for the probability $\mathbb{P}_{\mathbf{x},\mathbf{y}}\{\mathrm{d}(\mathbf{x},\mathbf{y}) \le 2\Delta\}$ and choose Δ as large as possible while keeping the probability sufficiently small. Note that the definition of the graph distance can be reduced to the existence of *self-avoiding paths*, i.e. paths in which each vertex appears at most once, since if there exists a path of length n between two given vertices there also exists a self-avoiding paths with shorter or equal length between those two. Hence, the paths considered throughout this section are assumed to be self-avoiding. The event $\{\mathrm{d}(\mathbf{x},\mathbf{y}) \le 2\Delta\}$ is equivalent to the existence of at least one path between $\mathbf{x}$ and $\mathbf{y}$ of length smaller than 2Δ. Hence,

$$\begin{aligned}\mathbb{P}_{\mathbf{x},\mathbf{y}}\{\mathrm{d}(\mathbf{x},\mathbf{y}) \le 2\Delta\} &= \mathbb{P}_{\mathbf{x},\mathbf{y}}\Bigg(\bigcup_{n=1}^{2\Delta}\ \bigcup_{\mathbf{x}_1,\dots,\mathbf{x}_{n-1}\in\mathscr{G}}^{\neq} \{\mathbf{x}_0 \sim \mathbf{x}_1 \sim \ldots \sim \mathbf{x}_{n-1} \sim \mathbf{x}_n\}\Bigg)\\ &\le \sum_{n=1}^{2\Delta} \mathbf{E}\Bigg[\sum_{\mathbf{x}_1,\dots,\mathbf{x}_{n-1}\in\mathscr{G}}^{\neq} \mathbb{P}_{\mathcal{X}\cup\{\mathbf{x},\mathbf{y}\}}\{\mathbf{x}_0 \sim \mathbf{x}_1 \sim \ldots \sim \mathbf{x}_{n-1} \sim \mathbf{x}_n\}\Bigg],\end{aligned}$$

where $\mathbf{x} = \mathbf{x}_0$, $\mathbf{y} = \mathbf{x}_n$, $\bigcup^{\neq}$ (resp. $\sum^{\neq}$) denotes the union (resp. sum) over all possible sets of pairwise distinct vertices $\mathbf{x}_0,\dots,\mathbf{x}_n$ of the Poisson process and $\mathbf{E}$ is the expectation with respect to the law of a Poisson process with unit intensity on $\mathbb{R}^d \times (0,1)$. To keep notation throughout this chapter short we will abbreviate the previous notation and write $\sum_{\mathbf{x}_1,\dots,\mathbf{x}_m}$ for the sum over all sets of m distinct vertices of the Poisson process. We get, by using Mecke's equation [76] and Assumption UBA that

$$\begin{aligned}&\mathbb{P}_{\mathbf{x},\mathbf{y}}\{\mathrm{d}(\mathbf{x},\mathbf{y}) \le 2\Delta\}\\ &\le \sum_{n=1}^{2\Delta} \int_{(\mathbb{R}^d\times(0,1))^{n-1}} \bigotimes_{i=1}^{n-1} \mathrm{d}\mathbf{x}_i\, \mathbb{E}\left[\mathbb{P}_{\mathcal{X}\cup\{\mathbf{x},\mathbf{x}_1,\dots,\mathbf{x}_{n-1},\mathbf{y}\}}\{\mathbf{x}_0 \sim \mathbf{x}_1 \sim \ldots \sim \mathbf{x}_{n-1} \sim \mathbf{x}_n\}\right]\\ &\le \sum_{n=1}^{2\Delta} \int_{(\mathbb{R}^d\times(0,1))^{n-1}} \bigotimes_{i=1}^{n-1} \mathrm{d}(x_i,t_i) \prod_{j=0}^{n-1} 1 \wedge \kappa(t_j \wedge t_{j+1})^{-\gamma\delta} (t_j \vee t_{j+1})^{\delta(\gamma-1)} \left|x_j - x_{j+1}\right|^{-\delta d}.\end{aligned}$$

This bound is only good enough if $\gamma < \frac{1}{2}$. If $\gamma \geq \frac{1}{2}$ the expectation on the right is dominated by paths which are typically not present in the graph. These are paths which connect $\mathbf{x}$ or $\mathbf{y}$ quickly to vertices with small mark t. Our strategy is therefore to truncate the admissible mark of the vertices of a possible path between $\mathbf{x}$ and $\mathbf{y}$. We define a decreasing sequence $(\ell_k)_{k\in\mathbb{N}_0}$ of thresholds and call a tuple of vertices $(\mathbf{x}_0, \dots, \mathbf{x}_n)$ *good* if their marks satisfy $t_k \wedge t_{n-k} \geq \ell_k$ for all $k \in \{0, \dots, n\}$. A path consisting of a good tuple of vertices is called a good path. We denote by $A_k^{(\mathbf{x})}$ the event that there exists a path starting in $\mathbf{x}$ which fails this condition after exactly k steps, i.e. a path $((x,t),(x_1,t_1),\dots(x_k,t_k))$ with $t \geq \ell_0, t_1 \geq \ell_1, \dots, t_{k-1} \geq \ell_{k-1}$, but $t_k < \ell_k$. Furthermore we denote by $B_n^{(\mathbf{x},\mathbf{y})}$ the event that there exists a good path of length n between $\mathbf{x}$ and $\mathbf{y}$. Then, for given vertices $\mathbf{x}$ and $\mathbf{y}$

$$\mathbb{P}_{\mathbf{x},\mathbf{y}}\{\mathrm{d}(\mathbf{x},\mathbf{y}) \leq 2\Delta\} \leq \sum_{n=1}^{\Delta} \mathbb{P}_{\mathbf{x}}(A_n^{(\mathbf{x})}) + \sum_{n=1}^{\Delta} \mathbb{P}_{\mathbf{y}}(A_n^{(\mathbf{y})}) + \sum_{n=1}^{2\Delta} \mathbb{P}_{\mathbf{x},\mathbf{y}}(B_n^{(\mathbf{x},\mathbf{y})}). \quad \text{(TMB)}$$

This decomposition is similar to the one for the mean-field models in [35]. The main aspect of the proof is to properly capture the influence of the geometry. It will turn out that the spatial correlations emerging in the discussed geometric random graphs which satisfy Assumptions UBA make it significant more difficult for a path to connect to a vertex with very small mark. Hence a slower decaying threshold sequence $(\ell_k)_{k\in\mathbb{N}_0}$ can be chosen such that the two first sums on the right of (TMB) are still small. Consequently, the third sum can be kept small for a larger choice of Δ. This requires a much deeper analysis of the graph and its spatial embedding.

In Section A.1 we give two examples for a direct application of (TMB) to geometric random graphs satisfying different assumptions to Assumption UBA such that they are much easier to handle. For these examples we state criteria when they are not ultrasmall and otherwise give asymptotic lower bounds on the chemical distance. The proofs of this results rely on simpler variants of arguments which are used in the following proofs of the main results.

2.3.2 Outline of the proof

The characteristic feature of the shortest path connecting two typical vertices is that, starting from both ends, the path contains a subsequence of increasingly powerful vertices. The two parts started at the ends meet roughly in the middle in a vertex of exceptionally high power depending on the distance between the starting vertices. In our framework powerful vertices are characterised by small marks. For geometric random graphs fulfilling Assumption UBA we show that arbitrary strategies connecting increasingly powerful vertices are dominated by an *optimal strategy* by which paths make connections between vertices of increasingly high power in a way depending on the parameters γ and δ in our assumption:

- If $\gamma > \frac{\delta}{\delta+1}$ we connect two powerful vertices $\mathbf{x}$ and $\mathbf{y}$ via a *connector*, a single vertex with a larger mark which is connected to both $\mathbf{x}$ and $\mathbf{y}$;
- if $\gamma < \frac{\delta}{\delta+1}$ we connect them by a single edge.

In both cases, we now sketch how our argument works on paths containing only the optimal type of connection between powerful vertices. The principal challenge of the proof will however be to show how these proposed optimal strategies dominate the entirety of other possible strategies. This is particularly hard in the former case, because a vast number of potential strategies leads to a massive entropic effect that needs to be controlled. Note also that at this point we need not show that the proposed optimal strategies actually work. This (easier) part of the proof requires Assumption LBA and is carried out in Section 2.4.

In the case $\gamma > \frac{\delta}{\delta+1}$ the optimal connection strategy is to follow a path of length $2n$ between $\mathbf{x}$ and $\mathbf{y}$, where we assume that n is even and that the vertices $\mathbf{x}_1 = (x_1, t_1), \dots, \mathbf{x}_{2n-1} = (x_{2n-1}, t_{2n-1})$ of the path satisfy $t_{2(k+1)} < t_{2k} < t_{2k+1}$ and $t_{2n-2(k+1)} < t_{2n-2k} < t_{2n-2k+1}$ for all $k = 0, \dots, n/2$, i.e. the vertices with even index can be seen as powerful vertices, while the ones with odd index represent the connectors between them, see Figure 2.1. Note that at this point we make no assumptions on the locations of these vertices.

For arbitrary $\varepsilon > 0$, we now determine a truncation sequence $(\ell_k)_{k\in\mathbb{N}_0}$, such that paths starting in $\mathbf{x}$, resp. $\mathbf{y}$, which are not good, only exist with a probability smaller than ε. To do so, we establish an upper bound for the probability of the

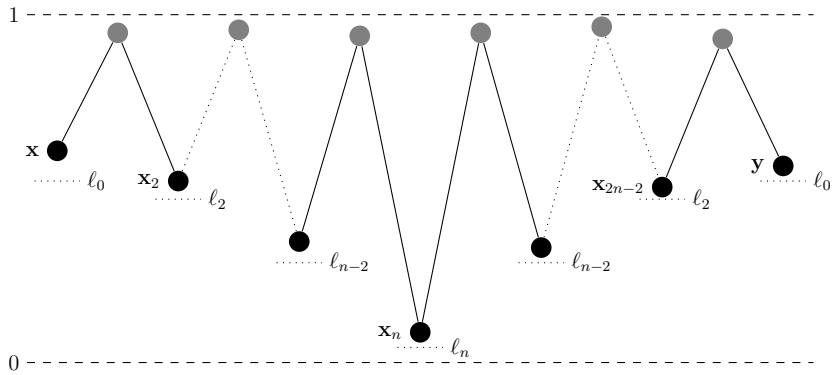

Figure 2.1: An example of a path with optimal connection type for $\gamma > \frac{\delta}{\delta+1}$. The horizontal axis corresponds to the sequential numbering of vertices on the path, the vertical axis represents the mark space. Powerful vertices (indicated by black dots) alternate with connectors (indicated by grey dots).

event $A_n^{(\mathbf{x})}$ that there exists a path starting in $\mathbf{x}$ whose n-th vertex is the first vertex which has a mark smaller than the corresponding ℓ_n. We denote by $N(\mathbf{x}, \mathbf{y}, n)$ the number of paths of length n from $\mathbf{x} = (x, t)$ to a vertex $\mathbf{y} = (y, s)$ whose vertices $(x_1, t_1), \dots (x_{n-1}, t_{n-1})$ fulfill $t_{2(k+1)} < t_{2k} < t_{2k+1}$ for all $k = 0, \dots, \lfloor n/2 \rfloor - 1$ and which is one half of a good path, i.e. $t \geq \ell_0, t_1 \geq \ell_1, \dots, t_{n-1} \geq \ell_{n-1}$. The mark of $\mathbf{y}$ is not restricted in this definition and is therefore allowed to be smaller than ℓ_n. Hence, in this case the event $A_n^{(\mathbf{x})}$ can only occur for n even, since by definition a connector is less powerful than the preceding and following vertex and therefore has a mark larger than the corresponding ℓ_n. For n even we have by Mecke's equation that

$$\mathbb{P}_{\mathbf{x}}(A_n^{(\mathbf{x})}) \leq \int\limits_{\mathbb{R}^d \times (0, \ell_n]} \mathrm{d}\mathbf{y}\, \mathbb{E}_{\mathbf{x},\mathbf{y}} N(\mathbf{x}, \mathbf{y}, n).$$

Since the existence of a path counted in $N(\mathbf{x}, \mathbf{y}, n)$ is equivalent to the existence of vertices $\mathbf{z}_1, \dots, \mathbf{z}_{n/2-1}$ such that the marks are bounded from below by $\ell_2, \ell_4, \dots, \ell_{n-2}$, with $\mathbf{z}_0 = \mathbf{x}, \mathbf{z}_{n/2} = \mathbf{y}$ the marks $u_0, \dots, u_{n/2}$ of $\mathbf{z}_0, \dots, \mathbf{z}_{n/2}$ are decreasing, and $\mathbf{z}_i, \mathbf{z}_{i+1}$ are connected via a single connector, Mecke's equation

yields

$$\mathbb{E}_{\mathbf{x},\mathbf{y}} N(\mathbf{x},\mathbf{y},n) \leq \int\limits_{\mathbb{R}^d\times(\ell_2,u_0]} \mathrm{d}\mathbf{z}_1 \cdots \int\limits_{\mathbb{R}^d\times(\ell_{n-2},u_{n/2-2}]} \mathrm{d}\mathbf{z}_{n/2-1} \mathbb{E}_{\mathbf{z}_0,\ldots,\mathbf{z}_{n/2}} \Bigg[\prod_{i=1}^{n/2} K(\mathbf{z}_i,\mathbf{z}_{i-1},2) \Bigg], \tag{2.6}$$

where $K(\mathbf{z}_i,\mathbf{z}_{i+1},2)$ is the number of connectors between $\mathbf{z}_i$ and $\mathbf{z}_{i+1}$. Using Mecke's equation and Assumption UBA we have

$$\mathbb{E}_{\mathbf{z}_0,\ldots,\mathbf{z}_{n/2}} \Bigg[\prod_{i=1}^{n/2} K(\mathbf{z}_i,\mathbf{z}_{i-1},2) \Bigg] \leq \prod_{i=1}^{n/2} e_K(\mathbf{z}_i,\mathbf{z}_{i-1},2),$$

where

$$e_K(\mathbf{z}_i,\mathbf{z}_{i-1},2) = \int\limits_{\mathbb{R}^d\times(u_{i-1}\vee u_i,1)} \mathrm{d}\mathbf{z}\, \rho(\kappa^{-1/\delta} u_{i-1}^{\gamma} u^{1-\gamma} |z_{i-1}-z|^d) \rho(\kappa^{-1/\delta} u_i^{\gamma} u^{1-\gamma} |z_i - z|^d),$$

for $\rho(x) := 1 \wedge x^{-\delta}$ and $\mathbf{z}_i = (z_i,u_i)$, $\mathbf{z}_{i-1} = (z_{i-1},u_{i-1})$. We see in Lemma 2.3 that there exists $C>0$ such that, for two given vertices $\mathbf{x}=(x,t)$ and $\mathbf{y}=(y,s)$ far enough from each other,

$$e_K(\mathbf{x},\mathbf{y},2) \leq C\rho\big(\kappa^{-1/\delta}(t\wedge s)^{\gamma}(t\vee s)^{\gamma/\delta} |x-y|^d\big). \tag{2.7}$$

This inequality holds for the optimal connection type between two powerful vertices of the path and we will see that this type of bound holds also for the case of multiple connectors between two powerful vertices (cf. Lemma 2.5). It also clearly displays the influence of the spatial embedding of the random geometric graph via the parameter δ. Assuming (2.7) for the moment, we obtain

$$\mathbb{P}_{\mathbf{x}}(A_n^{(\mathbf{x})}) \leq$$
$$\int\limits_{\mathbb{R}^d\times(\ell_2,u_0]} \mathrm{d}\mathbf{z}_1 \cdots \int\limits_{\mathbb{R}^d\times(\ell_{n-2},u_0]} \mathrm{d}\mathbf{z}_{n/2-1} \int\limits_{\mathbb{R}^d\times(0,\ell_n]} \mathrm{d}\mathbf{z}_{n/2} \prod_{i=1}^{n/2} C\rho\big(\kappa^{-1/\delta} u_i^{\gamma} u_{i-1}^{\gamma/\delta} |z_i - z_{i-1}|^d\big), \tag{2.8}$$

where $\mathbf{z}_i = (z_i,u_i)$ for $i=0,\ldots n/2$ and where we without loss of generality integrate up to u_0 in all but the last integral. When dealing with a general (rather than the optimal) connection strategy, we will use a classification of the strategies

in terms of binary trees. Left-to-right exploration of the tree will reveal the structure of the decomposition that replaces the straightforward decomposition in (2.6) and additional information on the location of the vertices will be encoded in terms of colouring of the leaves. Figure 2.2 displays the classifying binary tree for the optimal connection type.

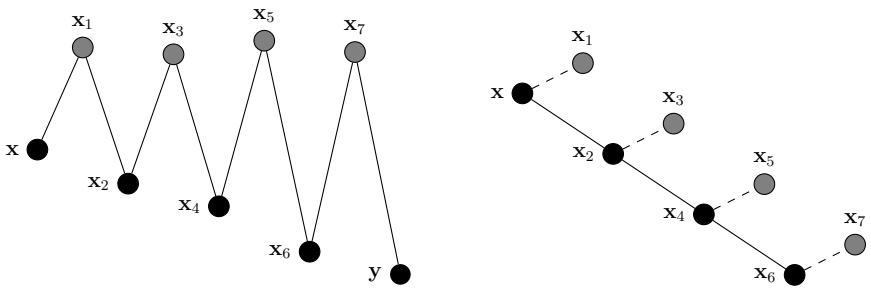

Figure 2.2: Representation of a path with optimal structure by a binary tree. For a less trivial example resulting from a general connection strategy, see Figure 2.5.

For a sufficiently large constant $c > 0$ the right-hand side of (2.8) can be bounded by

$$c^{n/2}\ell_n^{1-\gamma}\ell_0^{-\gamma/\delta}\prod_{i=1}^{n/2-1}\ell_{2i}^{1-\gamma-\gamma/\delta}$$

as shown in Lemma 2.7 considering all paths. With ℓ_0 smaller than the mark of $\mathbf{x}$ we choose the truncation sequence $(\ell_k)_{k\in\mathbb{N}_0}$ for $\varepsilon > 0$, such that

$$c^{n/2}\ell_n^{1-\gamma}\ell_0^{-\gamma/\delta}\prod_{i=1}^{n/2-1}\ell_{2i}^{1-\gamma-\gamma/\delta} = \frac{\varepsilon}{\pi^2 n^2}, \tag{2.9}$$

and we have

$$\sum_{n=1}^{\Delta}\mathbb{P}_{\mathbf{x}}(A_n^{(\mathbf{x})}) = \sum_{\substack{n=1\\ n\ even}}^{\Delta}\mathbb{P}_{\mathbf{x}}(A_n^{(\mathbf{x})}) \le \sum_{\substack{n=1\\ n\ even}}^{\Delta} c^{n/2}\ell_n^{1-\gamma}\ell_0^{-\gamma/\delta}\prod_{i=1}^{n/2-1}\ell_{2i}^{1-\gamma-\gamma/\delta} \le \sum_{n=1}^{\infty}\frac{\varepsilon}{\pi^2 n^2} = \frac{\varepsilon}{6}.$$

Writing $\eta_n := \ell_n^{-1}$ we can deduce from (2.9) a recursive description of $(\ell_n)_{n\in\mathbb{N}_0}$ such that

$$\eta_{n+2}^{1-\gamma} = \frac{(n+2)^2}{n^2}c\eta_n^{\gamma/\delta}.$$

Consequently there exist $b, B > 0$ such that $\eta_n \le b\exp(B(\gamma/(\delta(1-\gamma)))^{n/2})$. We

close the argument with heuristics that lead from this truncation sequence to a lower bound for the chemical distance. Let $\mathbf{x}$ and $\mathbf{y}$ be two given vertices. If there exists a path of length $n < \log|x-y|$ between them, there must exist at least one edge in this path which is longer than $\frac{|x-y|}{\log|x-y|}$. For $|x-y|$ large, this edge typically must have an endvertex whose mark is, up to a multiplicative constant, smaller than $|x-y|^{-d}$. Hence, if we choose

$$\Delta < (2+o(1))\frac{\log\log|x-y|}{\log\left(\frac{\gamma}{\delta(1-\gamma)}\right)}$$

we ensure ℓ_Δ is of larger order than $|x-y|^{-d}$. Therefore there is no good path whose vertices are powerful enough to be an endvertex of an edge longer than $\frac{|x-y|}{\log|x-y|}$ and consequently no good path of length shorter than 2Δ can exist between $\mathbf{x}$ and $\mathbf{y}$.

Turning to the case $\gamma < \frac{\delta}{\delta+1}$, we consider paths whose powerful vertices are connected directly to each other. For a path of length n between two given vertices $\mathbf{x}$ and $\mathbf{y}$ we assume that n is even and for the vertices $\mathbf{x}_1 = (x_1, t_1), \ldots, \mathbf{x}_{n-1} = (x_{n-1}, t_{n-1})$ of the path we assume that we have $t_0 > t_1 > \ldots > t_{n/2}$ and $t_n > t_{n-1} > \ldots > t_{n/2}$, where t_0 is the mark of $\mathbf{x}$ and t_n the mark of $\mathbf{y}$. We again make no restrictions on the locations of those vertices. Restricting the paths described in $A_n^{(\mathbf{x})}$ and $B_n^{(\mathbf{x},\mathbf{y})}$ to paths with this structure we follow the same argumentation as above to establish sufficiently small bounds for the event $A_n^{(x)}$ for a given vertex $\mathbf{x} = (x_0, t_0)$,

$$\mathbb{P}_{\mathbf{x}}(A_n^{(\mathbf{x})}) \leq \int\limits_{\mathbb{R}^d\times(\ell_1,t_0]} \mathrm{d}\mathbf{x}_1 \cdots \int\limits_{\mathbb{R}^d\times(\ell_{n-1},t_0]} \mathrm{d}\mathbf{x}_{n-1} \int\limits_{\mathbb{R}^d\times(0,\ell_n]} \mathrm{d}\mathbf{x}_n \prod_{i=1}^{n} C\rho\big(\kappa^{-1/\delta} t_i^{\gamma} t_{i-1}^{1-\gamma} |x_i - x_{i-1}|^d\big),$$

where we again without loss of generality integrate over a larger range. For $c > 0$ large enough, the right-hand side can be further bounded by

$$c^n \ell_n^{1-\gamma} \ell_0^{\gamma-1} \prod_{i=1}^{n-1} \log\left(\frac{1}{\ell_i}\right),$$

see Lemma 2.12. Choosing $\ell_0 < t_0$ and $(\ell_n)_{n\in\mathbb{N}_0}$ for $\epsilon > 0$, such that the last displayed term equals $\frac{\varepsilon}{\pi^2 n^2}$ ensures that $\sum_n \mathbb{P}_{\mathbf{x}}(A_n^{\mathbf{x}}) < \frac{\varepsilon}{6}$ and by induction we see that this choice is possible while for any $p > 1$ there exists $B > 0$ such that

$\eta_n \leq B^{n \log^p(n+1)}$. Following the same heuristics as before leads to the choice

$$\Delta \leq \frac{c \log |x-y|}{(\log \log |x-y|)^p}$$

for some constant $c > 0$ such that paths between $\mathbf{x}$ and $\mathbf{y}$ with length shorter than 2Δ do not exist with high probability.

2.3.3 The ultrasmall regime

We now start the full proof in the case $\gamma > \frac{\delta}{\delta+1}$ considering all possible connection strategies. We prepare this by first modifying the graph by adding edges between vertices which are sufficiently close to each other. We call a path *step minimizing* if it connects any pair of vertices on the path by a direct edge, if it is available. Note that the length of any path connecting two fixed vertices can be bounded from below by the length of a step mimimizing path connecting the two vertices. Two spatial constraints emerge from this: On the one hand, vertices on a step minimizing path in the modified graph that are not neighbours on the path cannot be near to each other. On the other hand, vertices connected by one of the added edges have to be near to each other. To make full use of these constraints we need to distinguish between original edges and edges added to the graph. This can be done efficiently by endowing every edge with a *conductance*, which is one for original and two for added edges.

More precisely, we consider a graph $\tilde{\mathscr{G}}$ where edges are endowed with conductances as follows: First, create a copy of $\mathscr{G}$ and assign to every edge conductance one. Then, between two vertices $\mathbf{x} = (x,t)$ and $\mathbf{y} = (y,s)$ of $\tilde{\mathscr{G}}$ an edge is added to $\tilde{\mathscr{G}}$ with conductance two whenever

$$|x-y|^d \leq \kappa^{1/\delta} (t \wedge s)^{-\gamma} (t \vee s)^{-\gamma/\delta}.$$

Since all conductances and edges of $\tilde{\mathscr{G}}$ are deterministic functionals of $\mathscr{G}$, there exists an almost sure correspondence between $\mathscr{G}$ and $\tilde{\mathscr{G}}$, under which an edge with conductance one in $\tilde{\mathscr{G}}$ implies the existence of the same edge in $\mathscr{G}$. With conductances assigned to every edge of $\tilde{\mathscr{G}}$, we define the conductance of a path $P = (\mathbf{x}_0, \ldots, \mathbf{x}_n)$ in $\tilde{\mathscr{G}}$ as the sum over all conductances of the edges of P and denote it by w_P.

We call a self-avoiding path $P = (\mathbf{x}_0, \dots, \mathbf{x}_n)$ in $\mathscr{G}$ or $\tilde{\mathscr{G}}$ *step minimizing*

$$\text{if there exists no edge between } \mathbf{x}_i \text{ and } \mathbf{x}_j \text{ for all } i, j \text{ with } |i-j| \geq 2. \quad (2.10)$$

Note that a step minimizing path in $\mathscr{G}$ is not necessarily step minimizing in $\tilde{\mathscr{G}}$, since there could exist an edge of conductance two between two vertices of the path that would reduce the number of steps. But by removing the vertices connecting such a pair of vertices from the path we can shorten the path to a step minimizing path in $\tilde{\mathscr{G}}$ whose length and conductance is no more than the length of the original path. Hence the chemical distance $\mathrm{d}(\mathbf{x}, \mathbf{y})$ between vertices $\mathbf{x}$ and $\mathbf{y}$ in $\mathscr{G}$ is larger or equal than the conductance $\mathrm{d}_w(\mathbf{x}, \mathbf{y}) := \min\{w_P : P \text{ is a path between } \mathbf{x} \text{ and } \mathbf{y}\}$ between them in $\tilde{\mathscr{G}}$.

To bound the probabilities occurring in (TMB), we express the events on $\mathscr{G}$ with the help of corresponding events on $\tilde{\mathscr{G}}$ by replacing the role of the length of a path by its conductance. The role of the conductance is crucial, as it allows us to distuingish newly added edges in a path, which is necessary to keep the bounds of the probabilities in (TMB) sufficiently small. We call a path $P = (\mathbf{x}_0, \dots, \mathbf{x}_n)$ in $\tilde{\mathscr{G}}$ *good* if its marks satisfy $t_k \geq \ell_{w_P(k)}$ and $t_{n-k} \geq \ell_{w_P - w_P(n-k)}$ for all $k = 0, \dots, n$, where $w_P(k)$ is the conductance of P between $\mathbf{x}_0$ and $\mathbf{x}_k$. We denote by $\tilde{A}_k^{\mathbf{x}}$ the event that there exists a step minimizing path starting in $\mathbf{x}$ in $\tilde{\mathscr{G}}$ with conductance k which fails to be good on its last vertex. Notice that if there exists a path described by the event $A_k^{\mathbf{x}}$, i.e. a path for which the k-th vertex is the first one whose mark is smaller than the corresponding truncation value ℓ_k, then due to the correspondence between $\mathscr{G}$ and $\tilde{\mathscr{G}}$ there also exists a step minimizing path P in $\tilde{\mathscr{G}}$ with $w_P \leq k$ which also fails the condition on its last vertex. Hence, the first two summands of the right-hand side of (TMB) can be bounded from above by $\sum_{n=1}^{\Delta} \mathbb{P}_{\mathbf{x}}(\tilde{A}_n^{(\mathbf{x})})$ and $\sum_{n=1}^{\Delta} \mathbb{P}_{\mathbf{y}}(\tilde{A}_n^{(\mathbf{y})})$.

To bound $\mathbb{P}_{\mathbf{x}}(\tilde{A}_n^{(\mathbf{x})})$, we count the expected number of paths occurring in the event $\tilde{A}_n^{(\mathbf{x})}$. Note that if $|x-y|^d \leq \kappa^{1/\delta}(t \wedge s)^{-\gamma}(t \vee s)^{-\gamma/\delta}$ holds for vertices $\mathbf{x}$ and $\mathbf{y}$, there exist no step minimizing paths between $\mathbf{x}$ and $\mathbf{y}$ with conductance larger or equal three and there exists one step minimizing path with conductance two, since there exists an edge of conductance two between the two vertices. This property also holds for any of the subclasses of step minimizing paths introduced in the following.

For given vertices $\mathbf{x} = (x, t)$ and $\mathbf{y} = (y, s)$ define the random variable $N(\mathbf{x}, \mathbf{y}, n)$ as the number of distinct step minimizing paths P between $\mathbf{x}$ and $\mathbf{y}$ with $w_P = n$, whose connecting vertices $(x_1, t_1), \dots (x_{m-1}, t_{m-1})$ all have a larger mark than $\mathbf{y}$ and fulfill $t \geq \ell_0, t_1 \geq \ell_{w_P(1)}, \dots, t_{m-1} \geq \ell_{w_P(m-1)}$. As $\tilde{A}_n^{(\mathbf{x})}$ is the event that there exists a path with conductance n, where the final vertex is the first and only one which has a mark smaller than the corresponding ℓ_n, the final vertex is also the most powerful vertex of the path. Hence, the number of paths described by the event $\tilde{A}_n^{(\mathbf{x})}$ can be written as the sum of $N(\mathbf{x}, \mathbf{y}, n)$ over all sufficiently powerful vertices $\mathbf{y}$ of the graph and, by Mecke's formula, we have

$$\mathbb{P}_{\mathbf{x}}(\tilde{A}_n^{(\mathbf{x})}) \leq \int\limits_{\mathbb{R}^d \times (0, \ell_n]} \mathrm{d}\mathbf{y}\, \mathbb{E}_{\mathbf{x},\mathbf{y}} N(\mathbf{x}, \mathbf{y}, n). \tag{2.11}$$

We now decompose $N(\mathbf{x}, \mathbf{y}, n)$. For $k = 1, \dots, n-1$, define $N(\mathbf{x}, \mathbf{y}, n, k)$ as the number of step minimizing paths P between $\mathbf{x}$ and $\mathbf{y}$ with $w_P = n$ and

- whose connecting vertices $(x_1, t_1), \dots (x_{m-1}, t_{m-1})$ have marks larger than the corresponding thresholds $\ell_{w_P(1)}, \dots, \ell_{w_P(m-1)}$ and larger than the mark of $\mathbf{y}$, and
- there exists $r \in \{1, \dots, m-1\}$ such that we have $w_P(r) = n - k$ and the connecting vertex $\mathbf{x}_r = (x_r, t_r)$ has the smallest mark among the connecting vertices and $\mathbf{x}$.

The vertex $\mathbf{x}_r$ can be understood as the powerful vertex of the path which connects to $\mathbf{y}$ via a path of less powerful vertices with conductance k. Consequently, we write $N(\mathbf{x}, \mathbf{y}, n, n)$ for the number of step minimizing paths of conductance n, which connect $\mathbf{x}$ and $\mathbf{y}$ via less powerful vertices. Then we have, for $n \in \mathbb{N}$,

$$N(\mathbf{x}, \mathbf{y}, n) \leq \sum_{k=1}^{n} N(\mathbf{x}, \mathbf{y}, n, k). \tag{2.12}$$

For $k = 1, \dots, n-1$, the existence of a path counted in $N(\mathbf{x}, \mathbf{y}, n, k)$ implies the existence of a vertex $\mathbf{z}$ such that a step minimizing path counted by $N(\mathbf{x}, \mathbf{z}, n-k)$ exists which connects to $\mathbf{y}$ via a path of less powerful vertices with conductance k. Hence

$$N(\mathbf{x}, \mathbf{y}, n, k) \leq \sum_{\substack{\mathbf{z}=(z,u) \\ \ell_{n-k} \vee s < u \leq t}} N(\mathbf{x}, \mathbf{z}, n-k)\, K(\mathbf{z}, \mathbf{y}, k), \tag{2.13}$$

for $n \in \mathbb{N}$ and $k = 1, \dots, n-1$, where we denote by $K(\mathbf{z}, \mathbf{y}, k)$ the number of step minimizing paths P between $\mathbf{z}$ and $\mathbf{y}$ with $w_P = k$ whose vertices have marks larger than the marks of $\mathbf{z}$ and $\mathbf{y}$. Note that unlike $N(\mathbf{x}, \mathbf{y}, n)$, this random variable is symmetric in its first two arguments and by definition we have that $N(\mathbf{x}, \mathbf{y}, n, n) = K(\mathbf{x}, \mathbf{y}, n)$. Observe that $K(\mathbf{z}, \mathbf{y}, 1)$ is the indicator whether $\mathbf{z}$ and $\mathbf{y}$ are connected by an edge with conductance one. We turn our attention to $K(\mathbf{z}, \mathbf{y}, k)$ in the case $k \geq 2$, i.e. two powerful vertices are connected via one or more connectors or an edge with conductance two.

Connecting powerful vertices.

First consider the random variable $K(\mathbf{x}, \mathbf{y}, 2)$. If $|x-y|^d \leq \kappa^{1/\delta}(t \wedge s)^{-\gamma}(t \vee s)^{-\gamma/\delta}$, the vertices $\mathbf{x}$ and $\mathbf{y}$ are connected by an edge with conductance two and we infer that $K(\mathbf{x}, \mathbf{y}, 2) = 1$. In the other case, $K(\mathbf{x}, \mathbf{y}, 2)$ is equal to the number of connectors between $\mathbf{x}$ and $\mathbf{y}$, i.e. the number of vertices with mark larger than the marks of $\mathbf{x}$ and $\mathbf{y}$, which form an edge of conductance one to $\mathbf{x}$ and $\mathbf{y}$. The following lemma shows the stated inequality (2.7) from Section 2.3.2 for this case. Recall that we write $\rho(x) := 1 \wedge x^{-\delta}$ and define $I_\rho := \int_{\mathbb{R}^d} \mathrm{d}x \rho(\kappa^{-1/\delta} |x|^d)$.

Lemma 2.3: Two-connection lemma

Let $\mathbf{x} = (x, t), \mathbf{y} = (y, s) \in \mathbb{R}^d \times (0, 1)$ be two given vertices with $|x-y|^d > \kappa^{1/\delta}(t \wedge s)^{-\gamma}(t \vee s)^{-\gamma/\delta}$. Then

$$\begin{aligned}\mathbb{E}_{\mathbf{x},\mathbf{y}} K(\mathbf{x}, \mathbf{y}, 2) &\leq \int_{\mathbb{R}^d \times (t \vee s, 1]} \mathrm{d}\mathbf{z} \rho\big(\kappa^{-1/\delta} t^\gamma u^{1-\gamma} |x-z|^d\big) \rho\big(\kappa^{-1/\delta} s^\gamma u^{1-\gamma} |y-z|^d\big) \\ &\leq C\kappa (t \wedge s)^{-\gamma\delta} (t \vee s)^{-\gamma} |x-y|^{-d\delta}\end{aligned}$$

where $C = \frac{I_\rho 2^{d\delta+1}}{(\gamma - (1-\gamma)\delta)}$.

Proof. The first inequality follows directly by summing over all possible connectors and applying Assumption UBA and Mecke's formula. Observe that for every vertex $\mathbf{z} = (z, u)$ either $|x-z| \geq \frac{|x-y|}{2}$ or $|y-z| \geq \frac{|x-y|}{2}$, as the open balls

$B_{\frac{|x-y|}{2}}(x)$ and $B_{\frac{|x-y|}{2}}(y)$ are disjoint. Hence, we have

$$\begin{aligned}
&\int_{\mathbb{R}^d\times(t\vee s,1]} \mathrm{d}\mathbf{z}\rho\big(\kappa^{-1/\delta}t^{\gamma}u^{1-\gamma}\,|x-z|^d\big)\rho\big(\kappa^{-1/\delta}s^{\gamma}u^{1-\gamma}\,|y-z|^d\big)\\
&\leq \int_{t\vee s}^{1}\mathrm{d}u\rho\big(2^{-d}\kappa^{-1/\delta}t^{\gamma}u^{1-\gamma}\,|x-y|^d\big)\int_{\mathbb{R}^d}\mathrm{d}z\rho\big(\kappa^{-1/\delta}s^{\gamma}u^{1-\gamma}\,|y-z|^d\big)\\
&\quad+\int_{t\vee s}^{1}\mathrm{d}u\rho\big(2^{-d}\kappa^{-1/\delta}s^{\gamma}u^{1-\gamma}\,|x-y|^d\big)\int_{\mathbb{R}^d}\mathrm{d}z\rho\big(\kappa^{-1/\delta}t^{\gamma}u^{1-\gamma}\,|x-z|^d\big)\\
&\leq I_\rho 2^{d\delta}\kappa\Bigg[\int_{t\vee s}^{1}\mathrm{d}u\; t^{-\gamma\delta}u^{(\gamma-1)\delta}\,|x-y|^{-d\delta}\,s^{-\gamma}u^{\gamma-1}\\
&\qquad\qquad+s^{-\gamma\delta}u^{(\gamma-1)\delta}\,|x-y|^{-d\delta}\,t^{-\gamma}u^{\gamma-1}\Bigg]\\
&\leq \tfrac{I_\rho 2^{d\delta}}{(\gamma-(1-\gamma)\delta)}\kappa\,|x-y|^{-d\delta}\left[t^{-\gamma\delta}s^{-\gamma}+s^{-\gamma\delta}t^{-\gamma}\right]\\
&\leq \tfrac{I_\rho 2^{d\delta+1}}{\gamma-(1-\gamma)\delta}\,\kappa(t\wedge s)^{-\gamma\delta}(t\vee s)^{-\gamma}\,|x-y|^{-d\delta}\,.
\end{aligned}$$

□

We consider the event that vertices $\mathbf{x}$ and $\mathbf{y}$ are connected by multiple vertices with larger marks. Recall that $K(\mathbf{x},\mathbf{y},k)$ is the number of step minimizing paths P between $\mathbf{x}$ and $\mathbf{y}$ with $w_P = k$ whose vertices have marks larger than the marks of $\mathbf{x}$ and $\mathbf{y}$. As before we call the vertices of such a path connectors. To control the number of such paths, notice that for any possible choice of connectors between $\mathbf{x}$ and $\mathbf{y}$, there exists an almost surely unique connector with smallest mark, i.e. the most powerful connector. For $i = 1,\dots,k$, we denote by $K(\mathbf{x},\mathbf{y},k,i)$ the number of step minimizing paths between $\mathbf{x}$ and $\mathbf{y}$ where the connectors have a larger mark than $\mathbf{x}$ and $\mathbf{y}$ and there is a vertex $\mathbf{x}_r$ with $w_P(r) = i$ which is the most powerful connector of those vertices. Then,

$$K(\mathbf{x},\mathbf{y},k)\leq\sum_{i=1}^{k-1}K(\mathbf{x},\mathbf{y},k,i).$$

Assume now that the connector $\mathbf{x}_r$ is the most powerful of all connectors and $w_P(r) = i$. In this case, the possible connectors $\mathbf{x}_1,\dots,\mathbf{x}_{r-1}$ and $\mathbf{x}_{r+1},\dots,\mathbf{x}_{m-1}$

need to have larger mark than $\mathbf{x}_r$. Hence, the paths between $\mathbf{x}_r$ and $\mathbf{x}$, resp. $\mathbf{y}$, considered on their own have the same structure as the initial path and this leads to

$$K(\mathbf{x},\mathbf{y},k) \leq \sum_{i=1}^{k-1} \sum_{\substack{\mathbf{z}=(z,u)\\ u>t\vee s}} K(\mathbf{x},\mathbf{z},i)K(\mathbf{z},\mathbf{y},k-i). \tag{2.14}$$

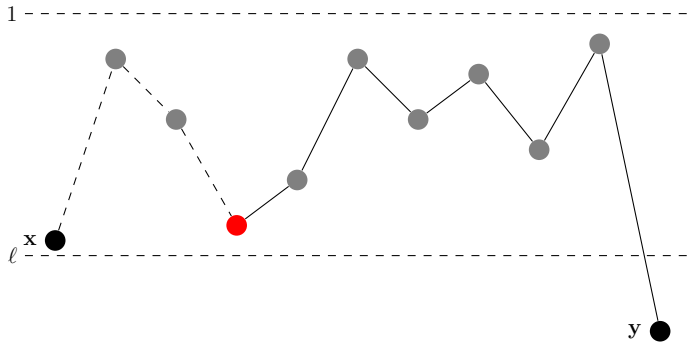

Figure 2.3: Decomposition of a path at the most powerful connector.

We use this decomposition together with Assumption UBA to find an upper bound for $\mathbb{E}_{\mathbf{x},\mathbf{y}}K(\mathbf{x},\mathbf{y},k)$. Recall that, when $|x-y|^d \leq \kappa^{1/\delta}(t\wedge s)^{-\gamma}(t\vee s)^{-\gamma/\delta}$, we have $K(\mathbf{x},\mathbf{y},k)=0$ if $k\geq 3$ and $K(\mathbf{x},\mathbf{y},k)=1$ if $k=2$ by definition. We now introduce a mapping

$$e_K\colon (\mathbb{R}^d\times(0,1))^2\times\mathbb{N}\to[0,\infty).$$

by $e_K(\mathbf{x},\mathbf{y},1)=\rho(\kappa^{-1/\delta}(t\wedge s)^{\gamma}(t\vee s)^{1-\gamma}\,|x-y|^d)$, for $\mathbf{x},\mathbf{y}\in\mathbb{R}^d\times(0,1)$, and, for $k\geq 2$ under the assumption that $|x-y|^d > \kappa^{1/\delta}(t\wedge s)^{-\gamma}(t\vee s)^{-\gamma/\delta}$,

$$e_K(\mathbf{x},\mathbf{y},k)=\sum_{i=1}^{k-1}\int_{\mathbb{R}^d\times(t\vee s,1)} \mathrm{d}\mathbf{z}\, e_K(\mathbf{x},\mathbf{z},i)e_K(\mathbf{z},\mathbf{y},k-i), \quad \text{for } \mathbf{x},\mathbf{y}\in\mathbb{R}^d\times(0,1), \tag{2.15}$$

and otherwise $e_K(\mathbf{x},\mathbf{y},2)=1$ and $e_K(\mathbf{x},\mathbf{y},k)=0$ for $k\geq 3$.

Lemma 2.4

Let $\mathbf{x}, \mathbf{y} \in \mathbb{R}^d \times (0,1)$ be two given vertices. Then, for all $k \in \mathbb{N}$, we have

$$\mathbb{E}_{\mathbf{x},\mathbf{y}} K(\mathbf{x}, \mathbf{y}, k) \leq e_K(\mathbf{x}, \mathbf{y}, k). \tag{2.16}$$

Note that by Assumption UBA and Lemma 2.3, we have $\mathbb{E}_{\mathbf{x},\mathbf{y}} K(\mathbf{x}, \mathbf{y}, 1) \leq e_K(\mathbf{x}, \mathbf{y}, 1)$ and $\mathbb{E}_{\mathbf{x},\mathbf{y}} K(\mathbf{x}, \mathbf{y}, 2) \leq e_K(\mathbf{x}, \mathbf{y}, 2)$. We prove the result for general k by induction using (2.14), but to do so we need to classify the possible connection strategies according to the way in which powerful vertices are placed. This classification is done by means of coloured binary trees. We write $\mathcal{T}_{k-1}$ for the set of all binary trees with $k-1$ vertices. Here a binary tree is a rooted tree in which every vertex can have either no child, a right child, a left child or both. We colour the vertices of a tree $T \in \mathcal{T}_{k-1}$ in such a way that the leaves of the tree can be either blue or red, and every other vertex is coloured blue. Thus, for each $T \in \mathcal{T}_{k-1}$ there exist 2^ℓ different colourings, where ℓ is the number of leaves of T. Let $\mathcal{T}^c_{k-1}$ be the set of all coloured trees.

Before proceeding we outline the role of the tree and its coloured vertices in regard to the information they capture. We will construct the tree so as to describe the precise order of the connectors' marks. In order to distuingish between connections of vertices that are sufficiently close to form an edge with conductance two and connections between vertices which are further apart, red vertices of the tree will represent the first case and blue the second.

To each step minimizing path of conductance k between $\mathbf{x}$ and $\mathbf{y}$ we associate a coloured tree $T \in \mathcal{T}^c_{k-1}$ in two steps, see Figure 2.4a:

(1) If the connectors of the step minimizing path P of conductance k are $\mathbf{x}_1, \ldots, \mathbf{x}_m$ with $m \leq k-1$, we associate a vector $\mathbf{u} = (u_1, \ldots, u_{k-1})$ to the path defined as follows. We set $u_{w_P(i)} := t_i$ for all $i \in 1, \ldots, m$ and $u_j = 1$ for all $j \in \{1, \ldots, k-1\} \backslash \{w_P(1), \ldots, w_P(m)\}$. Then

$$\mathbf{u} \in \mathcal{U}_{k-1} := \{\mathbf{u} = (u_1, \ldots, u_{k-1}) \in (0,1]^{k-1} \colon u_i \neq 1 \text{ if } u_{i-1} = 1\}.$$

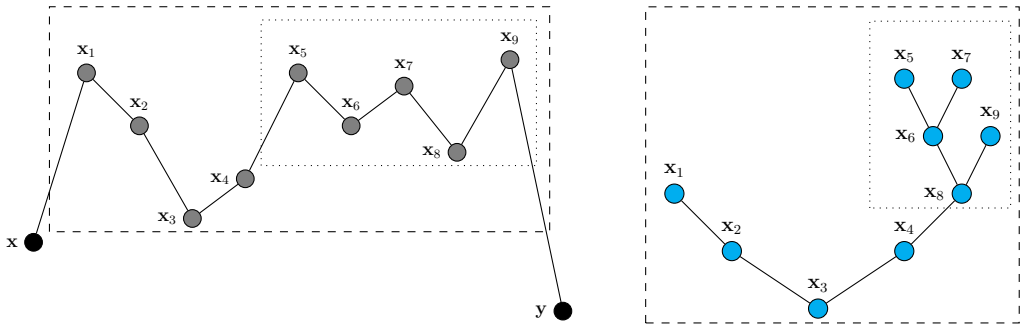

Figure 2.4a: Classification of a connection strategy by means of a binary tree. Local minima of the path correspond to branchpoints and local maxima to blue leaves of the corresponding binary tree T. Matching labels in the tree on the right are obtained by left-to-right labelling.

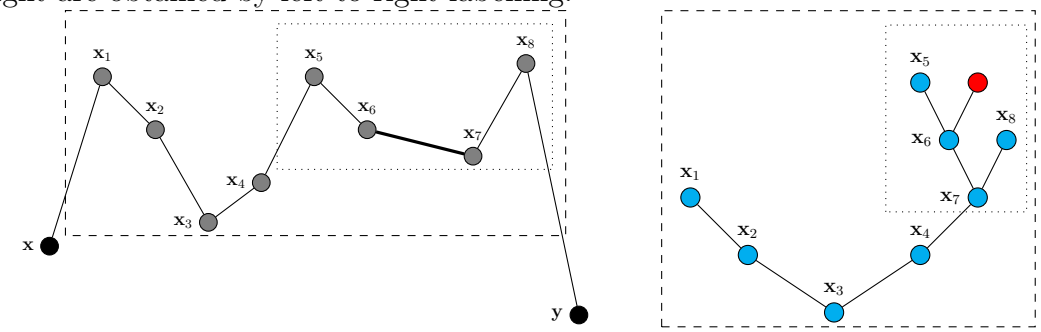

Figure 2.4b: One connector of the path in Figure 2.4a is replaced by an edge of conductance two. This edge corresponds to the red vertex in the tree to which no label and hence no vertex of the path is attached.

(2) To $\mathbf{u} \in \mathcal{U}_{k-1}$ we associate a coloured tree $T \in \mathcal{T}^c_{k-1}$ as follows:

- For $k = 2$ we have $\mathbf{u} = (u_1)$ and the set $\mathcal{T}^c_1$ contains two trees T, each consisting only of the root which may be coloured blue or red. If $\mathbf{u} = (1)$, then $\mathbf{u}$ is associated to the tree T with the red root and otherwise $\mathbf{u}$ is associated to the tree with the blue root.
- For $k > 2$, assume that to every tuple in $\mathbf{u} \in \mathcal{U}_{j-1}$ with $2 \leq j < k$ we have already associated a coloured tree $T \in \mathcal{T}^c_{j-1}$. Let $\mathbf{u} = (u_1, \ldots, u_{k-1})$ and let u_i be the smallest value of $\mathbf{u}$. Then, there exist trees $T_1 \in \mathcal{T}^c_{i-1}$ and $T_2 \in \mathcal{T}^c_{k-i-1}$ associated to $\mathbf{u}_1 = (u_1, \ldots, u_{i-1})$, resp. $\mathbf{u}_2 = (u_{i+1}, \ldots, u_{k-1})$. To $\mathbf{u}$ we associate the tree $T \in \mathcal{T}^c_{k-1}$, which has T_1 as the left subtree of the root and T_2 as the right subtree and colour the root blue.

Conversely, given a tree $T \in \mathcal{T}_{k-1}^c$ let m be the number of blue vertices of the tree. We define a labelling

$$\sigma_T : \{1, \dots, m\} \to T, i \mapsto \sigma_T(i),$$

of the blue vertices in T by letting $\sigma_T(i)$ be the ith vertex removed in a *left-to-right exploration* of the tree consisting of the blue vertices. This exploration starts with the vertex obtained by starting at the root and going left at any branching until this is no longer possible. Remove this vertex and repeat the procedure unless the removal disconnects a part from the tree or removes the root. If a part is disconnected explore this part (which is rooted in the right child of the last removed vertex) until it is fully explored and removed, and continue from there with the remaining tree. If the root is removed while it has a right child, explore the tree rooted in that child until it is fully explored and then stop. Similarly, define a bijection

$$\tau_T : \{1, \dots, k-1\} \to T, i \mapsto \tau_T(i),$$

by letting $\tau_T(i)$ be the ith vertex seen by a left-to-right exploration of *all* vertices on the tree T. We also set $\sigma_T^{-1}(\tau_T(0)) := 0$ and $\sigma_T^{-1}(\tau_T(k)) := m + 1$. Finally,

$$\varkappa_T : T \to \{0, \dots, k\}^2, v \mapsto \left(\varkappa_T^{(1)}(v), \varkappa_T^{(2)}(v)\right)$$

is defined recursively. For the root v of T, we set $\varkappa_T(v) = (0, k)$. As before, removing v splits T into a left subtree T_1 and a right subtree T_2. If these trees are nonempty, set $\varkappa_T(v_1) = \left(\varkappa_T^{(1)}(v), \tau_T^{-1}(v)\right)$ for the root v_1 of T_1, resp. $\varkappa_T(v_2) = \left(\tau_T^{-1}(v), \varkappa_T^{(2)}(v)\right)$ for the root v_2 of T_2. Repeat this for the subtrees until $\varkappa_T(v)$ is defined for all $v \in T$. Thus, for each vertex $v \in T$, its image $\varkappa_T(v)$ captures

- as its first entry the labelling τ_T^{-1} of the last vertex seen by a left-to-right exploration before the first vertex of the subtree rooted in v (and set to 0 if there is no such vertex),
- as its second entry the labelling τ_T^{-1} of the first vertex seen by a left-to-right exploration after the last vertex of the subtree rooted in v (and set to k if there is no such vertex)

With these labelings at hand, we now describe four restrictions that are satisfied by the marks and locations of the connectors $\mathbf{x}_1, \dots, \mathbf{x}_m$ of every step-minimizing path connecting $\mathbf{x}_0 = (x_0, t_0)$ and $\mathbf{x}_{m+1} = (x_{m+1}, t_{m+1})$ to which the coloured tree T is associated, namely

(i) if $\sigma_T(i)$ is the root in T, then $t_i > t_0, t_{m+1}$;

(ii) if $\sigma_T(i)$ is a child of $\sigma_T(j)$ in T, then $t_i > t_j$,

(iii) if there is a red leaf v with $i = \sigma_T^{-1}(\tau_T(\varkappa_T^{(1)}(v)))$ and $j = \sigma_T^{-1}(\tau_T(\varkappa_T^{(2)}(v)))$, then
$$|x_i - x_j|^d \leq \kappa^{1/\delta}(t_i \wedge t_j)^{-\gamma}(t_i \vee t_j)^{-\gamma/\delta};$$

(iv) if there is a blue vertex v with $i = \sigma_T^{-1}(\tau_T(\varkappa_T^{(1)}(v)))$ and $j = \sigma_T^{-1}(\tau_T(\varkappa_T^{(2)}(v)))$, then
$$|x_i - x_j|^d > \kappa^{1/\delta}(t_i \wedge t_j)^{-\gamma}(t_i \vee t_j)^{-\gamma/\delta}.$$

Note that whereas (i) and (ii) describe the order of the marks, (iii) and (iv) encode the spatial restrictions on the connectors via the colour of the tree vertices. In (iv), $\mathbf{x}_i$ (resp. $\mathbf{x}_j$) is the first vertex to the left (resp. right) with a smaller mark than $\mathbf{x}_{\sigma_T^{-1}(v)}$ and the inequality ensures that $\mathbf{x}_i$ and $\mathbf{x}_j$ are far enough apart that no edge with conductance two can exist between them. Conversely, the inequality in (iii) ensures the existence of an edge with conductance two. These conditions motivate the following definitions:

- M_T as the set of vectors $(t_1, \dots, t_m) \in (0,1)^m$ such that (i), (ii) hold,
- I_T^{rl} as the set of pairs $(i,j) \in \{0, \dots, m+1\}^2$ for which a *red leaf* v of T exists such that $i = \sigma_T^{-1}(\tau_T(\varkappa_T^{(1)}(v)))$ and $j = \sigma_T^{-1}(\tau_T(\varkappa_T^{(2)}(v)))$,
- I_T^{b} as the set of pairs $(i,j) \in \{0, \dots, m+1\}^2$ for which a *blue vertex* v of T exists such that $i = \sigma_T^{-1}(\tau_T(\varkappa_T^{(1)}(v)))$ and $j = \sigma_T^{-1}(\tau_T(\varkappa_T^{(2)}(v)))$,
- and I_T^{bc} as the set of pairs $(i, i+1) \in \{0, \dots, m+1\}^2$ for which we have that $\tau_T^{-1}(\sigma_T(i+1)) - \tau_T^{-1}(\sigma_T(i)) = 1$.

Whereas M_T captures the restrictions on the marks, I_T^{rl} and I_T^{b} contain the indices to which the the spatial restrictions (iii) and (iv) apply, as for $(i,j) \in I_T^{\mathrm{b}}$ the

vertices $\mathbf{x}_i$ and $\mathbf{x}_j$ cannot be near to each other and for $(i,j) \in I_T^{\mathrm{rl}}$ the vertices $\mathbf{x}_i$ and $\mathbf{x}_j$ have to be that near to each other so that an edge of conductance two exists between them. For each pair $(i,j) \in I_T^{\mathrm{rl}}$ we have $j = i+1$ and I_T^{rl}, I_T^{bc} form a partition of $\{(i,i+1) : i = 0,\dots,m\}$, because for any $(i,i+1) \in I_T^{\mathrm{bc}}$, there exists an edge of conductance one between the vertices $\mathbf{x}_i$ and $\mathbf{x}_{i+1}$.

Proof of Lemma 2.4. For $T \in \mathcal{T}_{k-1}^c$, we define $K_T(\mathbf{x},\mathbf{y})$ as the number of step minimizing paths P between $\mathbf{x}$ and $\mathbf{y}$ with $w_P = k$ whose vertices have marks larger than the marks of $\mathbf{x}$ and $\mathbf{y}$ to which T is associated. Then

$$\mathbb{E}_{\mathbf{x},\mathbf{y}} K(\mathbf{x},\mathbf{y},k) = \sum_{T \in \mathcal{T}_{k-1}^c} \mathbb{E}_{\mathbf{x},\mathbf{y}} K_T(\mathbf{x},\mathbf{y}).$$

If $k = 1$ (or equivalently $T = \emptyset$) we have that $K_T(\mathbf{x},\mathbf{y})$ is the indicator of the event that $\mathbf{x}$ and $\mathbf{y}$ are connected by an edge. For $k = 2$, if T is the tree consisting of the red root $K_T(\mathbf{x},\mathbf{y}) = \mathbf{1}\{|x-y|^d \le \kappa^{1/\delta}(t \wedge s)^{-\gamma}(t \vee s)^{-\gamma/\delta}\}$ and if T is the tree consisting of the blue root

$$K_T(\mathbf{x},\mathbf{y}) \le \mathbf{1}\{|x-y|^d > \kappa^{1/\delta}(t \wedge s)^{-\gamma}(t \vee s)^{-\gamma/\delta}\} \sum_{\substack{\mathbf{z}=(z,u) \\ u > t \vee s}} K_\emptyset(\mathbf{x},\mathbf{z}) K_\emptyset(\mathbf{z},\mathbf{y}).$$

For $k \ge 3$ we split the tree at the root, i.e.

$$K_T(\mathbf{x},\mathbf{y}) \le \mathbf{1}\{|x-y|^d > \kappa^{1/\delta}(t \wedge s)^{-\gamma}(t \vee s)^{-\gamma/\delta}\} \sum_{\substack{\mathbf{z}=(z,u) \\ u > t \vee s}} K_{T_1}(\mathbf{x},\mathbf{z}) K_{T_2}(\mathbf{z},\mathbf{y}). \tag{2.17}$$

where T_1 and T_2 are the left, resp. right, subtree of T obtained by cutting the root. Repeat the step (2.17) by consecutively splitting the tree at the vertices as seen in the order of a depth first search of the blue vertices in the tree, reducing the product to terms corresponding to empty or single red vertex trees. We get

$$\begin{aligned} K_T(\mathbf{x},\mathbf{y}) \le \sum_{\mathbf{x}_1,\dots,\mathbf{x}_m} & \mathbf{1}\{(t_1,\dots,t_m) \in M_T\} \\ & \prod_{(i,j) \in I_T^{\mathrm{b}}} \mathbf{1}\{|x_i - x_j|^d > \kappa^{1/\delta}(t_i \wedge t_j)^{-\gamma}(t_i \vee t_j)^{-\gamma/\delta}\} \\ & \prod_{(i,i+1) \in I_T^{\mathrm{rl}}} K_{v_{(i,i+1)}}(\mathbf{x}_i,\mathbf{x}_{i+1}) \prod_{(i,i+1) \in I_T^{\mathrm{bc}}} K_\emptyset(\mathbf{x}_i,\mathbf{x}_{i+1}), \end{aligned}$$

where $\mathbf{x}_0 = \mathbf{x}$, $\mathbf{x}_{m+1} = \mathbf{y}$ and $v_{(i,i+1)} \in T$ is the red leaf associated to (i,j) in the definition of I_T^{rl}. Note that the term $K_{v_{(i,i+1)}}$ contains further spatial restrictions on $\mathbf{x}_i$ and $\mathbf{x}_{i+1}$, ensuring that these vertices are sufficiently close. Taking expectations yields

$$\begin{aligned}\mathbb{E}_{\mathcal{X}} K_T(\mathbf{x},\mathbf{y}) \le \sum_{\mathbf{x}_1,\dots,\mathbf{x}_m} & \mathbf{1}\{(t_1,\dots,t_m)\in M_T\} \\ & \prod_{(i,j)\in I_T^{\mathrm{b}}} \mathbf{1}\{|x_i-x_j|^d > \kappa^{1/\delta}(t_i\wedge t_j)^{-\gamma}(t_i\vee t_j)^{-\gamma/\delta}\} \\ & \prod_{(i,i+1)\in I_T^{\mathrm{rl}}} \mathbf{1}\{|x_i-x_{i+1}|^d \le \kappa^{1/\delta}(t_i\wedge t_{i+1})^{-\gamma}(t_i\vee t_{i+1})^{-\gamma/\delta}\} \\ & \mathbb{E}_{\mathcal{X}} \prod_{(i,i+1)\in I_T^{\mathrm{bc}}} \mathbf{1}\{\mathbf{x}_i\sim\mathbf{x}_{i+1}\}.\end{aligned}$$

By Assumption UBA, we have

$$\mathbb{E}_{\mathcal{X}}\Big[\prod_{(i,i+1)\in I_T^{\mathrm{bc}}} \mathbf{1}\{\mathbf{x}_i\sim\mathbf{x}_{i+1}\}\Big] \le \prod_{(i,i+1)\in I_T^{\mathrm{bc}}} e_K(\mathbf{x}_i,\mathbf{x}_{i+1},1). \tag{2.18}$$

Hence, using the Mecke formula for m points, we get

$$\begin{aligned}\mathbb{E}_{\mathbf{x},\mathbf{y}} K_T(\mathbf{x},\mathbf{y}) \le \int \mathrm{d}\mathbf{x}_1\cdots\int \mathrm{d}\mathbf{x}_m\, & \mathbf{1}\{(t_1,\dots,t_m)\in M_T\} \\ & \prod_{(i,j)\in I_T^{\mathrm{b}}} \mathbf{1}\{|x_i-x_j|^d > \kappa^{1/\delta}(t_i\wedge t_j)^{-\gamma}(t_i\vee t_j)^{-\gamma/\delta}\} \\ & \prod_{(i,i+1)\in I_T^{\mathrm{rl}}} \mathbf{1}\{|x_i-x_{i+1}|^d \le \kappa^{1/\delta}(t_i\wedge t_{i+1})^{-\gamma}(t_i\vee t_{i+1})^{-\gamma/\delta}\} \\ & \prod_{(i,i+1)\in I_T^{\mathrm{bc}}} e_K(\mathbf{x}_i,\mathbf{x}_{i+1},1).\end{aligned} \tag{2.19}$$

What remains to be seen is that when the right-hand side in (2.19) is denoted $e_K^T(\mathbf{x},\mathbf{y})$ and summed over all $T\in\mathcal{T}_{k-1}^c$ we obtain $e_K(\mathbf{x},\mathbf{y},k)$. This is clearly true when $k=1$ and $k=2$. Otherwise we use (2.15) to decompose $e_K(\mathbf{x},\mathbf{y},k)$. By induction, the factors in this decomposition can be represented as in (2.19)

and we obtain

$$e_K(\mathbf{x},\mathbf{y},k) = \mathbf{1}\{|x-y|^d > \kappa^{1/\delta}(t\wedge s)^{-\gamma}(t\vee s)^{-\gamma/\delta}\} \sum_{i=1}^{k-1}\sum_{T_1\in\mathcal{T}^c_{i-1}}\sum_{T_2\in\mathcal{T}^c_{k-1-i}}\int_{\mathbb{R}^d\times(t\vee s,1)} \mathrm{d}\mathbf{z}\, e_K^{T_1}(\mathbf{x},\mathbf{z})e_K^{T_2}(\mathbf{z},\mathbf{y}).$$

Writing the terms $e_K^{T_1}(\mathbf{x},\mathbf{z})$ and $e_K^{T_2}(\mathbf{z},\mathbf{y})$ as in (2.19) as integrals over $\mathbf{x}_1,\dots,\mathbf{x}_{m_1}$ and $\mathbf{x}_{m_1+2},\dots,\mathbf{x}_m$ we can insert $\mathbf{z}$ as $\mathbf{x}_{m_1+1}$ and note that the conditions and terms emerging in that integral are exactly the same as in (2.19) for the tree T with T_1 and T_2 as left and right subtree of the root. Indeed,

- the vector $(t_1,\dots,t_m)$ of the marks of $\mathbf{x}_1,\dots,\mathbf{x}_m$ is an element of M_T iff $(t_1,\dots,t_{m_1})\in M_{T_1}$, $(t_{m_1+2},\dots,t_m)\in M_{T_2}$ and $t_{m_1+1} > s\vee t$,
- the spatial conditions described by I_T^{b} are fulfilled iff $x_1,\dots,x_{m_1}$ fulfills the ones decribed by $I_{T_1}^{\mathrm{b}}$, $x_{m_1+2},\dots,x_m$ the ones by $I_{T_2}^{\mathrm{b}}$ and

$$|x-y|^d > \kappa^{1/\delta}(t\wedge s)^{-\gamma}(t\vee s)^{-\gamma/\delta},$$

- I_T^{rl} is the union of $I_{T_1}^{\mathrm{rl}}$ and $I_{T_2}^{\mathrm{rl}}$ where the values of the pairs of $I_{T_2}^{\mathrm{rl}}$ have been increased by m_1+1 and in the same way I_T^{bc} directly emerges from $I_{T_1}^{\mathrm{bc}}$ and $I_{T_2}^{\mathrm{bc}}$.

Hence, $e_K(\mathbf{x},\mathbf{y},k)$ can be obtained by summing $e_K^T(\mathbf{x},\mathbf{y})$ over all $T\in\mathcal{T}^c_{k-1}$. □

Lemma 2.5: k-connection lemma

Let $\mathbf{x}=(x,t),\mathbf{y}=(y,s)\in\mathbb{R}^d\times(0,1)$ be two given vertices with $|x-y|^d > \kappa^{1/\delta}(t\wedge s)^{-\gamma}(t\vee s)^{-\gamma/\delta}$ and $0<\ell<\frac{1}{e}$ such that $\ell < t\vee s$. Then there exists $C>1$ such that, for $k\geq 3$, we have

$$e_K(\mathbf{x},\mathbf{y},k) \leq C^{k-1}\ell^{(\lfloor\frac{k}{2}\rfloor-1)(1-\gamma-\gamma/\delta)}\log(\tfrac{1}{\ell})^{k_*}\kappa(t\wedge s)^{-\gamma\delta}(t\vee s)^{-\gamma}\,|x-y|^{-d\delta}$$

where $k_* := k \mod 2$.

Proof. Choose $C>1$ such that C is larger than the constants appearing in

Lemma 2.3 and Lemmas A.3 and A.4 of Section A.2. We now show by induction that

$$e_K(\mathbf{x},\mathbf{y},k) \le \mathrm{Cat}(k-1)C^{k-1}\,\ell^{(\lfloor \frac{k}{2}\rfloor -1)(1-\gamma-\gamma/\delta)} \log(\tfrac{1}{\ell})^{k_*}\rho\big(\kappa^{-1/\delta}(t\wedge s)^{\gamma}(t\vee s)^{\gamma/\delta}\,|x-y|^d\big) \tag{2.20}$$

holds for all $k \ge 2$, where $\mathrm{Cat}(k-1)$ is the $(k-1)$-th Catalan number. Note that, for $k \ge 2$, it holds $e_K(\mathbf{x},\mathbf{y},k) \le 1$ for $|x-y|^d \le \kappa^{1/\delta}(t\wedge s)^{-\gamma}(t\vee s)^{-\gamma/\delta}$. Thus, it remains to show (2.20) under the condition $|x-y|^d > \kappa^{1/\delta}(t\wedge s)^{-\gamma}(t\vee s)^{-\gamma/\delta}$. For $k=2$, the bound (2.20) is already established by Lemma 2.3. If $k=3$ and $|x-y|^d > \kappa^{1/\delta}(t\wedge s)^{-\gamma}(t\vee s)^{-\gamma/\delta}$, by (2.15) we have

$$e_K(\mathbf{x},\mathbf{y},3) \le \int_{t\vee s}^1 \mathrm{d}u \int_{\mathbb{R}^d} \mathrm{d}z e_K(\mathbf{x},\mathbf{z},1)e_K(\mathbf{z},\mathbf{y},2) + \int_{t\vee s}^1 \mathrm{d}u \int_{\mathbb{R}^d} \mathrm{d}z e_K(\mathbf{x},\mathbf{z},2)e_K(\mathbf{z},\mathbf{y},1).$$

Using the bounds established in Lemma 2.3 together with Lemma A.4 leads to

$$e_K(\mathbf{x},\mathbf{y},3) \le 2C^2\log(\tfrac{1}{\ell})\kappa(t\wedge s)^{-\gamma\delta}(t\vee s)^{-\gamma}\,|x-y|^{-d\delta}\,.$$

Let $k \ge 4$ and assume that (2.20) holds for all $j = 2,\dots,k-1$. For $\mathbf{x},\mathbf{y}$ such that $|x-y|^d > \kappa^{1/\delta}(t\wedge s)^{-\gamma}(t\vee s)^{-\gamma/\delta}$, by (2.15),

$$e_K(\mathbf{x},\mathbf{y},k) = \sum_{i=1}^{k-1} \int_{\mathbb{R}^d\times(t\vee s,1)} \mathrm{d}\mathbf{z} e_K(\mathbf{x},\mathbf{z},i)e_K(\mathbf{z},\mathbf{y},k-i).$$

With (2.20) we hence get,

$$
\begin{aligned}
e_K(\mathbf{x},\mathbf{y},k) \leq \sum_{i=2}^{k-2} \Big[& C^{k-2}\ell^{(\lfloor \frac{i}{2}\rfloor+\lfloor\frac{k-i}{2}\rfloor-2)(1-\gamma-\gamma/\delta)} \log(\tfrac{1}{\ell})^{i_*+(k-i)_*} \operatorname{Cat}(i-1) \\
& \operatorname{Cat}(k-i-1) \int_{t\vee s}^{1} \mathrm{d}u \int_{\mathbb{R}^d} \mathrm{d}z \rho\big(\kappa^{-1/\delta} t^{\gamma} u^{\gamma/\delta} |x-z|^d\big) \rho\big(\kappa^{-1/\delta} s^{\gamma} u^{\gamma/\delta} |z-y|^d\big) \Big] \\
& + C^{k-2}\ell^{(\lfloor\frac{k-1}{2}\rfloor-1)(1-\gamma-\gamma/\delta)} \log(\tfrac{1}{\ell})^{(k-1)_*} \operatorname{Cat}(0)\operatorname{Cat}(k-2) \\
& \quad \times \int_{t\vee s}^{1} \mathrm{d}u \int_{\mathbb{R}^d} \mathrm{d}z \rho\big(\kappa^{-1/\delta} t^{\gamma} u^{1-\gamma} |x-z|^d\big) \rho\big(\kappa^{-1/\delta} s^{\gamma} u^{\gamma/\delta} |z-y|^d\big) \\
& + C^{k-2}\ell^{(\lfloor\frac{k-1}{2}\rfloor-1)(1-\gamma-\gamma/\delta)} \log(\tfrac{1}{\ell})^{(k-1)_*} \operatorname{Cat}(k-2)\operatorname{Cat}(0) \\
& \quad \times \int_{t\vee s}^{1} \mathrm{d}u \int_{\mathbb{R}^d} \mathrm{d}z \rho\big(\kappa^{-1/\delta} t^{\gamma} u^{\gamma/\delta} |x-z|^d\big) \rho\big(\kappa^{-1/\delta} s^{\gamma} u^{1-\gamma} |z-y|^d\big).
\end{aligned}
$$

Using Lemma A.3 and Lemma A.4 the last expression can be further bounded by

$$
\begin{aligned}
& \kappa(t\wedge s)^{-\gamma\delta}(t\vee s)^{-\gamma} |x-y|^{-d\delta} C^{k-1} \\
& \times \Big[\sum_{i=2}^{k-2} \operatorname{Cat}(i-1)\operatorname{Cat}(k-i-1) \ell^{(\lfloor\frac{i}{2}\rfloor+\lfloor\frac{k-i}{2}\rfloor-1)(1-\gamma-\gamma/\delta)} \log(\tfrac{1}{\ell})^{i_*+(k-i)_*} \\
& \qquad + 2l^{(\lfloor\frac{k-1}{2}\rfloor-1)(1-\gamma-\gamma/\delta)} \log(\tfrac{1}{\ell})^{(k-1)_*+1} \operatorname{Cat}(0)\operatorname{Cat}(k-2) \Big].
\end{aligned}
$$

If k is even, i and $k-i$ need to be either both even or both odd, for $i = 1,\dots,k-1$. Since $\ell > 0$ is chosen small enough that $\log(\frac{1}{\ell})^2 < \ell^{1-\gamma-\gamma/\delta}$, we have that in both cases

$$
\ell^{(\lfloor\frac{i}{2}\rfloor+\lfloor\frac{k-i}{2}\rfloor-1)(1-\gamma-\gamma/\delta)} \log(\tfrac{1}{\ell})^{i_*+(k-i)_*} < \ell^{(\lfloor\frac{k}{2}\rfloor-1)(1-\gamma-\gamma/\delta)}.
$$

If k is odd, an analogous observation leads to

$$
\ell^{(\lfloor\frac{i}{2}\rfloor+\lfloor\frac{k-i}{2}\rfloor-1)(1-\gamma-\gamma/\delta)} \log(\tfrac{1}{\ell})^{i_*+(k-i)_*} < \ell^{(\lfloor\frac{k}{2}\rfloor-1)(1-\gamma-\gamma/\delta)} \log(\tfrac{1}{\ell}).
$$

Hence, we have

$$\begin{aligned} e_K(\mathbf{x},\mathbf{y},k) &\le \kappa(t\wedge s)^{-\gamma\delta}(t\vee s)^{-\gamma}\,|x-y|^{-d\delta}\,C^{k-1}\ell^{(\lfloor\frac{k}{2}\rfloor-1)(1-\gamma-\gamma/\delta)} \\ &\qquad\times \log(\tfrac{1}{\ell})^{k_*}\sum_{i=1}^{k-1}\mathrm{Cat}(i-1)\,\mathrm{Cat}(k-i-1) \\ &\le \kappa(t\wedge s)^{-\gamma\delta}(t\vee s)^{-\gamma}\,|x-y|^{-d\delta}\,\mathrm{Cat}(k-1)C^{k-1}\ell^{(\lfloor\frac{k}{2}\rfloor-1)(1-\gamma-\gamma/\delta)}\log(\tfrac{1}{\ell})^{k_*} \end{aligned}$$

and (2.20) holds for k. The observation that $\mathrm{Cat}(k)\le 4^k$ concludes the proof. □

Probability bounds for bad paths.

With Lemma 2.5 we can establish a bound for $\mathbb{E}_{\mathbf{x},\mathbf{y}}N(\mathbf{x},\mathbf{y},n)$, recall the definitions in Section 2.3.3. As in (2.12) and (2.13), we have

$$N(\mathbf{x},\mathbf{y},n)\le K(\mathbf{x},\mathbf{y},n)+\sum_{k=1}^{n-1}\sum_{\substack{\mathbf{z}=(z,u)\\ t>u>\ell_{n-k}\vee s}} N(\mathbf{x},\mathbf{z},n-k)K(\mathbf{z},\mathbf{y},k)\ . \tag{2.21}$$

Here $\mathbf{z}$ is the most powerful vertex of the path disregarding $\mathbf{y}$ and connects to $\mathbf{y}$ via less powerful vertices. As done for $K(\mathbf{x},\mathbf{y},k)$ in the previous section we compare $\mathbb{E}_{\mathbf{x},\mathbf{y}}N(\mathbf{x},\mathbf{y},n)$ with a deterministic mapping

$$e_N\colon (\mathbb{R}^d\times(0,1))^2\times\mathbb{N}\to[0,\infty),$$

defined as

$$e_N(\mathbf{x},\mathbf{y},1)=\rho(\kappa^{-1/\delta}(t\wedge s)^{\gamma}(t\vee s)^{1-\gamma}\,|x-y|^d),\quad \text{for } \mathbf{x},\mathbf{y}\in\mathbb{R}^d\times(0,1),$$

and for $n\ge 2$

$$e_N(\mathbf{x},\mathbf{y},n)=e_K(\mathbf{x},\mathbf{y},n)+\sum_{i=1}^{n-1}\int_{\mathbb{R}^d\times(\ell_{n-k}\vee s,t]}\mathrm{d}\mathbf{z}\,e_N(\mathbf{x},\mathbf{z},n-k)e_K(\mathbf{z},\mathbf{y},k), \tag{2.22}$$

for $\mathbf{x},\mathbf{y}\in\mathbb{R}^d\times(0,1)$, if $|x-y|^d>\kappa^{1/\delta}(t\wedge s)^{-\gamma}(t\vee s)^{-\gamma/\delta}$, and otherwise $e_N(\mathbf{x},\mathbf{y},2)=1$ and $e_N(\mathbf{x},\mathbf{y},n)=0$ for $n\ge 3$.

Lemma 2.6

Let $\mathbf{x}, \mathbf{y} \in \mathbb{R}^d \times (0,1)$ be two given vertices. Then, for all $n \in \mathbb{N}$, we have

$$\mathbb{E}_{\mathbf{x},\mathbf{y}} N(\mathbf{x}, \mathbf{y}, n) \leq e_N(\mathbf{x}, \mathbf{y}, n). \tag{2.23}$$

Proof. First recall that for $|x-y|^d \leq \kappa^{1/\delta}(t \wedge s)^{-\gamma}(t \vee s)^{-\gamma/\delta}$ we have $N(\mathbf{x}, \mathbf{y}, n) = 0$ for $n \geq 3$ and $N(\mathbf{x}, \mathbf{y}, 2) = 1$. Thus in this case $N(\mathbf{x}, \mathbf{y}, n)$ is equal to $e_N(\mathbf{x}, \mathbf{y}, n)$ and consequently their expectations are equal. Otherwise, the proof follows the same argument as in Lemma 2.4, where we again classify the possible connection strategies between $\mathbf{x}$ and $\mathbf{y}$ through coloured binary trees. We therefore only briefly present the required class of trees, explain the association of a path to the corresponding tree and the restrictions on marks and space which a step minimizing path that associates to T has to satisfy.

Let $\mathcal{T}_n^{cb}$ be a class of coloured rooted binary trees with n vertices which are constructed as follows. For $k \leq n$, we have a *backbone* consisting of k vertices, starting with the root followed by $k-1$ vertices, each a left child of the previous one. The last vertex in this line is coloured red, the others blue. Let $i_1, \ldots, i_k \in \mathbb{N}$ with $i_1 + \ldots + i_k = n - k$. A tree $T \in \mathcal{T}_n^{cb}$ is formed by attaching to the j-th vertex (as seen by a left-to-right exploration of the backbone) a coloured subtree $T_j \in \mathcal{T}_{i_j}^{c}$ rooted in its right child, for $j = 1, \ldots, k$.

To any path $P = (\mathbf{x}_0, \mathbf{x}_1, \ldots, \mathbf{x}_{m+1})$ with $\mathbf{x}_0 = \mathbf{x}$ and $\mathbf{x}_{m+1} = \mathbf{y}$ where the connecting vertices have larger marks than $\mathbf{y}$ we associate a tree $T \in \mathcal{T}_n^{cb}$ as follows. We say $\mathbf{x}_i$ is a *powerful* vertex of P if $t_i \leq t_j$ for all $j = 0, \ldots, i-1$. By definition, the vertices $\mathbf{x}_0$ and $\mathbf{x}_{m+1}$ are always powerful vertices. We denote by $\{\mathbf{x}_{i_1}, \ldots, \mathbf{x}_{i_{k+1}}\}$ the set of powerful vertices keeping the order in the path. Then two consecutive powerful vertices $\mathbf{x}_{i_j}$ and $\mathbf{x}_{i_{j+1}}$ are, by definition, connected via a path of connectors $\mathbf{x}_{i_j+1}, \ldots \mathbf{x}_{i_{j+1}-1}$ of conductance $w_j := w_P(i_{j+1}) - w_P(i_j)$. If $w_j \geq 2$, associate the connectors of the path connecting $\mathbf{x}_{i_j}$ and $\mathbf{x}_{i_{j+1}}$ to a non-empty coloured tree $T_j \in \mathcal{T}_{w_j-1}^{c}$ as in the proof of Lemma 2.4. Let $T \in \mathcal{T}_n^{cb}$ be the coloured tree which has a backbone of length k and where T_j is attached to the j-th vertex (as seen by a left-to-right exploration of the backbone) such that its right child is the root of T_j, see Figure 2.5 for an example.

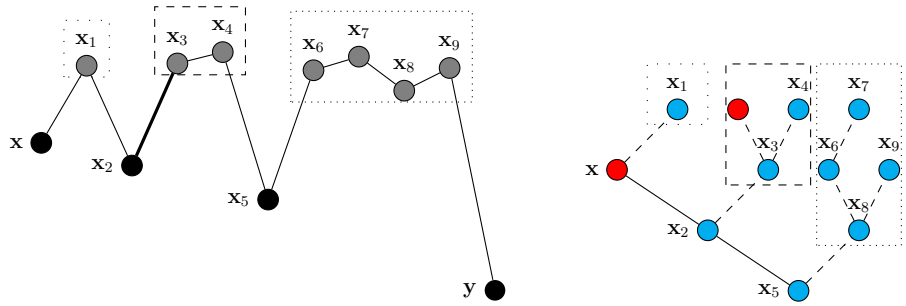

Figure 2.5: Associating a coloured binary tree to a path. The powerful vertices of the path are indicated in black. We have $k = 3$ vertices on the backbone. The three trees attached to the backbone are constructed as in Figure 2.4a, where the vertices with the smallest mark on the connecting paths are the roots which are attached as right children to the backbone.

Given a tree $T \in \mathcal{T}_n^{cb}$, let m be the number of blue vertices of the tree and k the number of vertices of the backbone. As in the proof of Lemma 2.4, we define a labelling

$$\sigma_T : \{0, \dots, m\} \to T, i \mapsto \sigma_T(i),$$

by letting $\sigma_T(0)$ be the red vertex on the backbone and $\sigma_T(i)$ be the ith vertex seen by a left-to-right exploration of the blue vertices of T. Define the bijection

$$\tau_T : \{0, \dots, n-1\} \to T, i \mapsto \tau_T(i),$$

by letting $\tau_T(0)$ be the red vertex on the backbone and $\tau_T(i)$ be the $(i+1)$st vertex seen by a left-to-right exploration of all other vertices of the tree. Denote by $v_1, \dots, v_k$ the vertices of the backbone of T and $T_1, \dots, T_k$ the subtrees rooted in their right child. Set $i_j := \sigma^{-1}(v_j)$, for $i = 1, \dots, k$, and $i_{k+1} := m + 1$. Then, the following restrictions on marks and space are satisfied by the vertices $\mathbf{x}_1, \dots, \mathbf{x}_m$ of any path connecting $\mathbf{x}_0 = \mathbf{x}$ and $\mathbf{x}_{m+1} = \mathbf{y}$ to which T is associated:

(i) $t_{i_j} > t_{i_{j+1}}$, for $j = 1, \dots, k$,

(ii) if there exists a vertex v_j of the backbone with $\tau_T^{-1}(v_j) \geq 2$, then

$$\left|x_0 - x_{i_j}\right|^d > \kappa^{1/\delta}(t_0 \wedge t_{i_j})^{-\gamma}(t_0 \vee t_{i_j})^{-\gamma/\delta},$$

(iii) for $j = 1, \dots, k$, the vertices $\mathbf{x}_{i_j+1}, \dots, \mathbf{x}_{i_{j+1}-1}$ satisfy the four restrictions

on marks and space given by the coloured tree T_i and $\mathbf{x}_{i_j}, \mathbf{x}_{i_{j+1}}$ as described prior to the proof of Lemma 2.4.

For $T \in \mathcal{T}_n^{cb}$, we define $N_T(\mathbf{x}, \mathbf{y})$ as the number of step minimizing paths to which T is associated. Denote again by $v_1, \dots, v_k$ the vertices of the backbone of T and set $i_j := \sigma^{-1}(v_j)$, $i_{k+1} := m + 1$. Splitting the tree at each blue vertex of the backbone leads to

$$N_T(\mathbf{x}, \mathbf{y}) \leq \sum_{\mathbf{x}_{i_2}, \dots, \mathbf{x}_{i_k}} \mathbf{1}\{t_{i_1} > \dots > t_{i_{k+1}}\} \prod_{\substack{2 \leq j \leq k \\ \tau_T^{-1}(v_j) \geq 2}} \mathbf{1}\{|x_0 - x_{i_j}|^d > \kappa^{1/\delta}(t_0 \wedge t_{i_j})^{-\gamma}(t_0 \vee t_{i_j})^{-\gamma/\delta}\} \prod_{1 \leq j \leq k} K_{T_j}(\mathbf{x}_{i_j}, \mathbf{x}_{i_{j+1}}),$$

where T_j is the subtree attached to the right child of v_j. Proceeding for each K_{T_j} and using the iterative structure of e_N as in the proof of Lemma 2.4 yields the result. □

As a path described by the event $\tilde{A}_n^{(\mathbf{x})}$ (recall the definition from Section 2.4) has a restriction on the mark but not on the location of its last vertex, we can use the integral

$$\int_{\mathbb{R}^d} \mathrm{d}y \; \mathbb{E}_{\mathbf{x},\mathbf{y}} N(\mathbf{x}, \mathbf{y}, n), \tag{2.24}$$

with $\mathbf{y} = (y, s)$ and s smaller than some yet to be determined value to bound $\mathbb{P}_{\mathbf{x}}(\tilde{A}_n^{(\mathbf{x})})$. Thus, we define for given $\mathbf{x} = (x, t)$ and $n \in \mathbb{N}$ the mapping $\mu_n^{\mathbf{x}} : (0, t] \to [0, \infty)$ by

$$\mu_n^{\mathbf{x}}(s) := \int_{\mathbb{R}^d} \mathrm{d}y \, e_N(\mathbf{x}, \mathbf{y}, n), \quad \text{for } s \in (0, t], \mathbf{y} = (y, s). \tag{2.25}$$

Recall that we write $k_* := k \pmod 2$ and $I_\rho := \int \mathrm{d}x \, \rho(\kappa^{-1/\delta} |x|^d)$. By the definition of $e_N(\mathbf{x}, \mathbf{y}, 1)$ we have $\mu_1^{\mathbf{x}}(s) \leq I_\rho s^{-\gamma} t^{\gamma - 1}$, for $s \in (0, t]$, and, for $n \geq 2$,

with a short calculation using Lemma 2.5 we get the recursive property

$$\mu_n^{\mathbf{x}}(s) \leq I_\rho C^{n-1} \ell_0^{(\lfloor \frac{n}{2} \rfloor - 1)(1-\gamma-\gamma/\delta)} \log(\tfrac{1}{\ell_0})^{n_*} s^{-\gamma} t^{-\gamma/\delta} \tag{2.26}$$

$$+ \sum_{k=2}^{n-1} I_\rho C^{k-1} \ell_{n-k}^{(\lfloor \frac{k}{2} \rfloor - 1)(1-\gamma-\gamma/\delta)} \log(\tfrac{1}{\ell_{n-k}})^{k_*} s^{-\gamma} \int_{\ell_{n-k}}^{t} \mathrm{d}u \mu_{n-k}^{\mathbf{x}}(u) u^{-\gamma/\delta} \tag{2.27}$$

$$+ I_\rho s^{-\gamma} \int_{\ell_{n-1}}^{t} \mathrm{d}u \, \mu_{n-1}^{\mathbf{x}}(u) u^{\gamma-1}, \quad \text{for } s \in (0,t], \tag{2.28}$$

where $C > 0$ is the constant from Lemma 2.5. Here, the first summand (2.26) corresponds to the first summand of (2.21), i.e. the number of paths with conductance n where the first vertex $\mathbf{x}$ and the last vertex with mark s are the two most powerful vertices of the path. The summands (2.27) and (2.28) describe the second summand of (2.21), where (2.28) covers the case that the last vertex of a path is directly connected to the preceding most powerful vertex.

Using the recursive inequality in (2.26) - (2.28) we now establish bounds for $\mu_n^{\mathbf{x}}$. To make the proof more transparent we continue working with a general sequence $(\ell_n)_{n\in\mathbb{N}_0}$ assuming only that it is at least exponentially decaying, i.e. for any $b > 0$ it holds that $\ell_{n+2} < b\ell_n$. We choose $b > 0$ small enough such that $\sum_{j=2}^{\infty} b^{(\gamma+\gamma/\delta-1)\frac{(j-3)(j-1)}{8}}$ converges. This choice is possible because in our regime $\gamma + \gamma/\delta$ is larger than one. We denote the limit of the series by $c_b > 1$. As we have already seen for the optimal path structure in Section 2.3.2, the chosen sequence $(\ell_n)_{n\in\mathbb{N}_0}$ decays much faster than any exponential rate so that this assumption will not have any effect on the result. Without loss of generality we may additionally assume $\ell_0 < \frac{1}{e}$.

Lemma 2.7

Let $\mathbf{x} = (x,t)$ be a given vertex and let the sequence $(\ell_n)_{n\in\mathbb{N}_0}$ be at least exponentially decaying with $\ell_0 < t \wedge \frac{1}{e}$. Then, there exists a constant c such that, for $n \in \mathbb{N}$, we have

$$\mu_n^{\mathbf{x}}(s) \le C_n s^{-\gamma}, \quad \text{for } s \in (0,t], \tag{2.29}$$

where

$$C_{n+2} = c^2 \ell_n^{1-\gamma-\gamma/\delta} C_n + c \log\left(\tfrac{1}{\ell_{n+1}}\right) C_{n+1} \tag{2.30}$$

and

$$C_1 = c\ell_0^{\gamma-1}, \quad C_2 = c^2 \ell_0^{-\gamma/\delta} + c\log(\tfrac{1}{\ell_1}) C_1.$$

Proof. We choose the constant $c > 0$ such that it is larger than $\frac{I_\rho c_b}{(\gamma+\gamma/\delta-1)\wedge 1}$ and larger than the constant C from Lemma 2.5. Since this also implies that $c > I_\rho$, by the definition of $\mu_1^{\mathbf{x}}$ we have

$$\mu_1^{\mathbf{x}}(s) = I_\rho s^{-\gamma} t^{\gamma-1} \le c\ell_0^{\gamma-1} s^{-\gamma} = C_1 s^{-\gamma} \quad \text{for } s \in (0,t].$$

For $n = 2$, the recursive inequality for $\mu_2^{\mathbf{x}}$ yields

$$\mu_2^{\mathbf{x}}(s) \le I_\rho C s^{-\gamma} t^{-\gamma/\delta} + I_\rho s^{-\gamma} \int_{\ell_1}^{t} \mathrm{d}u\, \mu_1^{\mathbf{x}}(u) u^{\gamma-1} \quad \text{for } s \in (0,t].$$

Using the already established bound for $n = 1$ we have

$$\begin{aligned}\mu_2^{\mathbf{x}}(s) &\le c^2 \ell_0^{-\gamma/\delta} s^{-\gamma} + I_\rho s^{-\gamma} \int_{\ell_1}^{t} \mathrm{d}u C_1 u^{-1} \\ &\le c^2 \ell_0^{-\gamma/\delta} s^{-\gamma} + c\log(\tfrac{1}{\ell_1}) C_1 s^{-\gamma} =: C_2 s^{-\gamma} \quad \text{for } s \in (0,t].\end{aligned}$$

Now let $n \ge 3$ and we assume that (2.29) holds for all $\tilde{n} \le n-1$. Then, using

the already established bounds and the recursive inequality property we have

$$\begin{aligned}
\mu_n^{\mathbf{x}}(s) &\le I_\rho C^{n-1}\ell_0^{(\lfloor\frac{n}{2}\rfloor-1)(1-\gamma-\gamma/\delta)}\log(\tfrac{1}{\ell_0})^{n_*}s^{-\gamma}t^{-\gamma/\delta} \\
&\quad + \sum_{k=2}^{n-1} I_\rho C^{k-1}\ell_{n-k}^{(\lfloor\frac{k}{2}\rfloor-1)(1-\gamma-\gamma/\delta)}\log(\tfrac{1}{\ell_{n-k}})^{k_*}s^{-\gamma}\int_{\ell_{n-k}}^{t}\mathrm{d}u C_{n-k}u^{-\gamma-\gamma/\delta} \\
&\quad + I_\rho s^{-\gamma}\int_{\ell_n-1}^{t}\mathrm{d}u\, C_{n-1}u^{-1} \\
&\le I_\rho C^{n-1}\ell_0^{(\lfloor\frac{n}{2}\rfloor-1)(1-\gamma-\gamma/\delta)}\log(\tfrac{1}{\ell_0})^{n_*}s^{-\gamma}t^{-\gamma/\delta} \\
&\quad + \sum_{k=2}^{n-1}\frac{I_\rho}{\gamma+\gamma/\delta-1}C^{k-1}\ell_{n-k}^{(\lfloor\frac{k}{2}\rfloor)(1-\gamma-\gamma/\delta)}\log(\tfrac{1}{\ell_{n-k}})^{k_*}C_{n-k}s^{-\gamma} \\
&\quad + I_\rho C_{n-1}\log(\tfrac{1}{\ell_{n-1}})s^{-\gamma} \quad \text{for } s\in(0,1).
\end{aligned}$$

Assume for the moment that

$$\begin{aligned}
&\sum_{k=2}^{n-1} c^{k-1}C_{n-k}\ell_{n-k}^{(\lfloor\frac{k}{2}\rfloor)(1-\gamma-\gamma/\delta)}\log(\tfrac{1}{\ell_{n-k}})^{k_*} + c^{n-1}\ell_0^{(\lfloor\frac{n}{2}\rfloor-1)(1-\gamma-\gamma/\delta)}\ell_0^{-\gamma/\delta}\log(\tfrac{1}{\ell_0})^{n_*} \\
&\qquad \le c_b c C_{n-2}\ell_{n-2}^{1-\gamma-\gamma/\delta}
\end{aligned} \tag{2.31}$$

holds. Then, as $c > C$, the term $\mu_n^{\mathbf{x}}(s)$ can be further bounded by

$$\tfrac{I_\rho c_b}{(\gamma+\gamma/\delta-1)\wedge 1}cC_{n-2}\ell_{n-2}^{1-\gamma-\gamma/\delta}s^{-\gamma} + I_\rho C_{n-1}\log(\tfrac{1}{\ell_{n-1}})s^{-\gamma},$$

which by (2.30) is smaller than $C_n s^{-\gamma}$ for $s\in(0,t]$. Hence, by induction the stated inequality holds for all $n\in\mathbb{N}$.

It remains to show that (2.31) holds. If k is even, a repeated application of (2.30) and $\ell_{n+2} < b\ell_n$ yields

$$c^{k-1}C_{n-k}\ell_{n-k}^{(\lfloor\frac{k}{2}\rfloor)(1-\gamma-\gamma/\delta)}\log(\tfrac{1}{\ell_{n-k}})^{k_*} \le cC_{n-2}\ell_{n-2}^{1-\gamma-\gamma/\delta}b^{(\gamma+\gamma/\delta-1)(\sum_{j=0}^{\frac{k-2}{2}}j)}.$$

If k is odd a similar calculation leads to

$$c^{k-1}C_{n-k}\ell_{n-k}^{(\lfloor\frac{k}{2}\rfloor)(1-\gamma-\gamma/\delta)}\log(\tfrac{1}{\ell_{n-k}})^{k_*} \le cC_{n-2}\ell_{n-2}^{1-\gamma-\gamma/\delta}b^{(\gamma+\gamma/\delta-1)(\sum_{j=0}^{\frac{k-3}{2}}j)}.$$

Distinguishing whether n is even or odd, the second term of (2.31) can be bounded in a similar way and so the whole expression can be bounded by

$$cC_{n-2}\ell_{n-2}^{1-\gamma-\gamma/\delta}\left(\sum_{\substack{k=2\\ \text{k even}}}^{n} b^{(\gamma+\gamma/\delta-1)\frac{(k-2)k}{8}} + \sum_{\substack{k=3\\ \text{k odd}}}^{n} b^{(\gamma+\gamma/\delta-1)\frac{(k-3)(k-1)}{8}}\right),$$

where the two sums can be bounded by c_b which implies that (2.31) holds. □

Notice that, as stated in Section 2.3.2, the inequality (2.31) shows us that the major contribution to the expected value of $N(\mathbf{x}, \mathbf{y}, n)$ comes from the paths where the two most powerful vertices are connected via a single connector. To see why, notice that the right-hand side of (2.31) is, up to a constant, the same as the $k = 2$ term of the left-hand side. In fact, Lemma 2.7 shows that the dominant class of possible paths is the one described in Section 2.3.2.

We are now ready to bound the probability of the event $\tilde{A}_n^{(\mathbf{x})}$, i.e. the event that there exists a path of conductance n where the final vertex is the first and only one which has a mark smaller than the corresponding ℓ_n. In particular the final vertex is the most powerful vertex of the path. By Mecke's equation, we have

$$\mathbb{P}_{\mathbf{x}}(\tilde{A}_n^{(\mathbf{x})}) \leq \int_{\mathbb{R}^d \times (0,\ell_n]} \mathrm{d}\mathbf{y}\, \mathbb{E}_{\mathbf{x},\mathbf{y}} N(\mathbf{x}, \mathbf{y}, n).$$

Hence, Fubini's theorem and Lemma 2.7 yield

$$\mathbb{P}_{\mathbf{x}}(\tilde{A}_n^{(\mathbf{x})}) \leq \int_0^{\ell_n} \mathrm{d}s \mu_n^{\mathbf{x}}(s) \leq \frac{1}{1-\gamma}\ell_n^{1-\gamma} C_n.$$

As in Section 2.3.2, with $\ell_0 < t \wedge \frac{1}{e}$ we choose the sequence $(\ell_n)_{n\in\mathbb{N}_0}$ for $\varepsilon > 0$, such that

$$\frac{1}{1-\gamma} C_n \ell_n^{1-\gamma} = \frac{\varepsilon}{\pi^2 n^2}, \tag{2.32}$$

and we have

$$\sum_{n=1}^{\Delta} \mathbb{P}_{\mathbf{x}}(A_n^{(\mathbf{x})}) \leq \sum_{n=1}^{\Delta} \mathbb{P}_{\mathbf{x}}(\tilde{A}_n^{(\mathbf{x})}) \leq \sum_{n=1}^{\Delta} \frac{1}{1-\gamma} C_n \ell_n^{1-\gamma} \leq \sum_{n=1}^{\infty} \frac{\varepsilon}{\pi^2 n^2} = \frac{\varepsilon}{6}.$$

Since C_n is defined recursively, we can obtain a recursive representation of the sequence $(\ell_n)_{n\in\mathbb{N}_0}$. Let $\eta_n := \ell_n^{-1}$ for $n \in \mathbb{N}_0$. Then, we have

$$\begin{aligned}\eta_{n+2}^{1-\gamma} &= \frac{\pi^2(n+2)^2}{3\varepsilon}\frac{1}{1-\gamma}C_{n+2} \\ &= \frac{\pi^2(n+2)^2}{3\varepsilon}\frac{1}{1-\gamma}\left[c^2\ell_n^{1-\gamma-\gamma/\delta}C_n + c\log\left(\frac{1}{\ell_{n+1}}\right)C_{n+1}\right] \\ &= \frac{(n+2)^2}{n^2}c^2\eta_n^{\gamma/\delta} + \frac{(n+1)^2}{n^2}c\log(\eta_{n+1})\eta_{n+1}^{1-\gamma}.\end{aligned} \tag{2.33}$$

Hence, there exists a different constant $c > 0$ such that $\eta_{n+2}^{1-\gamma} \le c\eta_n^{\gamma/\delta} + c\log(\eta_{n+1})\eta_{n+1}^{1-\gamma}$. By induction, we conclude that there exist $b > 0$ and $B > 0$ such that

$$\eta_n \le b\exp\left(B\left(\frac{\gamma}{\delta(1-\gamma)}\right)^{n/2}\right), \tag{2.34}$$

and thus the rate of decay of $(\ell_n)_{n\in\mathbb{N}_0}$ is faster than exponential.

Probability bounds for good paths.

We now proceed to establish a bound on the last summand $\sum_{n=1}^{2\Delta}\mathbb{P}_{\mathbf{x},\mathbf{y}}(B_n^{(\mathbf{x},\mathbf{y})})$ of (TMB). To do so we consider the original graph $\mathscr{G}$. Recall that $B_n^{(\mathbf{x},\mathbf{y})}$ is the event that there exists a good path of length n between $\mathbf{x}$ and $\mathbf{y}$. This can be bounded by the union of all possible good paths given by the vertices of the Poisson point process, i.e.

$$\mathbb{P}_{\mathbf{x},\mathbf{y}}(B_n^{(\mathbf{x},\mathbf{y})}) = \mathbb{P}_{\mathbf{x},\mathbf{y}}\left(\bigcup_{\substack{\mathbf{x}_1,\dots,\mathbf{x}_{n-1}\in\mathscr{G}\\(\mathbf{x}_0,\dots,\mathbf{x}_n)\text{ good}}}^{\neq}\{\mathbf{x}_0\sim\mathbf{x}_1\sim\ldots\sim\mathbf{x}_{n-1}\sim\mathbf{x}_n\}\right),$$

where $\mathbf{x} = \mathbf{x}_0$, $\mathbf{y} = \mathbf{x}_n$, $\bigcup^{\neq}$ denotes again the union across all possible sets of pairwise distinct vertices $\mathbf{x}_0,\dots,\mathbf{x}_n$ of the Poisson process. By Mecke's equation the right-hand side can be bounded from above by

$$\int_{\mathbb{R}^d\times(\ell_1,1]}\mathrm{d}\mathbf{x}_1\cdots\int_{\mathbb{R}^d\times(\ell_{\lfloor\frac{n}{2}\rfloor},1]}\mathrm{d}\mathbf{x}_{\lfloor\frac{n}{2}\rfloor}\cdots\int_{\mathbb{R}^d\times(\ell_1,1]}\mathrm{d}\mathbf{x}_{n-1}\,\mathbb{P}_{\mathbf{x},\mathbf{x}_1,\dots,\mathbf{x}_{n-1},\mathbf{y}}\{\mathbf{x}\sim\mathbf{x}_1\sim\ldots\sim\mathbf{x}_{n-1}\sim\mathbf{y}\}.$$

The following lemma reduces this bound to a non-spatial problem for paths of "reasonable" length which only depends on the marks of $\mathbf{x}_1, \dots, \mathbf{x}_{n-1}$ but not on their location. This allows us to use a similar strategy as the one used by Dereich et al. in [35], where lower bounds for the typical distance of non-spatial preferential attachment models are established.

Lemma 2.8

For given vertices $\mathbf{x} = (x, t)$ and $\mathbf{y} = (y, s)$, let $\Delta \leq c_\varepsilon |x - y|^\epsilon$ for some $1 > \varepsilon > 0$ and $c_\varepsilon > 0$. Then, there exist constants $a > 0$ and $\tilde{\kappa} > 0$ such that, for $n \leq \Delta$, we have

$$\int_{(\mathbb{R}^d)^{n-1}} \bigotimes_{i=1}^{n-1} \mathrm{d}x_i \mathbb{P}_{\mathbf{x},\mathbf{x}_1,\dots,\mathbf{x}_{n-1},\mathbf{y}}\{\mathbf{x} \sim \mathbf{x}_1 \sim \ldots \sim \mathbf{x}_{n-1} \sim \mathbf{y}\} \leq |x - y|^{-a} \prod_{k=1}^{n} \tilde{\kappa}(t_{k-1} \wedge t_k)^{-\gamma}(t_{k-1} \vee t_k)^{\gamma-1},$$

where $t_0 = t$ resp. $t_n = s$ are the marks of $\mathbf{x}$ resp. $\mathbf{y}$ and $\mathbf{x}_i = (x_i, t_i)$ for $i = 1, \dots, n-1$.

Remark 2.3.1. The constants a and $\tilde{\kappa}$ of Lemma 2.8 depend on the choice of ε and c_ε. But for $\Delta = O(\log |x - y|)$, for any $\epsilon > 0$ there exists a $c_\epsilon > 0$, such that, for $|x - y|$ large enough, we have $\Delta \leq c_\varepsilon |x - y|^\epsilon$. Thus, if $|x - y|$ is large enough, the choice of a and $\tilde{\kappa}$ does not depend on $|x - y|$.

Proof. Let $\{\mathbf{x}, \mathbf{x}_1, \dots, \mathbf{x}_{n-1}, \mathbf{y}\}$ be a set of given vertices. By Assumption UBA we have

$$\int_{(\mathbb{R}^d)^{n-1}} \bigotimes_{i=1}^{n-1} \mathrm{d}x_i \mathbb{P}_{\mathbf{x},\mathbf{x}_1,\dots,\mathbf{x}_{n-1},\mathbf{y}}\{\mathbf{x} \sim \mathbf{x}_1 \sim \ldots \sim \mathbf{x}_{n-1} \sim \mathbf{y}\} \leq \int_{(\mathbb{R}^d)^{n-1}} \bigotimes_{i=1}^{n-1} \mathrm{d}x_i \prod_{i=1}^{n} \rho\big(\kappa^{-1/\delta}(t_{i-1} \wedge t_i)^\gamma (t_{i-1} \vee t_i)^{1-\gamma} |x_{i-1} - x_i|^d\big).$$

As $n \leq c_\varepsilon |x - y|^\epsilon$, no matter the choice of vertices, there must exist at least one edge between two vertices $\mathbf{x}_{k-1} = (x_{k-1}, t_{k-1})$ and $\mathbf{x}_k = (x_k, t_k)$ with $|x_{k-1} - x_k| \geq$

$c_\varepsilon^{-1}\,|x-y|^{1-\varepsilon}$. Hence, the expression above can be further bounded by

$$\begin{aligned}
&\sum_{k=1}^{n-1}\int_{(\mathbb{R}^d)^{n-1}}\bigotimes_{i=1}^{n-1}\mathrm{d}x_i\rho\big(c_\varepsilon^{-d}\kappa^{-1/\delta}(t_{k-1}\wedge t_k)^{\gamma}(t_{k-1}\vee t_k)^{1-\gamma}\,|x-y|^{d(1-\varepsilon)}\big)\\
&\qquad\qquad\times\prod_{\substack{i=1\\ i\neq k}}^{n}\rho\big(\kappa^{-1/\delta}(t_{i-1}\wedge t_i)^{\gamma}(t_{i-1}\vee t_i)^{1-\gamma}\,|x_{i-1}-x_i|^{d}\big)\\
&\leq\sum_{k=1}^{n-1}\rho\big(c_\varepsilon^{-d}\kappa^{-1/\delta}(t_{k-1}\wedge t_k)^{\gamma}(t_{k-1}\vee t_k)^{1-\gamma}\,|x-y|^{d(1-\varepsilon)}\big)\\
&\qquad\qquad\times\prod_{\substack{i=1\\ i\neq k}}^{n}I_\rho(t_{i-1}\wedge t_i)^{-\gamma}(t_{i-1}\vee t_i)^{\gamma-1},
\end{aligned}$$

where the last inequality is achieved by integration over the location of the vertices. We choose $\tilde{\kappa}>2c_\varepsilon^d\kappa^{1/\delta}\vee 2I_\rho$. Since $\delta>1$, the term

$$\rho\big(c_\varepsilon^{-d}\kappa^{-1/\delta}(t_{k-1}\wedge t_k)^{\gamma}(t_{k-1}\vee t_k)^{1-\gamma}\,|x-y|^{d(1-\varepsilon)}\big)$$

can be bounded by $c_\varepsilon^d\kappa^{1/\delta}(t_{k-1}\wedge t_k)^{-\gamma}(t_{k-1}\vee t_k)^{\gamma-1}\,|x-y|^{-d(1-\varepsilon)}$ and therefore there exists a constant $a>0$ such that we have

$$\begin{aligned}
&\int_{(\mathbb{R}^d)^{n-1}}\bigotimes_{i=1}^{n-1}\mathrm{d}x_i\mathbb{P}_{\mathbf{x},\mathbf{x}_1,\ldots,\mathbf{x}_{n-1},\mathbf{y}}\{\mathbf{x}\sim\mathbf{x}_1\sim\ldots\sim\mathbf{x}_{n-1}\sim\mathbf{y}\}\\
&\leq|x-y|^{-a}\prod_{k=1}^{n}\tilde{\kappa}(t_{k-1}\wedge t_k)^{-\gamma}(t_{k-1}\vee t_k)^{\gamma-1}.
\end{aligned}$$

□

By Remark 2.3.1, with Lemma 2.8 and Fubini's theorem we obtain

$$\mathbb{P}_{\mathbf{x},\mathbf{y}}(B_n^{(\mathbf{x},\mathbf{y})})\leq|x-y|^{-a}\int_{\ell_1}^{1}\mathrm{d}t_1\cdots\int_{\ell_{\lfloor\frac{n}{2}\rfloor}}^{1}\mathrm{d}t_{\lfloor\frac{n}{2}\rfloor}\cdots\int_{\ell_1}^{1}\mathrm{d}t_{n-1}\prod_{k=1}^{n}\tilde{\kappa}(t_{k-1}\wedge t_k)^{-\gamma}(t_{k-1}\vee t_k)^{\gamma-1},$$

where $\mathbf{x} = (x, t_0)$ and $\mathbf{y} = (y, t_n)$. We define,

$$\begin{aligned}\nu_n^{\mathbf{x}}(s) = &\int_{\ell_1}^{1} \mathrm{d}t_1 \cdots \int_{\ell_{n-1}}^{1} \mathrm{d}t_{n-1} \\ &\tilde{\kappa}(t_{n-1} \wedge s)^{-\gamma}(t_{n-1} \vee s)^{\gamma-1} \prod_{k=1}^{n-1} \tilde{\kappa}(t_{k-1} \wedge t_k)^{-\gamma}(t_{k-1} \vee t_k)^{\gamma-1}\end{aligned} \tag{2.35}$$

and set $\nu_0^{\mathbf{x}}(s) = \delta_0(t - s)$. Then, the inequality above can be rewritten as

$$\mathbb{P}_{\mathbf{x},\mathbf{y}}(B_n^{(\mathbf{x},\mathbf{y})}) \leq |x - y|^{-a} \int_{\ell_{\lfloor \frac{n}{2} \rfloor}}^{1} \mathrm{d}s \nu_{\lfloor \frac{n}{2} \rfloor}^{\mathbf{x}}(s) \nu_{n-\lfloor \frac{n}{2} \rfloor}^{\mathbf{y}}(s).$$

Note that as defined, $\nu_n^{\mathbf{x}}(s)$ can be written recursively as

$$\nu_n^{\mathbf{x}}(s) = \int_{\ell_{n-1}}^{1} \mathrm{d}u \, \nu_{n-1}^{\mathbf{x}}(u) \tilde{\kappa}(u \wedge s)^{-\gamma}(u \vee s)^{\gamma-1}. \tag{2.36}$$

This allows us to establish an upper bound for $\nu_n^{\mathbf{x}}(s)$ analogous to the non-spatial case in [35]. The following lemma is a corollary of [35, Lemma 1].

Lemma 2.9

Let $(\ell_n)_{n\in\mathbb{N}}$ be a given non-increasing sequence and $\nu_n^{\mathbf{x}}(s)$ be as defined in (2.35), where $\mathbf{x} = (x, t)$ and $s \in (0, 1)$. Then, there exists a constant $c > 0$ such that, for all $n \in \mathbb{N}$,

$$\nu_n^{\mathbf{x}}(s) \leq \alpha_n s^{-\gamma} + \beta_n s^{\gamma-1}, \tag{2.37}$$

where

$$\begin{aligned}\alpha_{n+1} &= c\big(\alpha_n \log\left(\tfrac{1}{\ell_n}\right) + \beta_n\big) \\ \beta_{n+1} &= c\big(\alpha_n \ell^{1-2\gamma} + \beta_n \log\left(\tfrac{1}{\ell_n}\right)\big)\end{aligned} \tag{2.38}$$

and $\alpha_1 = \tilde{\kappa} t^{\gamma-1}$, $\beta_1 = \tilde{\kappa} t^{-\gamma}$.

Proof. For $n = 1$, we have by (2.35) that

$$\nu_1^{\mathbf{x}}(s) = \tilde{\kappa}(t \wedge s)^{-\gamma}(t \vee s)^{\gamma-1} = \mathbf{1}_{\{s \le t\}}\tilde{\kappa}s^{-\gamma}t^{\gamma-1} + \mathbf{1}_{\{s>t\}}\tilde{\kappa}t^{-\gamma}s^{\gamma-1} \le \alpha_1 s^{-\gamma} + \beta_1 s^{\gamma-1}.$$

Assume (2.37) holds for $n \in \mathbb{N}$. Then, by (2.36), we have that

$$\begin{aligned}
\nu_{n+1}^{\mathbf{x}}(s) &= \int_{\ell_n}^{1} \mathrm{d}u \nu_n^{\mathbf{x}}(u)\tilde{\kappa}(u \wedge s)^{-\gamma}(u \vee s)^{\gamma-1} \le \int_{\ell_n}^{1} \mathrm{d}u \nu_n^{\mathbf{x}}(u)\tilde{\kappa}\left(s^{-\gamma}u^{\gamma-1} + u^{-\gamma}s^{\gamma-1}\right) \\
&\le \tilde{\kappa}s^{-\gamma}\int_{\ell_n}^{1} \mathrm{d}u \left(\alpha_n u^{-1} + \beta_n u^{2\gamma-2}\right) + \tilde{\kappa}s^{\gamma-1}\int_{\ell_n}^{1} \mathrm{d}u \left(\alpha_n u^{-2\gamma} + \beta_n u^{-1}\right) \\
&\le \tilde{\kappa}s^{-\gamma}\left(\alpha_n \log\left(\tfrac{1}{\ell_n}\right) + \beta_n \frac{1}{2\gamma-1}\right) + \tilde{\kappa}s^{\gamma-1}\left(\alpha_n \frac{1}{2\gamma-1}\ell_n^{1-2\gamma} + \beta_n \log\left(\tfrac{1}{\ell_n}\right)\right) \\
&\le \alpha_{n+1}s^{-\gamma} + \beta_{n+1}s^{\gamma-1}.
\end{aligned}$$

Hence, by induction (2.37) holds for all $n \in \mathbb{N}$. □

Although Lemma 2.9 holds for an arbitrary sequence $(\ell_n)_{n\in\mathbb{N}}$, recall that we have chosen $(\ell_n)_{n\in\mathbb{N}}$ such that (2.32) holds. This implies by (2.33) that there exists a constant $c_1 > 0$ such that

$$\eta_{n+2} \ge c_1 \eta_n^{\gamma/\delta(1-\gamma)} \text{ for all } n \in \mathbb{N}_0, \tag{2.39}$$

where $\eta_n := \ell_n^{-1}$ as before. Additionally, notice that $(\alpha_n)_{n\in\mathbb{N}}$ and $(\beta_n)_{n\in\mathbb{N}}$ are non-decreasing sequences. By Lemma 2.9, we have that

$$\begin{aligned}
\sum_{n=1}^{2\Delta} \mathbb{P}_{\mathbf{x},\mathbf{y}}(B_n^{(\mathbf{x},\mathbf{y})}) &\le |x-y|^{-a} \sum_{n=1}^{2\Delta} \int_{\ell_{\lfloor \frac{n}{2} \rfloor}}^{1} \mathrm{d}s \nu_{\lfloor \frac{n}{2} \rfloor}^{\mathbf{x}}(s)\nu_{n-\lfloor \frac{n}{2} \rfloor}^{\mathbf{y}}(s) \\
&\le 2\,|x-y|^{-a} \sum_{n=1}^{\Delta} \int_{\ell_n}^{1} \mathrm{d}s \left(\alpha_n s^{-\gamma} + \beta_n s^{\gamma-1}\right)^2 \\
&\le \frac{4}{2\gamma-1}\,|x-y|^{-a} \sum_{n=1}^{\Delta} \alpha_n^2 \ell_n^{1-2\gamma} + \beta_n^2.
\end{aligned}$$

It follows from the definition of $(\alpha_n)_{n\in\mathbb{N}}$ and $(\beta_n)_{n\in\mathbb{N}}$ that $\beta_n \le c^{-1}\alpha_{n+1}$ and

$$\beta_n \le c\big(\alpha_n \ell_n^{1-2\gamma} + \alpha_n \log\big(\tfrac{1}{\ell_n}\big)\big),$$

where the second summand on the right-hand side is bounded by a multiple of the first. Therefore, there exists a constant $c_2 > 0$ such that $\beta_n^2 \le c_2 \alpha_{n+1}^2 \ell_{n+1}^{1-2\gamma}$. This and the monotonicity of the sequences $(\alpha_n)_{n\in\mathbb{N}}$ and $(\ell_n)_{n\in\mathbb{N}}$ gives that

$$\sum_{n=1}^{2\Delta} \mathbb{P}_{\mathbf{x},\mathbf{y}}(B_n^{(\mathbf{x},\mathbf{y})}) \le \frac{4(1+c_2)}{2\gamma-1}\,|x-y|^{-a} \sum_{n=1}^{\Delta} \alpha_{n+1}^2 \ell_{n+1}^{1-2\gamma}. \tag{2.40}$$

Recall that the sequence $(C_n)_{n\in\mathbb{N}}$ from Lemma 2.7 is defined as

$$C_{n+2} = c^2 \ell_n^{1-\gamma-\gamma/\delta} C_n + c \log\left(\tfrac{1}{\ell_{n+1}}\right) C_{n+1}$$

with $C_1 = c\ell_0^{\gamma-1}$ and $C_2 = c^2\ell_0^{-\gamma/\delta} + c\log(\frac{1}{\ell_1})C_1$. We compare this sequence to $(\alpha_n)_{n\in\mathbb{N}}$ in order to bound (2.40) further. By writing α_{n+2} in terms of α_n and β_n we have that

$$\alpha_{n+2} = c^2\left(\alpha_n\big(\ell_n^{1-2\gamma} + \log(\tfrac{1}{\ell_{n+1}})\log(\tfrac{1}{\ell_n})\big) + \beta_n\big(\log(\tfrac{1}{\ell_{n+1}}) + \log(\tfrac{1}{\ell_n})\big)\right).$$

As all summands on the right-hand side are bounded by a multiple of $\alpha_n\ell_n^{1-2\gamma}\log(1/\ell_{n+1})$ and $\log(1/\ell_{n+1})$ is smaller than a multiple of $\log(1/\ell_n)$, there exists a constant c_3 such that $\alpha_{n+2} \le c_3\alpha_n\ell_n^{1-2\gamma}\log(1/\ell_n)$. To compare $(\alpha_n)_{n\in\mathbb{N}}$ and $(C_n)_{n\in\mathbb{N}}$, notice that, up to a constant, α_1 and α_2 are equal to C_1 and C_2. Moreover

$$\frac{\alpha_{n+2}}{C_{n+2}} \le \frac{c_3\ell_n^{1-2\gamma}\log\left(\frac{1}{\ell_n}\right)\alpha_n}{c^2\ell_n^{1-\gamma-\gamma/\delta}C_n} = \frac{c_3}{c^2}\ell_n^{\gamma/\delta-\gamma}\log\left(\tfrac{1}{\ell_n}\right)\frac{\alpha_n}{C_n}.$$

Applying this inequality recursively and expressing α_{n+2} we obtain that for some $c_4 > 0$

$$\alpha_n \le C_n \prod_{i=1}^{\lceil \frac{n}{2}\rceil - 1} c_4 \ell_{n-2i}^{\gamma/\delta-\gamma}\log\left(\tfrac{1}{\ell_{n-2i}}\right) \quad \text{for all } n\in\mathbb{N}.$$

Hence, we have

$$\alpha_{n+1}^2 \ell_{n+1}^{1-2\gamma} \leq C_{n+1}^2 \ell_{n+1}^{1-2\gamma} \prod_{i=1}^{\lceil \frac{n+1}{2} \rceil - 1} c_4^2 \ell_{n+1-2i}^{2(\gamma/\delta-\gamma)} \log\left(\frac{1}{\ell_{n+1-2i}}\right)^2$$

$$\leq \left(\frac{3\varepsilon(1-\gamma)}{\pi^2(n+1)^2}\right)^2 \ell_{n+1}^{-1} \ell_{n+1}^{2(\gamma/\delta-\gamma)\sum_{i=1}^{\lceil \frac{n+1}{2} \rceil - 1}(\delta(1-\gamma)/\gamma)^i} \prod_{i=1}^{\lceil \frac{n+1}{2} \rceil - 1} c_1^{\sum_{j=1}^{i}(\delta(1-\gamma)/\gamma)^i} c_4^2 \log\left(\frac{1}{\ell_{n+1-2i}}\right)^2,$$

where the second inequality follows by (2.32) and (2.39). Observe that, as $\frac{\delta(1-\gamma)}{\gamma} < 1$, the series $\sum_{i=1}^{\infty} (\delta(1-\gamma)/\gamma)^i$ converges. Hence, there exists a constant which is larger than c_1 to the power $\sum_{j=1}^{i}(\delta(1-\gamma)/\gamma)^i$ for any $i \in \mathbb{N}$ and a constant $c_5 > 0$ such that

$$\ell_{n+1}^{2(\gamma/\delta-\gamma)\sum_{i=1}^{\lceil \frac{n+1}{2} \rceil - 1}(\delta(1-\gamma)/\gamma)^i} \leq \ell_{n+1}^{-c_5}.$$

Furthermore since we have established that η_n is of the order displayed in (2.34) it follows directly that the left-hand side multiplied with the product above can also be bounded by $\ell_{n+1}^{-c_5}$ for any sufficiently large constant $c_5 > 0$. Hence, there exists a further constant $c_6 > 0$ such that $\frac{4(1+c_2)}{2\gamma-1}\alpha_{n+1}^2 \ell_{n+1}^{1-2\gamma} \leq \frac{c_6}{(n+1)^4}\ell_{n+1}^{-(1+c_5)}$. Therefore, we have by using (2.34) once more that

$$\sum_{n=1}^{2\Delta} \mathbb{P}_{\mathbf{x},\mathbf{y}}(B_n^{(\mathbf{x},\mathbf{y})}) \leq \frac{c_6}{(\Delta+1)^3} |x-y|^{-a} \ell_{\Delta+1}^{-(1+c_5)}$$

$$\leq \frac{c_6 b}{(\Delta+1)^3} |x-y|^{-a} \exp\left(B(1+c_5)\left(\frac{\gamma}{\delta(1-\gamma)}\right)^{\frac{\Delta+1}{2}}\right).$$

Let $D > 0$ such that $B(1+c_5)(\gamma/(\delta(1-\gamma)))^{\frac{1-D}{2}} < a$ and choose $\Delta \leq \frac{2\log\log|x-y|}{\log(\gamma/\delta(1-\gamma)))} - D$. Then the above expression is of order $\mathcal{O}(\log\log|x-y|^{-2})$. Hence, for our choice of Δ, we have

$$\mathbb{P}_{\mathbf{x},\mathbf{y}}\{\mathrm{d}(\mathbf{x},\mathbf{y}) \leq 2\Delta\} \leq \varepsilon + \mathcal{O}\left(\log\log|x-y|^{-2}\right),$$

which implies the stated lower bound of Theorem 2.1(b).

2.3.4 The non-ultrasmall regime

In this section we consider the case $\gamma < \frac{\delta}{\delta+1}$ and show that the graph is not ultrasmall, i.e. the chemical distance in the graph is not of double logarithmic order of the Euclidean distance. In particular, we show the following.

Proposition 2.10

Let $\mathscr{G}$ be a geometric random graph which satisfies Assumption UBA for some $\delta > 1$ and $0 < \gamma < \frac{\delta}{\delta+1}$. Then, for any $p > 1$, there exists $c > 0$ such that, for $\mathbf{x}, \mathbf{y} \in \mathbb{R}^d \times (0,1)$, we have

$$\mathrm{d}(\mathbf{x}, \mathbf{y}) \geq c \frac{\log |x - y|}{(\log \log |x - y|)^p}$$

under $\mathbb{P}_{\mathbf{x},\mathbf{y}}$ with high probability as $|x - y| \to \infty$.

The proof is structurally analogous to the ultrasmall case, but significantly easier due to the simpler nature of the dominating strategy. As in Section 2.3.3, we bound the probabilities in (TMB) using a suitable truncation sequence $(\ell_n)_{n\in\mathbb{N}_0}$ such that the probability that bad paths starting in a vertex $\mathbf{x}$ exist can be made arbitrarily small. In this case, however, the truncation sequence decreases only exponentially. Similarly to the ultrasmall case, we construct a graph $\tilde{\mathscr{G}}$ which contains a copy of $\mathscr{G}$ and additionally an edge is added between two vertices $\mathbf{x} = (x, t)$ and $\mathbf{y} = (y, s)$ of $\tilde{\mathscr{G}}$ whenever

$$|x - y|^d \leq \kappa^{1/\delta} (t \wedge s)^{-\gamma} (t \vee s)^{\gamma - 1}.$$

Unlike done previously in Section 2.3.3, we assign no conductance to any edge in $\tilde{\mathscr{G}}$ and therefore only consider the lengths of paths. We declare a self-avoiding path $P = (\mathbf{x}_0, \ldots, \mathbf{x}_n)$ in $\tilde{\mathscr{G}}$ *step minimizing* if there exists no edge between $\mathbf{x}_i$ and $\mathbf{x}_j$ for all i, j with $|i - j| \geq 2$ and denote by $\tilde{A}_n^{\mathbf{x}}$ the event that there exists a step minimizing path starting in $\mathbf{x}$ of length n in $\tilde{\mathscr{G}}$, where the final vertex is the first vertex which has a mark smaller than the corresponding ℓ_n. Then the first two summands of the right-hand side of (TMB) can be bounded from above by $\sum_{n=1}^{\Delta} \mathbb{P}_{\mathbf{x}}(\tilde{A}_n^{(\mathbf{x})})$ and $\sum_{n=1}^{\Delta} \mathbb{P}_{\mathbf{y}}(\tilde{A}_n^{(\mathbf{y})})$, since for any path implying the event $A_n^{(\mathbf{x})}$ there exists a step minimizing path in $\tilde{\mathscr{G}}$ of smaller or equal length which also

fails to be good on its last vertex.

To bound these probabilities, we define the random variable $N(\mathbf{x}, \mathbf{y}, n)$ as the number of distinct step minimizing paths between $\mathbf{x}$ and $\mathbf{y}$ of length n, whose vertices $(x_1, t_1), \dots (x_{n-1}, t_{n-1})$ fulfill $t \geq \ell_0, t_1 \geq \ell_1, \dots, t_{n-1} \geq \ell_{n-1}$ and which all have a larger mark than $\mathbf{y}$. By Mecke's equation we have that

$$\mathbb{P}_{\mathbf{y}}(\tilde{A}_n^{(\mathbf{y})}) \leq \int_{\mathbb{R}^d \times (0,\ell_n]} dy\, \mathbb{E}_{\mathbf{x},\mathbf{y}} N(\mathbf{x}, \mathbf{y}, n), \qquad \text{for } n \in \mathbb{N}.$$

As before, the paths counted in $N(\mathbf{x}, \mathbf{y}, n)$ can be decomposed such that (2.21) holds, where $K(\mathbf{x}, \mathbf{y}, k)$ is the number of step minimizing paths between $\mathbf{x}$ and $\mathbf{y}$ of length k such that the vertices $\mathbf{x}_1, \dots, \mathbf{x}_{k-1}$ between them have marks larger than $\mathbf{x}$ and $\mathbf{y}$. We again refer to such vertices as connectors. Note that if $|x - y|^d \leq \kappa^{1/\delta}(t \wedge s)^{-\gamma}(t \vee s)^{\gamma-1}$, there exists no step minimizing paths of length larger or equal two between $\mathbf{x}$ and $\mathbf{y}$. Hence, we have $N(\mathbf{x}, \mathbf{y}, n) = K(\mathbf{x}, \mathbf{y}, n) = 0$ for $n \geq 2$ under this assumption.

We now bound the expectation of $K(\mathbf{x}, \mathbf{y}, k)$. As in Section 2.3.3, we define a mapping

$$e_K : (\mathbb{R}^d \times (0,1))^2 \times \mathbb{N} \to [0, \infty),$$

where $e_K(\mathbf{x}, \mathbf{y}, 1) = \rho(\kappa^{-1/\delta}(t \wedge s)^{\gamma}(t \vee s)^{1-\gamma} |x - y|^d)$, for $\mathbf{x}, \mathbf{y} \in \mathbb{R}^d \times (0,1)$ and

$$e_K(\mathbf{x}, \mathbf{y}, k) = \sum_{i=1}^{k-1} \int_{\mathbb{R}^d \times (t \vee s, 1)} \mathrm{d}\mathbf{z}\, e_K(\mathbf{x}, \mathbf{z}, i) e_K(\mathbf{z}, \mathbf{y}, k-i), \quad \text{for } k \geq 2, \mathbf{x}, \mathbf{y} \in \mathbb{R}^d \times (0,1),$$

if $|x - y|^d > \kappa^{1/\delta}(t \wedge s)^{-\gamma}(t \vee s)^{\gamma-1}$ and otherwise $e_K(\mathbf{x}, \mathbf{y}, k) = 0$. As before we use a binary tree to classify the connection strategies and use this together with Assumption UBA to obtain $\mathbb{E}_{\mathbf{x},\mathbf{y}} K(\mathbf{x}, \mathbf{y}, k) \leq e_K(\mathbf{x}, \mathbf{y}, k)$, for $k \in \mathbb{N}$.

Lemma 2.11

Let $\mathbf{x} = (x,t), \mathbf{y} = (y,s)$ be vertices with $|x-y|^d > \kappa^{1/\delta}(t \wedge s)^{-\gamma}(t \vee s)^{\gamma-1}$. Then there exists $C > 1$ such that, for $k \geq 2$, we have

$$e_K(\mathbf{x}, \mathbf{y}, k) \leq C^{k-1}\kappa(t \wedge s)^{-\gamma\delta}(t \vee s)^{(\gamma-1)\delta} |x-y|^{-d\delta}.$$

Proof. By [58, Lemma 2.2] there exists a constant $C > 1$ such that if $|x-y|^d > \kappa^{1/\delta}(t \wedge s)^{-\gamma}(t \vee s)^{\gamma-1}$ we have

$$\begin{aligned} e_K(\mathbf{x}, \mathbf{y}, 2) \leq & \int_{\mathbb{R}^d \times (t \vee s, 1]} \mathrm{d}\mathbf{z} \rho(\kappa^{-1/\delta} t^\gamma u^{1-\gamma} |x-z|^d) \rho(\kappa^{-1/\delta} s^\gamma u^{1-\gamma} |y-z|^d) \\ \leq & C\kappa(t \wedge s)^{-\gamma\delta}(t \vee s)^{(\gamma-1)\delta} |x-y|^{-d\delta}. \end{aligned} \tag{2.41}$$

We now show by induction that

$$e_K(\mathbf{x}, \mathbf{y}, k) \leq \mathrm{Cat}(k-1) C^{k-1}\kappa(t \wedge s)^{-\gamma\delta}(t \vee s)^{(\gamma-1)\delta} |x-y|^{-d\delta} \tag{2.42}$$

holds for all $k \geq 2$. This is sufficient, since $\mathrm{Cat}(k) \leq 4^k$. For $k = 2$ this follows from (2.41). Let $k \geq 3$ and assume (2.42) holds for all $j = 2, \ldots, k-1$. For $|x-y|^d > \kappa^{1/\delta}(t \wedge s)^{-\gamma}(t \vee s)^{\gamma-1}$ this, together with the definition of $e_K(\mathbf{x}, \mathbf{y}, k)$, yields

$$\begin{aligned} e_K(\mathbf{x}, \mathbf{y}, k) \leq & \sum_{i=1}^{k-1} \mathrm{Cat}(i-1)\,\mathrm{Cat}(k-i-1) C^{k-2} \times \\ & \int_{\mathbb{R}^d \times (t \vee s, 1]} \mathrm{d}\mathbf{z}\, \rho(\kappa^{-1/\delta} t^\gamma u^{1-\gamma} |x-z|^d) \rho(\kappa^{-1/\delta} s^\gamma u^{1-\gamma} |y-z|^d). \end{aligned}$$

With (2.41) the right-hand side can be further bounded by

$$\sum_{i=1}^{k-1} \mathrm{Cat}(i-1)\,\mathrm{Cat}(k-i-1) C^{k-1}\kappa(t \wedge s)^{-\gamma\delta}(t \vee s)^{(\gamma-1)\delta} |x-y|^{-d\delta}.$$

As $\sum_{i=1}^{k-1} \mathrm{Cat}(i-1)\,\mathrm{Cat}(k-i-1) = \mathrm{Cat}(k-1)$ we get that (2.42) holds for k. □

Probability bounds for bad paths Using Lemma 2.11 and (2.21) we find a suitable upper bound for $\int_{\mathbb{R}^d} \mathbb{E}_{\mathbf{x},\mathbf{y}} N(\mathbf{x},\mathbf{y},n)\mathrm{d}y$, with $\mathbf{y}=(y,s)$, which leads to a bound for $\mathbb{P}_{\mathbf{x}}(\tilde{A}_n^{\mathbf{x}})$. Recall that by (2.21) we have, for $n\in\mathbb{N}$,

$$N(\mathbf{x},\mathbf{y},n) \le K(\mathbf{x},\mathbf{y},n) + \sum_{k=1}^{n-1} \sum_{\substack{\mathbf{z}=(z,u)\\ t>u>\ell_{n-k}\vee s}} N(\mathbf{x},\mathbf{z},n-k)K(\mathbf{z},\mathbf{y},k).$$

As in Section 2.3.3, to establish an upper bound on $\mathbb{E}_{\mathbf{x},\mathbf{y}} N(\mathbf{x},\mathbf{y},n)$, we define a mapping

$$e_N\colon (\mathbb{R}^d\times(0,1))^2\times\mathbb{N}\to[0,\infty),$$

by setting $e_N(\mathbf{x},\mathbf{y},1)=\rho(\kappa^{-1/\delta}(t\wedge s)^{\gamma}(t\vee s)^{1-\gamma}\,|x-y|^d)$, for $\mathbf{x},\mathbf{y}\in\mathbb{R}^d\times(0,1)$, and for $n\ge 2$ if $|x-y|^d>\kappa^{1/\delta}(t\wedge s)^{-\gamma}(t\vee s)^{\gamma-1}$ we set $e_N(\mathbf{x},\mathbf{y},n)$ to be

$$e_N(\mathbf{x},\mathbf{y},n) + \sum_{i=1}^{n-1} \int_{\mathbb{R}^d\times(\ell_{n-k}\vee s,t]} \mathrm{d}\mathbf{z}\, e_N(\mathbf{x},\mathbf{z},n-k)e_K(\mathbf{z},\mathbf{y},k), \quad \text{for } \mathbf{x},\mathbf{y}\in\mathbb{R}^d\times(0,1), \tag{2.43}$$

and otherwise $e_N(\mathbf{x},\mathbf{y},n)=0$. As in Section 2.3.3 we have $\mathbb{E}_{\mathbf{x},\mathbf{y}} N(\mathbf{x},\mathbf{y},n)\le e_N(\mathbf{x},\mathbf{y},n)$, for $n\in\mathbb{N}$. Thus, for a given vertex $\mathbf{x}=(x,t)$ and $n\in\mathbb{N}$, an upper bound of $\int_{\mathbb{R}^d}\mathrm{d}y\mathbb{E}_{\mathbf{x},\mathbf{y}}N(\mathbf{x},\mathbf{y},n)$ is given by the mapping $\mu_n^{\mathbf{x}}:(0,t]\to[0,\infty)$ defined by

$$\mu_n^{\mathbf{x}}(s) := \int_{\mathbb{R}^d} \mathrm{d}y\, e_N(\mathbf{x},\mathbf{y},n), \quad \text{for } s\in(0,t], \tag{2.44}$$

where $\mathbf{y}=(y,s)$. We interpret s as the mark of the last vertex of a path counted by the random variable $N(\mathbf{x},\mathbf{y},n)$. With $I_\rho=\int \mathrm{d}x\rho(\kappa^{-1/\delta}\,|x|^d)$ we can see by the definition of $e_N(\mathbf{x},\mathbf{y},1)$ that $\mu_1^{\mathbf{x}}(s)\le I_\rho s^{-\gamma}t^{\gamma-1}$ for $s\in(0,t]$ and for $n\ge 2$ it follows by a short calculation and Lemma 2.11 that

$$\mu_n^{\mathbf{x}}(s) \le I_\rho C^{n-1}s^{-\gamma}t^{\gamma-1} + \sum_{k=1}^{n-1} I_\rho C^{k-1}s^{-\gamma}\int_{\ell_{n-k}}^{t} \mathrm{d}u\mu_{n-k}^{\mathbf{x}}(u)u^{\gamma-1} \quad \text{for } s\in(0,t],$$

where $C>1$ is the constant from Lemma 2.11. To establish a bound for $\mu_n^{\mathbf{x}}$ no further assumptions on the truncation sequence $(\ell_n)_{n\in\mathbb{N}_0}$ are necessary. As discussed in Section 2.3.2 we will see that the major contribution to the mass of $\mu_n^{\mathbf{x}}(s)$ comes from the paths where the two most powerful vertices are connected

directly and not via one or more connectors. This is indicated by the definition of the sequence $(C_n)_{n\in\mathbb{N}_0}$ and the inequality (2.46) in the proof of the following lemma.

Lemma 2.12

Let $\mathbf{x} = (x, t)$ be a given vertex and let the sequence $(\ell_n)_{n\in\mathbb{N}_0}$ be monotonically decreasing with $\ell_0 < t \wedge \frac{1}{e}$. Then, there exists $c > 0$ such that, for $n \in \mathbb{N}$,

$$\mu_n^{\mathbf{x}}(s) \le C_n s^{-\gamma} \quad \text{for } s \in (0, t], \tag{2.45}$$

where $C_1 = c\ell_0^{\gamma-1}$ and $C_{n+1} = c\log(\frac{1}{\ell_n})C_n$.

Proof. We choose the constant $c > 2(C \vee I_\rho)$, where C is as in Lemma 2.11. Then by definition of $\mu_1^{\mathbf{x}}$ we have $\mu_1^{\mathbf{x}}(s) = I_\rho s^{-\gamma} t^{\gamma-1} \le cs^{-\gamma}\ell_0^{\gamma-1} = C_1 s^{-\gamma}$ for $s \in (0, t]$. Let $n \ge 2$ and assume that (2.45) holds for all $\tilde{n} \le n-1$. Then, by (2.45),

$$\begin{aligned}\mu_n^{\mathbf{x}}(s) &= I_\rho C^{n-1} s^{-\gamma} t^{\gamma-1} + \sum_{k=1}^{n-1} I_\rho C^{k-1} s^{-\gamma} \int_{\ell_{n-k}}^{t} \mathrm{d}u \mu_{n-k}^{\mathbf{x}}(u) u^{\gamma-1} \\ &= I_\rho s^{-\gamma}\Big(C^{n-1}\ell_0^{\gamma-1} + \sum_{k=1}^{n-1} C_{n-k} C^{k-1} \log\big(\tfrac{1}{\ell_{n-k}}\big)\Big).\end{aligned}$$

We now want to show that

$$C^{n-1}\ell_0^{\gamma-1} + \sum_{k=1}^{n-1} C_{n-k} C^{k-1} \log\left(\tfrac{1}{\ell_{n-k}}\right) \le 2\log\left(\tfrac{1}{\ell_{n-1}}\right) C_{n-1}, \tag{2.46}$$

since assuming this leads to $\mu_n^{\mathbf{x}}(s) \le 2I_\rho \log(\frac{1}{\ell_{n-1}})C_{n-1}s^{-\gamma} \le c\log(\frac{1}{\ell_{n-1}})C_{n-1}s^{-\gamma}$ $= C_n s^{-\gamma}$, which completes the proof. By definition of the constants C_n we have that

$$C^{n-1}\ell_0^{\gamma-1} + \sum_{k=1}^{n-1} C_{n-k} C^{k-1} \log(\tfrac{1}{\ell_{n-k}}) \le \log(\tfrac{1}{\ell_{n-1}})C_{n-1} + \frac{1}{2}\sum_{k=2}^{n} C^{k-2} C_{n-k+1}.$$

As $\log(\frac{1}{\ell_n}) > 1$, for all $n \in \mathbb{N}_0$, we have $C_{n+1} \ge cC_n$ by definition of $(C_n)_{n\in\mathbb{N}_0}$,

and using that $c > 2C$, the right-hand side can be further bounded by

$$\log\left(\tfrac{1}{\ell_{n-1}}\right)C_{n-1} + \sum_{k=2}^{n}\left(\tfrac{1}{2}\right)^{k-1}c^{k-2}C_{n-k+1} \leq 2\log\left(\tfrac{1}{\ell_{n-1}}\right)C_{n-1},$$

which shows (2.46). □

Now we bound the probability of the event $\tilde{A}_n^{(\mathbf{x})}$, i.e. the event that there exists a path of length n, where the last vertex is the only vertex which has a mark smaller than its truncation bound ℓ_n. As in Section 2.3.3, Mecke's equation yields

$$\mathbb{P}(\tilde{A}_n^{(\mathbf{x})}) \leq \int_{\mathbb{R}^d\times(0,\ell_n]} \mathrm{d}\mathbf{y}\mathbb{E}_{\mathbf{x},\mathbf{y}}N(\mathbf{x},\mathbf{y},n) \leq \int_0^{\ell_n} \mathrm{d}s\mu_n^{\mathbf{x}}(s) \leq \frac{1}{1-\gamma}\ell_n^{1-\gamma}C_n,$$

where we have used Fubini's theorem in the second inequality and Lemma 2.12 in the third one. With $\ell_0 < t \wedge \frac{1}{e}$ we choose the sequence $(\ell_n)_{n\in\mathbb{N}}$ for $\epsilon > 0$, such that

$$\frac{1}{1-\gamma}C_n\ell_n^{1-\gamma} = \frac{\varepsilon}{\pi^2 n^2},$$

and get $P(\tilde{A}_n^{(\mathbf{x})}) \leq \frac{\varepsilon}{6}$. From the recursive definition of the sequence (C_n) we obtain a recursive representation of $(\ell_n)_{n\in\mathbb{N}_0}$. Let $\eta_n := \ell_n^{-1}$ for $n \in \mathbb{N}_0$, then

$$\eta_{n+1}^{1-\gamma} = \tfrac{\pi^2(n+1)^2}{3\varepsilon}\tfrac{1}{1-\gamma}C_{n+1} \quad = \tfrac{\pi^2(n+1)^2}{3\varepsilon}\tfrac{1}{1-\gamma}\left(c\log(\eta_n)C_n\right) = \tfrac{(n+1)^2}{n^2}c\log(\eta_{n+1})\eta_{n+1}^{1-\gamma}.$$

Hence, there exists a new constant $c > 0$ such that $\eta_{n+1}^{1-\gamma} \leq c\log(\eta_{n+1})\eta_{n+1}^{1-\gamma}$ and by induction we get that for any $p > 1$ there exists $B > 1$ large enough such that

$$\eta_n \leq B^{n\log^p(n+1)}. \tag{2.47}$$

Probability bounds for good paths We now consider the existence of good paths between two given vertices $\mathbf{x}$ and $\mathbf{y}$. We focus on the case $\gamma \in (\frac{1}{2}, \frac{\delta}{\delta+1})$, as the cases $\gamma = \frac{1}{2}$ and $\gamma < \frac{1}{2}$ follow with analogous or simpler arguments. As before we restrict the event $B_n^{\mathbf{x},\mathbf{y}}$ to the existence of a step minimizing good path of length n connecting $\mathbf{x}$ and $\mathbf{y}$ in $\tilde{\mathscr{G}}$. Deviating a bit from the method of Section 2.3.3 we relax the definition of $B_n^{\mathbf{x},\mathbf{y}}$ by defining $\tilde{B}_n^{\mathbf{x},\mathbf{y}}$ as the event that there exists a step minimizing path between $\mathbf{x}$ and $\mathbf{y}$ in $\tilde{\mathscr{G}}$ where the most powerful

vertex of the path has a mark larger than $\ell_{\lfloor \frac{n}{2} \rfloor}$. Then the term $\sum_{n=1}^{2\Delta} \mathbb{P}_{\mathbf{x},\mathbf{y}}(B_n^{\mathbf{x},\mathbf{y}})$ in (TMB) can be replaced by $\sum_{n=1}^{2\Delta} \mathbb{P}_{\mathbf{x},\mathbf{y}}(\tilde{B}_n^{\mathbf{x},\mathbf{y}})$.

We characterize the paths used in $\tilde{B}_n^{\mathbf{x},\mathbf{y}}$ by their powerful vertices, as done for regular paths in [58]. A vertex $\mathbf{x}_k$ of a path $(\mathbf{x}_0, \dots, \mathbf{x}_n)$ is *powerful* if $t_i \geq t_k$ for all $i = 0, \dots, k-1$ or if $t_i \geq t_k$ for all $i = k+1, \dots, n$. Note that by definition the vertices $\mathbf{x} = \mathbf{x}_0$ and $\mathbf{y} = \mathbf{x}_n$ are always powerful. The indices of the powerful vertices are a subset of $\{0, \dots, n\}$ which we denote by $\{i_0, i_1, \dots, i_{m-1}, i_m\}$, where $m+1$ is the number of powerful vertices in a path and $i_0 = 0$, $i_m = n$. As the most powerful vertex of a good path fulfils the assumption above, there exists a $k \in \{0, \dots, m\}$ such that $\mathbf{x}_{i_k}$ is the most powerful vertex of the path. We decompose the good paths at the powerful vertices first and then proceed to decompose the path between powerful vertices $\mathbf{x}_{i_j}$ and $\mathbf{x}_{i_{j-1}}$ in the same way as done for the random variable $K(\mathbf{x}_{i_{j-1}}, \mathbf{x}_{i_j}, i_j - i_{j-1})$ in Section 2.3.3. Using Mecke's equation, we get

$$
\begin{aligned}
&\mathbb{P}_{\mathbf{x},\mathbf{y}}(\tilde{B}_n^{(\mathbf{x},\mathbf{y})}) \\
&\leq \sum_{m=1}^{n} \sum_{k=0}^{m} \int_{\substack{(\mathbb{R}^d \times (0,1))^{m-1} \\ t_0 > \dots > t_k > \ell_{\lfloor \frac{n}{2} \rfloor} \\ t_k < \dots < t_m}} \bigotimes_{j=1}^{m-1} \mathrm{d}\mathbf{x}_j \sum_{\substack{\{i_1, \dots, i_{m-1}\} \\ \subset \{1, \dots, n-1\}}} \prod_{j=1}^{m} e_K(\mathbf{x}_{i_{j-1}}, \mathbf{x}_{i_j}, i_j - i_{j-1}) \\
&\leq \sum_{m=1}^{n} \binom{n-1}{m-1} C^{n-m} \sum_{k=0}^{m} \int_{\substack{(\mathbb{R}^d \times (0,1))^{m-1} \\ t_0 > \dots > t_k > \ell_{\lfloor \frac{n}{2} \rfloor} \\ t_k < \dots < t_m}} \bigotimes_{j=1}^{m-1} \mathrm{d}\mathbf{x}_j \\
&\qquad \prod_{j=1}^{m} \rho\left(\kappa^{-1/\delta} (t_{j-1} \wedge t_j)^{\gamma} (t_{j-1} \vee t_j)^{1-\gamma} \left|x_j - x_{j-1}\right|^d\right).
\end{aligned}
$$

Then, following the same arguments as in the proof of Lemma 2.8, there exists $a > 0$ and $\tilde{\kappa} > 0$ such that $\mathbb{P}_{\mathbf{x},\mathbf{y}}(\tilde{B}_n^{(\mathbf{x},\mathbf{y})})$ is bounded by

$$
|x-y|^{-a} \sum_{m=1}^{n} \binom{n-1}{m-1} C^{n-m} \tilde{\kappa}^{m-1} \sum_{k=0}^{m} \int_{\substack{(0,1)^{m-1} \\ t_0 > \dots > t_k > \ell_{\lfloor \frac{n}{2} \rfloor} \\ t_k < \dots < t_m}} \bigotimes_{j=1}^{m-1} \mathrm{d}t_j \prod_{j=1}^{m} (t_{j-1} \wedge t_j)^{-\gamma} (t_{j-1} \vee t_j)^{\gamma - 1}.
$$

By a simple calculation[1] the sum over k on the right-hand side can be bounded by a constant multiple of

$$\sum_{k=1}^{m-1} \binom{m-2}{k-1} \frac{\ell_{\lfloor \frac{n}{2} \rfloor}^{1-2\gamma} \log^{m-2}\left(\ell_{\lfloor \frac{n}{2} \rfloor}^{-1}\right)}{(m-2)!} + \frac{2\ell_0^{-1} \log^{m-1}\left(\ell_0^{-1}\right)}{(m-1)!}.$$

Since $\sum_{k=1}^{m-1} \binom{m-2}{k-1} \leq 2^{m-2}$ and the second summand can be bounded by a multiple of the first, there exists a constant $c_1 > 0$ such that $\mathbb{P}_{\mathbf{x},\mathbf{y}}(\tilde{B}_n^{(\mathbf{x},\mathbf{y})})$ is bounded by

$$\begin{aligned} &c_1 |x-y|^{-a} \sum_{m=1}^{n} \binom{n-1}{m-1} C^{n-m} \tilde{\kappa}^{m-1} \frac{\ell_{\lfloor \frac{n}{2} \rfloor}^{1-2\gamma} \log^{m-2}(\ell_{\lfloor \frac{n}{2} \rfloor}^{-1}) 2^{m-2}}{(m-2)!} \\ &\leq c_1 |x-y|^{-a} \sum_{m=1}^{n} \binom{n-1}{m-1} C^{n-m} \tilde{\kappa}^{m-1} B^{(2\gamma-1)\frac{n}{2}} \log^p\left(\tfrac{n+2}{2}\right) \frac{n^{m-2} \log^{p(m-2)}\left(\frac{n+2}{2}\right)}{(m-2)!}, \end{aligned}$$

where we have used (2.47) for the second inequality and denoted $(-1)! = 1$ and $\tilde{\kappa}$ might have changed between the steps. Since

$$\frac{n^{m-2} \log^{p(m-2)}\left(\frac{n+2}{2}\right)}{(m-2)!} \leq \frac{n^{n-2} \log^{p(n-2)}\left(\frac{n+2}{2}\right)}{(n-2)!}$$

for all $m = 1, \ldots, n$ and $\sum_{m=1}^{n} \binom{n-1}{m-1} \leq 2^n$, there exists a constant $c_2 \geq 2(C \vee \tilde{\kappa})$ such that the right-hand side above can be further bounded by

$$c_1 |x-y|^{-a} c_2^n B^{(2\gamma-1)\frac{n}{2}} \log^p\left(\tfrac{n+2}{2}\right) \frac{n^{n-2} \log^{p(n-2)}\left(\frac{n+2}{2}\right)}{(n-2)!}.$$

By Stirling's formula we have that $\frac{n^{n-2}}{(n-2)!} \leq e^n$. Hence, there exists $c_3 > 0$ such that

$$\begin{aligned} \sum_{n=1}^{2\Delta} \mathbb{P}_{\mathbf{x},\mathbf{y}}(\tilde{B}_n^{(\mathbf{x},\mathbf{y})}) &\leq c_1 |x-y|^{-a} \sum_{n=1}^{2\Delta} c_3^n e^{p(n-2)\log\log\left(\frac{n+2}{2}\right)} B^{(2\gamma-1)\frac{n}{2}} \log^p\left(\tfrac{n+2}{2}\right) \\ &\leq c_1 |x-y|^{-a} \, 2\Delta c_3^{2\Delta} e^{p(2\Delta-2)\log\log(\Delta+1)} B^{(2\gamma-1)\Delta \log^p(\Delta+1)}. \end{aligned}$$

We can see that $B^{(2\gamma-1)\Delta \log^p(\Delta+1)}$ dominates the right-hand side in the sense that

[1] For details see the proof of [58, Lemma 2.5], which differs from this calculation only in the fact that the mark of the first and last vertex of a path is fixed in our setting.

there exist constants $c_4, c_5 > 0$ such that

$$\sum_{n=1}^{2\Delta} \mathbb{P}_{\mathbf{x},\mathbf{y}}(\tilde{B}_n^{(\mathbf{x},\mathbf{y})}) \leq c_4 \, |x-y|^{-a} \, B^{c_5 \Delta \log^p(\Delta+1)}$$
$$= c_4 \exp\big(c_5 \log(B) \Delta \log^p(\Delta+1) - \log(|x-y|^a)\big).$$

We now set

$$\Delta \leq \frac{\log(|x-y|^a)}{c_5 \log(B)(\log\log(|x-y|^a))^p} - 1.$$

Then, we have that

$$c_5 \log(B) \Delta \log^p(\Delta+1) - \log(|x-y|^a)$$
$$\leq \log(|x-y|^a)\big(1 - \tfrac{p \log\log\log(|x-y|^a)}{\log\log(|x-y|^a)}\big)^p - \log(|x-y|^a).$$

A second order Taylor expansion shows that the right-hand side converges to $-\infty$ as $|x-y| \to \infty$. Hence, for such a choice of Δ, we have $\mathbb{P}_{\mathbf{x},\mathbf{y}}\{\mathrm{d}(\mathbf{x},\mathbf{y}) \leq 2\Delta\} \leq \varepsilon + o(1)$ which implies the statement of Proposition 2.10.

2.4 Proof of the upper bound for the chemical distance

To prove the upper bound for the chemical distance, we show the following proposition. Throughout this section let $\mathbf{0}$ be a fixed vertex with location 0.

Proposition 2.13

Suppose Assumption LBA holds for $\gamma > \frac{\delta}{\delta+1}$. Then for any vertex $\mathbf{x}$ there exists a path with no more than

$$(4+o(1))\frac{\log\log|x|}{\log\left(\frac{\gamma}{\delta(1-\gamma)}\right)}$$

vertices connecting $\mathbf{0}$ and $\mathbf{x}$, with high probability under $\mathbb{P}_{\mathbf{0},\mathbf{x}}(\ \cdot\ \mid \mathbf{0} \leftrightarrow \mathbf{x})$ as $|x| \to \infty$.

To prove this result, we rely on a strategy introduced in [64]. Since the vertices

of $\mathscr{G}$ are given by the points of a Poisson process, the most powerful vertex inside a box with volume of order $|x|^d$ around the midpoint between $\mathbf{0}$ and $\mathbf{x}$ typically has a mark smaller than $|x|^{-d}\log|x|$. Hence, it is sufficient to construct a short enough path from $\mathbf{0}$ resp. $\mathbf{x}$ to this most powerful vertex inside the box. Here, as in Section 2.3.2, the typical connection type between two powerful vertices is crucial. For $\gamma > \frac{\delta}{\delta+1}$ we expect two powerful vertices to be connected via a vertex with larger mark, which we again call a *connector*. In fact, the following lemma shows that for a powerful vertex with mark t and a suitable vertex with a sufficiently smaller mark, the probability that there exist no connector which neighbours each of the two vertices is decaying exponentially fast as the mark t gets small. This is a corollary of [64] and follows with the same calculations as in [58, Lemma 3.1]. We now fix for the rest of the section

$$\alpha_1 \in \big(1, \tfrac{\gamma}{\delta(1-\gamma)}\big) \quad \text{and} \quad \alpha_2 \in \big(\alpha_1, \tfrac{\gamma}{\delta}(1+\alpha_1\delta)\big)\,,$$

noting that our assumptions ensure that the intervals are nonempty.

Lemma 2.14

There exists $c > 0$ such that for two given vertices $\mathbf{x} = (x,t), \mathbf{y} = (y,s) \in \mathcal{X}$ with $t, s \le \frac{1}{4}$, $s \le t^{\alpha_1}$ and $|x-y|^d \le t^{-\alpha_2}$ we have

$$\mathbb{P}_{\mathbf{x},\mathbf{y}}\{\mathbf{x} \overset{2}{\leftrightarrow} \mathbf{y}\} \ge 1 - \exp\big(-ct^{(\alpha_2-\alpha_1\gamma)\delta-\gamma}\big).$$

Proof. We only consider connectors $\mathbf{z} = (z,u)$ with $u \ge \frac{1}{2}$ and $|x-z| < t^{-\frac{\gamma}{d}}$. Then, by the thinning theorem [76, Theorem 5.2] and Assumption LBA the number of such connectors is Poisson distributed with its mean bounded from below by

$$\int_{\frac{1}{2}}^{1} \mathrm{d}u \int_{B_{t^{-\gamma/d}}(x)} \mathrm{d}z\, \alpha^2 \rho(\kappa^{-1/\delta})\rho(\kappa^{-1/\delta}s^{\gamma}\,|y-z|^d) \\ \ge \frac{\alpha^2\rho(\kappa^{-1/\delta})}{2} t^{-\gamma}\rho(\kappa^{-1/\delta}s^{\gamma}(t^{-\gamma/d}+|x-y|)^d),$$

where $\rho(x) := 1 \wedge x^{-\delta}$ as in the previous section. As $|x-y|^d < t^{-\alpha_2}$ and $s < t^{\alpha_1}$ this can be bounded from below by $ct^{(\alpha_2-\alpha_1\gamma)\delta-\gamma}$, where $c = (\alpha^2\rho(\kappa^{-1/\delta})\kappa 2^{-(d\delta+1)}) \wedge (\alpha^2\rho(\kappa^{-1/\delta})/2)$. □

We now look into a box $H(x) = \frac{x}{2} + [-2|x|, 2|x|]^d$ and introduce a hierarchy of layers $L_1 \subset L_2 \subset \ldots \subset \mathcal{X} \cap H(x) \times (0,1)$ of vertices inside the box containing $\mathbf{0}$ and $\mathbf{x}$. While the layer L_1 only contains vertices with very small mark, vertices with larger and larger marks are included in layers with larger index. More precisely, as in [64] we set

$$L_k = \mathcal{X} \cap H(x) \times \left(0, (4|x|)^{-d\alpha_1^{-k}}\right]$$

and

$$K = \min\left\{k \geq 1 \colon (4|x|)^{-d\alpha_1^{-k}} \geq (\log(4|x|)^d)^{-\eta^{-1}}\right\} - 1,$$

where $\eta = (\gamma - (\alpha_2 - \alpha_1\gamma)\delta) \wedge (\alpha_2 - \alpha_1) > 0$. As the vertex set $\mathcal{X}$ is a Poisson process, by Lemma 2.14 for a given vertex in layer L_{k+1} there exists with high probability a suitable vertex in layer L_k such that both vertices are connected via a connector with high probability. As in [64] and [70] we can use an estimate as in Lemma 2.14 to see that a vertex in L_1 is either the most powerful vertex in the box or connected to it via a connector, with high probability as $|x| \to \infty$. Hence, we get that $\operatorname{diam}(L_K) \leq 4K$.

Since K is of order $(1 + o(1))\frac{\log\log|x|}{\log\alpha_1}$, to finish the proof it suffices to show that the vertices $\mathbf{0}$ and $\mathbf{x}$ are connected to the layer L_K in fewer than $o(\log\log|x|)$ steps. To do so, we first show that $\mathbf{0}$ (resp. $\mathbf{x}$) is connected to a vertex with sufficiently small mark and within distance smaller than $|x|$ in finitely many steps. Then, we show that this vertex is connected to a vertex of L_K in $o(\log\log|x|)$ steps. To keep the existence of these two paths sufficiently independent we rely on a sprinkling argument. For $b < 1$ we assign independently to each vertex in $\mathcal{X}$ the color *black* with probability b and *red* with probability $r = 1 - b$. Then, we denote by $\mathscr{G}^b$ the graph induced by restricting $\mathscr{G}$ to the black vertices and the edges between them. In the same way we define $\mathscr{G}^r$ for the black vertices. Note that $\mathscr{G}^r \cup \mathscr{G}^b$ is a subgraph of $\mathscr{G}$.

We use the black vertices to ensure the existence of the first part of the path in $\mathscr{G}^b$. Thus, we define for $\mathbf{0}$ (and similarly for $\mathbf{x}$) the event $E^b(D, s, v)$ that there exists a black vertex $\mathbf{z}$ with mark smaller than s and within distance shorter than v such that there exists a path in $\mathscr{G}^b$ of length smaller D between $\mathbf{0}$ and $\mathbf{z}$. Then, given $\mathbf{z}$, we use the red vertices to show that $\mathbf{z}$ is connected to the layer L_K in sufficiently few steps. We denote by L_k^r the restriction of L_k to its red vertices.

Observe that we still have $\operatorname{diam}(L_K^r) \leq 4K$ in $\mathscr{G}^r$, as Lemma 2.14 restricted to $\mathscr{G}^r$ also holds if the constant c is multiplied by r. We define F to be the event that $\mathbf{z}$ is connected by a path of length smaller than $o(\log\log|x|)$ to L_K^r in $\mathscr{G}^r$. Note that the event $\mathbf{0} \leftrightarrow \mathbf{x}$ implies that with high probability $\mathbf{0}$ and $\mathbf{x}$ are part of the unique infinite component K_∞ of $\mathscr{G}$, since $\mathbb{P}_{\mathbf{0},\mathbf{x}}(\{\mathbf{0} \leftrightarrow \mathbf{x}\}\backslash\{\mathbf{0},\mathbf{x} \in K_\infty\})$ converges to zero as $|x| \to \infty$. This is a consequence of the uniqueness of the infinite component K_∞ as $\{\mathbf{0} \leftrightarrow \mathbf{x}\}\backslash\{\mathbf{0},\mathbf{x} \in K_\infty\}$ implies that $\mathbf{0}$ and $\mathbf{x}$ are part of the same finite component whose asymptotic proportion of vertices is zero. Thus, to prove Proposition 2.13 it is sufficient to show that for any $s > 0$ there exists a almost surely finite random variable $D(s)$ such that

$$\lim_{b\nearrow 1}\liminf_{s\searrow 0}\liminf_{|x|\to\infty}\mathbb{P}_{\mathbf{0}}\left(\{\mathbf{0} \in K_\infty^b\} \cap E^b(D(s),s,|x|) \cap F\right) \geq \theta$$

where θ is the asymptotic proportion of vertices in the infinite component of $\mathscr{G}$ and K_∞^b is the infinite component of $\mathscr{G}^b$. Note that, as $\gamma > \frac{\delta}{\delta+1}$, the critical percolation parameter of the graph $\mathscr{G}$ is 0 by [58], and therefore K_∞^b exists and is unique. Now the probability above can be bounded from below by

$$\begin{aligned}
&\mathbb{P}_{\mathbf{0}}\left(\{\mathbf{0} \in K_\infty^b\} \cap E^b(D(s),s,|x|) \cap F\right)\\
&\geq \mathbb{P}_{\mathbf{0}}\{\mathbf{0} \in K_\infty^b\} - \mathbb{P}_{\mathbf{0}}\left(\{\mathbf{0} \in K_\infty^b\}\backslash E^b(D(s),s,|x|)\right) - \mathbb{P}_{\mathbf{0}}\left(E^b(D(s),s,|x|)\backslash F\right)\\
&= \mathbb{P}_{\mathbf{0}}\{\mathbf{0} \in K_\infty^b\} - \mathbb{P}_{\mathbf{0}}\left(\{\mathbf{0} \in K_\infty^b\}\backslash E^b(D(s),s,|x|)\right) - \mathbb{E}_{\mathbf{0}}\left[(1-\mathbb{P}_{\mathbf{z}}(F|\mathscr{G}^b))\mathbf{1}_{E^b(D(s),s,|x|)}\right].
\end{aligned}$$

We show in the following two lemmas that the last two terms converge to 0 as $s \to 0$ and $|x| \to \infty$ as in [64], which yields

$$\liminf_{s\searrow 0}\liminf_{|x|\to\infty}\mathbb{P}_{\mathbf{0}}\left(\{\mathbf{0} \in K_\infty^b\} \cap E^b(D(s),s,|x|) \cap F\right) \geq \theta_b,$$

where θ_b is the asymptotic proportion of vertices in the infinite component of $\mathscr{G}^b$. As in [70, Proposition 7] it can be shown that the percolation probability θ_b is continuous in b such that θ_b converges to θ as $b \nearrow 1$, which completes the proof.

Lemma 2.15

Let $b, s > 0$. Then, there exists an almost surely finite random variable $D(s)$ such that

$$\lim_{|x|\to\infty} \mathbb{P}_{\mathbf{0}}\left(\{\mathbf{0} \in K_\infty^b\} \backslash E^b(D(s), s, |x|)\right) = 0.$$

Proof. Let $E^b(D, s)$ be the event that there exists a black vertex $\mathbf{z}$ with mark smaller than s which is connected to $\mathbf{0}$ in less than D steps. If $\mathbf{0} \in K_\infty^b$ there exists a path connecting $\mathbf{0}$ to at least one black vertex with mark smaller than s. This follows from the results in [58] where it is shown that vertices with arbitrarily small mark are contained in the infinite component K_∞^b. In fact, the random variable $D_\infty = \min\{D : \text{ the event } E^b(D, s) \text{ occurs}\}$ is finite. Hence, if $|x|$ is large enough, $E^b(D_\infty, s, |x|)$ occurs if $\mathbf{0} \in K_\infty^b$ and thus $\lim_{|x|\to\infty} \mathbb{P}_{\mathbf{0}}\left(\{\mathbf{0} \in K_\infty^b\} \backslash E^b(D(s), s, |x|)\right) = 0$. □

Lemma 2.16

Let $b > 0$ and, on $E^b(D(s), s, |x|)$, denote by $\mathbf{z}$ the black vertex (x_0, t_0) with $t_0 < s$ within graph distance $D(s)$ from $\mathbf{0}$ in $\mathscr{G}^b$, which minimizes $|x_0|$. Then,

$$\lim_{s \searrow 0} \limsup_{|x|\to\infty} \mathbb{E}_{\mathbf{0}}\left[(1 - \mathbb{P}_{\mathbf{z}}(F|\mathscr{G}^b))\mathbf{1}_{E^b(D(s),s,|x|)}\right] = 0.$$

Proof. Starting in $\mathbf{z} = (x_0, t_0)$ we want to find a red vertex $\mathbf{x}_1 = (x_1, t_1) \in \mathcal{X} \cap H(x) \times (0, 1)$ with $|x_0 - x_1|^d \leq t_0^{-\alpha_2}$ and $t_1 \leq t_0^{\alpha_1}$ which is connected to $\mathbf{z}$ via one connector. Since $|x_0| \leq |x|$, we have that $x_0 \in H(x)$. Note that the volume of the intersection of $H(x)$ and the ball $B_{t_0^{-\alpha_2/d}}(x_0)$ is a positive proportion of the ball volume. Hence, there exists $c > 0$ such that the number of red vertices inside the box $H(x)$ with $|x_0 - x_1|^d \leq t_0^{-\alpha_2}$ and $t_1 \leq t_0^{\alpha_1}$ is Poisson-distributed with parameter larger than $crt_0^{\alpha_1-\alpha_2}$ and thus the probability that such a vertex does not exist is bounded by

$$p_1 = \exp(-crt_0^{\alpha_1-\alpha_2}) + \exp\big(-crt_0^{(\alpha_2-\alpha_1\gamma)\delta-\gamma}\big),$$

where the second summand is a consequence of Lemma 2.14 restricted to $\mathscr{G}^r$.

Repeating this strategy, the same arguments yield that for a vertex $\mathbf{x}_{j-1} = (x_{j-1}, t_{j-1})$ the probability that there does not exist a connection to a red vertex $\mathbf{x}_j = (x_j, t_j)$ inside $H(x)$ with $|x_{j-1} - x_j|^d \leq t_{j-1}^{-\alpha_2}$ and $t_j \leq t_{j-1}^{\alpha_1}$ is bounded by

$$p_j = \exp(-crt_{j-1}^{\alpha_1-\alpha_2}) + \exp\big(-crt_{j-1}^{(\alpha_2-\alpha_1\gamma)\delta-\gamma}\big).$$

As $\eta = (\gamma - (\alpha_2 - \alpha_1\gamma)\delta) \wedge (\alpha_2 - \alpha_1)$ and $t_j \leq t_{j-1}^{\alpha_1}$, the right-hand side can be further bounded such that $p_j \leq 2\exp(-ct_0^{-\eta\alpha_1^{j-1}})$. Applying a union bound, the probability of failing to reach L_K^r from $\mathbf{z}$ is bounded by

$$2\sum_{j=1}^{\infty} \exp\Big(-cs^{-\eta\alpha_1^{j-1}}\Big),$$

which converges to 0 as $s \searrow 0$, as shown in [64, Lemma A.4]. As $t_j \leq t_0^{\alpha^j}$, it takes at most $O(\log\log\log|x|)$ iterations of this strategy to arrive to a red vertex inside $H(x)$ with mark smaller than $(\log|x|)^{-\eta^{-1}}$. This completes the proof. □

CHAPTER 3

The contact process on scale-free geometric random graphs

In this chapter we discuss the behaviour of the contact process on geometric random graphs. For the main results of this chapter we consider the graphs in their ultrasmall regime, given by the results of Chapter 2. First, we study the non-extinction probability of the contact process and give precise asymptotics for this probability when the infection rate goes to zero, see Theorem 3.1. Second, we show that the extinction time of the contact process on a finite spatial restriction of the graphs is with high probability of exponential order of the number of vertices. As mentioned in Section 1.2.5, this chapter contains the work of [54], as the sections of this chapter can be found in [54]. For the discussion of the thesis' author's contribution to this work and minor changes see Section 1.2.5.

3.1 Introduction

In recent years the contact process has been studied extensively as a simple model for the spread of infection in a population or on a network. In this model each vertex of a given locally-finite graph has one of two states, 0 or 1 for each $t \geq 0$, indicating whether the vertex is healthy or infected at time t. An infected vertex

transmits the infection to a neighbouring vertex with rate $\lambda > 0$, independently of everything else, and *recovers* at rate 1. Precisely, the contact process on a locally-finite graph $G = (V, E)$ is a continuous-time Markov process $(\xi_t)_{t\geq 0}$ on the space $\{0,1\}^V$. By identifying ξ_t with the subset $\{x \in V : \xi_t(x) = 1\} \subset V$ for each $t \geq 0$ the transition rates are given by

$$\begin{aligned} \xi_t &\to \xi_t \backslash \{x\} \quad \text{for } x \in \xi_t \text{ at rate 1, and} \\ \xi_t &\to \xi_t \cup \{x\} \quad \text{for } x \notin \xi_t \text{ at rate } \lambda \big| \{y \in \xi_t : x \sim y\} \big|, \end{aligned} \tag{3.1}$$

where we denote like in the whole thesis by $x \sim y$ that x and y are connected by an edge.

Note that the contact process has a single absorbing state, corresponding to the configuration where all vertices are healthy. Thus, a natural question on the behaviour of the contact process is whether this state is reached in finite time, i.e. whether the *extinction time* of the contact process on G, defined by

$$\varpi_G := \inf\{t > 0 : \xi_t = \emptyset\},$$

is finite.

On the lattice $\mathbb{Z}^d$ there exists a critical value $\lambda_c(\mathbb{Z}^d)$ exhibiting a phase transition in whether the process dies out almost surely or not. If $\lambda \leq \lambda_c(\mathbb{Z}^d)$, the extinction time $\varpi_{\mathbb{Z}^d}$ is almost surely finite for any finite initial configuration where only finitely many sites are infected and we say it dies out, whereas if $\lambda > \lambda_c(\mathbb{Z}^d)$ there is a positive probability that the extinction time is infinite even if the infection only starts in a single vertex, see [77]. Looking at the contact process on finite graphs the extinction time is always almost surely finite and a more natural question in this setting is to ask how long the infection survives until it reaches the absorbing state. Interestingly, on the restriction of $\mathbb{Z}^d$ to finite boxes the critical value $\lambda_c(\mathbb{Z}^d)$ again exhibit a phase transition. If $\lambda < \lambda_c(\mathbb{Z}^d)$ the extinction time is of logarithmic order in the volume of the box whereas if $\lambda > \lambda_c(\mathbb{Z}^d)$ the contact process survives much longer and the extinction time is of exponential order in the volume of the box. In the later case the contact process is said to be in a *metastable* situation where it stabilizes for an exponentially long amount of time before it reaches the absorbing state where all vertices are healthy, see [77] for further details. The behaviour of the extinction time of

the contact process has been studied on various different finite graphs including on finite regular trees by Stacey [94], Cranston et al. [32] and Mountford et al. [86], on regular graphs by Mourrat and Valesin [88], on Erdós-Renyi graphs by Bhamidi et al. [12] and for a general large class of finite graphs by Mountford et al. [86] and Schapira and Valesin [93].

The situation changes dramatically if we consider random graphs with a scale-free degree distribution such as the configuration model or preferential attachment networks. On these graphs the critical value of λ is zero, therefore for any choice of $\lambda > 0$ the extinction time is of exponential order in the size of the graph, see [27] and [86] for the configuration model and [10] for preferential attachment networks. For these models further results on the metastability are given by Mountford et al. [87] on the configuration model, where they provide estimates on the rate of decay of the density of infected vertices in terms of λ at a time when the infection has not yet reached the absorbing states, for λ small and graph large enough. This rate of decay solely depends on the power-law exponent τ of the scale-free degree distribution, precisely it is given by

$$\rho_\tau(\lambda) = \begin{cases} \lambda^{1/(3-\tau)} & \text{if } \tau \in (2, \frac{5}{2}] \\ \frac{\lambda^{2\tau-3}}{\log(1/\lambda)^{\tau-2}} & \text{if } \tau \in (\frac{5}{2}, 3] \\ \frac{\lambda^{2\tau-3}}{\log(1/\lambda)^{2\tau-4}} & \text{if } \tau \in (3, \infty) \end{cases} . \tag{3.2}$$

This result seems to have a universal character as the same rate of decay has been shown for hyperbolic random graphs by Linker et al. [78]. The later can be seen as a geometric variant of the configuration model, as in both cases the probability to form an edge between two given vertices depends on the product of independent weights which are assigned to each vertex in the graph. For further results on the density of infected vertices at a time when the contact process is still alive on the configuration model with $\tau \in (1, 2]$ and preferential attachment networks see [25] and [24]. To obtain these estimates the analysis of the contact process on the corresponding limit graphs is important, i.e. the corresponding Galton-Watson process for the configuration model and the infinite hyperbolic model. In fact, for these models the rate of decay given by ρ_τ coincides with the rate of decay of the probability that the extinction time is infinite on the limit graphs when λ goes to zero. Thus, the study of the non-extinction probability is

a crucial step to obtain the stated metastability results.

In this chapter we will study the contact process on geometric random graphs as characterized in Section 1.2.2 which satisfy Assumption UBA* and LBA. In Chapter 2 we have seen that such graphs exhibit sufficiently short paths such that the graphs are ultrasmall if $\gamma > \frac{\delta}{\delta+1}$. In this regime we study in Section 3.2 the probability $\Gamma(\lambda)$ that the contact process starting in a typical vertex does not go extinct. We prove that the critical value λ_c is zero for these graphs and we give exact asymptotics on its rate of decay, when λ is small, see Theorem 3.1. In Section 3.3 we study a spatial restriction of the these graphs to boxes $[-\frac{n^{1/d}}{2}, \frac{n^{1/d}}{2}]^d$, still assuming that $\gamma > \frac{\delta}{\delta+1}$, and show that the extinction time exhibits no phase transition, i.e. for any $\lambda > 0$ the extinction time is of exponential order in the volume of the boxes, see Theorem 3.14.

3.1.1 The contact process and its graphical representation

The contact process on an arbitrary locally-finite graph $G = (V, E)$ with parameter λ is a continuous time Markov process $(\xi_t)_{t\geq 0}$ on the space $\{0,1\}^V$. At time t we say a vertex $x \in V$ is infected if $\xi_t(x) = 1$ and healthy if $\xi_t(x) = 0$. Thus, we can also view ξ_t as the subset $\{x : \xi_t(x) = 1\}$ of V of the infected vertices at time t. Infected vertices transmit the infection to each of their neighbours with rate λ and recover with rate 1, yielding the transition rates given by (3.1). We write $(\xi_t^A)_{t\geq 0}$ for the contact process with initial condition $A \subset V$, i.e. $\xi_0^A = A$ and $(\xi_t^x)_{t\geq 0}$ if $A = \{x\}$.

A very useful description of the contact process is its graphical representation given by a family of independent Poisson processes on $[0, \infty)$. Assign to each vertex $x \in V$ a Poisson process N_x on $[0, \infty)$ of rate 1. For each edge in G with endvertices x and y, assign to each of the pairs (x, y) and (y, x) a Poisson process $N_{(x,y)}$, resp. $N_{(y,x)}$, on $[0, \infty)$ with rate λ. We can think of every element $t \in N_x$ as a recovery mark at x at time t, and every element $t \in N_{(x,y)}$ as a transmission arrow from x to y at time t. Hence, on $V \times [0, \infty)$ we assign a recovery mark at (x, t) for all $t \in N_x$ and $x \in V$ and an arrow from (x, t) to (y, t) for all $t \in N_{(x,y)}$ and $x, y \in V$ which are connected by an edge. An *infection path* in the graphical construction is a a function $g : I \to V$ for some interval I

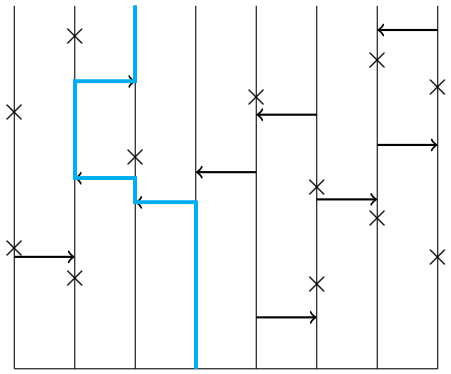

Figure 3.1: Sketch of the graphical representation of the contact process on $\mathbb{Z}$. Arrows represent (potential) infection transmissions and crosses represent the recovery marks. The blue path is one potential infection path in this representation starting in the fourth vertex.

such that the process $(g(t), t)_{t\in I}$ on $V \times [0, \infty)$ which goes up in time never hits a recovery mark and only changes values in the first component by travelling along an arrow in its given direction. We write $(x, t) \to (y, s)$ if there exists an infection path $g : [t, s] \to V$ from x to y, i.e. an infection path with $g(t) = x$ and $g(s) = y$. Then the contact process starting in A can be derived from infection paths of the graphical construction by

$$\xi_t^A(x) = \mathbf{1}\{A \times \{0\} \to (x, t)\}, \quad t \geq 0, x \in V,$$

see Figure 3.1 for an example. This graphical representation allows to derive important properties of the contact process easily, such as its monotonicity in the initial configuration, its additivity and its *self-duality* relation

$$\mathbb{P}(\xi_t^A \cap B \neq \emptyset) = \mathbb{P}(\xi_t^B \cap A \neq \emptyset) \quad \text{for } A, B \subset V.$$

For further properties of the contact process we refer to [77].

Throughout the following sections of this chapter we denote by $\mathbb{P}$ the joint law of the contact process and the underlying geometric random graph and with a slight abuse of notation denote by $\mathbb{P}_{\mathbf{x}_1,\dots,\mathbf{x}_n}$ and by $\mathbb{P}_{(0,T_0)}$ the joint law of the contact process and the respective geometric random graph law under the conditions given in Section 1.2.2.

3.2 Non-extinction probability

In this section we consider the probability $\Gamma(\lambda)$ that the contact process with parameter λ on $\mathscr{G}_{(0,T_0)}$ starting in the origin $(0,T_0)$ does not go extinct, i.e.

$$\Gamma(\lambda) = \mathbb{P}_{(0,T_0)}\big(\xi_t^{(0,T_0)} \neq \emptyset \ \forall t \geq 0\big). \tag{3.3}$$

Our main result describes the asymptotic behaviour of $\Gamma(\lambda)$ as λ becomes small. Here, we write $f(\lambda) \asymp g(\lambda)$, if there exist two positive constants $c, C > 0$ such that $cf(\lambda) \leq g(\lambda) \leq Cf(\lambda)$ for λ sufficiently small.

Theorem 3.1

Let $\mathscr{G}$ be a general geometric random graph which satisfies Assumption UBA* and Assumption LBA for $\gamma > \frac{\delta}{\delta+1}$. Then, as $\lambda \to 0$,

$$\Gamma(\lambda) \asymp \frac{\lambda^{2/\gamma-1}}{\log(1/\lambda)^{(1-\gamma)/\gamma}}. \tag{3.4}$$

As stated in the introduction for the ultrasmall regime the non-extinction probability is positive for any $\lambda > 0$ and therefore the critical value when the contact process dies out is almost surely zero. To compare the result of Theorem 3.1 to the rates (3.2) given in [87], resp. [78], for the contact process on the configuration model and on hyperbolic random graphs, note that $\gamma \in (\frac{\delta}{\delta+1}, 1)$ implies $\tau \in (2,3)$ since $\delta > 1$. As $\tau = 1 + \frac{1}{\gamma}$ the rate given in (3.4) matches the case $\tau \in (\frac{5}{2}, 3]$ in (3.2). To see the reason why for geometric random graphs satisfying Assumption UBA* and Assumption LBA only this case appears, it is helpful to look at the survival strategies of the infection leading to the two cases of (3.2) for which $\tau \in (2,3]$. If $\tau \in (2, \frac{5}{2}]$, the graph is so well connected that an infected vertex with a high degree, i.e. a small mark, has with high probability at least one neighbour with an even smaller mark to which the vertex transmits the infection. Thus, when the origin infects a relatively powerful vertex, i.e. a vertex with a small mark, with high probability the infection passes directly to more and more powerful vertices and therefore survives. This way of *direct spreading* does not work sufficiently well when $\tau \in (\frac{5}{2}, 3]$ as the graph is not connected well enough. In this case the survival strategy relies on the observation that, when a vertex with sufficiently high degree is infected, the infection survives so long in

the neighbourhood of the vertex which forms a star, that it reaches with high probability another vertex with similarly high degree from which this kind of *delayed spreading* can repeat, see [87, Section 3]. For geometric random graphs satisfying Assumption UBA* and Assumption LBA the strategy of direct spreading does not work, as for a vertex with mark t the expected number of neighbours with mark smaller than t does not increase when t becomes small, unlike in the configuration model or hyperbolic random graphs. Instead, two vertices with small mark are usually not connected directly but via a *connector*, a vertex with mark near one. This additional necessary step to transmit the infection to a vertex with smaller mark makes this strategy worse than the strategy of delayed spreading, which still works for the class of geometric random graphs, see Proposition 3.2, yielding that only the later one appears in Theorem 3.1. The same behaviour also holds for dynamical non-spatial preferential attachment with slow update rate, as studied in [68].

Remark 3.2.1. In Chapter 2 the upper bound assumption could be relaxed by omitting the assumption of independent occurence of the edges given the Poisson point process. This is not possible here, as the proof of the asymptotic upper bound given in Proposition 3.5 requires not only the ability to control the occurence of self-avoiding paths in the graph, but also the occurence of stars, i.e. the neighbourhoods of vertices with high degree. An upper bound assumption on the existence of paths as UBA does not yield any meaningful bound on the size of stars.

3.2.1 Lower bound

We dedicate this section to proving a lower bound for $\Gamma(\lambda)$ when λ is small. Namely, we will prove the following result.

Proposition 3.2

Let $\mathscr{G}$ be a general geometric random graph which satisfies Assumption LBA with $\gamma > \frac{\delta}{\delta+1}$. Then, there exists a constant $c > 0$ such that, for λ small, it holds

$$\Gamma(\lambda) > c\frac{\lambda^{2/\gamma-1}}{\log(1/\lambda)^{(1-\gamma)/\gamma}}. \tag{3.5}$$

For the proof of Proposition 3.2 we exploit the following observation. Let us denote by a *star* a connected graph where all but one vertex have degree one. Then, the contact process restricted to a subgraph isomorphic to a star survives for a constant time if the subgraph consists of at least order λ^{-2} vertices and survives even long enough to infect other neighbouring stars if the subgraph consists of order $\log(1/\lambda)\lambda^{-2}$ vertices, see [87]. We denote by $\mathbb{L}_r$ the graph consisting of the half-line $\mathbb{N}_0$, where to each even vertex $m \in \mathbb{N}_0$, r additional distinct neighbours are attached. Thus, $\mathbb{L}_r$ forms a half-line of stars consisting of $r+1$ vertices, where two consecutive stars are connected via a path of two edges. Throughout this section we denote the vertex $0 \in \mathbb{N}_0$ as the origin of $\mathbb{L}_r$. Notice that if the size r of the stars is of order $\log(1/\lambda)\lambda^{-2}$ and only the origin of $\mathbb{L}_r$ is infected, there exists a constant $p > 0$ such that the survival probability of the contact process on $\mathbb{L}_r$ is at least p. This is direct consequence of Lemma [78, Lemma 2.4], since the stars are sufficiently large so that whether two stars are connected by a single edge or a path of bounded length makes no difference. Thus, as a first step we will show that such a half-line of stars exists in $\mathscr{G}_{(0,T_0)}$. For $x \in \mathbb{R}^d$, denote by H_x the plane through x with normal vector x. Consequently, H_x divides $\mathbb{R}^d$ in two subsets and we denote by $\mathbb{R}^d_{\geq x}$ the subset that does not contain zero. As discussed in Section 1.2.2 the expected degree of a given vertex with mark t in a geometric random graph $\mathscr{G}$ which satisfies both Assumptions UBA* and LBA is of order $t^{-\gamma}$. We therefore call vertices with small mark powerful vertices. For $\beta > 0$ and $r := \beta \log(1/\lambda)\lambda^{-2}$, let $T_{\circledast} := r^{-1/\gamma}$ be the threshold such that vertices with smaller mark have an expected degree of order at least $\log(1/\lambda)\lambda^{-2}$.

Lemma 3.3

Let $\mathbf{x} = (x,t) \in \mathbb{R}^d \times (0,1)$ with $t < T_{\circledast}$. Then, given that $\mathbf{x}$ is a vertex of $\mathscr{G}_{(0,T_0)}$, we have with high probability as $\lambda \to 0$ that there exists a subgraph of $\mathscr{G}_{(0,T_0)}$ in $\mathbb{R}^d_{\geq x} \times (0,1)$ which is isomorphic to $\mathbb{L}_r$ such that the origin of $\mathbb{L}_r$ is identified with $\mathbf{x}$.

To prove the existence of such a subgraph, we decompose $\mathbb{R}^d_{\geq x} \times (0,1)$ into in distinct parts, where areas with small marks represent potential midpoints of stars and areas with large mark represent either neighbours of the midpoints or vertices which are connected by an edge to two distinct midpoints. Choose $\theta > 0$

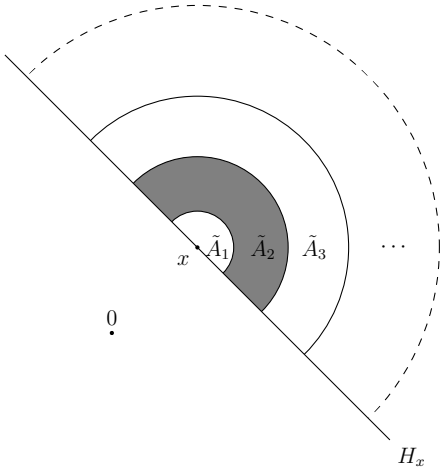

Figure 3.2: The anuli $(A_k)_{k\in\mathbb{N}}$ centered around x and truncated with respect to H_x, where the area $\tilde{A}_2$ is shaded grey.

such that $1 < \theta < \gamma + \gamma/\delta$ and note that his is always possible since $\gamma > \frac{\delta}{\delta+1}$. Set

$$T_k = T_{\circledast}^{\theta} e^{-k\theta} \text{ and } R_k = \tfrac{1}{2} T_{\circledast}^{-(\gamma+\gamma/\delta)/d} e^{k(\gamma+\gamma/\delta)/d}, \quad \text{for } k \in \mathbb{N}$$

and $R_0 = 0$. Given the vertex $\mathbf{x} = (x, t)$ define, for $k \in \mathbb{N}$, the anuli $A_k := B(\mathbf{x}, R_k) \cap B(\mathbf{x}, R_{k-1})^c$ and the sets

$$S_k := \tilde{A}_k \times [T_{k+1}, T_k), \quad S_k^{(1)} := \tilde{A}_k \times [1/2, 3/4) \text{ and } S_k^{(2)} := \tilde{A}_k \times [3/4, 1),$$

where $\tilde{A}_k := A_k \cap \mathbb{R}^d_{\geq x}$, see Figure 3.2. Notice that all these sets are disjoint and therefore the point processes restricted to these sets are independent. For the proof of Proposition 3.3 it will be helpful to interpret

- the vertices in S_k as the potential midpoints of the k-th star of the subgraph,
- the vertices in $S_k^{(1)}$ as the potential neighbours of the midpoints forming a sufficiently large star
- the vertices in $S_k^{(2)}$ as the potential *connectors* between consecutive midpoints, i.e. vertices which are connected to both midpoints.

Before we prove Lemma 3.3, we state the following lemma as a corollary of [70], which follows with similar calculations as done in Lemma 2.14. With this lemma

we can ensure that two vertices from consecutive areas S_k and S_{k+1} are connected via a connector with high probability.

Lemma 3.4

Given two vertices $\mathbf{x}_k \in S_k$ and $\mathbf{x}_{k+1} \in S_{k+1}$, the number of vertices in $S_k^{(2)}$ which form an edge to $\mathbf{x}_k$ and $\mathbf{x}_{k+1}$ is Poisson-distributed with parameter larger than

$$Ct_k^{-\gamma}\big(1 \wedge t_{k+1}^{-\gamma\delta}\big(\,|x_{k+1} - x_k| + t_k^{-\gamma/d}\big)^{-d\delta}\big), \tag{3.6}$$

where $C > 0$ is a constant not depending on k.

Proof. We consider the vertices $\mathbf{z} = (z, u) \in S_k^{(2)}$ with $|x_k - z|^d < t_k^{-\gamma}$. Note that the volume of $B\big(x_k, t_k^{-\gamma/d}\big) \cap \tilde{A}_k$ is a positive proportion $\rho > \frac{1}{2^{d+1}}$ of the ball volume, as $t_k^{-\gamma/d} < \frac{1}{2}(R_k - R_{k-1})$ for sufficiently small λ. Then, the number of those vertices which form an edge to $\mathbf{x}_k$ and $\mathbf{x}_{k+1}$ is Poisson-distributed with parameter bounded from below by

$$\begin{aligned}\int_{\frac{3}{4}}^{1} \int_{B(x_k, t_k^{-\gamma/d}) \cap \tilde{A}_k} & \mathrm{d}\mathbf{z}\alpha^2(1 \wedge \kappa)(1 \wedge \kappa t_{k+1}^{-\gamma\delta}\,|z - x_{k+1}|^{-d\delta}) \\ &\geq \frac{V_d \rho \alpha^2 (1 \wedge \kappa)}{4} t_k^{-\gamma}\big(1 \wedge \kappa t_{k+1}^{-\gamma\delta}\big(\,|x_{k+1} - x_k| + t_k^{-\gamma/d}\big)^{-d\delta}\big),\end{aligned}$$

where V_d is the volume of the d-dimensional unit ball and α and κ comes from Assumption LBA. Thus, there exist a constant $C > 0$ sufficiently small such that (3.6) holds. □

Proof of Lemma 3.3. Note that, for $k \in \mathbb{N}$, the number of vertices in S_k is Poisson-distributed with mean larger than

$$V_d(T_{k+1} - T_k)(R_{k+1}^d - R_k^d) \geq c_1 T_{\circledast}^{-(\gamma+\gamma/\delta-\theta)} e^{k(\gamma+\gamma/\delta-\theta)}$$

for some $c_1 > 0$, which does not depend on k. Thus, S_k is non-empty with probability larger than $1 - \exp(-c_1 T_{\circledast}^{-(\gamma+\gamma/\delta-\theta)} e^{k(\gamma+\gamma/\delta-\theta)})$. As the boxes $S_1, S_2, \ldots$ are disjoint, the numbers of vertices in each box are independent from each other.

Thus, it holds

$$\mathbb{P}(S_k \text{ is non-empty } \forall\, k \in \mathbb{N}) \geq \prod_{k=1}^{\infty} \left(1 - \exp(-c_1 T_{\circledast}^{-(\gamma+\gamma/\delta-\theta)} e^{k(\gamma+\gamma/\delta-\theta)})\right).$$

For $k \geq 2$, on the event that S_k is non-empty we denote by $\mathbf{x}_k$ the vertex in S_k with the smallest mark. For $k = 1$ we set $\mathbf{x}_1 := \mathbf{x}$ and always treat S_1 as non-empty. To keep notation cleaner we treat without loss of generality the mark of $\mathbf{x}_1$ as smaller than T_1 (this affects only the estimate in (3.7) below where $\gamma + \gamma\delta$ becomes $\gamma\delta$ which does not change the rest of the argument).

Given S_k and S_{k+1} are non-empty, the Euclidean distance of the corresponding vertices $\mathbf{x}_k$ and $\mathbf{x}_{k+1}$ is at most $2R_{k+1}$ and both vertices have a mark smaller T_k. Thus, by Lemma 3.4 there exists $c_2 > 0$ such that, for all $k \in \mathbb{N}$, the probability that $\mathbf{x}_k$ and $\mathbf{x}_{k+1}$ are connected via one connector in $S_k^{(2)}$ is larger than

$$1 - \exp(c_2 T_{\circledast}^{-(\gamma+\gamma\delta)(\theta-1)} e^{k(\gamma+\gamma\delta)(\theta-1)}). \tag{3.7}$$

Given S_k is non-empty, we now turn our attention to the number of neighbours of $\mathbf{x}_k$ in $S_k^{(1)}$. As in the proof of Lemma 3.4 we only consider the vertices $\mathbf{z} \in S_k^{(1)}$ with $|x_k - z|^d < T_k^{-\gamma}$. Note that the volume of $B(x_k, T_k^{-\gamma/d}) \cap A_k$ is again a positive proportion $\rho > \frac{1}{2^{d+1}}$ of the ball volume itself for λ small enough. These vertices are connected to $\mathbf{x}_k$ with probability bounded from below by $\alpha(1 \wedge \kappa)$. Thus, there exists $c > 0$ such that the number of neighbours of $\mathbf{x}_k$ in $S_k^{(1)}$ with $|x_k - z|^d < T_k^{-\gamma}$ is Poisson-distributed with mean larger than $cT_k^{-\gamma} \geq cre^{k\gamma}$. Thus, by a Chernoff-bound there exists $c_3 > 0$ such that, given S_k is non-empty, the probability that the number of neighbours of $\mathbf{x}_k$ is larger than r is at least $1 - \exp(-cre^{k\gamma})$, for all $k \in \mathbb{N}$.

We choose $0 < \varepsilon < \big(\gamma + \gamma/\delta - \theta\big) \wedge \big((\gamma + \gamma\delta)(\theta - 1)\big)$. Given all sets S_k are non-empty, the two previously discussed events only depend on disjoint subsets of the Poisson-process. Thus, the probability that, for all $k \geq 2$,

- S_k is non-empty,
- $\mathbf{x}_k$, the vertex with smallest mark in S_k, has at least r neighbours in $S_k^{(1)}$ and

- $\mathbf{x}_{k-1}$ and $\mathbf{x}_k$ are connected via a connector in $S_{k-1}^{(2)}$

is larger than

$$\prod_{k=1}^{\infty} \left(1 - \exp(-T_{\circledast}^{-\varepsilon} e^{k\varepsilon})\right)\left(1 - \exp(-cre^{k\gamma})\right)$$

which tends to one as $\lambda \to 0$ since r and $T_{\circledast}^{-\varepsilon}$ tend to infinity in this case. □

With Lemma 3.3 in hand we are now ready to complete the proof of Proposition 3.2. Starting at the origin we explore the Poisson point process by expanding a sphere centered at the origin $(0, T_0)$ until we find the nearest neighbour $\mathbf{x}$ of $(0, T_0)$ with mark smaller $T_{\circledast}$. As the number of neighbours of $(0, T_0)$ with mark smaller than $T_{\circledast}$ dominates a Poisson-distributed random variable with parameter of order $T_{\circledast}^{1-\gamma}$, the probability that we find such a neighbour $\mathbf{x}$ and there is a transmission from $(0, T_0)$ to $\mathbf{x}$ before $(0, T_0)$ recovers is larger than

$$\frac{c\lambda}{1+\lambda} T_{\circledast}^{1-\gamma} \geq \frac{c\lambda^{2/\gamma - 1}}{\log(1/\lambda)^{(1-\gamma)/\gamma}} \tag{3.8}$$

for some $c > 0$, where $\frac{\lambda}{\lambda+1}$ occurs as the probability that, given $\mathbf{x}$ is a neighbour of the origin $(0, T_0)$, $\mathbf{x}$ got infected by the origin before it recovers. Given the nearest neighbour $\mathbf{x} = (x, t)$ with mark smaller $T_{\circledast}$, by Lemma 3.3, there exists with probability larger than $\frac{1}{2}$ as λ is small a subgraph in the yet unexplored area $\mathbb{R}^d_{\geq x}$ which is isomorph to $\mathbb{L}_r$ with origin in $\mathbf{x}$. Conditioned on this subgraph being present and the origin of it being infected, the infection survives with a probability bounded away from zero, uniformly in λ, by [78, Lemma 2.4]. Hence, $\Gamma(\lambda)$ is up to a constant larger than the probability bound given in (3.8) which completes the proof of Proposition 3.2.

3.2.2 Upper bound

Proposition 3.5

Let $\mathscr{G}$ be a general geometric random graph which satisfies Assumption UBA* for $\gamma > \frac{1}{2}$ and $\delta > 1$. Then, there exists a constant $C > 0$ such that

$$\Gamma(\lambda) < C \frac{\lambda^{2/\gamma - 1}}{\log(1/\lambda)^{(1-\gamma)/\gamma}}. \tag{3.9}$$

To prove this we generalize and extend the arguments from [78] for the geometric random graphs characterized by the framework given in Section 1.2.2. Let the function $\rho : [0,\infty) \to [0,1]$ be defined by $\rho(x) := 1 \wedge x^{-\delta}$ and denote $I_\rho := \int_{\mathbb{R}^d} \mathrm{d}x \rho(\kappa |x|^d) < \infty$, where $\delta > 1$ and $\kappa > 0$ are given in Assumption UBA*. Note that, for geometric random graphs satisfying the Assumption UBA* and LBA, there exists constants $c, C > 0$ such that, for any vertex $\mathbf{x} = (x,t) \in \mathbb{R}^d \times (0,1)$, it holds $ct^{-\gamma} \leq \mathbb{E}_{\mathbf{x}} \deg \mathbf{x} \leq Ct^{-\gamma}$. With that in mind, we can think of $T(n) = n^{-1/\gamma}$ as the mark of a vertex with expected degree of order n in such a graph.

Throughout the proof we classify the vertices by their expected degree into different groups. Let $n_\star = \lambda^{-2}$ and, for some constant $\theta > 0$ to be specified later, $n_\circledast = \frac{\theta}{\lambda^2} \log\left(\frac{1}{\lambda}\right)$. Vertices with degree larger than $n_\star$ are the midpoints of stars on which the infection restricted to the star can survive for a constant time with a probability bounded away from zero, without necessarily surviving long enough such that it can reach other stars nearby. As we have seen in the proof of Proposition 3.2, this happens for stars with more than $n_\circledast$ vertices. For $\sigma > 0$, set $n_\sigma = \lambda^{-2+\sigma}$. Vertices with degree smaller than n_σ are centers of stars which are not sufficiently large, in the sense that the infection does not propagate through such stars and dies out when the graph is restricted to vertices with such small degree; see Lemma 3.13. We denote by

$$T_\star := T(n_\star), \quad T_\sigma := T(n_\sigma), \quad T_\circledast := T(n_\circledast)$$

the according mark of the vertices whose expected degree is by Assumption UBA* at most of the corresponding order.

Proof of Proposition 3.5. We consider now the contact process $(\xi_t^{(0,T_0)})_{t\geq 0}$ on $\mathscr{G}_{(0,T_0)}$ which starts from the origin $(0,T_0)$. For a vertex $\mathbf{x}$, on the event that $\mathbf{x}$ and $(0,T_0)$ are connected we denote by $I_{\mathbf{x}}$ the event that $\mathbf{x}$ got infected from the origin $(0,T_0)$ before $(0,T_0)$ recovers. On $I_{\mathbf{x}}$ we denote by $\tau_{\mathbf{x}}$ the time when $\mathbf{x}$ got infected by the origin and by $(\eta_t^{\mathbf{x}})_{t\geq\tau_{\mathbf{x}}}$ the contact process started at time $\tau_{\mathbf{x}}$ with a single infection at $\mathbf{x}$ determined by the same graphical construction as the original process $(\xi_t^{(0,T_0)})_{t\geq 0}$.

For $\sigma > 0$, denote by E_σ the event that each infection path g starting in the

origin which jumps first to a vertex with mark larger than T_σ is finite and never reaches a vertex with mark smaller than T_σ. We will see later that when the mark of the origin is itself larger than T_σ, the probability that E_σ occurs goes much quicker to one, when λ goes to zero, than the rate given in (3.4). In fact, we show in Lemma 3.13 that for $\sigma > 0$ sufficiently small, it holds

$$\mathbb{P}_{(0,T_0)}(E_\sigma^c \cap \{T_0 \geq T_\sigma\}) \leq \lambda^{2/\gamma - 1 + \varepsilon}. \tag{3.10}$$

Let $\sigma_0 > 0$ such that it holds $\sigma_0 > \sigma$ and let $T_{\sigma_0} = T(n_{\sigma_0})$ be the associated boundary of the mark of vertices with expected degree of order $\lambda^{-(2-\sigma_0)}$. Whereas T_σ and $T_\circledast$ will be used to distinguish the neighbours of the origin by their marks, for the survival of the contact process we consider whether $T_0 < T_{\sigma_0}$ or not. Then, we have

$$\begin{aligned} \mathbf{1}_{\{\xi_t^{(0,T_0)} \neq \emptyset \ \forall t \geq 0\}} \leq\ & \mathbf{1}_{\{T_0 < T_{\sigma_0}\}} + \mathbf{1}_{E_\sigma^c \cap \{T_0 \geq T_\sigma\}} \\ & + \sum_{\substack{\mathbf{x} \in \mathcal{X} \\ t \leq T_\circledast}} \mathbf{1}_{\{(0,T_0) \sim \mathbf{x}\}} \mathbf{1}_{I_\mathbf{x}} \mathbf{1}_{\{T_0 \geq T_{\sigma_0}\}} \\ & + \sum_{\substack{\mathbf{x} \in \mathcal{X} \\ T_\circledast < t < T_\sigma}} \mathbf{1}_{\{(0,T_0) \sim \mathbf{x}\}} \mathbf{1}_{I_\mathbf{x}} \mathbf{1}_{\{T_0 \geq T_{\sigma_0}\}} \mathbf{1}_{\{(\eta_t^\mathbf{x})_{t \geq \tau_\mathbf{x}} \text{ survives}\}} \end{aligned} \tag{3.11}$$

In fact, if the right-hand side is zero it holds that

- every infection path starting in the origin which jumps in its first step to a vertex with mark larger than T_σ is finite and never visits a vertex with mark smaller than T_σ,
- there exists no vertex with mark smaller than $T_\circledast$ which is a neighbour of the origin and got infected by it,
- there exists no vertex with mark inbetween T_σ and $T_\circledast$, which is a neighbour of the origin and got infected by it and the infection emerging from this vertex survives.

As these three points imply that the infection $(\xi_t^{(0,T_0)})_{t \geq 0}$ does not survive, the left-hand side is then also zero, from which the stated inequality follows. Note that this bound is especially not sharp in the second summand of the right-hand side, as we allow T_0 to take a larger range of values than needed. Taking

expectation on both sides of (3.11) yields an upper bound for the probability of interest and it is therefore sufficient to establish upper bounds for the expectation of each of the four summands of the right-hand side.

First, by the definition of T_{σ_0} we have that

$$\mathbb{P}(T_0 < T_{\sigma_0}) = \lambda^{(2-\sigma_0)/\gamma} < \lambda^{2/\gamma - 1/2}$$

for σ_0 and $\lambda > 0$ small enough and a bound for the second summand is given by (3.10), which will be proved in Lemma 3.13.

As mentioned beforehand, the third term on the right-hand side of (3.11) count the number of vertices with mark smaller than $T_\circledast$ which got infected by the origin $(0, T_0)$. We have seen in Section 3.2.1 that the contact process starting in such a vertex would ensure a spreading over a chain of infinitely many other stars with equally many neighbours. Thus, a sharp upper bound for the expected number of such vertices is crucial. By Mecke's equation, Assumption UBA* and since T_0 is independent of $\mathcal{X}$ it holds that

$$\begin{aligned}
\mathbb{E}_{(0,T_0)}\Bigg[\sum_{\substack{\mathbf{x}\in\mathcal{X}\\ t\le T_\circledast}} \mathbf{1}_{\{(0,T_0)\sim\mathbf{x}\}}\mathbf{1}_{I_\mathbf{x}}\mathbf{1}_{\{T_0\ge T_{\sigma_0}\}}\Bigg] &= \int_{T_{\sigma_0}}^1 \mathrm{d}t_0 \int_0^{T_\circledast} \mathrm{d}t \int_{\mathbb{R}^d} \mathrm{d}x\, \mathbb{E}_{(0,t_0),\mathbf{x}}[\mathbf{1}_{\{(0,t_0)\sim\mathbf{x}\}}\mathbf{1}_{I_\mathbf{x}}] \\
&\le \frac{\lambda}{\lambda+1}\int_{T_{\sigma_0}}^1 \mathrm{d}t_0 \int_0^{T_\circledast} \mathrm{d}t \int_{\mathbb{R}^d} \mathrm{d}x\, \rho(\kappa^{-1/\delta} t^\gamma t_0^{1-\gamma} |x|^d) \\
&\le \lambda \frac{I_\rho}{(1-\gamma)\gamma} T_\circledast^{1-\gamma} \le \frac{I_\rho}{(1-\gamma)\gamma} \frac{\lambda^{2/\gamma-1}}{\log(1/\lambda)^{(1-\gamma)/\gamma}}.
\end{aligned}$$

In fact, this is the dominant term of the right-hand side of (3.11) which contributes to the stated upper bound.

For the last summand of (3.11) we have by Mecke's equation, Assumption UBA*

and since T_0 is independent of $\mathcal{X}$ that

$$\begin{aligned}
&\mathbb{E}_{(0,T_0)}\Bigg[\sum_{\substack{\mathbf{x}\in\mathcal{X}\\ T_\circledast<t<T_\sigma}} \mathbf{1}_{\{(0,T_0)\sim\mathbf{x}\}}\mathbf{1}_{I_\mathbf{x}}\mathbf{1}_{\{T_0\geq T_{\sigma_0}\}}\mathbf{1}_{\{(\eta_t^\mathbf{x})_{t\geq\tau_\mathbf{x}} \text{ survives}\}}\Bigg]\\
&= \int_{T_{\sigma_0}}^1 \mathrm{d}t_0 \int_{T_\circledast}^{T_\sigma} \mathrm{d}t \int_{\mathbb{R}^d} \mathrm{d}x \mathbb{E}_{(0,t_0),\mathbf{x}}[\mathbf{1}_{\{(0,t_0)\sim\mathbf{x}\}}\mathbf{1}_{I_\mathbf{x}}\mathbf{1}_{\{(\eta_t^\mathbf{x})_{t\geq\tau_\mathbf{x}} \text{ survives}\}}]\\
&\leq \frac{\lambda}{\lambda+1}\int_{T_{\sigma_0}}^1 \mathrm{d}t_0 \int_{T_\circledast}^{T_\sigma} \mathrm{d}t \int_{\mathbb{R}^d} \mathrm{d}x \mathbb{E}_{(0,t_0),\mathbf{x}}[\mathbf{1}_{\{(\eta_t^\mathbf{x})_{t\geq\tau_\mathbf{x}} \text{ survives}\}} \,|\, (0,t_0)\sim\mathbf{x}, I_\mathbf{x}]\rho(\kappa^{-1/\delta}t^\gamma t_0^{1-\gamma}\,|y|^d).
\end{aligned}$$

In Lemma 3.12 we will show that there exist $\varepsilon > 0$ such that, for $\mathbf{x} = (x,t)$, $\mathbf{y} = (y,s) \in \mathbb{R}^d \times (0,1)$ with $t > T_\circledast$ and $s > T_{\sigma_0}$, it holds

$$\mathbb{P}_{\mathbf{x},\mathbf{y}}(\xi_t^\mathbf{x} \neq \emptyset \;\forall\; t \geq 0 \,|\, \mathbf{x}\sim\mathbf{y}) < \lambda^\varepsilon, \tag{3.12}$$

where $(\xi_t^\mathbf{x})_{t\geq 0}$ is the contact process of rate λ which starts in $\mathbf{x}$ and only in $\mathbf{x}$. By this inequality and the strong Markov-property of the contact process we have that

$$\begin{aligned}
&\mathbb{E}_{(0,T_0)}\Bigg[\sum_{\substack{\mathbf{x}\in\mathcal{X}\\ T_\circledast<t<T_\sigma}} \mathbf{1}_{\{(0,T_0)\sim\mathbf{x}\}}\mathbf{1}_{I_\mathbf{x}}\mathbf{1}_{\{T_0\geq T_{\sigma_0}\}}\mathbf{1}_{\{(\eta_t^\mathbf{x})_{t\geq\tau_\mathbf{x}} \text{ survives}\}}\Bigg]\\
&\leq \lambda^{1+\varepsilon}\int_{T_{\sigma_0}}^1 \mathrm{d}t_0 \int_{T_\circledast}^{T_\sigma} \mathrm{d}t \int_{\mathbb{R}^d} \mathrm{d}x \rho(\kappa^{-1/\delta}t^\gamma t_0^{1-\gamma}\,|x|^d)\\
&\leq \frac{I_\rho}{(1-\gamma)\gamma}\lambda^{2/\gamma-1+\varepsilon-\sigma(1/\gamma-1)} < \frac{I_\rho}{(1-\gamma)\gamma}\lambda^{2/\gamma-1+\varepsilon/2}
\end{aligned}$$

for $\sigma > 0$ and $\lambda > 0$ sufficiently small which completes the proof. □

We now proceed to establish the probability bounds (3.10) and (3.12) of the previous proof which have been left out. To show these bounds we need to have control over the occurence of infection paths which correspond to the both events, i.e. infection paths which jump from the origin to a vertex with mark larger than T_σ and infection paths starting in a vertex with mark between T_σ and $T_\circledast$. For these bounds we will rely on the arguments used in [78, Section 5], for which we will give a short overview.

We consider now a graph $G = (V,E)$ with root 0 and let P be the set of all finite

and infinite paths of vertices in the graph G. Instead of looking at infection paths themselves, we look at the paths of vertices which result from infection paths by capturing the visited vertices. Precisely, for an infection path $g : I \to V$ we define its *ordered trace* $p_g \in P$ as the path of vertices in G given by the vertices visited by g in the same order. The following result by [78] shows the usefulness of this definition, as to control the occurence of a given class of infection paths, it is sufficient to control the number of ordered traces corresponding to this class.

Lemma 3.6: [78, Lemma 5.1]

Let $\lambda < \frac{1}{2}$. Given $p \in P$, the probability that there exists $t \geq 0$ and an infection path $g : [0, t] \to V$ with p as its ordered trace is at most $(2\lambda)^{|p|}$.

We define the following subsets of P. Let $A \subset V$ such that the root 0 is not in A and define

- for $n \geq 1$, Q_A^n as the set of paths in G of length n starting in 0, where the first n vertices are distinct and not in A but the last vertex is in A,
- for $n \geq 3$, R_A^n as the set of paths in G of length n starting in 0, where the first n vertices are distinct and not in A but the last vertex is equal to a previous one.

We denote $Q_A := \bigcup_{k \geq 1} Q_A^k$ and $R_A := \bigcup_{k \geq 3} R_A^k$.

Typically A is a set of vertices with small mark, for example smaller than $T_\star$ or $T_\circledast$. These vertices are powerful as they have many neighbours and therefore ensure the survival of the infection for longer time. The set Q_A^n then describes all ordered traces which get to such a powerful vertex in its n-th step. The motivation for the second set R_A^n lies in the following result from [78]. Given a vertex $x \in V$, the contact process $(\xi_t)_{t \geq 0}$ starting in 0 is *thin on* x if there is no infection path $g : [0, t] \to V$ for some $t \geq 0$ with $g(0) = 0$ where x appears more than once in the ordered trace p_g of g. The contact process starting in 0 is thin on a set $V' \subset V$ if it is thin on every vertex of V'.

Lemma 3.7: [78, Lemma 5.4]

If $V_0 \subset V$ is finite, then on the event that $(\xi_t)_{t\geq 0}$ is thin on $(V_0)^c$, the contact process almost surely dies out, that is, almost surely there is $t \geq 0$ such that $\xi_t = \emptyset$.

Ordered traces which are not in $Q_A \cup R_A$ do not connect to a vertex with high degree and visit each vertex at most once. Thus, by the previous lemma infection paths which have such ordered traces typically do not contribute to the survival of the contact process. A consequence is the following key result by [78].

Lemma 3.8: [78, Lemma 5.5]

There exists $c > 0$ such that, for any $\lambda < \frac{1}{2}$, the following holds. Let G be a graph with root 0, $A \subset V$ and let $(\xi_t)_{t\geq 0}$ be the contact process on G starting in 0. Then,

$$\mathbb{P}(\xi_t \neq \emptyset \ \forall t \geq 0) \leq \frac{\exp\left(c\lambda^2 \deg(\mathbf{0})\right)}{T} + T \sum_{p \in Q_A \cup R_A} (2\lambda)^{|p|} \quad \text{for all } T > 0.$$

We consider again geometric random graphs given by our framework in Section 1.2.2 and proceed to establish bounds for the number of ordered traces in Q_A and R_A on $\mathscr{G}$ for a suitable choice of A. As A is a set of vertices typically defined in terms of their marks, the ordered traces in Q_A and R_A have restrictions on the marks of the vertices but not on their location. Thus, to control the number of such ordered traces we rely on the following definition as also used in Chapter 2. Let $\ell \in (0,1)$ be the truncation value and $\tilde{\kappa} \geq I_\rho$. We define, for $n \in \mathbb{N}$ and $t_0 \in (0,1)$,

$$\nu_{\ell,n}^{t_0}(s) := \int_\ell^1 \mathrm{d}t_1 \cdots \int_\ell^1 \mathrm{d}t_{n-1} \\ \tilde{\kappa}(t_{n-1} \wedge s)^{-\gamma}(t_{n-1} \vee s)^{\gamma-1} \prod_{k=1}^{n-1} \tilde{\kappa}(t_{k-1} \wedge t_k)^{-\gamma}(t_{k-1} \vee t_k)^{\gamma-1}, \quad (3.13)$$

for $s \in (0,1)$ and set $\nu_{\ell,0}^{t_0}(s) = \delta_0(t_0 - s)$. Note that as defined, $\nu_{\ell,n}^{\mathbf{x}}(s)$ can be

written recursively as

$$\nu_{\ell,n}^{t_0}(s) = \int_{\ell}^{1} \mathrm{d}u\, \nu_{\ell,n-1}^{t_0}(u)\tilde{\kappa}(u \wedge s)^{-\gamma}(u \vee s)^{\gamma-1}. \tag{3.14}$$

This allows us to establish an upper bound for $\nu_{\ell,n}^{\mathbf{x}}(s)$ analogous to the non-spatial case in [35, Lemma 1]. This is a corollary of Lemma 2.9.

Lemma 3.9

Let $\ell \in (0,1)$ and $\nu_{\ell,n}^{t_0}(s)$ be as defined in (3.13), where $\mathbf{x} = (x_0, t_0)$ and $s \in (0,1)$. Then, there exists a constant $c > 0$ such that, for all $n \geq 2$,

$$\nu_{\ell,n}^{t_0}(s) \leq \alpha_n s^{-\gamma} + \mathbf{1}_{\{s \geq \ell\}} \beta_n s^{\gamma-1}, \tag{3.15}$$

where

$$\begin{aligned} \alpha_{n+1} &= c\big(\alpha_n \log\left(\tfrac{1}{\ell}\right) + \beta_n\big) \\ \beta_{n+1} &= c\big(\alpha_n \ell^{1-2\gamma} + \beta_n \log\left(\tfrac{1}{\ell}\right)\big) \end{aligned} \tag{3.16}$$

and $\alpha_1 = \tilde{\kappa} t_0^{\gamma-1}$, $\beta_1 = \tilde{\kappa} t_0^{-\gamma}$.

Proof. This follows analogously to the proof of Lemma 2.9 by choosing a fixed truncation value ℓ instead of an arbitrary truncation sequence. □

The following result gives an explicit upper bound for the sequence $(\alpha_n)_{n\in\mathbb{N}}$.

Lemma 3.10

Let $\ell \in (0,1)$ and $(\alpha_n)_{n\in\mathbb{N}}$, $(\beta_n)_{n\in\mathbb{N}}$ the sequences defined by 3.16. Then, it holds

$$\alpha_n \leq (2c)^{n-2} c^2 \big(\ell^{\frac{1}{2}-\gamma} t_0^{\gamma-1} + t_0^{-\gamma}\big) \ell^{(1-2\gamma)(\frac{n}{2}-1)} \quad \text{for } n \geq 2 \tag{3.17}$$

for ℓ sufficiently small.

Proof. Let ℓ be small enough such that $c^{-2} < \log(\frac{1}{\ell})^2 < \frac{1}{3}\ell^{1-2\gamma}$, where $c > 0$ is

the constant given in Lemma 3.9. Then, it is easy to see that (3.17) holds for $n = 2$. We show that it holds that

$$\alpha_{n+2} \leq (2c)^2 \ell^{1-2\gamma} \alpha_n \text{ for } n \geq 2. \tag{3.18}$$

By the definition $(\alpha_n)_{n\in\mathbb{N}}$ and $(\beta_n)_{n\in\mathbb{N}}$ it holds that

$$\alpha_{n+2} = c^2 \big(\log(\tfrac{1}{\ell})^2 + \ell^{1-2\gamma} \big) \alpha_n + 2c^2 \log(\tfrac{1}{\ell}) \beta_n \quad \text{for } n \geq 1. \tag{3.19}$$

As (3.16) also implies that $\alpha_n \vee \beta_n \leq \alpha_{n+1}$ for $n \in \mathbb{N}$ it is easy to see that is also holds that

$$\log(\tfrac{1}{\ell}) \beta_n \leq \ell^{1-2\gamma} \alpha_n + \log(\tfrac{1}{\ell})^2 \alpha_n \text{ for } n \geq 2. \tag{3.20}$$

Combining both inequalities (3.19) and (3.20) yields (3.18). Note that (3.19) also implies that (3.17) holds for $n = 3$. Thus, (3.17) follows directly by induction with (3.18). □

Recall that

$$T_{\circledast} = \frac{\lambda^{2/\gamma}}{\theta^{1/\gamma}} \log(1/\lambda)^{-1/\gamma}, \; T_\star = \lambda^{2/\gamma} \text{ and } T_\sigma = \lambda^{(2-\sigma)/\gamma}.$$

For $\mathbf{x}, \mathbf{y} \in \mathbb{R}^d \times (0,1)$ with marks $t > T_{\circledast}$ and $s > T_{\sigma_0}$ we consider now the geometric random graph $\mathscr{G}$ under the law $\mathbb{P}_{\mathbf{x},\mathbf{y}}(\cdot \,|\, \mathbf{x} \sim \mathbf{y})$. On the event that $\mathbf{x}$ and $\mathbf{y}$ are vertices in $\mathscr{G}$, we declare $\mathbf{x}$ as the root of the graph and set

$$A := \{\mathbf{z} = (z,u) \in \mathcal{X} : u \leq T_\star\} \cup \{\mathbf{y}\} \tag{3.21}$$

as the set of vertices in $\mathscr{G}$ with mark smaller than $T_\star$ together with $\mathbf{y}$.

Lemma 3.11

Let $\mathbf{x} = (x,t), \mathbf{y} = (y,s) \in \mathbb{R}^d \times (0,1)$ with $t > T_{\circledast}$ and $s > T_{\sigma_0}$. Then, there exists $\varepsilon > 0$ not depending on the choice of θ such that for A given in (3.21) it holds

$$\mathbb{E}_{\mathbf{x},\mathbf{y}} \Big[\sum_{p \in Q_A \cup R_A} (2\lambda)^{|p|} \,\Big|\, \mathbf{x} \sim \mathbf{y} \Big] < \lambda^{\varepsilon}.$$

Proof. Let $0 < \varepsilon < (\frac{1}{\gamma} - 1) \wedge \sigma_0$, which is possible as $\frac{1}{\gamma} > 1$. For $n \geq 1$, denote by $\hat{Q}_A^n$ be the set of paths in Q_A^n which do not visit $\mathbf{y}$ in its last step and denote by $\hat{Q}_{\mathbf{y}}^n := Q_A^n \backslash \hat{Q}_A^n$ the set of paths in Q_A^n with $\mathbf{y}$ as its last vertex. Note that by definition the paths in $(Q_A \cup R_A)\backslash \hat{Q}_{\mathbf{y}}^1$ never consist of the given edge between the vertices $\mathbf{x}$ and $\mathbf{y}$. Thus, the occurence of paths in $\mathscr{G}$ which belong to $(Q_A \cup R_A)\backslash \hat{Q}_{\mathbf{y}}^1$ is independent of the edge between $\mathbf{x}$ and $\mathbf{y}$ by Assumption UBA*. Then, by Mecke's equation and Assumption UBA* we have, for $n \geq 2$, that

$$\begin{aligned}&\mathbb{E}_{\mathbf{x},\mathbf{y}}\big[|\hat{Q}_A^n| \,\big|\, \mathbf{x} \sim \mathbf{y}\big] \\ &\quad = \int_{\mathbb{R}^d \times (\ell,1]} \mathrm{d}\mathbf{x}_1 \cdots \int_{\mathbb{R}^d \times (0,\ell]} \mathrm{d}\mathbf{x}_n \prod_{i=1}^{n} \rho\big(\kappa^{-1/\delta}(t_i \wedge t_{i-1})^{1-\gamma}(t_i \vee t_{i-1})^{\gamma} |x_i - x_{i-1}|^d\big),\end{aligned}$$

where $\mathbf{x}_i = (x_i, t_i)$ for $i = 1, \ldots, n$ and $\mathbf{x} = (x_0, t_0)$. Integration over the locations on the right-hand side and using (3.17) yields, for $n \geq 2$, that

$$\begin{aligned}\mathbb{E}_{\mathbf{x},\mathbf{y}}\big[|\hat{Q}_A^n| \,\big|\, \mathbf{x} \sim \mathbf{y}\big] &\leq \int_0^{\ell} \mathrm{d}t_n \nu_{\ell,n}^{t_0}(t_n) = \alpha_n \tfrac{\ell^{1-\gamma}}{1-\gamma} \\ &\leq C^n \lambda^{(1/\gamma-2)n} \lambda^2 \big(\lambda^{-1/\gamma} \log(\tfrac{1}{\lambda})^{(1-\gamma)/\gamma} + \lambda^{-2} \log(\tfrac{1}{\lambda})\big)\end{aligned}$$

for some constant $C > 0$, where we have used in the last step that $t_0 > T_{\circledast}$. As it is easy to see that this bound also holds for the case $n = 1$, there exists $C > 0$ such that, for λ small enough, we have

$$\sum_{n=1}^{\infty} (2\lambda)^n \mathbb{E}_{\mathbf{x},\mathbf{y}}\big[|\hat{Q}_A^n| \,\big|\, \mathbf{x} \sim \mathbf{y}\big] \leq C\lambda^{1/\gamma+1}\big(\lambda^{-1/\gamma} \log(\tfrac{1}{\lambda})^{(1-\gamma)/\gamma} + \lambda^{-2} \log(\tfrac{1}{\lambda})\big) < 2C\lambda^{\varepsilon}.$$

By (3.16) there exists $c > 0$, such that $\alpha_n > c(\alpha_{n-1} + \beta_{n-1})$ for $n \geq 2$, and therefore similarly to the previous calculation it holds that

$$\begin{aligned}\mathbb{E}_{\mathbf{x},\mathbf{y}}\big[|R_A^n| \,\big|\, \mathbf{x} \sim \mathbf{y}\big] &\leq n \int_{\ell}^{1} \mathrm{d}t_{n-1} \nu_{\ell,n-1}^{t_0}(t_{n-1}) = cn\alpha_n \\ &\leq c^n \lambda^{(1/\gamma-2)(n-2)} \big(\lambda^{-1/\gamma} \log(\tfrac{1}{\lambda})^{(1-\gamma)/\gamma} + \lambda^{-2} \log(\tfrac{1}{\lambda})\big),\end{aligned}$$

where $c > 0$ changes throughout the lines and therefore there exists $C > 0$ such

that, for λ small enough, we have

$$\sum_{n=3}^{\infty}(2\lambda)^n\mathbb{E}_{\mathbf{x},\mathbf{y}}\big[|R_A^n|\,\big|\,\mathbf{x}\sim\mathbf{y}\big] \le C\lambda^{1/\gamma+1}\big(\lambda^{-1/\gamma}\log(\tfrac{1}{\lambda})^{(1-\gamma)/\gamma}+\lambda^{-2}\log(\tfrac{1}{\lambda})\big) < 2C\lambda^{\varepsilon}.$$

Note that with the same calculation this bound also holds for $\sum_{n=3}^{\infty}(2\lambda)^n\mathbb{E}|\hat{Q}_{\mathbf{y}}^n|$. Thus, it is left to find a bound for $2\lambda\mathbb{E}_{\mathbf{x},\mathbf{y}}\big[|\hat{Q}_{\mathbf{y}}^1|\,\big|\,\mathbf{x}\sim\mathbf{y}\big]$ and $(2\lambda)^2\mathbb{E}_{\mathbf{x},\mathbf{y}}\big[|\hat{Q}_{\mathbf{y}}^2|\,\big|\,\mathbf{x}\sim\mathbf{y}\big]$. By definition it directly follows that the first term is smaller than $2\lambda<\lambda^{\varepsilon}$. For the second term note that $|\hat{Q}_{\mathbf{y}}^2|$ is dominated by the number of neighbours of $\mathbf{y}$ which are not $\mathbf{x}$. As the expectation of this number is smaller than $\frac{I_\rho}{(1-\gamma)\gamma}T_{\sigma_0}^{-\gamma}$, we have $(2\lambda)^2\mathbb{E}_{\mathbf{x},\mathbf{y}}\big[|\hat{Q}_{\mathbf{y}}^2|\,\big|\,\mathbf{x}\sim\mathbf{y}\big]\le C\lambda^{\sigma_0}<C\lambda^{\varepsilon}$ for some $C>0$. □

Recall that there exists a constant $C>0$ such that for any vertex $\mathbf{x}=(x,t)\in\mathbb{R}^d\times(0,1)$, its expected degree is smaller than $Ct^{-\gamma}$. We now set θ in the definition of $T_{\circledast}$ as $\theta:=\frac{\varepsilon}{8Cc}$, where $\varepsilon>0$ is given by Lemma 3.11 and $c>0$ by Lemma 3.8. The following result is then a consequence of Lemma 3.11 and follows with the same argumentation as [78, Proposition 5.8]. It provides the bound (3.12) in the proof of Proposition 3.5.

Lemma 3.12

Let $\mathbf{x}=(x,t),\mathbf{y}=(y,s)\in\mathbb{R}^d\times(0,1)$ with $t>T_{\circledast}$ and $s>T_{\sigma_0}$ and $(\xi_t^{\mathbf{x}})_{t\ge0}$ be the contact process on $\mathscr{G}$ with rate λ which only starts in $\mathbf{x}$. Then, there exists $\varepsilon>0$ such that

$$\mathbb{P}_{\mathbf{x},\mathbf{y}}(\xi_t^{\mathbf{x}}\neq\emptyset\ \forall t\ge0\,|\,\mathbf{x}\sim\mathbf{y})\le\lambda^{\varepsilon}$$

when λ is small.

Proof. As seen before the expected degree of a vertex with mark larger than $T_{\circledast}$ is smaller than $\frac{C\theta}{\lambda^2}\log(\frac{1}{\lambda})$. Thus, to find an upper bound for the survival probability of $(\xi_t^{\mathbf{x}})_{t\ge0}$ we look at whether the degree of $\mathbf{x}$ is smaller than $\frac{2C\theta}{\lambda^2}\log(\frac{1}{\lambda})$ or not.

Then, by Lemma 3.8 with $T = \lambda^{-\varepsilon/2}$ and Lemma 3.11 it holds that

$$\begin{aligned}
&\mathbb{P}_{\mathbf{x},\mathbf{y}}(\xi_t^{\mathbf{x}} \neq \emptyset \ \forall t \geq 0 \,|\, \mathbf{x} \sim \mathbf{y}) \\
&\quad \leq \mathbb{P}_{\mathbf{x},\mathbf{y}}\big(\deg(\mathbf{x}) > \frac{2C\theta}{\lambda^2}\log(\tfrac{1}{\lambda}) \,|\, \mathbf{x} \sim \mathbf{y}\big) \\
&\qquad + \frac{\exp\big(\frac{\varepsilon}{4}\log(\frac{1}{\lambda})\big)}{T} + T\mathbb{E}_{\mathbf{x},\mathbf{y}}\big[\sum_{p \in Q_A \cup R_A} (2\lambda)^{|p|} \,|\, \mathbf{x} \sim \mathbf{y}\big] \\
&\quad \leq \mathbb{P}_{\mathbf{x},\mathbf{y}}\big(\deg(\mathbf{x}) > \frac{2C\theta}{\lambda^2}\log(\tfrac{1}{\lambda}) \,|\, \mathbf{x} \sim \mathbf{y}\big) + \lambda^{\varepsilon/4} + \lambda^{\varepsilon/2}.
\end{aligned}$$

As the number of neighbours of $\mathbf{x}$ different to $\mathbf{y}$ is Poisson distributed with parameter at most $\frac{C\theta}{\lambda^2}\log(\frac{1}{\lambda})$, using a Chernoff bound yields

$$\mathbb{P}_{\mathbf{x},\mathbf{y}}\big(\deg(\mathbf{x}) > \frac{2C\theta}{\lambda^2}\log(\tfrac{1}{\lambda}) \,|\, \mathbf{x} \sim \mathbf{y}\big) \leq \exp\big(-c_1\frac{\theta}{\lambda^2}\log(\tfrac{1}{\lambda})\big) < \lambda$$

for λ small enough, where $c_1 > 0$ is some constant. Thus, $\mathbb{P}_{\mathbf{x},\mathbf{y}}(\xi_t^{\mathbf{x}} \neq \emptyset \ \forall t \geq 0 \,|\, \mathbf{x} \sim \mathbf{y}) \leq 3\lambda^{\varepsilon/4}$ which completes the proof. □

As the last step to complete the proof of Proposition 3.5 we show inequality (3.10). Recall that, for $\sigma > 0$, E_σ denotes the event that each infection path of the contact process $(\xi_t^{(0,T_0)})_{t\geq 0}$ which jumps at first to a vertex with mark larger than T_σ is finite and never reaches a vertex with mark smaller than T_σ.

Lemma 3.13

There exists $\varepsilon > 0$ and $\sigma > 0$, such that

$$\mathbb{P}_{(0,T_0)}(E_\sigma^c \cap \{T_0 \geq T_\sigma\}) \leq \lambda^{2/\gamma - 1 + \varepsilon}.$$

Proof. We denote by

$$B_\sigma = \{\mathbf{x} \in \mathcal{X} : \mathbf{x} \neq \mathbf{0}, t \leq T_\sigma\}$$

the set of vertices with mark smaller or equal to T_σ and by $Q_{B_\sigma}^n$ and $R_{B_\sigma}^n$ the associated sets of paths, which either visit a vertex in B_σ in its last step or whose

vertices are not in B_σ but the last vertex is equal to a previous one. We set

$$Q_{B_\sigma} = \bigcup_{n\geq 2} Q^n_{B_\sigma}, \quad R_{B_\sigma} = \bigcup_{n\geq 3} R^n_{B_\sigma}$$

and $P_0 = \big\{\big((0,T_0),\mathbf{x},(0,T_0),\mathbf{y}\big) : \mathbf{x},\mathbf{y} \sim (0,T_0)\big\}$. By [78, Lemma 5.10] the event that no infection path starting in $(0,T_0)$ has an ordered trace in $P_0 \cup Q_{B_\sigma} \cup R_{B_\sigma}$ implies E_σ. In fact, if no infection path starting in $(0,T_0)$ has ordered trace in $P_0 \cup Q_{B_\sigma} \cup R_{B_\sigma}$, then each infection path $g : I \to V$ which starts at $(0,T_0)$ and jumps to a vertex $\mathbf{x} = (x,t)$ with $t \geq T_\sigma$ never visits a vertex in B_σ and never visits a vertex outside of B_σ more than once. Thus, by Lemma 3.7 any such infection path is finite, as the contact process starting in $(0,T_0)$ and restricted to B^c_σ is thin outside $(0,T_0)$ and dies out. Hence, it then holds

$$\begin{aligned}
&\mathbb{P}_{(0,T_0)}(E^c_\sigma \cap \{t_0 \geq T_\sigma\}) \\
&\quad \leq \mathbb{E}_{(0,T_0)}\big[\mathbf{1}\{t_0 \geq T_\sigma\} \sum_{p\in P_0\cup Q_{B_\sigma}\cup R_{B_\sigma}} (2\lambda)^{|p|}\big] \\
&\quad \leq (2\lambda)^3 \mathbb{E}_{(0,T_0)}[|P_0|\,\mathbf{1}\{t_0 > T_\sigma\}] + \sum_{n=2}^{\infty}(2\lambda)^n \mathbb{E}_{(0,T_0)}\left|Q^n_{B_\sigma}\right| + \sum_{n=3}^{\infty}(2\lambda)^n \mathbb{E}_{(0,T_0)}\left|R^n_{B_\sigma}\right|.
\end{aligned} \tag{3.22}$$

We will proceed to find upper bounds for the expected number of ordered traces corresponding to each of the three classes P_0, Q_{B_σ} and R_{B_σ}. First, it holds by Mecke's equation and integration over the location of the vertices that

$$\begin{aligned}
&(2\lambda)^3 \mathbb{E}_{(0,T_0)}[|P_0|\,\mathbf{1}\{T_0 > T_\sigma\}] \\
&\qquad \leq (2\lambda)^3 I_\rho^2 \int_{T_\sigma}^1 \mathrm{d}t_0 \int_0^1 \mathrm{d}s \int_0^1 \mathrm{d}t (t_0\wedge s)^{-\gamma}(t_0\wedge s)^{\gamma-1}(t_0\wedge t)^{-\gamma}(t_0\wedge t)^{\gamma-1} \\
&\qquad \leq (2\lambda)^3 (CI_\rho)^2 \int_{T_\sigma}^1 \mathrm{d}t_0 t_0^{-2\gamma} \\
&\qquad \leq C^3\lambda^{2/\gamma-1+\sigma(2-1/\gamma)} < C^3\lambda^{2/\gamma-1+\varepsilon},
\end{aligned}$$

for some small $\varepsilon > 0$ as $2/\gamma - 1 + \sigma(2-1/\gamma)$ is increasing in σ as $\gamma > \frac{1}{2}$. The positive constant C does not depend on λ and σ but may change throughout the lines.

Using Lemma 3.9 and (3.17) with $\ell = T_\sigma = \lambda^{2-\sigma}$ as done in the proof of Lemma

3.11 we have by Mecke's equation and Assumption UBA*, for $n \geq 2$, that

$$\begin{aligned}\mathbb{E}_{(0,T_0)}\left|Q^n_{B_\sigma}\right| &= \int_0^1 \mathrm{d}t_0 \int_0^\ell \mathrm{d}t_n \nu^{t_0}_{\ell,n}(t_n) \\ &\leq \frac{1}{1-\gamma}(2c)^{n-2}c^2\ell^{(1-2\gamma)(n/2-1)}\ell^{1-\gamma}\int_0^1 \mathrm{d}t_0(\ell^{1/2-\gamma}t_0^{1-\gamma}+t_0^{-\gamma}) \\ &\leq C^n\lambda^{(1/\gamma-2)(n/2-1)(2-\sigma)}\lambda^{(1/\gamma-1)(2-\sigma)}\lambda^{(1/(2\gamma)-1)(2-\sigma)},\end{aligned}$$

for some positive constant $C > 0$. Then, it follows that

$$\sum_{n=2}^{\infty}(2\lambda)^n\mathbb{E}_{(0,T_0)}\left|Q^n_{B_\sigma}\right| \leq C^2\lambda^{3/\gamma-1}\lambda^{(2-1/\gamma-1/(2\gamma))\sigma} < C^2\lambda^{2/\gamma-1+\varepsilon}$$

for $\sigma > 0$ sufficiently small. For the last summand Lemma 3.9 and (3.17) yield similarly that

$$\begin{aligned}\mathbb{E}_{(0,T_0)}\left|R^n_{B_\sigma}\right| &\leq n\int_0^1 \mathrm{d}t_0 \int_\ell^1 \mathrm{d}t_{n-1}\nu^{t_0}_{\ell,n-1}(t_{n-1}) \\ &\leq \frac{n}{c(1-\gamma)\gamma}\int_0^1 \mathrm{d}t_0\alpha_n \\ &\leq \frac{n}{(1-\gamma)\gamma}(2c)^{n-2}c\ell^{(1-2\gamma)(n/2-1)}\int_0^1 \mathrm{d}t_0(\ell^{1/2-\gamma}t_0^{1-\gamma}+t_0^{-\gamma}).\end{aligned}$$

and we have therefore

$$\begin{aligned}\sum_{n=3}^{\infty}(2\lambda)^n\mathbb{E}_{(0,T_0)}\left|R^n_{B_\sigma}\right| &\leq \sum_{n=3}^{\infty}C^n\lambda^{(1/\gamma-1)n}\lambda^{2-1/\gamma}\lambda^{(2-1/\gamma)(n/2-1/2)\sigma)} \\ &\leq C^3\lambda^{2/\gamma-1}\lambda^{(2-1/\gamma)\sigma} < \lambda^{2/\gamma-1+\varepsilon},\end{aligned}$$

since $2/\gamma - 1 + \sigma(2 - 1/\gamma)$ is again increasing in σ. As all three summands of the righthand side of (3.22) are bounded by $C\lambda^{2/\gamma-1+\varepsilon}$ for some constants $C > 0$ and $\varepsilon > 0$ sufficiently small this completes the proof. □

3.3 Exponential extinction time on finite restrictions

In this section we consider the graph sequence $(\mathscr{G}_n)_{n\in\mathbb{N}}$, where $\mathscr{G}_n$ is the spatial restriction of $\mathscr{G}$ on $[-\frac{n^{1/d}}{2}, \frac{n^{1/d}}{2}]^d$. As this is a sequence of finite graphs, the contact process with any potential initial condition will almost surely die out for all $n \in \mathbb{N}$. Thus, the more natural question is to estimate the time the infection survives on these graphs when the infection starts with the best possible initial condition, i.e. when the graph is fully infected. We denote by

$$\varpi_n := \inf\{t > 0 : \xi_t^{\mathscr{G}_n} = \emptyset\} \tag{3.23}$$

the extinction time of the contact process on $\mathscr{G}_n$. The main result of this section shows that for any choice of $\lambda > 0$ the extinction time is at least of exponential order in the number of vertices of $\mathscr{G}_n$ with high probability as n becomes large.

Theorem 3.14

Let $(\mathscr{G}_n)_{n\in\mathbb{N}}$ be the restricted finite graph sequence of a general geometric random graph which satisfies Assumption LBA for $\gamma > \frac{\delta}{\delta+1}$. For any $\lambda > 0$, there exists $c > 0$ such that

$$\lim_{n\to\infty} \mathbb{P}\{\varpi_n \geq e^{cn}\} = 1.$$

Remark 3.3.1. Note that the result of Theorem 3.14 also hold when we consider a graph sequence $(\mathscr{G}_n)_{n\in\mathbb{N}}$, where each graph $\mathscr{G}_n$ is defined on a Poisson process of unit intensity on the torus $\mathbb{T}_n$ with volume n and satisfies Assumption LBA, where the Euclidean distance is replaced by the torus metric.

As seen in the proof of Proposition 3.2 the infection survives well on the neighbourhood of sufficiently powerful vertices, the so called stars. Our main contribution is to show that there exists a connected subgraph in $\mathscr{G}_n$ which contains of order n stars. Then, with similar arguments as done in [86], it can be shown that the infection survives on this subgraph at least for a time of exponential order in n.

Proposition 3.15

Let $S > 0$ be given and $(\mathscr{G}_n)_{n\in\mathbb{N}}$ the restricted finite graph sequence of a general geometric random graph which satisfies Assumption LBA for $\gamma > \frac{\delta}{\delta+1}$. Then, there exists $b > 0$ and $\varepsilon > 0$ such that, for n sufficiently large, the probability that $\mathscr{G}_n$ has a connected subgraph containing $b \cdot n$ disjoint stars of at least S vertices each is larger than $1 - \exp(-n^{\varepsilon})$.

Proof. We fix $0 < a < \frac{1}{\log 2}$ and choose $\varepsilon_1 > 0$ small enough that $\log 2 > \frac{\varepsilon_1 + \log 2}{\gamma+\gamma/\delta}$, which is possible since $\gamma > \frac{\delta}{\delta+1}$. Similar the proof of Lemma 3.3, the vertices with mark smaller than $\frac{1}{2}$ will represent the potential midpoints of the stars of the subgraph, whereas the vertices with larger mark represent potential neighbours and connectors of the midpoints. For this proof it is not sufficient to use the arguments of Lemma 3.3 to show that a line of stars exists in $\mathscr{G}_n$, as such a subgraph would only consist of order $\log(n)$ many stars. Hence, we need to to break up the powerful vertices of $\mathscr{G}_n$ with mark smaller than $\frac{1}{2}$ more carefully into a system of boxes such that each of these boxes contains a midpoint of one potential star. Let $n_p = \lfloor n^{(1-a\log 2)/d} \rfloor$ and $k_p = \lfloor (a \log n)/d \rfloor$. For $k = 0, \dots k_p$, we define

$$V_k := \{0, \dots, n_p 2^{k_p - k} - 1\}^d.$$

and

$$A_{k,\mathbf{v}} := \bigtimes_{i=1}^{d} \left(2^k v_i, 2^k (v_i + 1)\right) \quad \text{for } k = 0, \dots, k_p \text{ and } \mathbf{v} = (v_1, \dots, v_d) \in V_k.$$

For each $k = 0, \dots, k_p$, the cubes $\{A_{k,\mathbf{v}} : \mathbf{v} \in V_k\}$ give a tessellation of $[0, \frac{n^{1/d}}{2}]^d$ into $(n_p 2^{k_p-k})^d$ cubes of volume 2^{kd} such that the finest tessellation is given for $k = 0$ and the coarsest for $k = k_p$. Furthermore, the cubes are nested in each other in the sense that for each cube $A_{k+1,\mathbf{v}}$ the cubes $\{A_{k,2\mathbf{v}+\mathbf{e}} : \mathbf{e} \in \{0,1\}^d\}$ are a tessellation of $A_{k+1,\mathbf{v}}$.

Set $\theta > 0$ such that $\log 2 > \theta > \frac{\varepsilon_1 + \log 2}{\gamma+\gamma/\delta}$ and define

$$B_{k,\mathbf{v}} := A_{k,\mathbf{v}} \times (\tfrac{1}{2} e^{-(k+1)\theta d}, \tfrac{1}{2} e^{-k\theta d}) \quad \text{for } k = 0, \dots k_p \text{ and } \mathbf{v} = (v_1, \dots, v_d) \in V_k.$$

We denote with the parameter $k = 0, \dots k_p$ the layer of the boxes $\{B_{k,\mathbf{v}} : \mathbf{v} \in \mathcal{V}_k\}$

which defines the range of the marks of points of $\mathcal{X}$ inside the boxes and the level of coarsness of the tessellation of the space. Thus, large values of k imply more powerful vertices and a coarser set of boxes to separate them. As an example, the boxes of the most powerful layer k_p have width of order $n^{a\log 2}$ and the marks of the vertices therein are of order $n^{-a\theta\log 2}$. As we have already seen that the cubes $\{A_{k,\mathbf{v}} : k = 0,\dots,k_p, \mathbf{v} \in V_k\}$ are nested in each other, the system of boxes $\{B_{k,\mathbf{v}} : k = 0,\dots,k_p, \mathbf{v} \in V_k\}$ can be made to have a tree structure by treating $B_{k+1,\mathbf{v}}$ as the parent of each box $B_{k,2\mathbf{v}+\mathbf{e}}$, for $\mathbf{e} \in \{0,1\}^d$, see Figure 3.3. This leads to n_p^d distinct $2d$-regular trees with roots $\{B_{k_p,\mathbf{v}} : \mathbf{v} \in V_{k_p}\}$.

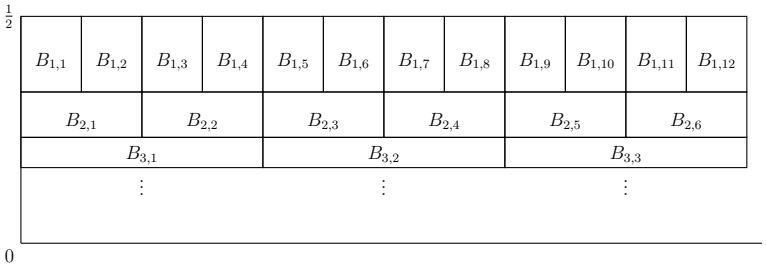

Figure 3.3: Sketch of the structure of the boxes $B_{k,\mathbf{v}}$ in dimension one. The y-axis represents the mark of the vertices and the x-axis the location.

Note that the amount of vertices in a box $B_{k,\mathbf{v}}$ is Poisson-distributed with parameter

$$2^{kd}\left(\tfrac{1}{2}e^{-k\theta d} - \tfrac{1}{2}e^{-(k+1)\theta d}\right) > ce^{kd(\log 2-\theta)}$$

for some constant $c > 0$ not depending on k and $\mathbf{v}$. Thus, for $\varepsilon_2 = \log 2 - \theta > 0$ it holds that

$$\mathbb{P}\{B_{k,\mathbf{v}} \text{ is non-empty}\} \geq 1 - \exp\left(ce^{kd\varepsilon_2}\right). \tag{3.24}$$

On the event that $B_{k,\mathbf{v}}$ is non-empty we denote by $\mathbf{x}_{k,\mathbf{v}}$ the vertex with the smallest mark in the box.

As mentioned above each of these boxes corresponds to one potential midpoint of the stars. For each such midpoint, i.e. for each such box we need a distinct set of potential neighbours and connectors. To this end, we colour the vertices with mark larger than $\frac{1}{2}$. Choose $0 < \varepsilon_3 < \theta\gamma \wedge \delta\varepsilon_1$ such that $\sum_{k=0}^{\infty} e^{-kd(\theta\gamma\wedge\delta\varepsilon_1-\varepsilon_3)}$ converges and color the points of $\mathcal{X}$ on $\mathbb{R}^d \times [\frac{1}{2}, 1)$ by the colour set $\mathbb{N}$ independently such that the points with color $k \in \mathbb{N}$ form a Poisson point process $\mathcal{X}_k$ on $\mathbb{R}^d \times [\frac{1}{2}, 1)$ with an intensity proportional to $e^{-kd(\theta\gamma\wedge\delta\varepsilon_1-\varepsilon_3)}$. For $k = 0,\dots,k_p$

and $\mathbf{v} \in V_k$, we denote by

- $N_{k,\mathbf{v}} = \mathcal{X}_k \cap A_{k,\mathbf{v}} \times [\frac{1}{2}, \frac{3}{4})$ the potential neighbours of $\mathbf{x}_{k,\mathbf{v}}$, if $B_{k,\mathbf{v}}$ is non-empty and by
- $C_{k,\mathbf{v}} = \mathcal{X}_k \cap A_{k,\mathbf{v}} \times [\frac{3}{4}, 1)$ the potential connectors, which we will use to connect $\mathbf{x}_{k,\mathbf{v}}$ to other midpoints.

Note that the intensity of these Poisson point processes is decreasing in k, as it is easier for vertices with smaller mark to find sufficiently many neighbours and connectors in the corresponding boxes, so we require fewer candidates to succeed.

Since $\theta\gamma < \log 2$, there exists $c > 0$ such that, for all $k = 0, \dots, k_p$, on the event that $B_{k,\mathbf{v}}$ is non-empty it holds $ct_{k,\mathbf{v}}^{-\gamma/d} < 2^k$, where $t_{k,\mathbf{v}}$ is the mark of $\mathbf{x}_{k,\mathbf{v}}$. Thus for each $k = 0, \dots, k_p$, the volume of $B(\mathbf{x}_{k,\mathbf{v}}, ct_{k,\mathbf{v}}^{-\gamma/d}) \cap A_{k,\mathbf{v}}$ is a positive proportion $\rho > \frac{1}{2^d}$ of the volume of the ball itself. As in the proof of Lemma 3.3 this leads to two observations. First, given $B_{k,\mathbf{v}}$ is non-empty, by the same arguments as in the proof of Lemma 3.4 the number of neighbours of $x_{k,\mathbf{v}}$ in $N_{k,\mathbf{v}}$ is Poisson-distributed with parameter larger than $ce^{-kd(\theta\gamma\wedge\delta\varepsilon_1-\varepsilon_3)}e^{kd\theta\gamma} > ce^{kd\varepsilon_3}$ for some constant $c > 0$ not depending on k. We denote by $\mathrm{Star}(k, \mathbf{v})$ the event that $B_{k,\mathbf{v}}$ is non-empty and $\mathbf{x}_{k,\mathbf{v}}$ has at least S neighbours in $N_{k,\mathbf{v}}$. Then, by a Chernoff bound there exists $c > 0$ and k_0 sufficiently large and not depending on n such that for all $k \geq k_0$ and $\mathbf{v} \in V_k$ it holds

$$\mathbb{P}\big(\,\mathrm{Star}(k, \mathbf{v}) \,|\, B_{k,\mathbf{v}} \text{ is non-empty}\big) \geq 1 - \exp(-ce^{kd\varepsilon_3}). \tag{3.25}$$

Second, given the box $B_{k+1,\mathbf{v}}$ and one of its children $B_{k,2\mathbf{v}+\mathbf{e}}$ are non-empty, note that $\mathbf{x}_{k+1,\mathbf{v}}$ and $\mathbf{x}_{k,2\mathbf{v}+\mathbf{e}}$ have distance at most $\sqrt{d}2^{k+1}$ and both have marks smaller $\frac{1}{2}e^{-k\theta d}$. Thus, by the same argument as used in the proof of Lemma 2.3, there exists a constant $c > 0$ such that the number of vertices in $C_{k,2\mathbf{v}+\mathbf{e}}$ which form an edge to both $\mathbf{x}_{k+1,\mathbf{v}}$ and $\mathbf{x}_{k,2\mathbf{v}+\mathbf{e}}$ is Poisson-distributed with parameter larger than

$$ce^{-kd(\theta\gamma\wedge\delta\varepsilon_1-\varepsilon_3)}t_{k,2\mathbf{v}+\mathbf{e}}^{-\gamma}\big(1 \wedge t_{k+1,\mathbf{v}}^{-\gamma\delta}(|x_{k,2\mathbf{v}+\mathbf{e}} - x_{k+1,\mathbf{v}}| + t_{k,2\mathbf{v}+\mathbf{e}}^{\gamma/d})^{-d\delta}\big) > ce^{kd\varepsilon_3}$$

where the constant $c > 0$ changes through the steps but does not depend on k

and $\mathbf{v}$ and we have used that $\theta > \frac{\varepsilon_1+\log 2}{\gamma+\gamma/\delta}$. Denote by $\mathbf{x}_{k+1,\mathbf{v}} \overset{2}{\leftrightarrow} \mathbf{x}_{k,2\mathbf{v}+\mathbf{e}}$ the event that the boxes $B_{k+1,\mathbf{v}}$ and $B_{k,2\mathbf{v}+\mathbf{e}}$ are non-empty and the vertices $\mathbf{x}_{k+1,\mathbf{v}}$ and $\mathbf{x}_{k,2\mathbf{v}+\mathbf{e}}$ are connected via a vertex in $C_{k,2\mathbf{v}+\mathbf{e}}$. Then, we have for all $k \in \mathbb{N}$ and $\mathbf{v} \in V_k$ that

$$\mathbb{P}(\mathbf{x}_{k+1,\mathbf{v}} \overset{2}{\leftrightarrow} \mathbf{x}_{k,2\mathbf{v}+\mathbf{e}} \,|\, B_{k+1,\mathbf{v}} \text{ and } B_{k,2\mathbf{v}+\mathbf{e}} \text{ are non-empty}) \geq 1 - \exp(-ce^{kd\varepsilon_3}). \tag{3.26}$$

With the structure of the boxes and the bounds (3.24)-(3.26) at hand we will show that there exists a connected subgraph containing of order n distinct stars with at least S vertices each. This will be done in two steps. First, we show that the vertices in the most powerful layer k_p form a connected subgraph containing n_p^d distinct stars, where each box $B_{k_p,\mathbf{v}}$ contains one of the midpoints of these stars. Second, recall that each box $B_{k_p,\mathbf{v}}$ for $\mathbf{v} \in V_{k_p}$ represents the root of a 2^d-regular tree. We will show that the trees resulting only from boxes contributing a star to the connected subgraph are percolated 2^d-regular trees with a depth of order k_p containing of order $2^{k_p d}$ distinct stars. As there are n_p^d many trees like this, this will lead to a connected subgraph of $\mathscr{G}_n$ with of order n distinct stars.

To simplify notation we redefine the labeling of the boxes of layer k_p. Let

$$\sigma : \{0, \dots, n_p^d - 1\} \to V_k$$

be a bijection such that $B_{k_p,\sigma(0)} = B_{k_p,\mathbf{0}}$ and the boxes $B_{k_p,\sigma(i)}$, $B_{k_p,\sigma(i+1)}$ are adjacent to each other for $i = 0, \dots, n_p^d - 2$. In the same way we relabel the vertices with the smallest mark in a box, i.e. on the event that $B_{k_p,\sigma(i)}$ is non-empty we denote by $\mathbf{x}_{k_p,\sigma(i)}$ the vertex with the smallest mark in that box. We say $B_{k_p,\sigma(0)}$ is good if and only if the box is non-empty and the vertex $\mathbf{x}_{k_p,\sigma(0)}$ has at least S neighbours in $N_{k_p,\sigma(0)}$. By (3.24) and (3.25), there exists $c > 0$ such that

$$\mathbb{P}(B_{k_p,\sigma(0)} \text{ is good}) \geq \big(1 - \exp(-ce^{k_p d\varepsilon_2})\big)\big(1 - \exp(-ce^{k_p d\varepsilon_3})\big).$$

For $i = 0, \dots, n_p^d - 2$, we say $B_{k_p,\sigma(i+1)}$ is good if

(i) $B_{k_p,\sigma(i)}$ is good,

(ii) $B_{k_p,\sigma(i+1)}$ is non-empty,

(iii) $\mathbf{x}_{k_p,\sigma(i+1)}$ has at least S neighbours in $N_{k_p,\sigma(i+1)}$ and

(iv) $\mathbf{x}_{k_p,\sigma(i+1)}$ and $\mathbf{x}_{k_p,\sigma(i)}$ are connected via a connector in $C_{k_p,\sigma(i+1)}$

and otherwise bad. Let $\varepsilon_4 < \varepsilon_2 \wedge \varepsilon_3$. Then, by (3.24)-(3.26), there exists $c > 0$ such that, for $i = 0, \dots, n_p^d - 2$, it holds

$$\mathbb{P}(B_{k_p,\sigma(i+1)} \text{ is good} \,|\, B_{k_p,\sigma(i)} \text{ is good}) \geq \big(1 - \exp(-ce^{kd\varepsilon_4})\big).$$

Thus we can deduce that

$$\mathbb{P}(B_{k_p,\mathbf{v}} \text{ is good for all } \mathbf{v} \in V_{k_p}) \geq 1 - n_0^d \exp(-ce^{k_p d\varepsilon_4}) \geq 1 - n^{1-a\log 2} \exp(-cn^{a\varepsilon_4}). \tag{3.27}$$

We continue the definition of good boxes on the other layers. For $\mathbf{v} \in \mathbb{N}$ denote by $\lfloor \frac{\mathbf{v}}{2} \rfloor$ the vector $(\lfloor \frac{v_1}{2} \rfloor, \dots, \lfloor \frac{v_d}{2} \rfloor)$. Then, for each $k = 0, \dots, k_p - 1$ and $\mathbf{v} \in V_k$ the parent box of $B_{k,\mathbf{v}}$ is given by $B_{k+1,\lfloor \frac{\mathbf{v}}{2} \rfloor}$. For $k = 0, \dots, k_p - 1$ and $\mathbf{v} \in V_k$, we say that $B_{k,\mathbf{v}}$ is good if

(i) $B_{k+1,\lfloor \frac{\mathbf{v}}{2} \rfloor}$ is good,

(ii) $B_{k,\mathbf{v}}$ is non-empty,

(iii) $\mathbf{x}_{k,\mathbf{v}}$ has at least S neighbours in $N_{k,\mathbf{v}}$ and

(iv) $\mathbf{x}_{k,\mathbf{v}}$ and $\mathbf{x}_{k+1,\lfloor \frac{\mathbf{v}}{2} \rfloor}$ are connected via a connector in $C_{k,\mathbf{v}}$

and otherwise we say that $B_{k,\mathbf{v}}$ is bad. Note that again (3.24)-(3.26) implies that there exists $c > 0$ such that for all $k = 0, \dots, k_p - 1$, $\mathbf{v} \in V_k$ and $\mathbf{e} \in \{0,1\}^d$, it holds

$$\mathbb{P}(B_{k,2\mathbf{v}+\mathbf{e}} \text{ is good} \,|\, B_{k+1,\mathbf{v}} \text{ is good}\} \geq 1 - \exp(-ce^{kd\varepsilon_4}) \tag{3.28}$$

and given $B_{k+1,\mathbf{v}}$ is good, the events that $B_{k,2\mathbf{v}+\mathbf{e}}$ is good are independent of each other and any other box on this layer, since they depend on disjoint subsets of $\mathcal{X}$ and edges occur independently. Therefore, the number of good children of $B_{k+1,\mathbf{v}}$, given this box is good, is Binomial-distributed with parameters 2^d and $p_k > 1 - \exp(-ce^{kd\varepsilon_4})$ and, given the good boxes on layer $k+1$, the numbers of good children of each of those good boxes are independent of each other. Consequently, denote by $|B_k|$ the number of good boxes in layer k. Then, given $|B_{k+1}|$, $|B_k|$ is Binomial-distributed with parameters $2^d\,|B_{k+1}|$ and p_k.

With this observation we are able to give estimates on the number of good

boxes in each layer and show that sufficiently many good boxes exists. For $k = 0, \dots, k_p - 1$, we denote by $E_k := \{|B_k| > 2^d(1 - k^{-2})\,|B_{k+1}|\}$ the event that layer k has sufficiently many good boxes in comparison to layer $k+1$ of the next more powerful vertices and we denote by E_{k_p} the event that all boxes in layer k_p are good. Then, the event $E_k \cap \ldots \cap E_{k_p}$ implies that

$$|B_k| > \left|B_{k_p}\right| \prod_{i=k}^{k_p-1} 2^d(1 - i^{-2}) > c n_0^d 2^{d(k_p-k-1)} > c 2^{-kd} n,$$

where $c = \prod_{i=1}^{\infty}(1 - i^{-2})$. Thus, it is sufficient to show that there exists k_0 such that $E_{k_0} \cap \ldots \cap E_{k_p}$ holds with high probability. We choose k_0 large enough that (3.25) still holds for all $k \geq k_0$ and $\mathbf{v} \in V_k$ and that $1 - \exp(ce^{k_0 d\varepsilon_4}) > 1 - k_0^{-2}$. Then, by a Chernoff bound for Binomial-distributed random variables it holds

$$P\big(E_k^c \,\big|\, |B_{k+1}|\,\big) \leq \exp\Big(-\frac{2^{d-1}\,|B_{k+1}|\,ce^{kd\varepsilon_4}}{k^2}\Big)$$

for all $k \geq k_0$. As a consequence, there exists $c > 0$ such that

$$\mathbb{P}(E_k \,|\, E_{k+1} \cap \ldots \cap E_{k_p}) \geq 1 - \exp(-c\frac{e^{kd\varepsilon_4} 2^{-kd} n^d}{k^2}) \geq 1 - \exp\Big(-c\frac{n^{ad\varepsilon_4}}{(\log n)^2}\Big).$$

Hence, it follows together with (3.27) that

$$\mathbb{P}(E_{k_0} \cap \ldots \cap E_{k_p}) \geq \mathbb{P}(E_{k_p})\left(1 - \lfloor a \log n \rfloor \exp\Big(-c\frac{n^{ad\varepsilon_4}}{(\log n)^2}\Big)\right) \geq 1 - \exp(-n^{\varepsilon})$$

for some ε not depending on n. As $E_{k_0} \cap \ldots \cap E_{k_p}$ implies the existence of up to a constant at least $2^{-k_0} n$ good boxes and therefore the existence of a connected subgraph of $\mathscr{G}_n$ containing bn distinct stars, for some $b > 0$, this completes the proof. □

Proof of Theorem 3.14. Given the subgraph $G_n = (V_n, E_n)$ provided by Proposition 3.15 note that G_n is a connected tree by construction. Denote by $M_n \subset V_n$ the set of vertices which are the midpoints of the stars containing S vertices. For $\mathbf{x}, \mathbf{y} \in M_n$, write $\mathbf{x} \overset{2}{\leftrightarrow} \mathbf{y}$ if there exists a connector in G_n which forms an edge to $\mathbf{x}$ and $\mathbf{y}$. By definition all vertices $\mathbf{x}, \mathbf{y} \in M_n$ with $\mathbf{x} \overset{2}{\leftrightarrow} \mathbf{y}$ have graph distance

at most two in G_n. The graph H_n given by the vertex set M_n and the edge set

$$F_n := \{\{\mathbf{x}, \mathbf{y}\} : \mathbf{x}, \mathbf{y} \in M_n, \mathbf{x} \overset{2}{\leftrightarrow} \mathbf{y}\}$$

is a connected tree with degree bounded by $2^d + 2$ and for each pair $\mathbf{x}, \mathbf{y} \in M_n$ with $\mathbf{x} \overset{2}{\leftrightarrow} \mathbf{y}$ the connector is unique. Hence, for any $\lambda > 0$ and with $S > 0$ chosen sufficiently large depending on λ by the same arguments as used in the proof of [86, Theorem 1.4] together with [86, Proposition 5.2] it holds $\lim_{n\to\infty} \mathbb{P}\{\varpi_n \geq e^{cn}\} = 1$ for some constant $c > 0$. □

CHAPTER 4

Application of results to concrete examples of scale-free geometric random graphs

In this chapter we introduce and discuss various different examples of scale-free geometric random graphs. Those models are either part of the discussed class characterized in Section 1.2.2 or are well-studied models from the literature which serve as a comparison to the first. We discuss the application of the main results of this thesis to these models, with the first two sections being the core of the chapter, as in these we discuss the two main examples, the age-dependent random connection model and the soft Boolean model.

4.1 The age-dependent random connection model

In the *age-dependent random connection model* each vertex is a point of a Poisson point process of unit intensity on $\mathbb{R}^d$ which carries an independent uniform distributed birth time in $(0,1)$. Thus, the vertex set is given by a Poisson point process of unit intensity on $\mathbb{R}^d \times (0,1)$ and, for a vertex $\mathbf{x} = (x,t)$, the first entry x is its *location* in $\mathbb{R}^d$ and the second entry is the *birth time* of the vertex, as introduced in Section 1.2.1. Let $\gamma \in (0,1)$ and $\beta > 0$. Then, given the vertex set,

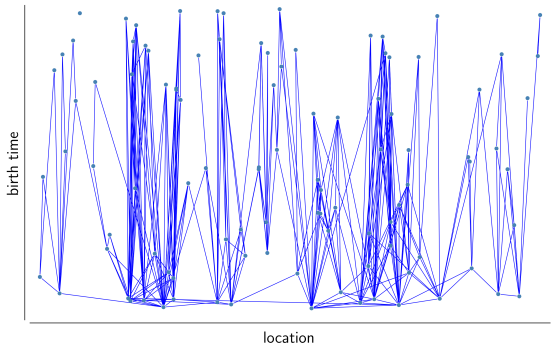

Figure 4.1: Snapshot of a simulation of the age-dependent random connection model on $\mathbb{R} \times (0,1)$. Values on the horizontal axis represent the location of the vertices and values on the vertical axis their birth times. For the simulation we set $\beta = 1$, $\gamma = 0.75$ and $\varphi(x) := 1 \wedge x^{-\delta}$ with $\delta = 1.5$. For comparison see Figure 4.8.

we connect two vertices $\mathbf{x} = (x,t)$ and $\mathbf{y} = (y,s)$ independently with probability

$$\varphi\big(\beta^{-1}(t \wedge s)^{\gamma}(t \vee s)^{1-\gamma}\,|x-y|\,\big), \tag{4.1}$$

where $\varphi : [0,\infty) \to [0,1]$ is a non-increasing integrable function. See Section 4.1.1 for comments on the role and the interplay of the parameters γ and β and the *profile function* φ.

Applying our main results proven in Chapter 2 we are able to give a sharp transition for the occurence of ultrasmallness under assumptions on the profile function φ. If there exists $\delta > 0$ such that, for every $\varepsilon > 0$, there is $C > 0$ for which it holds $\varphi(r) \leq Cr^{-(\delta-\varepsilon)}$ for $r \geq 0$, then the age-dependent random connection model satisfies Assumption UBA*, and consequently Assumption UBA, for the parameters γ and $\delta - \varepsilon$ for every small $\varepsilon > 0$. Thus by Theorem 2.1, ultrasmallness fails under this assumption on φ when $\gamma < \frac{\delta}{\delta+1}$. In particular, this implies that there is no ultrasmallness if the profile function φ only has bounded support since the parameter δ can be chosen arbitrarily large in this case.

However, if the profile function φ also satisfies that, for every $\varepsilon > 0$, there is $c > 0$ for which $\varphi(r) \geq cr^{-(\delta+\varepsilon)}$, for all $r \geq 1$, then the model satisfies Assumption LBA for the parameters γ and $\delta + \varepsilon$ for every $\varepsilon > 0$. Hence, if $\gamma > \frac{\delta}{\delta+1}$ the model is ultrasmall and, since the asymptotic lower and upper bounds given in Theorem

2.1 and Proposition 2.13 hold for the parameter γ and one arbitrarily close to δ, we obtain the full limit theorem stated in (2.5). In summary, we obtain the following theorem.

Theorem 4.1

Let $\delta > 1$ and $\varphi : [0, \infty) \to [0, 1]$ such that, for every sufficiently small $\varepsilon > 0$, there are $c, C > 0$ such that

$$cr^{-(\delta+\varepsilon)} \leq \varphi(r) \leq Cr^{-(\delta-\varepsilon)} \quad \text{for all } r \geq 1. \tag{A1}$$

Then, the age-dependent random connection model

- is **not ultrasmall** if $\gamma < \frac{\delta}{\delta+1}$ and
- is **ultrasmall** if $\gamma > \frac{\delta}{\delta+1}$ and, for $\mathbf{x}, \mathbf{y} \in \mathbb{R}^d \times (0, 1)$, we have

$$\mathrm{d}(\mathbf{x}, \mathbf{y}) = (4 + o(1)) \frac{\log \log |x - y|}{\log \left(\frac{\gamma}{\delta(1-\gamma)}\right)} \tag{4.2}$$

under $\mathbb{P}_{\mathbf{x},\mathbf{y}}(\ \cdot\ \mid \mathbf{x} \leftrightarrow \mathbf{y})$ with high probability as $|x - y| \to \infty$.

Under the same assumption on the profile function φ we also obtain the main results of Chapter 3 for the age-dependent random connection model. Thus, as a consequence of Theorem 3.1 the non-extinction probability

$$\Gamma(\lambda) := \mathbb{P}_{(0,T_0)}(\xi_t^{(0,T_0)} \neq \emptyset \ \forall\, t \geq 0)$$

of the contact process $(\xi_t^{(0,T_0)})_{t\geq 0}$ starting in the origin $(0, T_0)$ of the Palm-version of the age-dependent random connection model is positive for any $\lambda > 0$ and decays at the rate given in the following result when λ is small.

Theorem 4.2

Let $\delta > 1$ and $\varphi : [0, \infty) \to [0, 1]$ a profile function which it satisfies (A1). When $\gamma > \frac{\delta}{\delta+1}$, there exists $c, C > 0$ such that, as $\lambda \to 0$, it holds

$$c \frac{\lambda^{2/\gamma-1}}{\log(1/\lambda)^{(1-\gamma)/\gamma}} \leq \Gamma(\lambda) \leq C \frac{\lambda^{2/\gamma-1}}{\log(1/\lambda)^{(1-\gamma)/\gamma}}. \tag{4.3}$$

For the second main result of Chapter 3 we do not consider the age-dependent random connection model itself, but a sequence of random graphs $(\mathscr{G}^n)_{n\in\mathbb{N}}$ defined on a homogeneous Poisson point process on $\mathbb{T}_n^d \times (0,1)$, where, given the Poisson point process, edges occur independently with probability given by (4.1) with the Euclidean distance replaced by the torus metric given by $\mathbb{T}_n^d$. To see how this fits as a rescaled version of the age-based spatial preferential attachment network see Section 4.1.2. Theorem 3.14 and Remark 3.3.1 then yield the following result for the extinction time $\varpi_n := \inf\{t > 0 : \xi_t^{\mathscr{G}^n} = \emptyset\}$ of the initially fully infected contact process $(\xi_t^{\mathscr{G}^n})_{t\geq 0}$ on $\mathscr{G}^n$.

Theorem 4.3

Let $\varphi : [0,\infty) \to [0,1]$ a profile function which satisfies (A1) such that $\gamma > \frac{\delta}{\delta+1}$. For any $\lambda > 0$, there exists $c > 0$ such that

$$\lim_{n\to\infty} \mathbb{P}\{\varpi_n \geq e^{cn}\} = 1.$$

As discussed in Section 1.2.1, the age-dependent random connection model can be motivated as the weak local limit graph of the *age-based spatial preferential attachment network*. We introduce this network in Section 4.1.1 and in Section 4.1.2 we give a rescaling argument which leads to a weak local limit theorem, see Theorem 4.4, where the limiting graph is in fact the age-dependent random connection model. By this weak local limit theorem and the analysis of the age-dependent random connection model we are able to analyse various properties of the age-based spatial preferential attachment network. In Section 4.1.3 we look at the neighbourhood of a typical vertex in these random graphs and show that they have a scale-free degree distribution with power-law exponent $\tau = 1 + \frac{1}{\gamma}$. In Section 4.1.4 we discuss the behaviour of the global and average clustering coefficient when the age-based spatial preferential attachment network grows large and in Section 4.1.5 we discuss the typical edge length in this network. Throughout the following sections we denote the age-dependent random connection model by $\mathscr{G}^\infty$ to emphasize its property as a limit graph. Note that in the following the limit graph $\mathscr{G}^\infty$ is defined on a Poisson process on $\mathbb{R}^d \times (0,1]$, however this has no influence on the results of this thesis.

As mentioned in Section 1.2.5, the following subsections form the work in [55] as

they can be found in [55] with slight changes in text and notation. See Section 1.2.5 for a discussion of the thesis' author's contribution to this work.

4.1.1 The age-based spatial preferential attachment network

The *age-based spatial preferential attachment model* is a growing sequence of graphs $(\mathscr{G}_n)_{n>0}$ in continuous time. The vertices of the graphs are embedded in the d-dimensional torus $\mathbb{T}_1^d = (-1/2, 1/2]^d$ of side-length one, endowed with the torus metric $d_{\mathbb{T}_1^d}$ defined by

$$d_{\mathbb{T}_1^d}(x, y) = \min\left\{|x - y + u| : u \in \{-1, 0, 1\}^d\right\} \text{ for } x, y \in \mathbb{T}_1^d,$$

where $|\cdot|$ denotes the Euclidean norm as in the whole thesis. Vertices are denoted by $\mathbf{x} = (x, t)$ and they are characterised by their birth time $t > 0$ and by their location $x \in \mathbb{T}_1^d$.

At time $n = 0$ the graph $\mathscr{G}_0$ has no vertices or edges. Then

- Vertices arrive according to a standard Poisson process in time and are placed independently uniformly on the d-dimensional torus $\mathbb{T}_1^d$.
- Given the graph $\mathscr{G}_{n-}$ a vertex $\mathbf{x} = (x, t)$ born at time $t = n$ and placed in location x is connected by an edge to each existing node $\mathbf{y} = (y, s)$ independently with probability

$$\varphi\left(\frac{t \cdot d_{\mathbb{T}_1^d}(x, y)^d}{\beta \cdot \left(\frac{t}{s}\right)^\gamma}\right), \tag{4.4}$$

where

(a) $\varphi\colon [0, \infty) \to [0, 1]$ is the *profile function*. It is nonincreasing, integrable and normalized in the sense that

$$\int_{\mathbb{R}^d} \varphi(|x|^d)\, dx = 1. \tag{4.5}$$

The profile function can be used to control the occurrence of long edges.

(b) $\gamma \in (0,1)$ is a parameter that quantifies the strength of the preferential attachment mechanism. We shall see that it alone determines the power-law exponent of the network.

(c) $\beta \in (0,\infty)$ is a parameter to control the edge density, which is asymptotically equal to $\frac{\beta}{1-\gamma}$, hence the smaller β, the sparser the graph.

Some comments on our choices in (4.4) are in order.

(i) For any $r > 0$, the profile function φ and parameter β define the same model as the profile function $x \mapsto \varphi(rx)$ and parameter $r\beta$. Hence the normalization convention (4.5) represents no loss of generality. Similarly, if the intensity of the arrival process is taken as $\lambda > 0$ the process $(\mathscr{G}_{n/\lambda})_{n>0}$ is the original process with the same profile function φ and parameter $\beta\lambda$.

(ii) The form of the connection probability (4.4) is natural for the following reasons: To ensure that the probability of a new vertex connecting to its nearest neighbour does not degenerate, as $n \to \infty$, it is necessary to scale $d_{\mathbb{T}_1^d}(x,y)$ by $n^{-1/d}$, which is the order of the distance of a point to its nearest neighbour at time n. Further, the integrability condition of φ ensures that the expected number of edges connecting a new vertex to the already existing ones, remains bounded from zero and infinity, as $n \to \infty$.

(iii) In the degree-based spatial preferential attachment model of Jacob and Mörters [69], introduced in Section 1.1.1, the term $(t/s)^\gamma$ that creates the age dependence in our model is replaced by a function of the indegree, the number of younger vertices $\mathbf{y}$ is connected to at time t. If this function is asymptotically linear with slope γ, the network is scale-free with power-law exponent $\tau = 1 + \frac{1}{\gamma}$. In this case, the expected indegree is of order $(t/s)^\gamma$ so that the models remain comparable and this is the natural choice to ensure that our network model will be scale-free.

(iv) For the profile function φ, one has different choices. We normally assume that φ is either regularly varying at infinity with index $-\delta$, for some $\delta > 1$, or φ decays quicker than any regularly varying function, in which case we set $\delta = \infty$. In the latter case a natural choice is to consider $\varphi(x) = \frac{1}{2a}\mathbf{1}_{[0,a]}(x)$ for $a \geq 1/2$. In this case, a vertex born at time s is linked to a new vertex at time t with probability $1/(2a)$ if and only if their locations

are within distance

$$\left(\frac{1}{t}\beta a\,(t/s)^{\gamma}\right)^{1/d}.$$

In the case $a = 1/2$, the profile function φ only takes the values zero and one, thus the decision is not random and we connect two vertices whenever they are close enough. The degree-based preferential attachment model in discrete time for this choice of φ was introduced in [1] and further studied in [30] and [71]. This particular choice for the profile function helps to get a better understanding of the problems and properties of this model, see for example Section 4.1.4. However, as seen in the introduction of this example this choice is too restrictive as it does not allow the networks to be ultrasmall.

4.1.2 Weak local limit

In this section, we introduce a graphical representation of the network $\mathscr{G}_n$. This representation allows a simple rescaling, and the rescaled graphs turn out to converge to a limiting graph, which is the already introduced *age-dependent random connection model*. This also turns out to be the weak local limit of the graph sequence $(\mathscr{G}_n)_{n\geq 0}$, which enables us to achieve results for the network $(\mathscr{G}_n)_{n\geq 0}$ by studying the age-dependent random connection model.

Let $\mathcal{X}$ denote a Poisson point process of unit intensity on $\mathbb{R}^d \times (0,\infty)$. We say a point $\mathbf{x} = (x,t) \in \mathcal{X}$ is born at time t and placed at location x. Observe that, almost surely, two points of $\mathcal{X}$ neither have the same birth time nor the same location. We say that (x,t) is *older* than (y,s) if $t < s$. For $n > 0$ write $\mathcal{X}_n$ for $\mathcal{X} \cap (\mathbb{T}_1^d \times (0,n])$, the set of vertices on the torus already born at time n. We denote by

$$E(\mathcal{X}) := \{(\mathbf{x},\mathbf{y}) \in \mathcal{X} \times \mathcal{X} \colon \mathbf{x} \text{ younger than } \mathbf{y}\}$$

the set of *potential edges* in $\mathcal{X}$. Given $\mathcal{X}$ we introduce a family $\mathcal{V}$ of independent random variables, uniformly distributed on $(0,1)$, indexed by the set of potential edges. We denote these variables by $\mathcal{V}_{\mathbf{x},\mathbf{y}}$ or $\mathcal{V}(\mathbf{x},\mathbf{y})$. A realization of $\mathcal{X}_n$ and $\mathcal{V}_n$, defined as the restriction of $\mathcal{V}$ to indices in $\mathcal{X}_n \times \mathcal{X}_n$, defines a network $\mathcal{G}(\mathcal{X}_n,\mathcal{V}_n)$ with vertex set $\mathcal{X}_n$ placing an edge between $\mathbf{x} = (x,t)$ and $\mathbf{y} = (y,s)$ with $s < t$,

if and only if

$$\mathcal{V}(\mathbf{x},\mathbf{y}) \leq \varphi\left(\frac{t \cdot d_{\mathbb{T}_1^d}(x,y)^d}{\beta\,\left(\frac{t}{s}\right)^\gamma}\right). \tag{4.6}$$

Observe that the graph sequence $(\mathcal{G}(\mathcal{X}_n,\mathcal{V}_n))_{n>0}$ has the law of our age-based spatial preferential attachment network and is therefore constructed on the probability space carrying the Poisson process $\mathcal{X}$ and the sequence $\mathcal{V}$. Moreover, $\mathcal{G}$ extends to a deterministic mapping associating a graph structure to any locally finite set of points in $\mathcal{Y} \subseteq \mathbb{T}_a^d \times (0,\infty)$ and sequence $\mathcal{V}$ in $(0,1)$ indexed by $E(\mathcal{Y}) = \{(\mathbf{x},\mathbf{y}) \in \mathcal{Y}\times\mathcal{Y}\colon \mathbf{x} \text{ younger than } \mathbf{y}\}$, where $\mathbb{T}_a^d = (-\frac{1}{2}a^{1/d}, \frac{1}{2}a^{1/d}]^d$ is the torus of volume a equipped with its canonical metric $d_{\mathbb{T}_a^d}(\cdot,\cdot)$, and $\mathbf{x}$, $\mathbf{y}$ are connected if and only if (4.6) holds. We permit the case $a=\infty$, with $\mathbb{T}_\infty^d = \mathbb{R}^d$ equipped with the Euclidean metric.

For finite $n > 0$, we define the *rescaling mapping*

$$\begin{array}{rccc} h_n: & \mathbb{T}_1^d \times (0,n] & \longrightarrow & \mathbb{T}_n^d \times (0,1], \\ & (x,t) & \longmapsto & \big(n^{1/d}x, t/n\big), \end{array}$$

which expands space by a factor of $n^{1/d}$ and time by a factor of $1/n$. The mapping h_n operates canonically on the set $\mathcal{X}_n$ as well as on $\mathcal{V}_n$ by $h_n(\mathcal{V}_n)(h_n(\mathbf{x}),h_n(\mathbf{y})) := \mathcal{V}_n(\mathbf{x},\mathbf{y})$, and also on graphs with vertex set in $\mathcal{X}_n$ by mapping points $\mathbf{x}$ to $h_n(\mathbf{x})$ and introducing an edge between $h_n(\mathbf{x})$ and $h_n(\mathbf{y})$ if and only if there is one between $\mathbf{x}$ and $\mathbf{y}$. As

$$\varphi\left(\frac{t/n \cdot d_{\mathbb{T}_n^d}(n^{1/d}x, n^{1/d}y)^d}{\beta\,\left(\frac{t/n}{s/n}\right)^\gamma}\right) = \varphi\left(\frac{t \cdot d_{\mathbb{T}_1^d}(x,y)^d}{\beta\,\left(\frac{t}{s}\right)^\gamma}\right)$$

the operation h_n preserves the rule (4.6) and therefore

$$\mathcal{G}(h_n(\mathcal{X}_n), h_n(\mathcal{V}_n)) = h_n(\mathcal{G}(\mathcal{X}_n,\mathcal{V}_n)).$$

In plain words, it is the same to construct the graph and then rescale the picture, or to first rescale the picture and then construct the graph on the rescaled picture, see Figure 4.2.

We now denote $\mathcal{X}^n = \mathcal{X} \cap (\mathbb{T}_n^d \times (0,1])$ and by $\mathcal{V}^n$ the restriction of $\mathcal{V}$ to indices

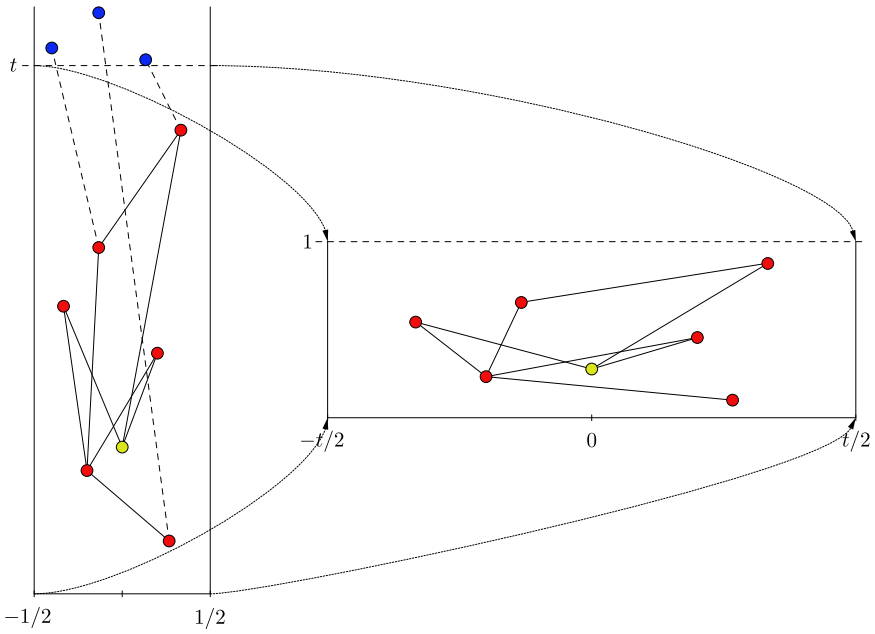

Figure 4.2: The graph $\mathscr{G}_n$ on the left and its rescaling $h_n(\mathscr{G}_n)$ on the right. The blue vertices are born after time n and, therefore, the corresponding edges do not exist yet and the vertices are not part of the rescaled graph. The yellow vertex is placed at location 0 and remains in the centre after the rescaling.

in $\mathcal{X}^n \times \mathcal{X}^n$. This gives rise to a graph $\mathscr{G}^n := \mathcal{G}(\mathcal{X}^n, \mathcal{V}^n)$. As $h_n(\mathcal{X}_n)$ is a Poisson point process of unit intensity on $\mathbb{T}_n^d \times (0,1]$ and $h_n(\mathcal{V}_n)$ are independent uniform marks attached to the potential edges, for fixed finite n, the graph $\mathscr{G}^n$ has the same law as $\mathcal{G}(h_n(\mathcal{X}_n), h_n(\mathcal{V}_n))$ and therefore as $h_n(\mathscr{G}_n)$. However, the process $(\mathscr{G}^n)_{n>0}$ behaves differently from the original process $(\mathscr{G}_n)_{n>0}$. Indeed, while the degree of any fixed vertex in $(\mathscr{G}_n)_{n>0}$ goes to infinity, the degree of any fixed vertex in $(\mathscr{G}^n)_{n>0}$ stabilizes and the graph sequence converges to the graph $\mathscr{G}^\infty := \mathcal{G}(\mathcal{X}^\infty, \mathcal{V}^\infty)$; see the theorem below.

In order to formulate also a local version of this convergence result we add a point at the origin to our Poisson process denoting $\mathcal{X}_{(0,T_0)} := \mathcal{X} \cup \{(0,T_0)\}$ where T_0 is an independent, uniformly on $(0,1]$ distributed birth time. As before let $\mathcal{V}_{(0,T_0)}$ be a family of independent uniformly distributed random variables indexed by the potential edges in $\mathcal{X}_{(0,T_0)}$, and, for $0 < n \leq \infty$, let $\mathcal{X}^n_{(0,T_0)} = \mathcal{X}_{(0,T_0)} \cap (\mathbb{T}_n^d \times (0,1])$ and denote by $\mathcal{V}^n_{(0,T_0)}$ the restriction of $\mathcal{V}_{(0,T_0)}$ to indices in $\mathcal{X}^n_{(0,T_0)} \times \mathcal{X}^n_{(0,T_0)}$. We

define rooted graphs $\mathscr{G}^n_{(0,T_0)} := \mathcal{G}(\mathcal{X}^n_{(0,T_0)}, \mathcal{V}^n_{(0,T_0)})$ with the root being the vertex placed at the origin. For $p > 0$ define the class $\mathcal{H}_p$ of nonnegative functions H acting on locally finite rooted graphs and depending only on a bounded graph neighbourhood of the root with the property that

$$\sup_{0<n<\infty} \mathbb{E}[H(\mathscr{G}^n_{(0,T_0)})^p] < \infty.$$

Theorem 4.4

(i) $\mathscr{G}^\infty$ is almost surely locally finite, i.e. almost surely all its vertices have finite degree.

(ii) Almost surely, the graph sequence $(\mathscr{G}^n)$ converges to $\mathscr{G}^\infty$ in the sense that for each $\mathbf{x} \in \mathcal{X}^\infty$ the neighbours of $\mathbf{x}$ in $\mathscr{G}^n$ and in $\mathscr{G}^\infty$ coincide for large n.

(iii) In probability, the graph sequence $(\mathscr{G}_n)$ converges weakly locally to $\mathscr{G}^\infty_{(0,T_0)}$ in the sense that for any $H \in \mathcal{H}_p$, $p > 1$, we have

$$\lim_{n\to\infty} \frac{1}{n} \sum_{\mathbf{x}\in\mathscr{G}_n} H(\theta_{\mathbf{x}}\mathscr{G}_n) = \mathbb{E}[H(\mathscr{G}^\infty_{(0,T_0)})] \qquad \text{in probability,} \tag{4.7}$$

where $\theta_{\mathbf{x}}$ acts on points $\mathbf{y} = (y, s)$ as $\theta_{\mathbf{x}}(\mathbf{y}) = (y - x, s)$ and on graphs accordingly.

Theorem 4.4 will be proved in Section 4. As mentioned beforehand the limiting graph $\mathscr{G}^\infty$ in (ii) is the *age-dependent random connection model*. The rooted graph $\mathscr{G}^\infty_{(0,T_0)}$ occurring as the local limit is the *Palm version* of the age-dependent random connection model $\mathscr{G}^\infty$; loosely speaking the graph $\mathscr{G}^\infty$ with a typical vertex shifted to the origin.

Remark 4.1.1.

- Weak local limits were introduced by Benjamini and Schramm [9] as distributional limits for determinstic sequences of finite graphs randomized by a uniform choice of root. The result in (iii) allows that H additionally depends continuously on the ages of the vertices and the length of the edges if taken in the scaled graphs $h_n(\theta_{\mathbf{x}}\mathscr{G}_n)$. Further generalisations of the results

hold, see Yukich and Penrose [92] for seminal work on random geometric graphs and Jacob and Mörters [69] for a similar proof in the case of the degree-based model which can be adapted to our situation. We will not need these more general results here.

- The age-dependent random connection model is in a different universality class than other established models of infinite spatial scale-free graphs. Examples as scale-free percolation, see Section 4.3, or ultra-small scale-free geometric networks, see Section 4.4, do not arise naturally from sequences of growing finite random graphs on a fixed space as the age-dependent random connection model does.

- There is a similar convergence result for the degree-based spatial preferential attachment model, but the limiting graph is not as natural as the age-dependent random connection model as the existence of edges between vertices with given location and age depends in this graph on the existence of edges between the older vertex and other vertices that may lie arbitrarily far away, see Jacob and Mörters [69].

4.1.3 Convergence of neighbourhoods and degree distributions

In this section we will study the asymptotic degree distribution and show that the age-based spatial preferential attachment model is scale-free. To this end we study the neighbourhood of a fixed vertex $\mathbf{x} = (x, t)$ in the graphs $\mathscr{G}^n$. We think of edges as oriented from the younger to the older endvertex, so that the *indegree* of $\mathbf{x}$ is the number of younger vertices that connect to it, and the *outdegree* is the number of older vertices it connects to. As our construction is based on Poisson processes and conditionally independent edges, the indegree and outdegree of a fixed vertex are independent and Poisson distributed.

If G is a graph with vertices in $\mathbb{T}_n^d \times (0, \infty)$, we write $\mathbf{x} \sim \mathbf{y}$ to indicate that there is an edge between $\mathbf{x}$ and $\mathbf{y}$ in G. Now, let $\mathbf{x} = (x, t)$ be a vertex in G and define its older neighbours,

$$\mathcal{Y}_{\mathbf{x}}(G) := \{\mathbf{y} = (y, s) \in G \colon \mathbf{x} \sim \mathbf{y}, s \leq t\},$$

and its younger neighbours born before time s,

$$\mathcal{Z}_{\mathbf{x}}(s, G) := \{\mathbf{y} = (y, r) \in G \colon \mathbf{y} \sim \mathbf{x}, t < r \leq s\}.$$

For $n \in (0, \infty]$ and $0 < t < s \leq 1$, we write $\mathcal{Y}_{\mathbf{x}}^n := \mathcal{Y}_{\mathbf{x}}(\mathscr{G}^n)$ and $\mathcal{Z}_{\mathbf{x}}^n(s) := \mathcal{Z}_{\mathbf{x}}(s, \mathscr{G}^n)$, adding the point $\mathbf{x} = (x, t)$ to the underlying Poisson process $\mathcal{X}$ if it is not already there.

Proposition 4.5

(a) For every $n \in (0, \infty]$, the older neighbours $\mathcal{Y}_{\mathbf{x}}^n$ of $\mathbf{x} = (x, t)$ form a Poisson point process on $\mathbb{T}_n^d \times [0, t)$ with intensity measure

$$\lambda_{\mathcal{Y}_{\mathbf{x}}^n} := \varphi\left(\beta^{-1} t \left(\frac{s}{t}\right)^{\gamma} d_{\mathbb{T}_n^d}(x, y)^d\right) dy\, ds.$$

(b) For every $n \in (0, \infty]$, the younger neighbours $\mathcal{Z}_{\mathbf{x}}^n(s_0)$ of $\mathbf{x} = (x, t)$ at time $s_0 \in (t, 1]$ form a Poisson point process on $\mathbb{T}_n^d \times (t, s_0]$ with intensity measure

$$\lambda_{\mathcal{Z}_{\mathbf{x}}^n(s_0)} := \varphi\left(\beta^{-1} s \left(\frac{t}{s}\right)^{\gamma} d_{\mathbb{T}_n^d}(x, y)^d\right) dy\, ds.$$

(c) The outdegree of the origin in $\mathscr{G}_{(0,T_0)}^{\infty}$ is Poisson distributed with parameter $\frac{\beta}{1-\gamma}$ and independent of the birth time T_0 of the origin.

(d) The indegree of the origin in $\mathscr{G}_{(0,T_0)}^{\infty}$ is mixed Poisson distributed, where the mixing distribution has the density

$$f(\lambda) = \beta^{1/\gamma}(\gamma\lambda + \beta)^{-(1+1/\gamma)} \qquad \text{for } \lambda > 0. \tag{4.8}$$

Proof. The older neighbours of $\mathbf{x} = (x, t)$ are all neighbours with birth time smaller than t, therefore, $\mathcal{X} \cap (\mathbb{T}_n^d \times [0, t))$ is the set of all potential vertices connected to $\mathbf{x}$ by an outgoing edge. Now, given $\mathcal{X}$ a vertex $\mathbf{y} = (y, s) \in \mathcal{X} \cap (\mathbb{T}_n^d \times [0, t))$ is connected to $\mathbf{x}$ independently with probability $\varphi(\beta^{-1} t^{1-\gamma} s^{\gamma} d_{\mathbb{T}_n^d}(x, y)^d)$. Thus, $\mathcal{Y}_{\mathbf{x}}^n$ defines a thinning of $\mathcal{X} \cap (\mathbb{T}_n^d \times [0, t))$ and (a) follows. The analogous argument for the vertices in $\mathcal{X} \cap (\mathbb{T}_n^d \times (t, s_0])$ proves (b).

Applying (a) to $\mathbf{x} = (0, t)$ and $n = \infty$ gives that the number of older neighbours is Poisson distributed with parameter

$$\begin{aligned}\lambda_{\mathcal{Y}_{\mathbf{x}}^{\infty}}\big(\mathbb{R}^d \times [0,t]\big) &= \int_0^t \mathrm{d}s \int_{\mathbb{R}^d} \mathrm{d}y\, \varphi\big(\beta^{-1} t^{1-\gamma} s^{\gamma} |y|^d\big) \\ &= \int_0^t \mathrm{d}s\, \beta t^{\gamma-1} s^{-\gamma} \int_{\mathbb{R}^d} \mathrm{d}y \varphi\big(|y|^d\big) = \frac{\beta}{1-\gamma},\end{aligned}$$

using the normalisation of φ. The claimed independence follows as the distribution does not depend on t, completing the proof of (c).

Applying (b) to $\mathbf{x} = (0, t)$ and $n = \infty$ gives that the number of younger neighbours up to time s is Poisson distributed with parameter

$$\begin{aligned}&\lambda_{\mathcal{Z}_{\mathbf{x}}^{\infty}(s)}\big(\mathbb{R}^d \times (t,s]\big) \\ &\quad= \int_t^s \mathrm{d}v \int_{\mathbb{R}^d} \mathrm{d}y\, \varphi\big(\beta^{-1} v^{1-\gamma} t^{\gamma} |y|^d\big) = \beta \int_t^s \mathrm{d}v\, t^{-\gamma} v^{\gamma-1} \int_{\mathbb{R}^d} \mathrm{d}y\, \varphi(|y|^d) \\ &\quad= \beta \int_t^s \mathrm{d}v\, t^{-\gamma} v^{\gamma-1} = \beta \frac{s^{\gamma} t^{-\gamma} - 1}{\gamma}.\end{aligned}$$

As T_0 is independent of $\mathcal{X}$ and $\mathcal{V}$ the probability that the indegree equals k is therefore

$$\begin{aligned}&\int_0^1 \mathrm{d}t \exp\Big(-\beta \frac{t^{-\gamma}-1}{\gamma}\Big) \cdot \frac{\big(\beta \frac{t^{-\gamma}-1}{\gamma}\big)^k}{k!} \\ &\qquad= \int_0^{\infty} \mathrm{d}\lambda \exp(-\lambda) \cdot \frac{\lambda^k}{k!} \cdot \big(\beta^{1/\gamma}(\gamma\lambda + \beta)^{-(1+1/\gamma)}\big),\end{aligned}$$

as claimed. □

Remark: Since, by construction, $\mathcal{Y}_{\mathbf{x}}^n$ and $\mathcal{Z}_{\mathbf{x}}^n(1)$ are independent Poisson point processes, the neighbourhood of a point $\mathbf{x} = (x, t)$ added (if necessary) to $\mathscr{G}^n$ is a Poisson point process with intensity $\lambda_{\mathcal{Z}_{\mathbf{x}}^n(1)} + \lambda_{\mathcal{Y}_{\mathbf{x}}^n}$. Let now n be finite and pick a vertex $\mathbf{x}$ uniformly at random from the finite graph $\mathscr{G}_n$. We easily see that $h_n(\theta_{\mathbf{x}}\mathscr{G}_n) = \mathscr{G}^n_{(0,T_0)}$ in distribution. Hence Proposition 4.5 part (a) and (b) give a precise description of the neighbourhood of a randomly chosen vertex in $\mathscr{G}_n$.

Proof of Theorem 4.4(i). By Proposition 4.5 part (c) and (d), almost surely, the origin has finite degree in $\mathscr{G}^{\infty}_{(0,T_0)}$. Hence, by the refined Campbell theorem (see

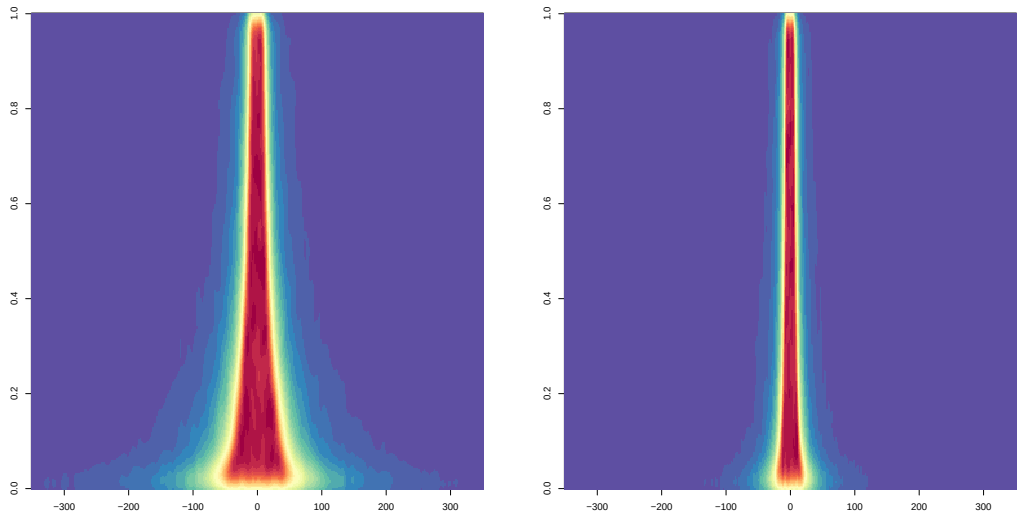

Figure 4.3: Heatmaps of the neighbourhood of a relatively old root (left, birth time 0.2) and of a relatively young root (right, birth time 0.8) in $\mathscr{G}^{\infty}_{(0,T_0)}$ with $\beta = 5$, $\gamma = 1/3$ and $\varphi(x) = 1 \wedge x^{-2}$.

Theorem 9.1 in [76]), almost surely, every vertex in $\mathscr{G}^{\infty}$ has finite degree. □

Proof of Theorem 4.4(ii). We work conditionally on $\mathbf{x} = (x, t) \in \mathcal{X}^{\infty}$. Our aim is to show that there exists an almost surely finite random variable M such that, for all $n \in (0, \infty]$ and $\mathbf{y} \in \mathcal{X}^{\infty}$ with distance at least M from $\mathbf{x}$, the vertices $\mathbf{x}$ and $\mathbf{y}$ are not connected in $\mathscr{G}^n$. To this end, observe that the distance between $\mathbf{x}$ and any $\mathbf{y} \in \mathbb{T}^d_n$ can be up to $2\sqrt{d}\,|x|$ smaller than it would be in $\mathbb{R}^d$. Consider the model where the vertices within distance $2\sqrt{d}\,|x|$ of $\mathbf{x}$ are deleted from $\mathcal{X}^{\infty}$ and all the other vertices are moved towards $\mathbf{x}$ by a distance of $2\sqrt{d}\,|x|$. It is easy to see that all vertices $\mathbf{y} \in \mathcal{X}^{\infty}$, that are at least $2\sqrt{d}\,|x|$ away from $\mathbf{x}$ and connected to $\mathbf{x}$ in the finite graph $\mathscr{G}^n$ for some $n > 0$, are also linked to $\mathbf{x}$ in this new model. Furthermore, the degree of $\mathbf{x}$ is still almost surely finite. Hence, we define the random variable M as the distance of $\mathbf{x}$ to the furthest vertex it is linked to in this new model, plus $2\sqrt{d}\,|x|$. Then M is almost surely finite and, as for $n > |x| + M$ the vertices in $\mathcal{X}^{\infty}$ and in $\mathcal{X}^n$ within distance M from $\mathbf{x}$ coincide, the edges of $\mathbf{x}$ linking it to another vertex $\mathbf{y}$ that is at most M away coincide in $\mathscr{G}^n$ and $\mathscr{G}^{\infty}$ for sufficiently large n. □

Proof of Theorem 4.4(iii). We can replace the left-hand side in (4.7) by the limit

of $\frac{1}{n}\sum_{\mathbf{x}\in\mathscr{G}^n} H(\theta_{\mathbf{x}}\mathscr{G}^n)$, which has the same distribution and, due to Campbell's formula, has expectation $\mathbb{E}[H(\mathscr{G}^n_{(0,T_0)})]$. Furthermore, the neighbourhoods of the origin in $\mathscr{G}^n_{(0,T_0)}$ and in $\mathscr{G}^\infty_{(0,T_0)}$ agree for sufficiently large n. As the family $(H(\mathscr{G}^n_{(0,T_0)}))_{n>0}$ is bounded in L^p and therefore uniformly integrable, we infer that $\mathbb{E}[H(\mathscr{G}^n_{(0,T_0)})]$ converges to $\mathbb{E}[H(\mathscr{G}^\infty_{(0,T_0)})]$. Hence the first moments in (4.7) converge, and we now argue that for bounded H the second moments converge, too.

Spelling out the second moment of $\frac{1}{n}\sum_{\mathbf{x}\in\mathscr{G}^n} H(\theta_{\mathbf{x}}\mathscr{G}^n)$ we get a term corresponding to choosing the same $\mathbf{x}\in\mathscr{G}^n$ twice, which by the first moment calculation applied to H^2 converges to zero, and the term

$$\mathbb{E}\Big[\frac{1}{n^2}\sum_{\substack{\mathbf{x},\mathbf{x}'\in\mathscr{G}^n\\ \mathbf{x}\neq\mathbf{x}'}} H(\theta_{\mathbf{x}}\mathscr{G}^n)H(\theta_{\mathbf{x}'}\mathscr{G}^n)\Big].$$

Using the boundedness of H we can chose $\varepsilon>0$ so that the contribution from pairs $\mathbf{x},\mathbf{x}'$ for which one is born before time ε is arbitrarily small. We can then find a large radius R so that the graph neighbourhood of the origin on which H depends is contained in $\{\mathbf{y}\colon d_{\mathbb{T}^d_1}(0,y)\le R\}$ for $\theta_{\mathbf{x}}\mathscr{G}^n$ for a proportion of vertices $\mathbf{x}\in\mathscr{G}^n$ born after time ε arbitrarily close to one, for all sufficiently large n. We can neglect the small proportion of exceptional vertices as well as pairs $\mathbf{x},\mathbf{x}'$ with distance smaller than R using again the boundedness of H. On the remaining part the expectation factorizes and we see that second moment converges to $\mathbb{E}[H(\mathscr{G}^\infty_{(0,T_0)})]^2$. Hence we get convergence in L^2.

It remains to remove the condition of boundedness of H. Let $k\in\mathbb{N}$ and observe that our result applies to the bounded functional $H\wedge k$. Note that

$$\mathbb{E}\Big[\frac{1}{n}\sum_{\mathbf{x}\in\mathscr{G}^n} H(\theta_{\mathbf{x}}\mathscr{G}^n)-H\wedge k(\theta_{\mathbf{x}}\mathscr{G}^n)\Big]=\mathbb{E}\big[H(\mathscr{G}^n_{(0,T_0)})-H\wedge k(\mathscr{G}^n_{(0,T_0)})\big]$$

and the right hand side goes to zero uniformly in n as $k\to\infty$ by the uniform integrability implied in our L^p bound. This implies the required convergence. □

We define the *empirical outdegree distribution* ν_n of the graph $\mathscr{G}_n$ by

$$\nu_n(k)=\frac{1}{n}\sum_{\mathbf{x}\in\mathscr{G}_n}\mathbf{1}_{\{|\mathcal{Y}_{\mathbf{x}}(\mathscr{G}_n)|=k\}}\qquad\text{for } k\in\mathbb{N}_0,$$

and note that (for convenience) we have normalised ν_n so that its mass converges to one without necessarily being equal to one for small n. We now show that the empirical outdegree distribution ν_n converges to a deterministic limit.

Theorem 4.6

For any function $g : \mathbb{N}_0 \to [0, \infty)$ growing no faster than exponentially we have

$$\frac{1}{n} \sum_{\mathbf{x} \in \mathscr{G}_n} g\big(|\mathcal{Y}_{\mathbf{x}}(\mathscr{G}_n)|\big) = \int \mathrm{d}\nu_n \, g \longrightarrow \int \mathrm{d}\nu \, g,$$

in probability, as $n \to \infty$, where ν is the Poisson distribution with parameter $\beta/(1-\gamma)$.

Proof. For a finite graph G with vertices marked by birth times and a root vertex $\mathbf{x}$ we can define $H(G) = g(|\mathcal{Y}_{\mathbf{x}}(G)|)$ where $\mathcal{Y}_{\mathbf{x}}(G)$ is the set of edges from the root to older vertices in G. Note that the function H depends only on the neighbourhood of the root within graph distance one and the relative birth times of these vertices. Moreover, $H(\mathscr{G}^n_{(0,T_0)}) = g(|\mathcal{Y}_{\mathbf{x}}(\mathscr{G}^n_{(0,T_0)})|)$ where $\mathbf{x} \in \mathscr{G}^n_{(0,T_0)}$ is the vertex placed at the origin, for arbitrary n, and as $|\mathcal{Y}_{\mathbf{x}}(\mathscr{G}^n_{(0,T_0)})|$ is Poisson distributed with a bounded parameter, the integrability condition $H \in \mathcal{H}_p$ is satisfied as long as g is not growing faster than exponentially. As $H(\theta_{\mathbf{x}}\mathscr{G}_n) = g(|\mathcal{Y}_{\mathbf{x}}(\mathscr{G}_n)|)$ for all $\mathbf{x} \in \mathcal{X}_n$ and finite n, we infer the result from Theorem 4.4(iii). □

Define the *empirical indegree distribution* μ_n of the graph $\mathscr{G}_n$ by

$$\mu_n(k) = \frac{1}{n} \sum_{\mathbf{x} \in \mathscr{G}_n} \mathbf{1}_{\{|\mathcal{Z}_{\mathbf{x}}(n, \mathscr{G}_n)| = k\}}.$$

Similar to above, the empirical indegree distribution μ_n also converges to a deterministic limit.

Theorem 4.7

For any function $g : \mathbb{N}_0 \to [0, \infty)$ growing no faster than linearly we have

$$\frac{1}{n} \sum_{\mathbf{x} \in \mathscr{G}_n} g\big(|\mathcal{Z}_{\mathbf{x}}(n, \mathscr{G}_n)|\big) = \int \mathrm{d}\mu_n \, g \longrightarrow \int \mathrm{d}\mu \, g,$$

in probability, as $n \to \infty$, where μ is the mixed Poisson distribution with density f as in (4.8)

Proof. For a finite graph G with vertices marked by birth times and a root vertex $\mathbf{x}$ we can define $H(G) = g(|\mathcal{Z}_{\mathbf{x}}(G)|)$ where $\mathcal{Z}_{\mathbf{x}}(G)$ is the set of edges from younger vertices in G to the root. Note that the function H depends only on the neighbourhood of the root within graph distance one and the relative birth times of these vertices. Moreover, $H(\mathscr{G}^n_{(0,T_0)}) = g(|\mathcal{Z}_{\mathbf{x}}(\mathscr{G}^n_{(0,T_0)})|)$ where $\mathbf{x} \in \mathscr{G}^n_{(0,T_0)}$ is the vertex placed at the origin, for arbitrary n. Now $|\mathcal{Z}_{\mathbf{x}}(\mathscr{G}^n_{(0,T_0)})|$ is dominated by $|\mathcal{Z}_{\mathbf{x}}(\mathscr{G}^\infty_{(0,T_0)})|$ whose distribution μ has tails (calculated in Lemma 4.8 below) that vanish fast enough to ensure that $H \in \mathcal{H}_p$ for some $p > 1$. As $H(\theta_{\mathbf{x}}\mathscr{G}_n) = g(|\mathcal{Z}_{\mathbf{x}}(\mathscr{G}_n)|)$ for all $\mathbf{x} \in \mathcal{X}_n$ and finite n, we infer the result from Theorem 4.4(iii). □

To complete the proof that the age-based preferential attachment model is scale-free with power-law exponent $\tau = 1 + \frac{1}{\gamma}$ we observe that, by a similar argument as in Theorem 4.6 and Theorem 4.7, the empirical degree distribution in $\mathscr{G}_n$ converges in probability to the convolution of ν and μ. As ν has superexponentially light tails, the tail behaviour of the convolution is inherited from that of μ, which we now calculate.

Lemma 4.8

$\mu(k) = k^{-(1+\frac{1}{\gamma})+o(1)}$ as $k \to \infty$.

Proof. Observe that

$$\begin{aligned}\mu(k) &= \beta^{1/\gamma} \int_0^\infty \mathrm{d}\lambda \, \frac{\lambda^k}{k!} e^{-\lambda} (\gamma\lambda + \beta)^{-(1+\frac{1}{\gamma})} \leq \frac{\beta^{1/\gamma}\gamma^{-1-\frac{1}{\gamma}}}{\Gamma(k+1)} \int_0^\infty \mathrm{d}\lambda \, \lambda^{(k-\frac{1}{\gamma})-1} e^{-\lambda} \\ &= \frac{\beta^{1/\gamma}}{\gamma^{1+1/\gamma}} \frac{\Gamma(k-\frac{1}{\gamma})}{\Gamma(k+1)} = k^{-1-\frac{1}{\gamma}+o(1)},\end{aligned}$$

as $k \to \infty$, by Stirling's formula. On the other hand, note that for some fixed bound $A > 0$, there exists a constant $c > 0$ such that $\gamma x + \beta \leq c\gamma x$ for all $x \geq A$. Hence

$$\begin{aligned}\mu(k) &\geq \frac{c^{-1-\frac{1}{\gamma}}\beta^{1/\gamma}}{\Gamma(k+1)} \int_A^\infty \mathrm{d}\lambda \, \lambda^k e^{-\lambda} (\gamma\lambda)^{-1-\frac{1}{\gamma}} \\ &= \tilde{c} \frac{\Gamma(k-\frac{1}{\gamma})}{\Gamma(k+1)} - \frac{\tilde{c}}{\Gamma(k+1)} \int_0^A \mathrm{d}\lambda \, \lambda^{(k-\frac{1}{\gamma})-1} e^{-\lambda},\end{aligned}$$

for some positive constant $\tilde{c}$. As the subtracted term, for fixed A, is of smaller order, as $k \to \infty$, we obtain the lower bound. □

Remark 4.1.2. Note that by Proposition 4.5 the degree distribution of the origin in $\mathscr{G}^\infty_{(0,T_0)}$ is given by the convolution of ν and μ. Thus, Lemma 4.8 implies that the age-dependent random connection model is scale-free with power-law exponent $\tau = 1 + \frac{1}{\gamma}$. We will use the arguments presented in Proposition 4.5 and 4.8 to show that later examples of geometric random graphs are scale-free as well.

4.1.4 Global and local clustering coefficients

To show that the age-based spatial preferential attachment model has clustering features we recall two metrics introduced in Section 1.1.1 which are well established in the applied networks literature, see e.g. [90, 97] for some early papers. If G is a finite graph, we call a pair of edges in G a *wedge* if they share an endpoint (called its *tip*). Recall that the *global clustering coefficient* or *transitivity* of G is

given by

$$c^{\text{glob}}(G) := 3\frac{\text{Number of triangles in } G}{\text{Number of wedges in } G},$$

if there is at least one wedge in G and $c^{\text{glob}}(G) := 0$ otherwise.

Another way of thinking about clusters is locally; i.e. to count only the triangles and wedges containing a fixed vertex $\mathbf{x}$. For a vertex $\mathbf{x}$ with at least two neighbours, the *local clustering coefficient* is given by

$$c^{\text{loc}}_{\mathbf{x}}(G) := \frac{\text{Number of triangles in } G \text{ containing vertex } \mathbf{x}}{\text{Number of wedges with tip } \mathbf{x} \text{ in } G},$$

which is also an element of $[0, 1]$. Let $V_2(G) \subseteq G$ be the set of vertices in G with degree at least two, and define the *average clustering coefficient* by

$$c^{\text{av}}(G) := \frac{1}{|V_2(G)|} \sum_{\mathbf{x} \in V_2(G)} c^{\text{loc}}_{\mathbf{x}}(G),$$

if $V_2(G)$ is not empty and by $c^{\text{av}}(G) := 0$ otherwise. Note that this metric places more weight on the low degree nodes, while the transitivity places more weight on the high degree nodes.

Theorem 4.9: Clustering Coefficients

(a) For the average clustering coefficient we have

$$c^{\mathrm{av}}(\mathscr{G}_n) \longrightarrow \int_0^1 \pi(\mathrm{d}t)\, \mathbb{P}\big\{(Y_t^{(1)}, S_t^{(1)}) \sim (Y_t^{(2)}, S_t^{(2)})\big\},$$

in probability as $n \to \infty$, where $(Y_t^{(1)}, S_t^{(1)})$ resp. $(Y_t^{(2)}, S_t^{(2)})$ are two independent random variables on $\mathbb{R}^d \times [0,1]$ with distribution

$$\frac{1}{\lambda_t}\Big(\varphi(\beta^{-1}s^{1-\gamma}t^{\gamma}|y|^d)\mathbf{1}_{(t,1]}(s) + \varphi(\beta^{-1}t^{1-\gamma}s^{\gamma}|y|^d)\mathbf{1}_{[0,t]}(s)\Big)\,\mathrm{d}y\,\mathrm{d}s, \quad (4.9)$$

where $\lambda_t = \frac{\beta}{\gamma}(\frac{2\gamma-1}{1-\gamma} + t^{-\gamma})$ is the normalising factor, and π is the probability measure on $[0,1]$ with density proportional to $1 - e^{-\lambda_t} - \lambda_t e^{-\lambda_t}$.

(b) For the global clustering coefficient, there exists a number $c_\infty^{\mathrm{glob}} \geq 0$ such that

$$c^{\mathrm{glob}}(\mathscr{G}_n) \longrightarrow c_\infty^{\mathrm{glob}}$$

in probability, as $n \to \infty$. The limiting global clustering coefficient c_∞^{glob} is positive if and only if $\gamma < 1/2$.

Remark 4.1.3. The limiting average clustering coefficient can be interpreted as the probability that in $\mathscr{G}^{\infty}_{(0,T_0)}$ two neighbours of the vertex at the origin are connected by an edge. The density of the birthtime of the vertex at the origin here is not uniform but given by the measure π, which is the conditional distribution of the birthtime of a vertex given that it has degree at least two. Observe that this coefficient is always positive. By contrast the global clustering coefficient vanishes asymptotically when preferential attachment to old nodes is strong (i.e. when γ is large). In this case the collection of wedges is dominated by those with an untypically old tip. These vertices have small local clustering as they are endvertices to a significant amount of long edges.

Proof. Let G be a finite rooted graph and define the function $H(G) = c_{\mathbf{x}}^{\mathrm{loc}}(G)$ if the root $\mathbf{x}$ has degree at least two, and $H(G) = 0$ otherwise. As H is bounded,

we have $H \in \mathcal{H}_p$ for any $p > 1$ and, by Theorem 4.4 (iii), we get

$$\frac{1}{n} \sum_{\mathbf{x} \in \mathscr{G}_n} H(\theta_{\mathbf{x}} \mathscr{G}_n) \longrightarrow \mathbb{E}\left[H(\mathscr{G}^{\infty}_{(0,T_0)})\right]$$

in probability, as $n \to \infty$. To calculate the limit, observe that, for a vertex $\mathbf{x}$ with degree k, the number of wedges with tip $\mathbf{x}$ is $k(k-1)/2$. It follows that

$$\begin{aligned}
&\mathbb{E}\left[H(\mathscr{G}^{\infty}_{(0,T_0)})\right] \\
&\quad = \int_0^1 \mathrm{d}t \sum_{k \geq 2} \mathbb{E}\Bigg[\frac{2}{k(k-1)} \sum_{(y,s) \sim (0,t)} \sum_{\substack{(z,u) \sim (0,t) \\ u < s}} \mathbf{1}_{\{(y,s) \sim (z,u)\}} \mathbf{1}_{\{|\mathcal{Y}^{\infty}_{(0,t)}| + |\mathcal{Z}^{\infty}_{(0,t)}(1)| = k\}}\Bigg].
\end{aligned}$$

By Proposition 4.5, the neighbourhood of the root $(0,t)$ is given by a Poisson point process with intensity measure

$$\lambda_{\mathcal{Z}^{\infty}_{(0,t)}(1)} + \lambda_{\mathcal{Y}^{\infty}_{(0,t)}}.$$

Conditioned on the number of neighbours, the neighbours of the root $(0,t)$ are independent and identically distributed by the normalized intensity measure of the neighbourhood given in (4.9), see [76, Proposition 3.8]. Therefore,

$$\mathbb{E}\left[H(\mathscr{G}^{\infty}_{(0,T_0)})\right] = \int_0^1 \mathrm{d}t\, \mathbb{P}\big\{(Y_t^{(1)}, S_t^{(1)}) \sim (Y_t^{(2)}, S_t^{(2)})\big\}\, \mathbb{P}\big\{|\mathcal{Y}^{\infty}_{(0,t)}| + |\mathcal{Z}^{\infty}_{(0,t)}(1)| \geq 2\big\},$$

where $(Y_t^{(1)}, S_t^{(1)})$ and $(Y_t^{(2)}, S_t^{(2)})$ are independent and identically distributed as claimed. Choosing $H(G)$ as the indicator of the event that the root has degree at least two, Theorem 4.4 (iii) gives

$$\frac{|V_2(\mathscr{G}_n)|}{n} \longrightarrow \int_0^1 \mathrm{d}t\, \mathbb{P}\big\{|\mathcal{Y}^{\infty}_{(0,t)}| + |\mathcal{Z}^{\infty}_{(0,t)}(1)| \geq 2\big\}\, dt,$$

in probability. As $|\mathcal{Y}^{\infty}_{(0,t)}| + |\mathcal{Z}^{\infty}_{(0,t)}(1)|$ is Poisson distributed with intensity λ_t we conclude that

$$c^{\mathrm{av}}(\mathscr{G}_n) \longrightarrow \frac{\int_0^1 \mathrm{d}t\, \mathbb{P}\big\{(Y_t^{(1)}, S_t^{(1)}) \sim (Y_t^{(2)}, S_t^{(2)})\big\}\, \big(1 - e^{-\lambda_t} - \lambda_t e^{-\lambda_t}\big)}{\int_0^1 \mathrm{d}t\, 1 - e^{-\lambda_t} - \lambda_t e^{-\lambda_t}},$$

as claimed in part (a).

For the global clustering coefficient, we count the number of triangles and wedges separately. To this end, define $H(G)$ to be the number of triangles which have their youngest vertex in the root of G, and $\hat{H}(G)$ to be the number of wedges with tip in the root $\mathbf{x}$ of G. Note that $H(\mathscr{G}^n_{(0,T_0)}) \leq |\mathcal{Y}_{\mathbf{x}}(\mathscr{G}^\infty_{(0,T_0)})|^2$ and thus $H \in \mathcal{H}_p$ for any $p > 1$. Moreover,

$$\begin{aligned}\hat{H}(\mathscr{G}^n_{(0,T_0)}) &= \frac{1}{2}|\mathcal{Y}^n_{\mathbf{x}}|(|\mathcal{Y}^n_{\mathbf{x}}|-1) + \frac{1}{2}|\mathcal{Z}^n_{\mathbf{x}}(1)|(|\mathcal{Z}^n_{\mathbf{x}}(1)|-1) + |\mathcal{Y}^n_{\mathbf{x}}||\mathcal{Z}^n_{\mathbf{x}}(1)| \\ &\leq 2\big(|\mathcal{Y}^\infty_{\mathbf{x}}|^2 + |\mathcal{Z}^\infty_{\mathbf{x}}(1)|^2\big).\end{aligned}$$

If $\gamma < 1/2$ and $1 < p < 1/(2\gamma)$, we hence have $\hat{H} \in \mathcal{H}_p$ and Theorem 4.4(iii) gives that

$$c^{\mathrm{glob}}(\mathscr{G}_n) = \frac{\sum_{\mathbf{x}\in\mathscr{G}_n} H(\theta_{\mathbf{x}}\mathscr{G}_n)}{n} \cdot \frac{n}{\sum_{\mathbf{x}\in\mathscr{G}_n} \hat{H}(\theta_{\mathbf{x}}\mathscr{G}_n)} \longrightarrow \frac{\mathbb{E}[H(\mathscr{G}^\infty_{(0,T_0)})]}{\mathbb{E}[\hat{H}(\mathscr{G}^\infty_{(0,T_0)})]} > 0$$

in probability. If $\gamma > 1/2$, applying the theorem to the bounded functions $\hat{H}(\mathscr{G}_n) \wedge k$ and then sending k to ∞, we get $\frac{1}{n}\sum_{\mathbf{x}\in\mathscr{G}_n} \hat{H}(\theta_{\mathbf{x}}\mathscr{G}_n) \to \infty$ and hence $c^{\mathrm{glob}}(\mathscr{G}_n) \to 0$ in probability, as $n \to \infty$. □

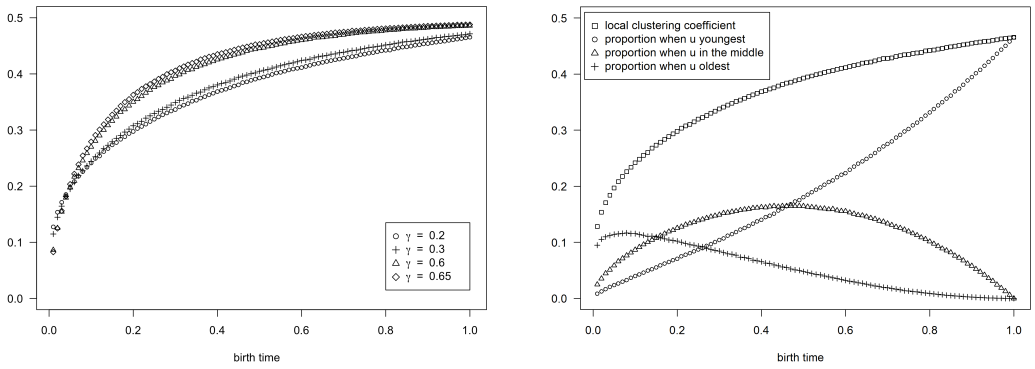

Figure 4.4: Local clustering coefficient of a vertex $(0,t)$ for parameters $a = 1$ and $\beta = c_{\mathrm{ed}}(1-\gamma)$ chosen such that the asymptotic edge density is fixed at c_{ed}. The plot on the left displays the behaviour of the model for high edge density ($c_{\mathrm{ed}} = 10$) for various values of γ. We remark that the shown behaviour is qualitatively independent of the edge density. In the plot on the right, the clustering coefficient for $\gamma = 0.2$ is shown, along with the probabilities of the event that t is younger (resp. in the middle or older) than two randomly picked neighbours, which are connected.

The local and average clustering coefficients cannot be calculated explicitly, but can be simulated; see the appendix of this paper for a discussion on the simulation techniques used here. We focus on the profile functions $\varphi = \frac{1}{2a}\mathbf{1}_{[0,a]}$, for $a \geq 1/2$, dimension $d = 1$, and fixed edge density $\beta/(1-\gamma)$. Figure 4.4 shows the local clustering coefficient of a vertex of age t in $\mathscr{G}^{\infty}$ showing monotone dependence on the age, i.e. the empirical probability that two neighbours of a given vertex are connected to each other is larger for younger vertices. This coincides with our intuitive understanding of the local structure of the networks, in which a young vertex, typically, is connected to either very close or very old vertices such that two randomly chosen neighbours have a decent chance of being connected to each other as well. By contrast, an old vertex typically has more long edges to younger vertices. Thus, two of its neighbours are typically further apart, which reduces the chance of them being each others neighbour. This monotonicity occurs independently of the choice of β, γ and a.

In Figure 4.5 we see that the dependence of the average clustering coefficient with respect to the width a of the profile function is of order $\frac{1}{a}$, a scaling that we also see in the analysis of the global clustering coefficient in the case $\gamma < \frac{1}{2}$. Hence, the average clustering coefficient and the global clustering coefficient (if $\gamma < \frac{1}{2}$) can be varied by the choice of φ and can be made arbitrarily small by choosing a large. Unlike with the global clustering coefficient, there is a mild dependence on β. Again, roughly speaking, large width of φ encourages long edges and reduces clustering.

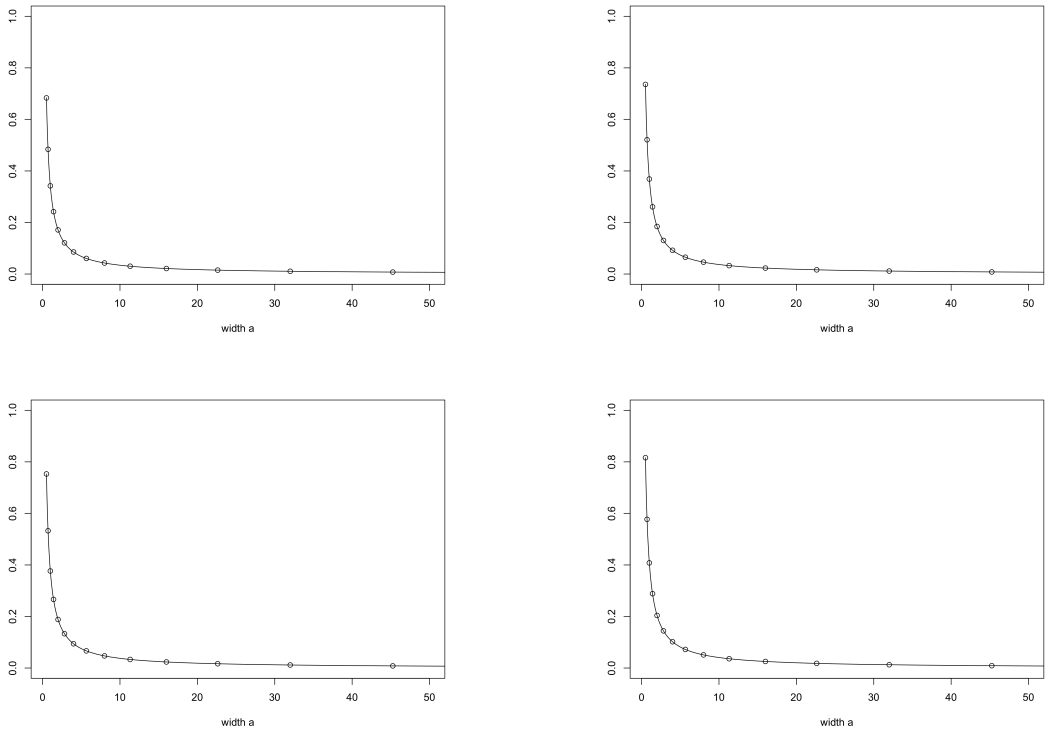

Figure 4.5: Average clustering coefficient for the network with profile function $\varphi = \frac{1}{2a}\mathbf{1}_{[0,a]}$ plotted against the width a, for $\gamma = 0.3$ in the left resp. $\gamma = 0.6$ in the right graphs. The graphs in the top row correspond to fixed edge density 1 while the bottom row corresponds to edge density 10.

4.1.5 Asymptotics for typical edge lengths

In this section we study the distribution of the length of typical edges in $\mathscr{G}_n$. We denote by $E(G)$ the set of edges of the graph G and define λ_n, the (rescaled) *empirical edge length distribution* in $\mathscr{G}_n$, by

$$\lambda_n = \frac{1}{|E(\mathscr{G}_n)|} \sum_{(\mathbf{x},\mathbf{y})\in E(\mathscr{G}_n)} \delta_{n^{1/d} d_{\mathbb{T}^d_1}(x,y)}.$$

Theorem 4.10

For every continuous and bounded $g\colon [0,\infty) \to \mathbb{R}$, we have

$$\frac{1}{|E(\mathscr{G}_n)|} \sum_{(\mathbf{x},\mathbf{y})\in E(\mathscr{G}_n)} g\big(n^{1/d} d_{\mathbb{T}_1^d}(x,y)\big) = \int \mathrm{d}\lambda_n\, g \to \int \mathrm{d}\lambda\, g,$$

in probability, as $n \to \infty$, where the limiting probability measure λ on $(0,\infty)$ is given by

$$\lambda([a,b)) = \frac{1-\gamma}{\beta} \int_0^1 \mathrm{d}t \int_0^t \mathrm{d}s \int_{a\le|y|<b} \mathrm{d}y\, \varphi\big(\beta^{-1} t^{1-\gamma} s^{\gamma} |y|^d\big). \tag{4.10}$$

Proof. For a finite graph G with vertices positioned in $\mathbb{R}^d$ and marked by birth times and with a root vertex $\mathbf{x}$ placed at the origin define, for $a < b \in [0,\infty]$, the function

$$H_{a,b}(G) = \sum_{\mathbf{y}\in\mathcal{Y}_{\mathbf{x}}(G)} \mathbf{1}_{[a,b)}(|y|). \tag{4.11}$$

Observe that the law of $\lambda_n([a,b))$ in $\mathscr{G}_n$ equals the law of

$$\frac{1}{|E(\mathscr{G}^n)|} \sum_{\mathbf{x}\in\mathcal{X}^n} H_{a,b}(\theta_{\mathbf{x}}\mathscr{G}^n).$$

As mentioned in the remark following the theorem, Theorem 4.4 is applicable to functions $H_{a,b}$ depending on the length of edges in the rescaled graphs $(\mathscr{G}^n)_{n>0}$. Since the sum in (4.11) is dominated by the outdegree, $H_{a,b} \in \mathcal{H}_p$ for some $p > 1$. We thus get

$$\frac{1}{n} \sum_{\mathbf{x}\in\mathcal{X}^n} H_{a,b}(\theta_{\mathbf{x}}\mathscr{G}^n) \longrightarrow \mathbb{E}[H_{a,b}(\mathscr{G}^{\infty}_{(0,T_0)})],$$

and since Theorem 4.4 (iii) also gives $|E(\mathscr{G}^n)|/n \to \frac{\beta}{1-\gamma}$ and it also holds that $\lambda([a,b)) = \frac{1-\gamma}{\beta}\mathbb{E}[H_{a,b}(\mathscr{G}^{\infty}_{(0,T_0)})]$ we infer that $\lambda_n([a,\infty)) \longrightarrow \lambda([a,\infty))$ in probability, as $n \to \infty$. Therefore, convergence in probability of λ_n to λ in the space of probability measures on $\mathbb{R}_+$, equipped with the Lévy-Prokhorov metric, follows. □

Remark 4.1.4. Suppose there exists $\delta > 1$ such that the profile function satisfies $\varphi(x^d) \asymp 1 \wedge x^{-d\delta}$. Then the explicit formula for λ in (4.10) can be used to calculate the tail behaviour of λ. More precisely, separating the integration into several domains, depending on whether we are integrating over the tail domain of φ or not, results in the terms of order d, $d(\frac{1}{\gamma} - 1)$ and $d(\delta - 1)$. This gives that $\lambda([K, \infty)) \asymp 1 \wedge (\beta^{-1/d} K)^{-\eta}$, where

$$\eta := \min\big\{d, d(\frac{1}{\gamma} - 1), d(\delta - 1)\big\}. \tag{4.12}$$

In particular, λ has finite expectation if $\eta > 1$ and infinite expectation if $\eta < 1$.

We denote by $M^{\infty}_{(0,T_0)}$ the length of the longest outgoing edge of the origin in $\mathscr{G}^{\infty}_{(0,T_0)}$. By the construction of λ above, $\lambda([K, \infty))$ is the expected number of outgoing edges of length bigger than K divided by the total number of outgoing edges from the origin. If K is large this should be of similar order to the probability that $M^{\infty}_{(0,T_0)} \geq K$. This is confirmed in the following lemma.

Lemma 4.11

Suppose there exists $\delta > 1$ such that the profile function satisfies $\varphi(x^d) \asymp 1 \wedge x^{-d\delta}$. Then, $\mathbb{E}\left[(M^{\infty}_{(0,T_0)})^a\right]$ is finite if $a < \eta$ and infinite if $a > \eta$, where η is as defined in (4.12).

Proof. We show that the tail probability $\mathbb{P}\{(M^{\infty}_{(0,T_0)})^a \geq K\}$ is of order $K^{-\eta/a}$ as $K \to \infty$. The number of outgoing edges with length at least $K^{1/a}$ in $\mathscr{G}^{\infty}_{(0,T_0)}$ from the vertex $(0, t)$ at the origin are Poisson distributed with parameter

$$\lambda_{K^{1/a},t} := \lambda_{\mathcal{Y}^{\infty}_{(0,t)}}\big(\mathbb{R}^d \backslash (\{|x| < K^{1/a}\}) \times (0, t]\big),$$

and hence

$$\mathbb{P}\{(M^{\infty}_{(0,T_0)})^a \geq K\} = \int_0^1 \mathrm{d}t\, 1 - \exp\big(-\lambda_{K^{1/a},t}\big) \asymp \int_0^1 \mathrm{d}t\, \lambda_{K^{1/a},t} \asymp \lambda([K^{1/a}, \infty)),$$

recalling the asymptotic edge length distribution λ defined in (4.10). The established tail behaviour of the measure λ yields $\mathbb{P}\{(M^{\infty}_{(0,T_0)})^a \geq K\} \asymp 1 \wedge K^{-\eta/a}$. □

Using this, we can establish a result about the average rescaled length in the

network $\mathscr{G}_n$.

Theorem 4.12

Suppose that there exists $\delta > 1$ such that the profile function satisfies $\varphi(x^d) \asymp 1 \wedge x^{-d\delta}$. Then, for all $a > 0$ and $b \in [0, \frac{\eta}{a})$, there exists a positive constant C, depending on $a, b, \gamma, \beta, \varphi$, such that

$$\frac{1}{|E(\mathscr{G}_n)|} \sum_{\mathbf{x} \in \mathscr{G}_n} \Big(\sum_{\mathbf{y} \in \mathcal{Y}_{\mathbf{x}}(\mathscr{G}_n)} \Big(n^{1/d} d_{\mathbb{T}_1^d}(x, y) \Big)^a \Big)^b \to C \tag{4.13}$$

in probability, as $n \to \infty$.

Remark 4.1.5. If $\eta > 1$ one can choose $a = b = 1$ and this yields that the mean edge length in $\mathscr{G}_n$ is of order $n^{-1/d}$. If $\eta < 1$ (and in particular always if $d = 1$) the mean edge length is of larger order.

Proof. Consider again a finite graph G with vertices positioned in $\mathbb{R}^d$ and marked by birth times and with a root vertex $\mathbf{x}$ placed at the origin. Define

$$H(G) := \Big(\sum_{\mathbf{y} \in \mathcal{Y}_{\mathbf{x}}(G)} |y|^a \Big)^b$$

and observe that the law of the left-hand side in (4.13) equals the law of

$$\frac{1}{|E(\mathscr{G}^n)|} \sum_{\mathbf{x} \in \mathcal{X}^n} H(\theta_{\mathbf{x}} \mathscr{G}^n).$$

It suffices to show that $H \in \mathcal{H}_p$ for some $p > 1$, since Theorem 4.4 (iii) then ensures the convergence in probability to $\frac{1-\gamma}{\beta} \mathbb{E}[H(\mathscr{G}^\infty_{(0,T_0)})]$, which is a positive constant. To this end recall $M^\infty_{(0,T_0)}$, the length of the longest outgoing edge of the root $\mathbf{x}$ in $\mathscr{G}^\infty_{(0,T_0)}$ and observe that, almost surely, $H(\mathscr{G}^n_{(0,T_0)}) \le (M^\infty_{(0,T_0)})^{ab} |\mathcal{Y}^\infty_{\mathbf{x}}|^b$. Since, by choice, $ab < \eta$, there exist some $p, q > 1$, such that $\alpha := pqab < \eta$. Lemma 4.11 then ensures $\mathbb{E}[(M^\infty_{(0,T_0)})^\alpha] < \infty$ and, by applying Hölder's inequality to the observed bound for $H(\mathscr{G}^n_{(0,T_0)})$, we get

$$\sup_{n>0} \mathbb{E}\left[H(\mathscr{G}^n_{(0,T_0)})^p \right] \le \left(\mathbb{E}\left[(M^\infty_{(0,T_0)})^\alpha \right] \right)^{1/q} \left(\mathbb{E}\left[|\mathcal{Y}^\infty_{\mathbf{x}}|^{\frac{\alpha}{a(q-1)}} \right] \right)^{\frac{q-1}{q}} < \infty.$$

□

4.2 The soft Boolean model

As explained in Section 1.2.1 in the (soft) Boolean model on $\mathbb{R}^d$ each point x of a Poisson point process of unit intensity carries an independent identically distributed radius R_x and we assign to each unordered pair of vertices $\{x, y\}$ an independent identically distributed random variable $X(x, y)$. Given these random variables two vertices are connected by an edge if and only if

$$\frac{|x-y|}{R_x + R_y} < X(x, y). \tag{4.14}$$

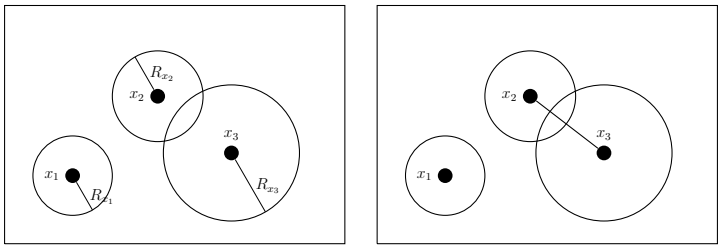

Figure 4.6a: Sketch of the construction of the hard version of the Boolean model. Balls centered around the vertices are drawn with the corresponding radii and edges are drawn when two balls intersect, leading to the graph given in the right picture.

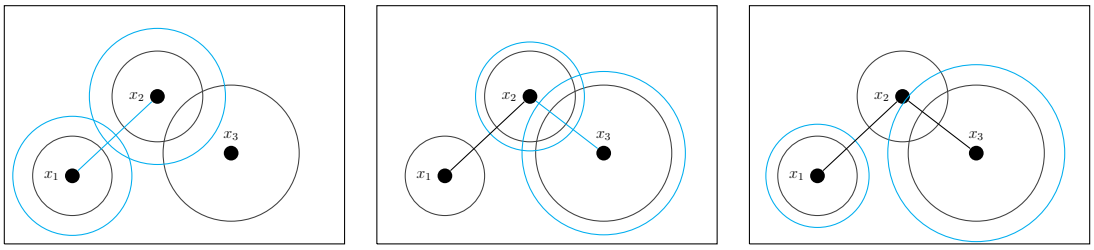

Figure 4.6b: The coloured balls are the copies of the balls in Figure 4.6a, whose radius is multiplied by the corresponding random variable X which is drawn for each pair of vertices. Edges are drawn when the coloured balls intersect, leading to a soft version of the model.

The choice $X = 1$, where X is an identically distributed copy of the random variables $X(x, y)$, corresponds to the hard version of the Boolean model where an edge is drawn between x and y if and only if the balls centered around x, resp.

y, with radius R_x, resp. R_y, intersect. An alternative choice of the distribution of X allows us to relax this condition and enforce the occurence of long edges in that way. As mentioned in Section 1.2.1 this influence can be interpreted in the following way. Take for each pair of vertices $\{x, y\}$ a copy from both corresponding balls and modify them by multiplying their radii R_x and R_y by $X(x, y)$. Then, form an edge between the vertices if and only if the modified balls intersect, see Figure 4.6b. To ensure that the expected number of neighbours of a given vertex $\mathbf{x}$ is bounded away from zero and infinity, we have an integrability condition on X. Namely, we assume that $0 < \int_{\mathbb{R}^d} \mathrm{d}y\, \mathbb{P}(X > |y|) < \infty$.

This model can be put in our framework by taking a Poisson process of unit intensity on $\mathbb{R}^d \times (0, 1)$ as the vertex set and setting the radius of a vertex $\mathbf{x} = (x, t)$ as $R_x := F^{-1}(1 - t)$ where F is the distribution function of the radius and $F^{-1}(t) = \inf\{u : F(u) > t\}$ is the generalised inverse function. It then holds for a uniform random variable U on $(0, 1)$ that

$$\mathbb{P}(F^{-1}(1 - U) \leq z) = \mathbb{P}(U > 1 - F(z)) = F(z).$$

When the radius distribution is heavy-tailed, more precisely, if there exist $\gamma \in (0, 1)$ and $c_1, c_2 > 0$ such that, for all $r \geq 1$, it holds

$$c_1 r^{-d/\gamma} \leq \mathbb{P}(R_x > r) \leq c_2 r^{-d/\gamma}, \tag{4.15}$$

the (soft) Boolean model has a scale-free degree distribution, i.e. in the Palm version $\mathscr{G}_{(0,T_0)}$ of the model the degree distribution of the origin $(0, T_0)$ is scale-free with power-law exponent $\tau = 1 + \frac{1}{\gamma}$. We will show this by using the following result, which is a corollary of Proposition 4.5 and Lemma 4.8.

Lemma 4.13

Let $\gamma \in (0,1)$ and U be a uniform on $(0,1)$ distributed random variable. Furthermore set $\Lambda : (0,1) \to \mathbb{R}_+$ to be a function for which there exists $c_1, c_2 > 0$ such that it holds $c_1 u^{-\gamma} \leq \Lambda(u) \leq c_2 u^{-\gamma}$ for all $u \in (0,1)$. Denote by μ the mixed Poisson-distribution with mixing distribution $\Lambda(U)$. Then, it holds

$$\mu(k) = k^{-(1+1/\gamma)+o(1)} \quad \text{as } k \to \infty.$$

Proof. Let ν_1, resp. ν_2, be mixed Poisson distributions with mixing distribution $c_1 U^{-\gamma}$, resp. $c_2 U^{-\gamma}$. By a coupling argument it holds, for all $k \in \mathbb{N}_0$, that $\nu_1(\{k,\dots,\infty\}) \leq \mu(\{k,\dots,\infty\}) \leq \nu_2(\{k,\dots,\infty\})$. Hence, it is sufficient to show that, for a mixed Poisson distribution ν with mixing distribution $cU^{-\gamma}$, $c > 0$, $\nu(k)$ decays polynomially at rate $1 + \frac{1}{\gamma}$ as $k \to \infty$. As U is uniform distributed it holds, for $k \in \mathbb{N}_0$, that

$$\begin{aligned}\nu(k) &= \int_0^1 \mathrm{d}u \exp(-cu^{-\gamma}) \frac{(cu^{-\gamma})^k}{k!} \\ &= \int_c^\infty \mathrm{d}\lambda \frac{c^{1/\gamma}}{\gamma} \exp(-\lambda) \frac{\lambda^k}{k!} \lambda^{-(1+1/\gamma)} = \frac{c^{1/\gamma}}{\gamma} \frac{\Gamma(k-\frac{1}{\gamma})}{\Gamma(k+1)} - \frac{c^{1/\gamma}}{\gamma} \int_0^c \mathrm{d}\lambda \lambda^{k-1-1/\gamma} e^{-\lambda}.\end{aligned}$$

As the second term is of smaller order, by Stirling's formula we obtain that $\nu(k) = k^{-(1+1/\gamma)+o(1)}$ as $k \to \infty$. □

Proposition 4.14

The origin in the Palm version $\mathscr{G}_{(0,T_0)}$ of the (soft) Boolean model satisfying (4.15) for $\gamma \in (0,1)$ has a scale-free degree distribution μ for which it holds

$$\mu(k) = k^{-(1+1/\gamma)+o(1)} \quad \text{as } k \to \infty.$$

Proof. Since edges are formed independently given the Poisson point process, by the same arguments as in the proof of Proposition 4.5 the degree of a vertex

$\mathbf{x} = (0, t)$ is Poisson distributed with parameter

$$\begin{aligned}\int_0^1 \mathrm{d}s \int_{\mathbb{R}^d} \mathrm{d}y\, \mathbb{P}\left(X \geq \frac{|y|}{F^{-1}(1-t) + F^{-1}(1-s)}\right) \\ = C \int_0^1 \mathrm{d}s\, (F^{-1}(1-t) + F^{-1}(1-s))^d\end{aligned}$$

for some constant $C > 0$ given by the integrability condition on X. For functions $f : (0,1) \to \mathbb{R}$, $g : (0,1) \to \mathbb{R}$ we write $f(t) \asymp g(t)$ if there exist constants $c_1, c_2 > 0$ such that $c_1 g(t) \leq f(t) \leq c_2 g(t)$ for all $t \in (0,1)$. Then, by (4.15) it holds

$$\begin{aligned}C \int_0^1 \mathrm{d}s\, (F^{-1}(1-t) + F^{-1}(1-s))^d &\asymp \int_0^1 \mathrm{d}s (t^{-\gamma/d} + s^{-\gamma/d})^d \\ &\asymp \int_0^1 \mathrm{d}s (t \wedge s)^{-\gamma} \asymp t^{-\gamma}.\end{aligned}$$

As the mark T_0 of the origin $(0, T_0)$ in the Palm version of the model is independent of the other vertices and of the random variables $X(x, y)$, the degree distribution μ of the origin is mixed Poisson-distributed with a mixing distribution given by a functional of T_0 which satisfies the condition in Lemma 4.13 and therefore it holds $\mu(k) = k^{-(1+1/\gamma)+o(1)}$ as $k \to \infty$. □

The claims of the main results of the previous chapters take hold fully if we assume X to be heavy-tailed, see Figure 4.7 for a simulation of such a model. First, we assume that there exists $\delta > 1$ such that, for every small $\varepsilon > 0$, there is a constant c_3 such that $P(X > r) \leq c_4 r^{-d(\delta-\varepsilon)}$ for all $r \geq 0$. As the right inequality of (4.15) implies that $F^{-1}(1-t) \leq c_2^{\gamma/d} t^{-\gamma/d}$ we infer that the probability to form an edge between $\mathbf{x}$ and $\mathbf{y}$ is bounded by

$$c_4 \frac{(F^{-1}(1-t) + F^{-1}(1-s))^{d(\delta-\varepsilon)}}{|x-y|^{d(\delta-\varepsilon)}} \leq c_4 c_3^{\gamma(\delta-\varepsilon)} (t \vee s)^{-\gamma(\delta-\varepsilon)}.$$

Hence, using the conditional independence of the edges, Assumption UBA* and consequently Assumption UBA holds for the parameters γ and $\delta - \varepsilon$ for all $\varepsilon > 0$. By Theorem 2.1 the assumption then implies no ultrasmallness if $\gamma < \frac{\delta}{\delta+1}$. In particular this implies that the hard version of the Boolean model is not ultrasmall for any radius distribution satisfying $\mathbb{P}(R_x > r) \leq c_2 r^{-d/\gamma}$ for any

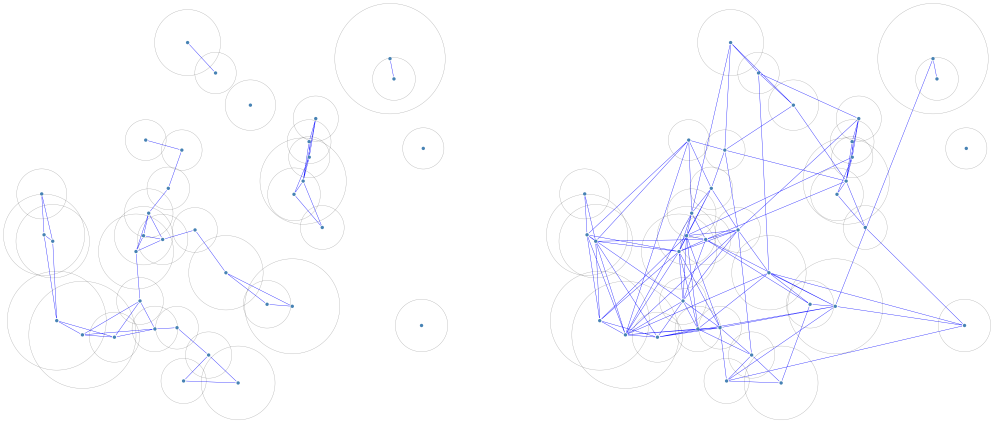

Figure 4.7: The left picture shows a simulation of the two-dimensional hard Boolean model with $\gamma = 0.75$. The picture on the right-hand side gives a soft version of the model, where X is heavy-tailed with $\delta = 1.5$. For comparison, the same other parameters and realisation of the Poisson point process as the hard model have been used in this case. Note that the left graph is a subgraph of the one on the right-hand side.

$\gamma \in (0, 1)$ or having only bounded support almost surely.

If we additionally assume that for every $\varepsilon > 0$ there is a constant $c_3 > 0$ such that for all $r \geq 1$ it holds $P(X > r) \geq c_3 r^{-d(\delta+\varepsilon)}$ then both Assumptions UBA and LBA hold for parameters arbitrarily close to γ and δ and hence by Theorem 2.1 and Theorem 2.2 the model is ultrasmall if $\gamma > \frac{\delta}{\delta+1}$ and in this case we obtain the full limit theorem stated in (2.5). In particular, we obtain the following theorem.

Theorem 4.15

Let the radii distribution satisfy (4.15) for some $\gamma \in (0,1)$ and let $\delta > 1$ such that, for every ε, there are $c_3, c_4 > 0$ such that

$$c_3 r^{-d(\delta+\varepsilon)} \leq \mathbb{P}(X > r) \leq c_4 r^{-(\delta-\varepsilon)} \quad \text{for all } r \geq 1. \tag{A2}$$

Then, the soft Boolean model

- is **not ultrasmall** if $\gamma < \frac{\delta}{\delta+1}$ and
- is **ultrasmall** if $\gamma > \frac{\delta}{\delta+1}$ and, for $\mathbf{x}, \mathbf{y} \in \mathbb{R}^d \times (0,1)$, we have

$$\mathrm{d}(\mathbf{x}, \mathbf{y}) = (4 + o(1)) \frac{\log\log|x-y|}{\log\left(\frac{\gamma}{\delta(1-\gamma)}\right)} \tag{4.16}$$

under $\mathbb{P}_{\mathbf{x},\mathbf{y}}(\ \cdot\ \mid \mathbf{x} \leftrightarrow \mathbf{y})$ with high probability as $|x-y| \to \infty$.

Under the same assumptions we obtain the results of Chapter 3 for the soft Boolean model. We denote by $\Gamma(\lambda)$ the non-extinction probability of the contact process starting in the origin $(0, T_0)$ of the Palm-version of the soft Boolean model and by ϖ_n the extinction time of the contact process on the soft-Boolean model restricted to the box $[-\frac{n^{1/d}}{2}, \frac{n^{1/d}}{2}]$ with a fully infected initial condition. Then, by Theorem 3.1 and 3.14 the following results hold for the contact process on the soft Boolean model.

Theorem 4.16

Let the radii distribution satisfy (4.15) for some $\gamma \in (0,1)$ and let $\delta > 1$ such that (A2) is satisfied. When $\gamma > \frac{\delta}{\delta+1}$, there exists $c, C > 0$ such that, as $\lambda \to 0$, it holds

$$c \frac{\lambda^{2/\gamma-1}}{\log(1/\lambda)^{(1-\gamma)/\gamma}} \leq \Gamma(\lambda) \leq C \frac{\lambda^{2/\gamma-1}}{\log(1/\lambda)^{(1-\gamma)/\gamma}}. \tag{4.17}$$

Theorem 4.17

Let the radii distribution satisfy (4.15) for some $\gamma \in (0,1)$ and let $\delta > 1$ such that (A2) is satisfied and it holds $\gamma > \frac{\delta}{\delta+1}$. For any $\lambda > 0$, there exists $c > 0$ such that

$$\lim_{n\to\infty} \mathbb{P}\{\varpi_n \geq e^{cn}\} = 1.$$

An alternative soft Boolean model

An alternative version of the soft Boolean model is obtained by changing the connection rule slightly. Instead of forming an edge between two vertices when their balls intersect, we now create an edge if at least one vertex lies in the ball of the other vertex. This means that we form an edge between two vertices if and only if

$$\frac{|x-y|}{R_x \vee R_y} < X(x,y) \tag{4.18}$$

where R_x, R_y and $X(x,y)$ play the same role as in (4.14). The hard version of this model has been discussed by Hirsch [63], where he also gives a lower bound for the chemical distance, which is of the form $|x-y| / \log|x-y|$. As

$$(R_x + R_y)/2 \leq R_x \vee R_y \leq R_x + R_y,$$

both versions of the (soft) Boolean model behave similarly. In fact, our results also show that the hard model is not ultrasmall and Proposition 4.14, Theorem 4.15, Theorem 4.16 and Theorem 4.17 hold as stated also for this version of the (soft) Boolean model.

4.3 Scale-free percolation

Scale-free percolation is defined on the lattice $\mathbb{Z}^d$ or on a Poisson point process with unit intensity on $\mathbb{R}^d$, where each vertex x is equipped with a random independent identically distributed weight W_x, where we assume the weights to be heavy-tailed, i.e. there exists $\gamma \in (0,1)$ such that

$$\mathbb{P}(W > w) = w^{-1/\gamma}, \quad \text{for } w \geq 1, \tag{4.19}$$

where W is a random variable with same distribution as the weights. Then, given the vertex set and the weights edges are drawn independently and a pair of vertices x, y is connected by an edge with probability

$$\varphi\big(\beta^{-1} W_x W_y \, |x-y|^d\big),$$

where $\varphi : [0,\infty) \to [0,1]$ is a non-increasing integrable function and $\beta > 0$ controls the edge density. This model has been introduced and discussed for the lattice by Deijfen et al. [33] and studied on a Poisson point process by Deprez et al. [34].

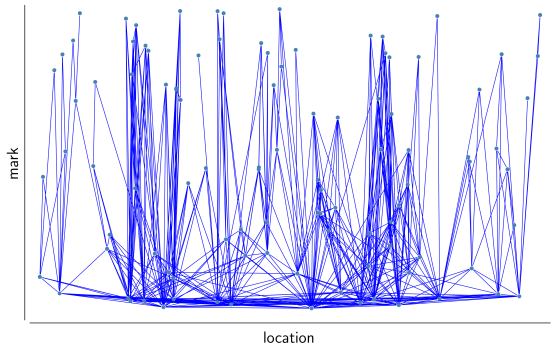

Figure 4.8: Snapshot of a simulation of scale-free percolation on a Poisson point process on $\mathbb{R} \times (0,1)$. For comparison, the same parameters and realisation as in Figure 4.1 were used for this simulation. Notice that we can see in this simulation that vertices with small mark are much better connected than in the age-dependent random connection model, where two vertices with small mark are connected via connectors.

We can put this model in our framework in the same way as done for the soft Boolean model. Set a Poisson process of unit intensity on $\mathbb{R}^d \times (0,1)$ as the vertex set. Denote by F the distribution function of W and set the weight of a vertex $\mathbf{x} = (x,t)$ as $W_x := F^{-1}(1-t)$ where $F^{-1}(t) = \inf\{u : F(u) > t\}$. As (4.19) implies that $F^{-1}(1-t) = t^{-\gamma}$ in our framework an edge is formed independently between two vertices $\mathbf{x}$ and $\mathbf{y}$ with probability

$$\varphi\big(\beta^{-1} t^{-\gamma} s^{-\gamma} \, |x-y|^d\big).$$

The model has a scale-free degree distribution, see [33, Theorem 2.2] and [34, Theorem 3.1], which we can easily see in our framework as the degree of a given

vertex $\mathbf{x} = (x, t)$ is Poisson-distributed with parameter $ct^{-\gamma}$ for some $c > 0$. Hence, by the same arguments as in Section 4.2 and Lemma 4.13 it follows that the degree distribution of the origin of the Palm version of scale-free percolation is scale-free with power-law exponent $1 + \frac{1}{\gamma}$.

As mentioned in Section 2.1 the dependence on the weights in this model is so strong that the geometry does not play a significant role and the techniques developed in Chapter 2 and Chapter 3 are not needed to understand the behaviour of the model. In fact, Assumption UBA* only holds for $\gamma < \frac{1}{2}$, which recovers the well-known result that the graph is not ultrasmall in this case. Recent work for the behaviour of the chemical distance when $\gamma < \frac{1}{2}$ has been done by Hao and Heydenreich [61]. Adapting the upper bound assumption to the structure of scale-free percolation improves our results on the chemical distance. The scale-free percolation satisfies Assumption A.1 for any $\gamma \in (0, 1)$, when there exists $\delta > 1$ such that for all $\varepsilon > 0$, there is $C > 0$ such that $\varphi(r) \leq Cr^{-(\delta-\varepsilon)}$ for all $r \geq 1$. Then, by Theorem A.1 we obtain again that scale-free percolation is not ultrasmall if $\gamma < \frac{1}{2}$ and in the case $\gamma > \frac{1}{2}$ we obtain an asymptotic lower bound on the chemical distance which is sharp in comparison to well-known results from the literature, see [21] and [33]. In comparison to Section 2.3 we can see that the proof of Theorem A.1 is structurally much simpler than the proofs of the main results, as the geometry, described in our framework by the choice of φ, turns out to have no influence at all. This observation agrees with the results, shown in [21] and [33], that the geometry has no influence on the occurence of ultrasmallness.

As mentioned in Chapter 3 the behaviour of the contact process on hyperbolic random graphs has been studied in [78] and show the rate of decay of the non-extinction probability $\Gamma(\lambda)$ given in (3.2). This differs from Theorem 3.1 as there exists another survival strategy leading to a different rate of decay on hyperbolic random graphs when τ is near to two, i.e. γ near one. For this choice of γ an infected vertex with relatively small mark has typically many neighbouring powerful vertices with even smaller mark to which the infection can spread directly. As a consequence the infection spreads to more and more powerful vertices and survives in that way. We expect to see this behaviour also on scale-free percolation with an arbitrary non-increasing integrable function φ, as the expected number of neighbours of a given vertex $\mathbf{x} = (x, t)$ with mark

smaller than t increases when t becomes small and therefore ensures there are sufficiently many more powerful to which the infection can spread.

4.4 Ultrasmall scale-free geometric networks

In [99] Yukich introduces a model which is built up in a similar way as the soft Boolean model either on the lattice or on a Poisson point process on $\mathbb{R}^d$. Each vertex x carries an independent identically distributed radius R_x and an edge is formed between two vertices x and y if both vertices lie in the ball centered at the other vertex with its corresponding radius. In other words we draw an edge if and only if

$$\frac{|x-y|}{R_x \wedge R_y} < 1. \tag{4.20}$$

This condition is structurally different to the ones presented in Section 4.2, as this condition only depends on the smaller radius associated to the two vertices whereas the conditions (4.14) or (4.18) of the hard Boolean model are mainly influenced by the larger radius. Thus, it is easy to see that this condition is much stricter, leading to a sparser graph when taking the same radii for this model and the hard Boolean model. In fact, when the radius distribution satisfies condition (4.15) the model is not scale-free. This is compensated by taking larger radii, see Figure 4.9. Let $\gamma > 0$ and $\alpha > 0$ throughout this section. As done in [99], we assign to each vertex x an independent uniform random variable U_x on $(0,1)$ and the radius of x is given by $R_x := \alpha^{1/d} U_x^{-(1+\gamma)/d}$.

This model can be put easily in our framework as the mark of each vertex is a uniformly on the interval $(0,1)$ distributed random variable. Thus, we form an edge between two vertices $\mathbf{x} = (x,t)$ and $\mathbf{y} = (y,s)$ if and only if

$$\frac{|x-y|^d}{\alpha(t \vee s)^{-(1+\gamma)}} < 1. \tag{4.21}$$

As shown in [99, Theorem 1.1] the model is scale-free with power-law exponent $\tau = 1 + \frac{1}{\gamma}$, which we can again check easily in our framework, since the number of neighbours of a given a vertex $\mathbf{x} = (x,t)$ is Poisson-distributed with parameter $\Lambda(t)$ depending only on the mark of the vertex for which there exists $c, C > 0$ such that $ct^{-\gamma} < \Lambda(t) < Ct^{-\gamma}$ for all $t \in (0,1)$. Hence, by Lemma 4.13 the origin

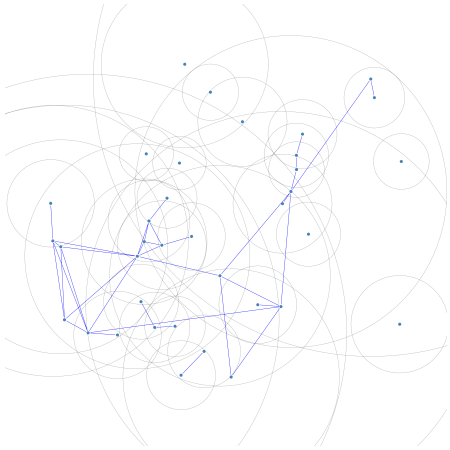

Figure 4.9: Simulation of the two-dimensional ultrasmall scale-free geometric network with parameter $\gamma = 0.75$ and $\alpha = 2$.

in the Palm-version of the model has a scale-free degree distribution.

In [99, Theorem 1.2] it is shown that this model is ultrasmall for every $\gamma > 0$ by proving an asymptotic upper bound of the chemical distance of two given vertices which is of doubly logarithmic order in their Euclidean distance when the vertices are far apart. Our results in Chapter 2 provide an asymptotic lower bound, which is smaller than the proven upper bound, see Theorem A.2. This lower bound turns out to be sharp, as shown in [81] for the model on the lattice.

4.5 The reinforced-age-dependent random connection model

In this section we consider a reinforced version of the age-dependent random connection model described in Section 4.1, where the connection probability between vertices is reinforced by additional weights of the nodes. The following discussion can be found in part in [56]. Interestingly, although edges do not occur independently of each other due to the additional weights, the results of Chapter 2 still apply in full generality. Let the vertex set be a Poisson point process $\mathcal{X}$ on $\mathbb{R}^d \times (0, 1)$ as before. We assign in addition to each point $\mathbf{x} \in \mathcal{X}$ an independent identically distributed *reinforcement weight* $W_{\mathbf{x}}$, for which we assume the second moment exists and that it is almost surely bounded away from zero, i.e. there exists $\alpha > 0$ such that $\mathbb{P}(W \geq \alpha) = 1$, where W is an identically distributed

random variable as $W_{\mathbf{x}}$. Given $\mathcal{X}$ and the reinforcement weights, edges are then formed independently between $\mathbf{x} = (x, t)$ and $\mathbf{y} = (y, s)$ with probability

$$\varphi\left(\tfrac{(W_{\mathbf{x}}W_{\mathbf{y}})^{-1/\delta}}{\beta}(t \wedge s)^{\gamma}(t \vee s)^{1-\gamma}\,|x-y|^{d}\right),$$

where φ is as in Example 4.1. Let $I \subset \mathcal{X}^2$ be a set of pairs of vertices where each vertex appears at most twice. If there is $C > 0$ such that $\varphi(r) \leq Cr^{-\delta}$ for all $r > 0$, then

$$\begin{aligned}
&\mathbb{E}_{\mathcal{X}}\Bigg[\prod_{(\mathbf{x}_i,\mathbf{y}_i)\in I}\mathbf{1}\{\mathbf{x}_i \sim \mathbf{y}_i\}\Bigg] \\
&\quad\leq \mathbb{E}_{\mathcal{X}}\Bigg[\prod_{(\mathbf{x}_i,\mathbf{y}_i)\in I} C W_{\mathbf{x}_i}W_{\mathbf{y}_i}\beta^{\delta}(t_i \wedge s_i)^{-\gamma\delta}(t_i \vee s_i)^{(\gamma-1)\delta}\,|x_i-y_i|^{-\delta d}\Bigg] \\
&\quad\leq \prod_{(\mathbf{x}_i,\mathbf{y}_i)\in I} C\beta^{\delta}(t_i \wedge s_i)^{-\gamma\delta}(t_i \vee s_i)^{(\gamma-1)\delta}\,|x_i-y_i|^{-\delta d}\,(\mathbb{E}[W_{\mathbf{x}_i}^2] \vee 1)(\mathbb{E}[W_{\mathbf{y}_i}^2] \vee 1),
\end{aligned}$$

where the second inequality holds since each reinforcement weight appears at most twice in the product and they are independent of $\mathcal{X}$. As the second moment of the weights exists, Assumption UBA holds for an appropriately chosen κ. Hence, ultrasmallness fails if $\gamma < \frac{\delta}{\delta+1}$. Note that in the same way Assumption UBA is satisfied for parameter γ and one arbitrarily close to δ, when we assume on φ that for every small $\varepsilon > 0$ there exists $C > 0$ such that $\varphi(r) \leq Cr^{-(\delta-\varepsilon)}$ for all $r > 0$, since the moment assumption on W implies that $\mathbb{E}[W^{2-\varepsilon}] < \infty$ for all small $\varepsilon > 0$. On the other hand, we can easily couple the reinforced age-dependent random connection model to an age-dependent random connection model with a modified density parameter, such that the latter is a subgraph of the former. Indeed, for each pair of vertices we draw an independent uniform random variable $U(\mathbf{x}, \mathbf{y})$. Given the Poisson process $\mathcal{X}$, the reinforcement weights and the family $(U(\mathbf{x}, \mathbf{y}))_{\mathbf{x},\mathbf{y}\in\mathcal{X}}$, we can construct the age-dependent random connection model and the reinforced model simultaneously in the following way. First, add an edge between any pair of vertices when

$$U(\mathbf{x}, \mathbf{y}) \leq \varphi\left(\frac{\alpha^{-2/\delta}}{\beta}(t \wedge s)^{\gamma}(t \vee s)^{1-\gamma}\,|x-y|^{d}\right).$$

This leads to the age-dependent random connection model with new density parameter $\tilde{\beta} = \beta\alpha^{-2/\delta}$. Since $W \geq \alpha$ almost surely, each such edge is also added

in the reinforced model. To get the full reinforced model, we add additional edges to hitherto unconnected pairs of vertices if

$$U(\mathbf{x},\mathbf{y}) \leq \varphi\left(\frac{(W_{\mathbf{x}}W_{\mathbf{y}})^{-1/\delta}}{\beta}(t\wedge s)^{\gamma}(t\vee s)^{1-\gamma}\,|x-y|^{d}\right).$$

As the age-dependent random connection model is ultrasmall when $\gamma > \frac{\delta}{\delta+1}$ and if for every $\epsilon > 0$, there exists $c > 0$ with $\varphi(r) \geq cr^{-(\delta+\epsilon)}$ for all $r \geq 1$, the reinforced model is ultrasmall as well and we get the asymptotic chemical distance as stated in (2.5) under both tail assumptions stated for φ in this section. Combining these results provides a characterization of the occurence of ultrasmallness of the same scope as for the age-dependent random connection model.

Theorem 4.18

Let $\delta > 1$ and $\varphi : [0,\infty) \to [0,1]$ such that, for every sufficiently small $\varepsilon > 0$, there are $c, C > 0$ such that

$$cr^{-(\delta+\varepsilon)} \leq \varphi(r) \leq Cr^{-(\delta-\varepsilon)} \quad \text{for all } r \geq 1.$$

Furthermore, assume that the second moment of W exists and that it is almost surely bounded away from zero. Then, the reinforced age-dependent random connection model

- is **not ultrasmall** if $\gamma < \frac{\delta}{\delta+1}$ and
- is **ultrasmall** if $\gamma > \frac{\delta}{\delta+1}$ and, for $\mathbf{x},\mathbf{y} \in \mathbb{R}^d \times (0,1)$, we have

$$\mathrm{d}(\mathbf{x},\mathbf{y}) = (4+o(1))\frac{\log\log|x-y|}{\log\left(\frac{\gamma}{\delta(1-\gamma)}\right)} \tag{4.22}$$

under $\mathbb{P}_{\mathbf{x},\mathbf{y}}(\ \cdot\ \mid \mathbf{x}\leftrightarrow\mathbf{y})$ with high probability as $|x-y|\to\infty$.

Remark 4.5.1. To depict the influence of the weights on the degree distribution, we assign to each vertex $\mathbf{x}$ an independent on $(0,1)$ uniform distributed random variable $U_{\mathbf{x}}$ and for $\alpha,\eta > 0$ we set the weight of the vertex as $W_{\mathbf{x}} := \alpha U_{\mathbf{x}}^{-\eta}$. As the assigned uniform random variables are additional independent marks of the Poisson point process we can think of the model defined on a Poisson point

process of unit intensity on $\mathbb{R}^d \times (0,1) \times (0,1)$, where for a vertex $\mathbf{x} = (x,t,w)$ the first two entries are the same as in the age-dependent random connection model and the last entry w describes the uniform mark which defines the weight of the vertex. In this case, two vertices $\mathbf{x} = (x,t,w)$ and $\mathbf{y} = (y,s,v)$ form an edge independently with probability

$$\varphi\left(\tfrac{(wv)^{\eta/\delta}}{\beta}(t \wedge s)^{\gamma}(t \vee s)^{1-\gamma}\,|x-y|^d\right).$$

Thus, with the same arguments as in the proof of Proposition 4.5 the degree of a given vertex $\mathbf{x} = (x,t,w)$ is Poisson-distributed with parameter $\Lambda(t,w)$, where there exists $c, C > 0$ such that $cw^{-\eta/\delta}t^{-\gamma} \leq \Lambda(t,w) \leq Cw^{-\eta/\delta}t^{-\gamma}$ for all $t, w \in (0,1)$. An easy calculation similar to the proof of Lemma 4.13 shows that the degree distribution of the origin $(0,U,W)$ of the Palm-version is scale-free with power-law exponent $\tau = 1 + \frac{1}{\gamma}$ if $\eta/\delta < \gamma$ and otherwise with power-law exponent $\tau = 1 + \frac{\delta}{\eta}$ as in this case the weights contribute more to the connection probability than the marks of the vertices. Note that the second moment assumption on the weight distribution implies $\eta < \frac{1}{2}$. Hence, as the results in Theorem 4.18 are especially relevant for $\gamma > \frac{1}{2}$, the power-law exponent in this case does not differ from the age-dependent random connection model.

Note that examples presented in Section 4.2 can similarly be reinforced, and similar conclusions to the ones in this section can consequently be drawn.

4.6 Ellipses percolation

In [95] Teixeira and Ungaretti introduce a model on $\mathbb{R}^2$ as a collection of random ellipses centred on points of a Poisson process $\mathcal{X}$ on $\mathbb{R}^2 \times (0,1)$ with uniform marks t, from which the size of the major half-axis is derived as $t^{-\gamma/2}$ while its direction is sampled uniformly. The size of the minor half-axis is one. The random graph is then constructed by taking the Poisson process as the vertex set and forming edges given the collection of random ellipses between pairs of points of the point process if their ellipses intersect. Hilário and Ungaretti [62] show that, for $\gamma \in (1,2)$, the model is ultrasmall.

We introduce a soft version of this model, where for each pair of vertices $\mathbf{x}, \mathbf{y}$ we consider copies of their ellipses where the size of the major axes are multiplied

with independent, identically distributed positive heavy-tailed random variables $X = X(\mathbf{x}, \mathbf{y})$ with $\mathbb{P}(X > r) \sim r^{-2\delta}$ for some $\delta > 1$. An edge between $\mathbf{x}$ and $\mathbf{y}$ is then formed if the new ellipses intersect. Note that given $\mathcal{X}$ edges are not drawn independently of each other, as the neighbourhood of each vertex depends on the orientation of the ellipses. The results of Chapter 2 show that, for $\gamma \in [0, 1)$, the original model is never ultrasmall and the soft model is not ultrasmall if $\gamma < \frac{\delta}{\delta+1}$. We see that if an edge is formed between $\mathbf{x} = (x, t)$ and $\mathbf{y} = (y, s)$, this implies that balls around x and y with radii $X(\mathbf{x}, \mathbf{y})t^{-\gamma/2}$ and $X(\mathbf{x}, \mathbf{y})s^{-\gamma/2}$ intersect. Thus, there exists $\kappa > 0$ such that

$$\mathbb{P}_{\mathcal{X}}\{\mathbf{x} \sim \mathbf{y}\} \leq \mathbb{P}\big(X \geq \tfrac{|x-y|}{t^{-\gamma/2}+s^{-\gamma/2}}\big) \leq \kappa(t \wedge s)^{-\gamma\delta}(t \vee s)^{(\gamma-1)\delta} |x - y|^{-2\delta} .$$

Since the random variables $X(\mathbf{x}, \mathbf{y})$ are independent, Assumption UBA holds for $\gamma \in [0, 1)$ and $\delta > 1$ and the claimed result follows.

4.7 The weight-dependent random connection model

Gracar et al. have introduced a framework for geometric random graphs in [57] which include many but not all of the presented examples of this chapter. The weight-dependent random connection model is defined on a Poisson point process $\mathcal{X}$ of unit intensity on $\mathbb{R}^d \times (0, 1)$ and for a vertex $\mathbf{x} = (x, t)$ we denote by x the location of the vertex and by t its mark as done in Section 1.2.2. Given the vertex set, edges are drawn independently and between two vertices $\mathbf{x} = (x, t)$ and $\mathbf{y} = (y, s)$ an edge is formed with probability

$$\varphi(g(t, s) |x - y|^d),$$

where $\varphi : [0, \infty) \to [0, 1]$ is the *profile function* which is non-increasing, integrable and normalized such that

$$\int_{\mathbb{R}^d} \mathrm{d}x \, \varphi(|x|^d) = 1$$

and the *kernel function* $g : (0, 1) \times (0, 1) \to [0, \infty)$ is symmetric and non-decreasing in both arguments. Hence, preferences are given to connections between near vertices and vertices with small marks. However, a suitable choice

of the profile function enforces the occurence of long edges in the model, similar to the role of φ in the previous examples, see for example Section 4.1. The kernel function g on the other hand describes the influence of the marks on the connection probability. This function is defined in terms of $\gamma > [0, 1)$ and $\beta > 0$, where β controls the edge density and γ determines the strength of the influence especially of small marks on the connection probability. Special selections of this function lead to some of the examples introduced in the previous sections of this chapter.

- The *preferential attachment kernel*

$$g^{pa}(t, s) := \frac{1}{\beta}(t \wedge s)^{\gamma}(t \vee s)^{1-\gamma}$$

  leads directly to the age-dependent random connection model, see Section 4.1.

- We define the *sum kernel* as

$$g^{sum}(t, s) := \frac{1}{\beta}(t^{-\gamma/d} + s^{-\gamma/d})^{-d}.$$

  We can easily see that this leads to the soft Boolean model, see Section 4.2, when interpreting $(\beta t^{-\gamma})^{1/d}$, resp. $(\beta s^{-\gamma})^{1/d}$ as the random radii of the two vertices. The variant of the soft Boolean model given by the connection rule 4.18 can be obtained with the *min kernel* which is defined as

$$g^{min}(t, s) := \frac{1}{\beta}(t \wedge s)^{\gamma}.$$

- As already shown in Section 4.3, we obtain a continuum version of the scale-free percolation model of Deijfen et al. [33] when taking the *product kernel*

$$g^{prod}(t, s) := \frac{1}{\beta}t^{\gamma}s^{\gamma}.$$

- The final example is the *max kernel* defined as

$$g^{max}(t, s) := \frac{1}{\beta}(t \vee s)^{1+\gamma}$$

which leads to a continuum version of the ultra-small scale-free geometric networks of Yukich [99], see Section 4.4. For this kernel function any parameter $\gamma > 0$ is suitable.

As we have already seen in the previous sections all these potential choices for the kernel function lead to a geometric random graph which has a scale-free degree distribution with power-law exponent $\tau = 1 + \frac{1}{\gamma}$. In fact, this holds for arbitrary choices for the kernel function satisfying one integral assumption.

Proposition 4.19

Let $\gamma > 0$ and $g : (0,1) \times (0,1) \to [0,\infty)$ be a function for which there exists $c, C > 0$ such that $ct^{-\gamma} \leq \int_0^1 \mathrm{d}s \, \frac{1}{g(t,s)} \leq Ct^{-\gamma}$ for all $t \in (0,1)$. Then, the origin in the Palm-version of the weight-dependent connection model with kernel function g has a scale-free degree distribution with power-law exponent $\tau = 1 + \frac{1}{\gamma}$.

Proof. By the same arguments as in the proof of Proposition 4.5, the neighbourhood of a given vertex $\mathbf{x} = (x,t)$ forms a Poisson point process with intensity measure

$$\varphi(g(t,s)\,|x-y|^d)\mathrm{d}y\mathrm{d}s.$$

Thus, the degree of the vertex is Poisson distributed with parameter $\lambda(t)$ given by

$$\lambda(t) = \int_0^1 \mathrm{d}s \int_{\mathbb{R}^d} \mathrm{d}y \varphi(g(t,s)\,|x-y|^d) = I_\varphi \int_0^1 \mathrm{d}s \, \frac{1}{g(t,s)},$$

where $I_\varphi = \int_{\mathbb{R}^d} \mathrm{d}y \, \varphi(|y|^d)$. As the mark T_0 of the origin $(0,T_0)$ in the Palm version of the model is independent of the Poisson process, the degree of the origin follows a mixed Poisson-distribution μ which satisfies the condition in Lemma 4.13 and the weight-dependent random connection model is scale-free with power-law exponent $1 + \frac{1}{\gamma}$. □

It is easy to see that the weight-dependent random connection models with the preferential attachment kernel and the min kernel work as the boundary cases of geometric random graphs satisfying Assumption UBA* and Assumption LBA. In fact, the weight-dependent random connection model with a kernel g such that

$g \leq g^{pa}$ satisfies Assumption UBA* and the weight-dependent random connection model with a kernel g such that $g \geq g^{min}$ satisfies Assumption LBA. Hence, all results of Chapter 2 and Chapter 3 hold for the weight-dependent random connection model with any kernel g satisfying $g^{min} \leq g \leq g^{pa}$ in the same way as for the age-dependent random connection model and the soft Boolean model.

CHAPTER 5

Conclusion and further research possibilities

As we have seen in the last chapter there are various different examples of scale-free geometric random graphs which fit into the class discussed in this thesis. In each model the vertices are given by a Poisson point process in $\mathbb{R}^d \times (0,1)$, which determines their location in $\mathbb{R}^d$ together with one other property, for example their birth time in the age-dependent random connection model or the corresponding radius of their ball in the soft Boolean model. Given this Poisson point process, in most examples edges are drawn independently, as in the models included in the weight-dependent random connection model, but we also provided examples as the reinforced-age-dependent random connection model for which this is not the case.

For these geometric random graphs we have shown in Chapter 2 a novel behaviour in the occurence of short paths, as the absence and occurence of ultrasmallness does not solely depend on the parameter γ determining the power-law exponent of the scale-free degree distribution by $\tau = 1 + \frac{1}{\gamma}$. Instead, it depends also on the rate of decay of the connection probability of two vertices with typical marks when their Euclidean distance is large, determined by the parameter δ. This is remarkably different to well-known scale-free spatial models as scale-free

percolation or geometric inhomogeneous random graphs, for which the regime boundary depends only on the power-law exponent, or the ultrasmall scale-free geometric networks model, which is ultrasmall for any positive choice of γ. The universality of this novel behaviour is supported by the work by Gracar et al. [58] which investigates the existence of a subcritical percolation phase and reveals the same regime boundary depending on the parameters γ and δ. As seen in Chapter 2 the occurence of ultrasmallness in the geometric random graphs relies on the observation that a vertex with a small mark is typically connected to a vertex with even smaller mark via a connector, i.e. a vertex with mark near one. This argument can be repeated, such that there exists a path to vertices with arbitrarily small marks, with high probability. We have seen that this type of connection between two powerful vertices, i.e vertices with small mark, highly depends on their Euclidean distance as the connector only forms an edge to both powerful vertices with high probability if the influence of the Euclidean distance is small, i.e. if δ is small, or the neighbourhoods of the two powerful vertices are large, i.e. if γ is large. The major contribution of Chapter 2 has been to show the corresponding lower bounds on the chemical distance in the ultrasmall regime and a sharp criterion for the absence of ultrasmallness, especially under the condition that we do not assume edges to be drawn independently, given the Poisson point process. To establish sharp bounds for the probability of the existence of short paths between two given vertices, we have developed in Chapter 2 a classification of possible path structures appearing in the geometric random graphs by the means of coloured binary tree. They do not only capture the influence of the marks on the existence of such paths but also the subtle influence of the spatial embedding in terms of δ.

The effects of such short paths on the spread of infection has been studied in Chapter 3, where it is shown that in the ultrasmall regime the geometric random graphs are so well connected, that the contact process with any positive infection rate does not go extinct with positive probability. This strong behaviour of the contact process is underlined by the shown result that, on a finite restriction of the geometric random graphs, the extinction time of the contact process is of exponential order in the size of the graph, again not depending on the choice of the infection rate. Both results rely on the local survival of the contact process on the neighbourhood of powerful vertices, i.e. vertices with small marks, on which

the contact process survives so long that the process can be transmitted to the distinct neighbourhood of an other vertex with small mark. Thus, the short paths between powerful vertices which lead to the occurence of ultrasmallness turn out to also be crucial for the survival of the infection.

We conclude this thesis by addressing various open problems and further research possibilities which are related to the work of the author presented in this thesis.

Chemical distance in the non-ultrasmall regime In this thesis we provide in Proposition 2.10 a lower bound on the chemical distance of two spatially distant vertices in the non-ultrasmall regime. What remains to show is a suitable upper bound indicating for which choice of $\gamma \in [0, 1)$ and $\delta > 1$ the geometric random graphs exhibit small-world behaviour. We do not expect our stated lower bound to be sharp, as it can easily be improved for the soft Boolean model to a lower bound of logarithmic order in the Euclidean distance of the two vertices. Instead we might expect the existence of a polylogarithmic regime, as apparent in scale-free percolation, see [33] and [61]. The methods presented in Chapter 2 do not seem to be suitable to show such type of lower bounds as they were designed to exhibit a sharp distinction between the occurence and absence of ultrasmallness. In [13] Biskup introduces a hierarchic classification of the vertices which leads to polylogarithmic behaviour of the chemical distance in long-range percolation which has been adapted by Hao and Heydenreich [61] to scale-free percolation. It would be interesting to see whether with this type of argument one can establish polylogarithmic upper and lower bound for a suitable choice of γ and δ in the discussed class of geometric random graphs.

Survival of the contact process in the non-ultrasmall regime Similar to the sharp upper and lower bounds for the chemical distance, the behaviour of the contact process on geometric random graphs in the non-ultrasmall regime remains an open problem. For the configuration model it has been shown in [87] that for any power-law exponent $\tau > 2$ the contact process with any given positive infection rate λ does not go extinct with positive probability and for non-spatial preferential attachment type models a metastable behaviour with metastable density of order $\lambda^{2\tau-3+o(1)}$ has been identified for any $\tau > 2$ in [68]. As seen in Chapter 2 the spatial dependence of the connection probabilities

reduces the possibility of short paths between powerful vertices which remain crucial for the survival of the infection. Thus, it would be interesting to see whether the discussed geometric random graphs exhibit a regime in which the contact process goes extinct almost surely.

Algorithmic small-world phenomenon in the age-dependent random connection model In [22] an algorithmic view of the small-world phenomenon on the model of geometric inhomogeneous random graphs is studied. In this work, Milgram's experiment described in the beginning of this thesis is modelled by a decentralized greedy routing protocol, which sends a message from a starting vertex to a target vertex. Given these two vertices, in each step of greedy routing the message is sent from the current vertex to the neighbour which has the highest connection probability with the target vertex. Bringmann et al. show that by greedy routing the message is sent to the target person with positive probability and in case of success the length of the resulting path is of the same order as the length of the shortest path between the two vertices. Thus, greedy routing provides an algorithmic way to find a shortest path between two given vertices. An interesting question would be the application of greedy routing in the age-dependent random connection model or the soft Boolean model. As discussed in Section 2.1 the typical structure of a short path differs to the one in geometric inhomogeneous random graphs as two powerful vertices are typically not connected directly but via a connector. This leads to the question whether this protocol works in the same way for the age-dependent random connection model as it does for geometric inhomogeneous random graphs or if the difference in the structure of short paths in this models is so large that the greedy routing protocol needs to be adapted to it.

Contact process with hibernation As the contact process survives well for different scale-free random graphs models it might be interesting to study a variant of the process in which the vertices gain the ability to defend themselves from the infection. We propose a variant of the contact process in which each healthy vertex has the ability to *hibernate* depending on the spread of the infection in its neighbourhood, thus preventing itself from being infected. Precisely, a healthy vertex hibernates at rate proportional to the proportion of its infected neighbours, which we can understand in the friendship network as self-isolation of a

person if sufficiently many of its friends are infected. After some time, a hibernating vertex wakes up and can become infected like before. To implement this to the contact process, we add the following dynamics to the process, determined by the *hibernation rate* $\rho > 0$ and the *wake-up rate* $w > 0$. An infected vertex lets a neighbouring vertex hibernate at rate $\rho/\deg$, independently of everything else, where deg is the degree of the neighbouring vertex, and a hibernating vertex wakes up at rate w.

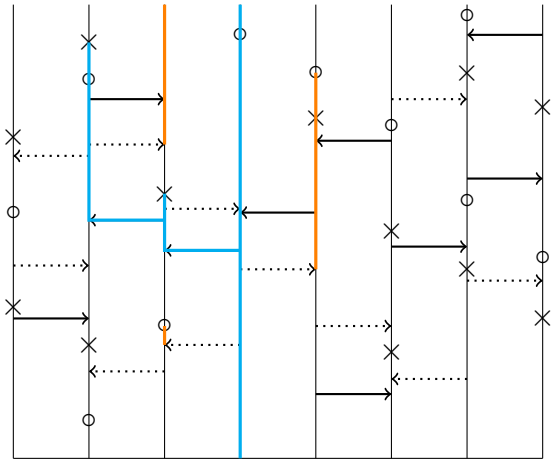

Figure 5.1: Sketch of a contact process with hibernation on $\mathbb{Z}$, where hibernation arrows and wake-up marks are added to the given representation of the contact process in Figure 3.1. The wake-up marks $\circ$ are given for each vertex by an independent Poisson process with rate θ and the dotted arrows indicate the hibernation of a vertex due to an infected neighbour. For each ordered pair of neighbours the dotted arrows are given by an independent Poisson process with rate $\rho/2$. The blue paths indicate the contact process with initial condition on the fourth vertex, whereas the orange parts show phases of hibernation induced by neighbouring infected vertices.

This variant is still a Markov process and can still be studied with the help of a graphical representation. However, due to the hibernation mechanism the variant loses crucial properties such as additivity and monotonicity in the initial configuration, as we can see in Figure 5.1, which makes the study of the model itself interesting.

CHAPTER 6

Acknowledgement

First of all, I would like to thank Prof. Dr. Peter Mörters for his excellent supervision over the past few years. From the many fruitful discussions, over his intuition about what is and is not possible, to his advice and approach to problem solving as well as his trust in his PhD students, all contributed greatly to the results of this thesis.

I am grateful to have been part of his research group that has been built up in Cologne over the last several years. In particular, I would like to thank my co-authors Prof. Dr. Peter Mörters, Peter Gracar and Lukas Lüchrath for their collaboration and the great time together, which has led to many results in this thesis. I will miss our joint discussions.

Special thanks go to my colleagues at the University for my very pleasant time in Cologne. In particular, Alexis Prévost, Lars Schmitz, Leonie Brinker, Katharina Bata, Céline Kerriou, Marylin Düsterbeck and Gioele Gallo.

I would also like to thank Prof. Dr. Alexander Drewitz for being a great personal mentor. Additionally, I am very grateful to Prof. Dr. Steffen Dereich for agreeing to read this thesis and taking on the role of examiner.

The unconditional support and encouragement received from my family has been invaluable. I would like to thank my parents and my brothers for all the energy and time they have given me. Special thanks to my brother Jens for his helpful physicists perspective on my work.

Finally, my thanks go to Sol. Without her loving support, tireless patience, and her motivation and encouragement when I needed it most this thesis would not have been possible.

APPENDIX A

Appendix

A.1 Application of the truncated first moment bound for other geometric random graphs

As mentioned in Section 2.3.1, we will give in the following an application of the truncated first moment bound method to geometric random graphs, which are not in the class of geometric random graphs discussed in this thesis but satisfy alternative upper bound assumptions on their connection probabilities. By this assumptions we will prove asymptotic lower bounds on the chemical distance as well as sharp criteria when the corresponding geometric random graphs are not ultrasmall. These proofs are much simpler than the one given in Chapter 2, as no subtle influence of the spatial embedding occurs.

Assumption: The product-kernel

Let $\mathscr{G}$ be a graph with vertex set given by a Poisson process on unit intensity on $\mathbb{R}^d \times (0,1)$ as described in Section 2.2.1 and let $\delta > 1$ and $0 \leq \gamma < 1$ be the parameter of the following assumption.

Assumption A.1

There exists $\kappa > 0$ such that, for every finite set of pairs of vertices $I \subset \mathcal{X}^2$ in which each vertex appears at most twice, we have

$$\mathbb{P}_{\mathcal{X}}\Big(\bigcap_{(\mathbf{x}_i,\mathbf{y}_i)\in I} \{\mathbf{x}_i \sim \mathbf{y}_i\}\Big) \leq \prod_{(\mathbf{x}_i,\mathbf{y}_i)\in I} \kappa\, t_i^{-\gamma\delta} s_i^{-\gamma\delta} |x_i - y_i|^{-\delta d}$$

where $\mathbf{x}_i = (x_i, t_i)$, $\mathbf{y}_i = (y_i, s_i)$.

Contrary to Assumption UBA, for each pair of vertices, the influence of the marks of both vertices in Assumption A.1 is given by their product to the same power $-\gamma\delta$. Thus, this assumption corresponds to geometrically embedded graphs where each vertex has a random weight and the connection probability between two vertices depends on the product of those weights and their Euclidean distance. As mentioned in Section 2.1 one major example of this is the *scale-free percolation model*, which is discussed in Section 4.3. This assumption leads to the following lower bounds on chemical distances in the graph.

Theorem A.1

Let $\mathscr{G}$ be a general geometric random graph which satisfies Assumption A.1 for some $\gamma \in [0, 1)$ and $\delta > 1$.

(a) If $\gamma < \frac{1}{2}$, then $\mathscr{G}$ is **not ultrasmall**, i.e. for $\mathbf{x}, \mathbf{y} \in \mathbb{R}^d \times (0, 1)$, under $\mathbb{P}_{\mathbf{x},\mathbf{y}}$, the distance $\mathrm{d}(\mathbf{x}, \mathbf{y})$ is of larger order than $\log\log|x - y|$ with high probability as $|x - y| \to \infty$.

(b) If $\gamma > \frac{1}{2}$, then for $\mathbf{x}, \mathbf{y} \in \mathbb{R}^d \times (0, 1)$, under $\mathbb{P}_{\mathbf{x},\mathbf{y}}$, we have

$$\mathrm{d}(\mathbf{x}, \mathbf{y}) \geq (2 + o(1)) \frac{\log\log|x - y|}{\log\left(\frac{\gamma}{1-\gamma}\right)}$$

with high probability as $|x - y| \to \infty$.

Proof. First, let $\gamma < \frac{1}{2}$. As discussed beforehand truncation of the marks in a path between the vertices $\mathbf{x}$ and $\mathbf{y}$ is not necessary in this case. As done in the beginning of Section 2.3.1 we get by using Mecke's equation and Assumption A.1

that

$$\mathbb{P}_{\mathbf{x},\mathbf{y}}\{\mathrm{d}(\mathbf{x},\mathbf{y}) \le 2\Delta\} \le \sum_{n=1}^{2\Delta} \int_{(\mathbb{R}^d\times(0,1))^{n-1}} \bigotimes_{i=1}^{n-1} \mathrm{d}(x_i,t_i) \prod_{j=0}^{n-1} 1 \wedge \kappa t_j^{-\gamma\delta} t_{j+1}^{-\gamma\delta} \left|x_j - x_{j+1}\right|^{-\delta d},$$

where $\mathbf{x} = (x_0, t_0)$ and $\mathbf{y} = (x_n, t_n)$. With similar arguments as in the proof of Lemma 2.8, for given vertices $\mathbf{x}$ and $\mathbf{y}$, there exists constants $a > 0$ and $\tilde{\kappa} > 0$, which do not depend on $|x - y|$ when it is large enough, such that for $n = O(\log|x - y|)$, we have

$$\int_{(\mathbb{R}^d)^{n-1}} \bigotimes_{i=1}^{n-1} \mathrm{d}x_i \prod_{j=0}^{n-1} 1 \wedge \kappa t_j^{-\gamma\delta} t_{j+1}^{-\gamma\delta} \left|x_j - x_{j+1}\right|^{-\delta d} \le |x-y|^{-a} \prod_{j=0}^{n-1} \tilde{\kappa} t_j^{-\gamma} t_{j+1}^{-\gamma}. \quad \text{(A.1)}$$

Thus (A.1) and Fubini's Lemma yield

$$\begin{aligned}\mathbb{P}_{\mathbf{x},\mathbf{y}}\{\mathrm{d}(\mathbf{x},\mathbf{y}) \le 2\Delta\} &\le |x-y|^{-a} \sum_{n=1}^{\Delta} \int_{(0,1)^{n-1}} \bigotimes_{i=1}^{n-1} \mathrm{d}t_i \prod_{j=0}^{n-1} \tilde{\kappa} t_j^{-\gamma} t_{j+1}^{-\gamma} \\ &\le |x-y|^{-a} \sum_{n=1}^{2\Delta} t_0^{-\gamma} t_n^{-\gamma} \left(\tfrac{1}{1-2\gamma}\right)^{n-1}\end{aligned}$$

As the marks of $\mathbf{x}$ and $\mathbf{y}$ are fixed, there exists constant $c, C > 0$ such that

$$\mathbb{P}_{\mathbf{x},\mathbf{y}}\{\mathrm{d}(\mathbf{x},\mathbf{y}) \le \Delta\} \le |x-y|^{-a} \sum_{n=1}^{\Delta} C^n \le |x-y|^{-a}\, cC^{\Delta}.$$

Choose $0 < b < a$, then for $\Delta \le \frac{b\log|x-y|}{\log C}$, it holds

$$\mathbb{P}_{\mathbf{x},\mathbf{y}}\{\mathrm{d}(\mathbf{x},\mathbf{y}) \le \Delta\} \le c\,|x-y|^{b-a} = o(1)$$

as $|x - y| \to \infty$. Thus, for $\gamma < \frac{1}{2}$, the chemical distance is with high probability at least of logarithmic order in $|x - y|$ as the Euclidean distance tends to infinity.

For $\gamma > \frac{1}{2}$, we will use a truncation of the marks leading to inequality (TMB). First, we establish an upper bound for $\mathbb{P}_{\mathbf{x}}(A_n^{(\mathbf{x})})$ for a given vertex $\mathbf{x}$. Denote by $N(\mathbf{x}, \mathbf{y}, n)$ the number of paths from $\mathbf{x}$ to $\mathbf{y}$ where the vertices of the path fulfill

$t_i \geq \ell_i$ for all $i = 0, \dots, n-1$. By Mecke's equation we have

$$\mathbb{P}_{\mathbf{x}}(A_n^{(\mathbf{x})}) \leq \int_{\mathbb{R}^d \times (0,\ell_n]} \mathrm{d}\mathbf{y} \mathbb{E}_{\mathbf{x},\mathbf{y}} N(\mathbf{x}, \mathbf{y}, n).$$

By Assumption A.1 and Mecke's equation the expected number of such paths is bounded by

$$\int_{\mathbb{R}^d \times (\ell_1,1]} \mathrm{d}\mathbf{x}_1 \dots \int_{\mathbb{R}^d \times (\ell_{n-1},1]} \mathrm{d}\mathbf{x}_{n-1} \rho(\kappa^{-1/\delta} t_i^{\gamma} t_{i+1}^{\gamma} |x_i - x_{i+1}|^d)$$

where $\rho(x) := 1 \wedge x^{-\delta}$ and $\mathbf{x} = (x_0, t_0)$, $\mathbf{y} = (x_n, t_n)$. We set $I_\rho := \int_{\mathbb{R}^d} \mathrm{d}x \rho(\kappa^{-1/\delta} |x|^d)$. Then, integrating over the locations of the vertices yields that

$$\mathbb{P}_{\mathbf{x}}(A_n^{(\mathbf{x})}) \leq I_\rho^n \int_{\ell_1}^1 \mathrm{d}t_1 \dots \int_{\ell_{n-1}}^1 \mathrm{d}t_{n-1} \int_0^{\ell_n} \mathrm{d}t_n t_0^{-\gamma} t_n^{-\gamma} \prod_{j=1}^{n-1} t_j^{-2\gamma}.$$

To find a sharp bound of the right-hand side, we define

$$\mu_n^{\mathbf{x}}(s) = K^n \int_{\ell_1}^1 \mathrm{d}t_1 \dots \int_{\ell_{n-1}}^1 \mathrm{d}t_{n-1} t_0^{-\gamma} s^{-\gamma} \prod_{j=1}^{n-1} t_j^{-2\gamma} \quad \text{for } s \in (0,1),$$

where $K > 0$ is a constant. This is a simpler version of the definition given in (2.25) in the proof of the main results of Chapter 2. Then, it holds $\mathbb{P}_{\mathbf{x}}(A_n^{(\mathbf{x})}) \leq \int_0^{\ell_n} \mathrm{d}s \mu_n^{\mathbf{x}}(s)$, when we choose K sufficiently large. Note that $\mu_n^{\mathbf{x}}(s)$ has a recursive structure given by

$$\mu_n^{\mathbf{x}}(s) = K \int_{\ell_{n-1}}^1 \mathrm{d}t_{n-1} s^{-\gamma} t_{n-1}^{-\gamma} \mu_{n-1}^{\mathbf{x}}(t_{n-1}) \quad \text{for } n \geq 2.$$

This leads to the following upper bound for $\mu_n^{\mathbf{x}}$. Let $(\ell_k)_{k \in \mathbb{N}_0}$ be the yet to be fixed truncation sequence such that $\ell_0 < t$. Then there exists a constant $c > 0$ such that, for $n \in \mathbb{N}$ and a given vertex $\mathbf{x}$, it holds

$$\mu_n^{\mathbf{x}}(s) \leq C_n s^{-\gamma} \quad \text{for } s \in (0,1), \tag{A.2}$$

where $C_{n+1} = c\ell_n^{1-2\gamma} C_n$ and $C_1 = c\ell_0^{-\gamma}$ (see Lemma 2.7 for the corresponding bound in the proof of the main results of Chapter 2). In fact, it holds $\mu_1^{\mathbf{x}}(s) =$

$Kt_0^{-\gamma}s^{-\gamma} \leq c\ell_0^{-\gamma}s^{-\gamma}$, when $c \geq K$. And for $n \geq 2$, we have

$$\begin{aligned}\mu_n^{\mathbf{x}}(s) &= K\int_{\ell_{n-1}}^1 \mathrm{d}t_{n-1}s^{-\gamma}t_{n-1}^{-\gamma}\mu_{n-1}^{\mathbf{x}}(t_{n-1}) \\ &\leq KC_{n-1}s^{-\gamma}\int_{\ell_{n-1}}^1 \mathrm{d}t_{n-1}t_{n-1}^{-2\gamma} \leq cC_{n-1}\ell_n^{1-2\gamma}s^{-\gamma} = C_n s^{-\gamma}.\end{aligned}$$

By inequality (A.2) it holds $\mathbb{P}_{\mathbf{x}}(A_n^{(\mathbf{x})}) \leq \frac{C_n}{1-\gamma}\ell_n^{1-\gamma}$.

Now, we can choose the truncation sequence $(\ell_k)_{k\in\mathbb{N}_0}$ such that the first two summands of (TMB) can be kept sufficiently small. For $\varepsilon > 0$, we choose the truncation sequence with $\ell_0 < t$ such that $\frac{C_n\ell_n^{1-\gamma}}{1-\gamma} = \frac{\varepsilon}{\pi^2 n^2}$. Thus, by this choice we have $\sum_{n=1}^{\Delta}\mathbb{P}_{\mathbf{x}}(A_n^{(\mathbf{x})}) \leq \frac{\varepsilon}{6}$. Note that, for $n \in \mathbb{N}$, it holds with $\eta_n := \ell_n^{-1}$ that

$$\eta_{n+1}^{1-\gamma} = \frac{\pi^2(n+1)^2}{\varepsilon(1-\gamma)}C_{n+1} = \frac{\pi^2(n+1)^2}{\varepsilon(1-\gamma)}cC_n\eta_n^{2\gamma-1} = \big(\tfrac{n+1}{n}\big)^2 c\eta_n^{\gamma} \tag{A.3}$$

and $\eta_1^{1-\gamma} = \frac{c\pi^2}{\varepsilon(1-\gamma)}\eta_0^{\gamma}$. Thus, there exists constants $b, B > 0$ such that

$$\eta_n \leq b\exp\big(B\big(\frac{\gamma}{1-\gamma}\big)^n\big). \tag{A.4}$$

In fact, there exists a constant $c > 0$ such that by using (A.3) repeatedly, it holds

$$\eta_n \leq c\eta_{n-1}^{\frac{\gamma}{1-\gamma}} \leq \big(c^{\sum_{i=1}^n(\frac{1-\gamma}{\gamma})^i}\eta_0\big)^{(\frac{\gamma}{1-\gamma})^n}.$$

Since $\gamma > \frac{1}{2}$, the row $\sum_{i=1}^{\infty}(\frac{1-\gamma}{\gamma})^i$ converges and there exists a new constant $c > 0$ such that $\eta_n \leq (c\eta_0)^{(\frac{\gamma}{1-\gamma})^n}$. Choosing $B > \log(c\eta_0)$ completes the proof of inequality (A.4).

Proceeding with a probability bound for the occurence of good paths between two vertices $\mathbf{x}$ and $\mathbf{y}$, by Mecke's equation and (A.1), it holds

$$\begin{aligned}&\mathbb{P}_{\mathbf{x},\mathbf{y}}(B_n^{(\mathbf{x},\mathbf{y})}) \\ &\leq \int_{\mathbb{R}^d\times(\ell_1,1]}\mathrm{d}\mathbf{x}_1\cdots\int_{\mathbb{R}^d\times(\ell_{\lfloor\frac{n}{2}\rfloor},1]}\mathrm{d}\mathbf{x}_{\lfloor\frac{n}{2}\rfloor}\cdots\int_{\mathbb{R}^d\times(\ell_1,1]}\mathrm{d}\mathbf{x}_{n-1}\prod_{j=0}^{n-1}1\wedge\kappa t_j^{-\gamma\delta}t_{j+1}^{-\gamma\delta}\,|x_j - x_{j+1}|^{-\delta d} \\ &\leq |x-y|^{-a}\int_{\ell_1}^1\mathrm{d}t_1\cdots\int_{\ell_{\lfloor\frac{n}{2}\rfloor}}^1\mathrm{d}t_{\lfloor\frac{n}{2}\rfloor}\cdots\int_{\ell_1}^1\mathrm{d}t_{n-1}\tilde{\kappa}^n\prod_{j=0}^{n-1}t_j^{-\gamma}t_{j+1}^{-\gamma},\end{aligned}$$

where $\mathbf{x}_j = (x_j, t_j)$ and $\mathbf{x} = (x_0, t_0)$, $\mathbf{y} = (x_n, t_n)$. Thus, choosing the constant K in the definition of $\mu_n^{\mathbf{x}}$ sufficiently large, it holds that

$$\mathbb{P}_{\mathbf{x},\mathbf{y}}(B_n^{(\mathbf{x},\mathbf{y})}) \leq |x-y|^{-a} \int_{\ell_{\lfloor \frac{n}{2} \rfloor}}^1 \mathrm{d}s \mu^{\mathbf{x}}_{\lfloor \frac{n}{2} \rfloor}(s) \mu^{\mathbf{y}}_{n-\lfloor \frac{n}{2} \rfloor}(s).$$

Then by the estimates (A.2) and (A.4) it follows that

$$\begin{aligned}\sum_{n=1}^{2\Delta} \mathbb{P}_{\mathbf{x},\mathbf{y}}(B_n^{(\mathbf{x},\mathbf{y})}) &\leq |x-y|^{-a} \sum_{n=1}^{\Delta} \int_{\ell_n}^1 \mathrm{d}s C_n^2 s^{-2\gamma} \leq |x-y|^{-a} \frac{\Delta}{2\gamma - 1} C_\Delta^2 \ell_\Delta^{1-2\gamma} \\ &\leq |x-y|^{-a} \frac{1}{\Delta^3} \eta_\Delta \leq \frac{b}{\Delta^3} \exp\big(B\big(\frac{\gamma}{1-\gamma}\big)^n\big).\end{aligned}$$

Choosing $\Delta \leq \frac{\log\log|x-y|}{\log \frac{\gamma}{1-\gamma}} - D$, where $D > 0$ such that $B\big(\frac{\gamma}{1-\gamma}\big)^{-D} < a$, yields

$$\sum_{n=1}^{2\Delta} \mathbb{P}_{\mathbf{x},\mathbf{y}}(B_n^{(\mathbf{x},\mathbf{y})}) = o(\log\log|x-y|^{-3})$$

which by using (TMB) completes the proof of Theorem A.1. □

Assumption: The weak-kernel

As before, let $\mathscr{G}$ be a graph with vertex set given by a Poisson process on unit intensity on $\mathbb{R}^d \times (0,1)$ as described in Section 2.2.1. Let $\gamma > 0$ be the parameter of the following assumption.

Assumption A.2

There exists $\kappa > 0$ such that, for every set of pairs of vertices $I \subset \mathcal{X}^2$, we have

$$\mathbb{P}_{\mathcal{X}}\Big(\bigcap_{(\mathbf{x}_i,\mathbf{y}_i)\in I} \{\mathbf{x}_i \sim \mathbf{y}_i\}\Big) \leq \prod_{(\mathbf{x}_i,\mathbf{y}_i)\in I} \mathbf{1}\{|x_i - y_i|^d \leq \kappa (t_i \vee s_i)^{-(1+\gamma)}\}$$

where $\mathbf{x}_i = (x_i, t_i)$, $\mathbf{y}_i = (y_i, s_i)$.

By this assumption, for each pair of vertices only the mark of the weaker one, i.e. the larger mark, influences the right-hand side. This is contrary to the

examples which satisfy Assumption UBA, where the more powerful vertex with the smaller mark has more influence on the connection probability. In fact, the dependence on the weaker vertex is more restrictive than the previously stated assumptions. This restrictive dependence on the marks of the vertices is compensated by taking the marks to a much larger negative power than in Assumption UBA and Assumption A.1 such that ultrasmallness can still occur in examples satisfying Assumption A.2. The main example is a continuous version of *ultra-small scale-free geometric networks* which is further discussed in Section 4.4.

Theorem A.2

Let $\mathscr{G}$ be a general geometric random graph which satisfies Assumption A.2 for some $\gamma > 0$, then for $\mathbf{x}, \mathbf{y} \in \mathbb{R}^d \times (0,1)$, under $\mathbb{P}_{\mathbf{x},\mathbf{y}}$, we have

$$\mathrm{d}(\mathbf{x}, \mathbf{y}) \geq (2 + o(1)) \frac{\log\log|x - y|}{\log(1+\gamma)}$$

with high probability as $|x - y| \to \infty$.

Proof. Again, we use the classification of good and bad paths by a truncation sequence $(\ell_k)_{k\in\mathbb{N}_0}$ which leads to (TMB). First we consider the occurence of bad paths starting in $\mathbf{x}$, resp. $\mathbf{y}$. Let $I_{\tilde{\rho}} := \int_{\mathbb{R}^d} \mathrm{d}x \mathbf{1}\{|x|^d \leq \kappa\}$. Then, it holds by Mecke's equation and Assumption A.2

$$\begin{aligned}
\mathbb{P}_x(A_n^{\mathbf{x}}) &\leq \int_{\mathbb{R}^d\times(\ell_1,1]} \mathrm{d}\mathbf{x}_1 \ldots \int_{\mathbb{R}^d\times(\ell_{n-1},1]} \mathrm{d}\mathbf{x}_{n-1} \int_{\mathbb{R}^d\times(0,\ell_n]} \mathrm{d}\mathbf{x}_n \\
&\qquad \prod_{i=0}^{n-1} \mathbf{1}\{|x_i - x_{i+1}|^d \leq \kappa (t_i \vee t_{i+1})^{-(1+\gamma)}\} \\
&\leq (I_{\tilde{\rho}})^n \int_{\ell_1}^1 \mathrm{d}t_1 \ldots \int_{\ell_{n-1}}^1 \mathrm{d}t_{n-1} \int_0^{\ell_n} \mathrm{d}t_n \prod_{i=0}^{n-1} (t_i \vee t_{i+1})^{-(1+\gamma)} \\
&\leq (I_{\tilde{\rho}})^n \int_{\ell_1}^1 \mathrm{d}t_1 \ldots \int_{\ell_{n-1}}^1 \mathrm{d}t_{n-1} \int_0^{\ell_n} \mathrm{d}t_n \prod_{i=0}^{n-1} t_i^{-(1+\gamma)} \\
&\leq c^n \ell_0^{-(1+\gamma)} \ell_n \prod_{i=1}^{n-1} \ell_i^{-\gamma}
\end{aligned}$$

for $c > 0$ sufficiently large. We choose the truncation sequence such that it holds $c^n \ell_0^{-(1+\gamma)} \ell_n \prod_{i=1}^{n-1} \ell_i^{-\gamma} = \frac{\varepsilon}{\pi^2 n^2}$ for all $n \in \mathbb{N}$. Similar to the proof of Theorem A.1 we have as a direct consequence that $\sum_{n=1}^{\Delta} \mathbb{P}_{\mathbf{x}}(A_n^{(\mathbf{x})}) \leq \frac{\varepsilon}{6}$. Letting $\eta_n := \ell_n^{-1}$ for $n \in \mathbb{N}$ we see that the given definition of the truncation sequence implies $\eta_1 = \frac{c\pi^2}{\varepsilon} \eta_0^{1+\gamma}$ and

$$\eta_{n+1} = \frac{\pi(n+1)^2}{\varepsilon} c \eta_n^{1+\gamma} \big(c^n \eta_0^{1+\gamma} \eta_n^{-1} \prod_{i=1}^{n-1} \eta_i^{\gamma} \big) = \big(\tfrac{n+1}{n} \big)^2 c \eta_n^{1+\gamma}.$$

Thus, by similar arguments as used in the proof of Theorem A.1, there exist constants $b, B > 0$ such that $\eta_n \leq b \exp\big(B(1+\gamma)^n\big)$ for $n \in \mathbb{N}$.

Considering the good paths between the given vertices $\mathbf{x}$ and $\mathbf{y}$, note that by definition, vertices of a good path between $\mathbf{x}$ and $\mathbf{y}$ with length at most 2Δ must have marks larger than ℓ_Δ. Thus by Assumption A.2, the longest edge of such a good path must be shorter than $(\kappa \eta_\Delta^{1+\gamma})^{1/d}$. Choosing $\Delta \leq \frac{\log\log|x-y|}{\log(1+\gamma)} - D$, where $D > 0$ such that $(1+\gamma)^{1-D}\big(B + \log(\kappa b^{1+\gamma})\big) < d(1-\xi)$ for some $\xi > 0$, then yields that the edges of a good path of length at most 2Δ between $\mathbf{x}$ and $\mathbf{y}$ must be shorter than $|x-y|^{1-\xi}$. But a path between $\mathbf{x}$ and $\mathbf{y}$ of that length must have at least one edge of length larger than $\frac{|x-y|}{\log|x-y|}$ since 2Δ is of smaller order than $\log|x-y|$. Hence, for $|x-y|$ large enough there cannot exist a good path between $\mathbf{x}$ and $\mathbf{y}$ and it holds $\sum_{n=1}^{2\Delta} \mathbb{P}_{\mathbf{x},\mathbf{y}}(B_n^{(\mathbf{x},\mathbf{y})}) = 0$ for the given choice of Δ and $|x-y|$ sufficiently large. □

A.2 Further calculations for the ultrasmall regime used in Section 2.3

Lemma A.3

Let $x, y \in \mathbb{R}^d$, $t, s \in (0,1)$ and $\ell > 0$ with $\ell < t \vee s$. For $\gamma > \frac{\delta}{\delta+1}$,

$$\int_{t\vee s}^{1} \mathrm{d}u \int_{\mathbb{R}^d} \mathrm{d}z \rho\big(\kappa^{-1/\delta} t^{\gamma} u^{\gamma/\delta} |x-z|^d\big) \rho\big(\kappa^{-1/\delta} s^{\gamma} u^{\gamma/\delta} |y-z|^d\big) \leq \tilde{c} \ell^{1-\gamma-\gamma/\delta} \kappa (t\wedge s)^{-\gamma\delta} (t\vee s)^{-\gamma} |x-y|^{-d\delta},$$

where $\tilde{c} = \frac{2^{d\delta+1} I_\rho}{(\gamma+\gamma/\delta-1)} \vee 1$.

Proof. Assume $t < s$, then we have

$$\begin{aligned}
&\int_{s}^{1} \mathrm{d}u \int_{\mathbb{R}^d} \mathrm{d}z \rho\big(\kappa^{-1/\delta} t^{\gamma} u^{\gamma/\delta} |x-z|^d\big) \rho\big(\kappa^{-1/\delta} s^{\gamma} u^{\gamma/\delta} |y-z|^d\big) \\
&\quad \leq \int_{\ell}^{1} \mathrm{d}u\, \rho\big(2^{-d} \kappa^{-1/\delta} t^{\gamma} u^{\gamma/\delta} |x-y|^d\big) \int_{\mathbb{R}^d} \mathrm{d}z\, \rho\big(\kappa^{-1/\delta} s^{\gamma} u^{\gamma/\delta} |y-z|^d\big) \\
&\qquad + \int_{\ell}^{1} \mathrm{d}u\, \rho\big(2^{-d} \kappa^{-1/\delta} s^{\gamma} u^{\gamma/\delta} |x-y|^d\big) \int_{\mathbb{R}^d} \mathrm{d}z\, \rho\big(\kappa^{-1/\delta} t^{\gamma} u^{\gamma/\delta} |x-z|^d\big) \\
&\quad \leq I_\rho 2^{d\delta} \kappa \Big[t^{-\gamma\delta} s^{-\gamma} |x-y|^{-d\delta} \int_{\ell}^{1} \mathrm{d}u\, u^{-\gamma-\gamma/\delta} + t^{-\gamma} s^{-\gamma\delta} |x-y|^{-d\delta} \int_{\ell}^{1} \mathrm{d}u\, u^{-\gamma-\gamma/\delta} \Big] \\
&\quad \leq \tfrac{I_\rho 2^{d\delta}}{\gamma+\gamma/\delta-1} \kappa \ell^{1-\gamma-\gamma/\delta} \Big[t^{-\gamma\delta} s^{-\gamma} |x-y|^{-d\delta} + s^{-\gamma\delta} t^{-\gamma} |x-y|^{-d\delta} \Big] \\
&\quad \leq \tfrac{I_\rho 2^{d\delta+1}}{\gamma+\gamma/\delta-1} \kappa \ell^{1-\gamma-\gamma/\delta} t^{-\gamma\delta} s^{-\gamma} |x-y|^{-d\delta},
\end{aligned}$$

where we used for the first inequality that, for $z \in \mathbb{R}^d$, either $|x-z|$ or $|y-z|$ is larger than $\frac{|x-y|}{2}$ and for the third inequality that $\gamma > \frac{\delta}{\delta+1}$ implies $\gamma + \gamma/\delta - 1 > 0$. □

Lemma A.4

Let $x, y \in \mathbb{R}^d$, $t, s \in (0,1)$ and $\frac{1}{e} > \ell > 0$ with $\ell < t \vee s$. For $\gamma > \frac{\delta}{\delta+1}$,

$$\int_{t\vee s}^{1} \mathrm{d}u \int_{\mathbb{R}^d} \mathrm{d}z\, \rho(\kappa^{-1/\delta} t^{\gamma} u^{\gamma/\delta} |x-z|^d) \rho(\kappa^{-1/\delta} s^{\gamma} u^{1-\gamma} |y-z|^d) \leq \tilde{c} \log(\ell^{-1}) \kappa (t \wedge s)^{-\gamma\delta} (t \vee s)^{-\gamma} |x-y|^{-d\delta},$$

where $\tilde{c} = \frac{I_\rho 2^{d\delta+1}}{(\delta-1)(\gamma+\gamma/\delta-1)\wedge 1}$.

Proof. Since, for $z \in \mathbb{R}^d$, either $|x-z|$ or $|y-z|$ is larger than $\frac{|x-y|}{2}$, we have

$$\begin{aligned}
&\int_{t\vee s}^{1} \mathrm{d}u \int_{\mathbb{R}^d} \mathrm{d}z\, \rho(\kappa^{-1/\delta} t^{\gamma} u^{\gamma/\delta} |x-z|^d) \rho(\kappa^{-1/\delta} s^{\gamma} u^{1-\gamma} |y-z|^d) \\
&\leq \int_{\ell}^{1} \mathrm{d}u\, \rho(2^{-d} \kappa^{-1/\delta} t^{\gamma} u^{\gamma/\delta} |x-y|^d) \int_{\mathbb{R}^d} \mathrm{d}z\, \rho(\kappa^{-1/\delta} s^{\gamma} u^{1-\gamma} |y-z|^d) \\
&\quad + \int_{\ell}^{1} \mathrm{d}u\, \rho(2^{-d} \kappa^{-1/\delta} s^{\gamma} u^{1-\gamma} |x-y|^d) \int_{\mathbb{R}^d} \mathrm{d}z\, \rho(\kappa^{-1/\delta} t^{\gamma} u^{\gamma/\delta} |x-z|^d) \\
&\leq I_\rho 2^{d\delta} \kappa \left[t^{-\gamma\delta} s^{-\gamma} |x-y|^{-d\delta} \int_{\ell}^{1} \mathrm{d}u\, u^{-1} + s^{-\gamma\delta} t^{-\gamma} |x-y|^{-d\delta} \int_{\ell}^{1} \mathrm{d}u\, u^{-\gamma/\delta + (\gamma-1)\delta} \right].
\end{aligned}$$

As $\gamma > \frac{\delta}{\delta+1}$ and $\delta > 1$, we have $-\gamma/\delta + (\gamma-1)\delta > -1$. Hence, the last expression can be further bounded by

$$\begin{aligned}
&I_\rho 2^{d\delta} \kappa \big[\log(\ell^{-1}) t^{-\gamma\delta} s^{-\gamma} |x-y|^{-d\delta} + \tfrac{1}{(\delta-1)(\gamma+\gamma/\delta-1)} s^{-\gamma\delta} t^{-\gamma} |x-y|^{-d\delta} \big] \\
&\leq \tfrac{I_\rho 2^{d\delta+1}}{(\delta-1)(\gamma+\gamma/\delta-1)\wedge 1} \log(\ell^{-1}) \kappa (t \wedge s)^{-\gamma\delta} (t \vee s)^{-\gamma} |x-y|^{-d\delta},
\end{aligned}$$

since $\log(\ell^{-1}) > 1$. □

A.3 Simulation of the age-dependent random connection model

In this section, we give an overview of the code used to generate the pictures shown throughout Section 4.1. It is also used for estimating the limiting average clustering coefficient in Section 4.1.4. The code can be freely accessed at: `http://www.mi.uni-koeln.de/~moerters/LoadPapers/adrc-model.R`.

The main objective of the code is to sample neighbours of a given vertex (x,t) in the age-dependent random connection model in dimension 1 for given parameters β and γ and the profile function φ. Due to Proposition 4.5, which gives an explicit description of the neighbourhood of a given vertex, we can use rejection sampling to achieve this. The distribution in (4.9), defined on $\mathbb{R} \times (0,1]$, that we use to sample the neighbours of (x,t) may be unbounded and heavy tailed in the first parameter. To deal with this, we restrict the sampling to a region with mass $q = 0.99$ with respect to this distribution. This sampling works for arbitrary but reasonable choices of the profile function φ and parameters β, γ; we provide and use an optimized sampling algorithm for $\varphi = \frac{1}{2a}\mathbf{1}_{[0,a]}$ with $a \geq \frac{1}{2}$. The advantage of studying this class of φ is that expressions can be analytically simplified, which allows us to improve the algorithm by dividing the region from which the points are sampled into sub-regions with equal mass with respect to φ, thus increasing the acceptance rate for points sampled far away from (x,t). That is, the code first selects one of these equally likely sub-regions uniformly at random and then points are sampled therein until one is accepted. The numerical optimization method `nlminb` is used to calculate the boundaries of the ranges, i.e. quantiles of the distribution from (4.9).

A first application of the sampling is the estimation of the expected local clustering coefficient of a vertex $(0,t)$ in the age-dependent random connection model (see Figure 4.4) and by Theorem 4.9 also the average clustering coefficient for the age-based preferential attachment network (see Figure 4.5). To this end, the code samples pairs of neighbours of $(0,t)$ and averages the probability that the pair is connected.

A second application of the sampling is generating heatmaps of the neighborhoods of a given vertex (see Figure 4.3). The heatmaps are generated using the

R library `MASS` and function `kde2d` by estimating the heat kernel for the sampled neighbouring vertices. Further properties thereof can be studied with additional heatmap generating functions that we provide.

APPENDIX B

List of Principal Notation

Basic Notation

$\mathbb{N}$	Natural numbers $\{1, 2, 3, \ldots\}$
$\mathbb{N}_0$	$\mathbb{N} \cup \{0\}$
$\mathbb{R}$	Real numbers
$\mathbb{Z}^d$	d-dimensional lattice
$\mathbb{R}^d$	d-dimensional Euclidean space
$\lvert x - y \rvert$	Euclidean distance between x and y
$\mathbb{T}_n^d$	d-dimensional torus of width n
$d_{\mathbb{T}_n^d}$	standard torus metric
$a \wedge b$	$\min\{a, b\}$ for $a, b \in \mathbb{R}$
$a \vee b$	$\max\{a, b\}$ for $a, b \in \mathbb{R}$
$\mathbf{1}_A$ and $\mathbf{1}A$	Indicator function
$\mathbb{P}$	Probability measure
$\mathbb{E}$	Expectation with respect to $\mathbb{P}$

$f \in o(g)$	f/g converges to zero
$f \in O(g)$	f/g is bounded away from infinity
$f \asymp g$	f/g is bounded away from zero and infinity

Graph metrics

$G = (V, E)$	Graph G with vertex set V and edge set E	p. 5
$x \sim y$	Vertices x and y are connected by an edge	p. 5
$x \leftrightarrow y$	Vertices x and y belong to the same connected component	p. 6
$\deg(x)$	Degree of vertex x	p. 5
$\mathrm{d}(x, y)$	Graph (chemical) distance between two vertices x and y	p. 6
$c^{\mathrm{glob}}(G)$	Global clustering coefficient	p. 6
$c^{\mathrm{av}}(G)$	Average clustering coefficient	p. 7
τ	Power-law exponent of a scale-free degree distribution	p. 7

Geometric random graphs

$\mathscr{X}$	Poisson point process of unit intensity on $R^d \times (0, 1)$	p. 16
$\mathscr{G}$	Geometric random graph defined on $\mathscr{X}$	p. 16
$\mathbf{x} = (x, t)$	Vertex $\mathbf{x}$ of $\mathscr{G}$ with location x and mark t	p. 16
γ	Characterisation parameter - mark influence	p. 16
δ	Characterisation parameter - spatial influence	p. 16
$\mathbb{P}_{\mathbf{x_1},\ldots,\mathbf{x_n}}$	Law of $\mathscr{G}$ conditioned on the event that $\mathbf{x_1}, \ldots, \mathbf{x_n}$ are points of $\mathscr{X}$	p. 17
$\mathscr{G}_{(0,T_0)}$	Palm-version of $\mathscr{G}$	p. 17
$(0, T_0)$	Origin of the Palm-version	p. 17
$\mathbb{P}_{(0,T_0)}$	Law of the Palm-version	p. 17

Contact process

λ	Infection rate	p. 90
ϖ_G	Extinction time of the contact process	p. 90
$(\xi_t^A)_{t\geq 0}$	Contact process with initial condition $A \subset V$	p. 92
$\Gamma(\lambda)$	Non-extinction probability of the contact process with infection rate λ	p. 94

Bibliography

[1] W. Aiello, A. Bonato, C. Cooper, J. Janssen and P. Prałat. 'A spatial web graph model with local influence regions'. *Internet Mathematics* 5.1-2 (2008), pp. 175–196.

[2] Réka Albert and Albert-László Barabási. 'Statistical mechanics of complex networks'. *Reviews of Modern Physics* 74.1 (2002), pp. 47–97.

[3] Peter Antal and Agoston Pisztora. 'On the chemical distance for supercritical Bernoulli percolation'. *The Annals of Probability* 24.2 (1996), pp. 1036–1048.

[4] Lars Backstrom, Paolo Boldi, Marco Rosa, Johan Ugander and Sebastiano Vigna. 'Four degrees of separation'. *Proceedings of the 4th Annual ACM Web Science Conference on - WebSci '12*. (2012).

[5] Albert-László Barabási and Réka Albert. 'Emergence of scaling in random networks'. *American Association for the Advancement of Science. Science* 286.5439 (1999), pp. 509–512.

[6] Albert-László Barabási, Réka Albert and Hawoong Jeong. 'Mean-field theory for scale-free random networks'. *Physica A: Statistical Mechanics and its Applications* 272.1 (1999), pp. 173–187.

[7] Itai Benjamini and Noam Berger. 'The diameter of long-range percolation clusters on finite cycles'. *Random Structures & Algorithms* 19.2 (2001), pp. 102–111.

[8] Itai Benjamini, Harry Kesten, Yuval Peres and Oded Schramm. 'Geometry of the uniform spanning forest: transitions in dimensions $4, 8, 12, \dots$'. *Annals of Mathematics. Second Series* 160.2 (2004), pp. 465–491.

[9] Itai Benjamini and Oded Schramm. 'Recurrence of distributional limits of finite planar graphs'. *Electronic Journal of Probability* 6 (2001), pp. 1–13.

[10] Noam Berger, Christian Borgs, Jennifer T. Chayes and Amin Saberi. 'On the spread of viruses on the internet'. *Proceedings of the Sixteenth Annual ACM-SIAM Symposium on Discrete Algorithms*. (2005), pp. 301–310.

[11] Smriti Bhagat, Moira Burke, Carlos Diuk, Sergey Edunov and Ismail Onur Filiz. *Three and a half degrees of separation*. (2016). URL: `https://research.facebook.com/blog/2016/2/three-and-a-half-degrees-of-separation/` (visited on 09/09/2022).

[12] Shankar Bhamidi, Danny Nam, Oanh Nguyen and Allan Sly. 'Survival and extinction of epidemics on random graphs with general degree'. *The Annals of Probability* 49.1 (2021), pp. 244–286.

[13] Marek Biskup. 'On the scaling of the chemical distance in long-range percolation models'. *The Annals of Probability* 32.4 (2004), pp. 2938–2977.

[14] Marek Biskup and Jeffrey Lin. 'Sharp asymptotic for the chemical distance in long-range percolation'. *Random Structures & Algorithms* 55.3 (2019), pp. 560–583.

[15] Béla Bollobás. 'A probabilistic proof of an asymptotic formula for the number of labelled regular graphs'. *European Journal of Combinatorics* 1.4 (1980), pp. 311–316.

[16] Béla Bollobás, Svante Janson and Oliver Riordan. 'The phase transition in inhomogeneous random graphs'. *Random Structures & Algorithms* 31.1 (2007), pp. 3–122.

[17] Béla Bollobás and Oliver Riordan. 'The diameter of a scale-free random graph'. *Combinatorica. An International Journal on Combinatorics and the Theory of Computing* 24.1 (2004), pp. 5–34.

[18] Béla Bollobás, Oliver Riordan, Joel Spencer and Gábor Tusnády. 'The degree sequence of a scale-free random graph process'. *Random Structures & Algorithms* 18.3 (2001), pp. 279–290.

[19] Béla Bollobás and Oliver M. Riordan. 'Mathematical results on scale-free random graphs'. *Handbook of graphs and networks*. (2002), pp. 1–34.

[20] Karl Bringmann, Ralph Keusch and Johannes Lengler. 'Sampling geometric inhomogeneous random graphs in linear time'. *25th European Symposium on Algorithms*. Vol. 87. Leibniz Int. Proc. Inform. (2017), 20:1–20:15.

[21] Karl Bringmann, Ralph Keusch and Johannes Lengler. 'Average Distance in a General Class of Scale-Free Networks with Underlying Geometry' (2018). arXiv: `1602.05712 [cs.DM]`.

[22] Karl Bringmann, Ralph Keusch, Johannes Lengler, Yannic Maus and Anisur R. Molla. 'Greedy routing and the algorithmic small-world phenomenon'. *Journal of Computer and System Sciences* 125 (2022), pp. 59–105.

[23] S. R. Broadbent and J. M. Hammersley. 'Percolation processes. I. Crystals and mazes'. *Proceedings of the Cambridge Philosophical Society* 53 (1957), pp. 629–641.

[24] Van Hao Can. 'Metastability for the contact process on the preferential attachment graph'. *Internet Mathematics* (2017), p. 45.

[25] Van Hao Can and Bruno Schapira. 'Metastability for the contact process on the configuration model with infinite mean degree'. *Electronic Journal of Probability* 20 (2015), pp. 1–22.

[26] Jiří Černý and Serguei Popov. 'On the internal distance in the interlacement set'. *Electronic Journal of Probability* 17 (2012), pp. 1–25.

[27] Shirshendu Chatterjee and Rick Durrett. 'Contact processes on random graphs with power law degree distributions have critical value 0'. *The Annals of Probability* 37.6 (2009), pp. 2332–2356.

[28] Fan Chung and Linyuan Lu. 'The average distance in a random graph with given expected degrees'. *Internet Mathematics* 1.1 (2003), pp. 91–113.

[29] Fan Chung and Linyuan Lu. *Complex graphs and networks*. Vol. 107. CBMS Regional Conference Series in Mathematics. (2006), pp. viii+264.

[30] Colin Cooper, Alan Frieze and Paweł Prałat. 'Some typical properties of the spatial preferred attachment model'. *Algorithms and models for the web graph*. Vol. 7323. Lecture Notes in Comput. Sci. (2012), pp. 29–40.

[31] Don Coppersmith, David Gamarnik and Maxim Sviridenko. 'The diameter of a long-range percolation graph'. *Random Structures & Algorithms* 21.1 (2002), pp. 1–13.

[32] Michael Cranston, Thomas Mountford, Jean-Christophe Mourrat and Daniel Valesin. 'The contact process on finite homogeneous trees revisited'. *ALEA*.

Latin American Journal of Probability and Mathematical Statistics 11.1 (2014), pp. 385–408.

[33] Maria Deijfen, Remco van der Hofstad and Gerard Hooghiemstra. 'Scale-free percolation'. *Annales de l'Institut Henri Poincaré Probabilités et Statistiques* 49.3 (2013), pp. 817–838.

[34] Philippe Deprez and Mario V. Wüthrich. 'Scale-free percolation in continuum space'. *Communications in Mathematics and Statistics* 7.3 (2019), pp. 269–308.

[35] Steffen Dereich, Christian Mönch and Peter Mörters. 'Typical distances in ultrasmall random networks'. *Advances in Applied Probability* 44.2 (2012), pp. 583–601.

[36] Steffen Dereich and Peter Mörters. 'Random networks with sublinear preferential attachment: degree evolutions'. *Electronic Journal of Probability* 14 (2009), pp. 1222–1267.

[37] Steffen Dereich and Peter Mörters. 'Random networks with sublinear preferential attachment: the giant component'. *The Annals of Probability* 41.1 (2013), pp. 329–384.

[38] Amogh Dhamdhere and Constantine Dovrolis. 'Ten years in the evolution of the internet ecosystem'. *Proceedings of the 8th ACM SIGCOMM conference on Internet measurement conference - IMC '08.* (2008), pp. 183–196.

[39] Jian Ding and Allan Sly. 'Distances in critical long range percolation' (2015). arXiv: `1303.3995 [math.PR]`.

[40] Peter Sheridan Dodds, Roby Muhamad and Duncan J. Watts. 'An Experimental Study of Search in Global Social Networks'. *Science* 301.5634 (2003), pp. 827–829.

[41] Sander Dommers, Remco van der Hofstad and Gerard Hooghiemstra. 'Diameters in preferential attachment models'. *Journal of Statistical Physics* 139.1 (2010), pp. 72–107.

[42] S. N. Dorogovtsev, J. F. F. Mendes and A. N. Samukhin. 'Structure of Growing Networks with Preferential Linking'. *Physical Review Letters* 85.21 (2000), pp. 4633–4636.

[43] Alexander Drewitz, Balázs Ráth and Artëm Sapozhnikov. 'On chemical distances and shape theorems in percolation models with long-range correlations'. *Journal of Mathematical Physics* 55.8 (2014), p. 083307.

[44] P. Erdős and A. Rényi. 'On random graphs. I'. *Publicationes Mathematicae Debrecen* 6 (1959), pp. 290–297.

[45] P. Erdős and A. Rényi. 'On the evolution of random graphs'. *A Magyar Tudományos Akadémia. Matematikai Kutató Intézetének Közleményei* 5 (1960), pp. 17–61.

[46] P. Erdős and A. Rényi. 'On the strength of connectedness of a random graph'. *Acta Mathematica. Academiae Scientiarum Hungaricae* 12 (1964), pp. 261–267.

[47] Michalis Faloutsos, Petros Faloutsos and Christos Faloutsos. 'On power-law relationships of the Internet topology'. *ACM SIGCOMM Computer Communication Review* 29.4 (1999), pp. 251–262.

[48] Abraham D. Flaxman, Alan M. Frieze and Juan Vera. 'A geometric preferential attachment model of networks'. *Internet Mathematics* 3.2 (2006), pp. 187–205.

[49] Olivier Garet and Régine Marchand. 'Asymptotic shape for the chemical distance and first-passage percolation on the infinite Bernoulli cluster'. *ESAIM. Probability and Statistics* 8 (2004), pp. 169–199.

[50] Olivier Garet and Régine Marchand. 'Large deviations for the chemical distance in supercritical Bernoulli percolation'. *The Annals of Probability* 35.3 (2007), pp. 833–866.

[51] J. Gärtner and S. A. Molchanov. 'Parabolic problems for the Anderson model. I. Intermittency and related topics'. English. *Communications in Mathematical Physics* 132.3 (1990), pp. 613–655.

[52] E. N. Gilbert. 'Random graphs'. *Annals of Mathematical Statistics* 30 (1959), pp. 1141–1144.

[53] E. N. Gilbert. 'Random plane networks'. *Journal of the Society for Industrial and Applied Mathematics* 9 (1961), pp. 533–543.

[54] Peter Gracar and Arne Grauer. 'The contact process on scale-free geometric random graphs' (2022). arXiv: `2208.08346 [math.PR]`.

[55] Peter Gracar, Arne Grauer, Lukas Lüchtrath and Peter Mörters. 'The age-dependent random connection model'. *Queueing Systems. Theory and Applications* 93.3-4 (2019), pp. 309–331.

[56] Peter Gracar, Arne Grauer and Peter Mörters. 'Chemical Distance in Geometric Random Graphs with Long Edges and Scale-Free Degree Distribution'. *Communications in Mathematical Physics* (2022).

[57] Peter Gracar, Markus Heydenreich, Christian Mönch and Peter Mörters. 'Recurrence versus transience for weight-dependent random connection models'. *Electronic Journal of Probability* 27 (2022), pp. 1–31.

[58] Peter Gracar, Lukas Lüchtrath and Peter Mörters. 'Percolation phase transition in weight-dependent random connection models'. *Advances in Applied Probability* 53.4 (2021), pp. 1090–1114.

[59] G. R. Grimmett and J. M. Marstrand. 'The supercritical phase of percolation is well behaved'. *Proceedings of the Royal Society. London. Series A. Mathematical, Physical and Engineering Sciences* 430.1879 (1990), pp. 439–457.

[60] Geoffrey Grimmett. *Percolation*. Second. Vol. 321. Fundamental Principles of Mathematical Sciences. (1999), pp. xiv+444.

[61] Nannan Hao and Markus Heydenreich. 'Graph distances in scale-free percolation: the logarithmic case' (2021). arXiv: `2105.05709 [math.PR]`.

[62] Marcelo Hilário and Daniel Ungaretti. 'Euclidean and chemical distances in ellipses percolation' (2021). arXiv: `2103.09786 [math.PR]`.

[63] Christian Hirsch. 'From heavy-tailed Boolean models to scale-free Gilbert graphs'. *Brazilian Journal of Probability and Statistics* 31.1 (2017), pp. 111–143.

[64] Christian Hirsch and Christian Mönch. 'Distances and large deviations in the spatial preferential attachment model'. *Bernoulli. Official Journal of the Bernoulli Society for Mathematical Statistics and Probability* 26.2 (2020), pp. 927–947.

[65] Remco van der Hofstad. *Random graphs and complex networks. Vol. 1*. Cambridge Series in Statistical and Probabilistic Mathematics. (2017), pp. xvi+321.

[66] Remco van der Hofstad. *Random Graphs and Complex Networks II*. (to appear in 2023).

[67] Remco van der Hofstad, Gerard Hooghiemstra and Dmitri Znamenski. 'Distances in random graphs with finite mean and infinite variance degrees'. *Electronic Journal of Probability* 12 (2007), no. 25, 703–766.

[68] Emmanuel Jacob, Amitai Linker and Peter Mörters. 'The contact process on dynamical scale-free networks' (2022). arXiv: `2206.01073 [math.PR]`.

[69] Emmanuel Jacob and Peter Mörters. 'Spatial preferential attachment networks: power laws and clustering coefficients'. *The Annals of Applied Probability* 25.2 (2015), pp. 632–662.

[70] Emmanuel Jacob and Peter Mörters. 'Robustness of scale-free spatial networks'. *The Annals of Probability* 45.3 (2017), pp. 1680–1722.

[71] Jeannette Janssen and Rory Prałat Paweł and Wilson. 'Geometric graph properties of the spatial preferred attachment model'. *Advances in Applied Mathematics* 50.2 (2013), pp. 243–267.

[72] Jonathan Jordan. 'Degree sequences of geometric preferential attachment graphs'. *Advances in Applied Probability* 42.2 (2010), pp. 319–330.

[73] Jonathan Jordan. 'Geometric preferential attachment in non-uniform metric spaces'. *Electronic Journal of Probability* 18.none (2013), pp. 1–15.

[74] Jonathan Jordan and Andrew R. Wade. 'Phase transitions for random geometric preferential attachment graphs'. *Advances in Applied Probability* 47.2 (2015), pp. 565–588.

[75] Dmitri Krioukov, Maksim Kitsak, Robert S. Sinkovits, David Rideout, David Meyer and Marián Boguñá. 'Network Cosmology'. *Scientific Reports* 2.1 (2012).

[76] Günter Last and Mathew Penrose. *Lectures on the Poisson process*. Vol. 7. Institute of Mathematical Statistics Textbooks. (2018), pp. xx+293.

[77] Thomas M. Liggett. *Stochastic interacting systems: contact, voter and exclusion processes*. Vol. 324. Fundamental Principles of Mathematical Sciences. (1999), pp. xii+332.

[78] Amitai Linker, Dieter Mitsche, Bruno Schapira and Daniel Valesin. 'The contact process on random hyperbolic graphs: metastability and critical exponents'. *The Annals of Probability* 49.3 (2021), pp. 1480–1514.

[79] Priya Mahadevan, Dmitri Krioukov, Marina Fomenkov, Xenofontas Dimitropoulos, Claire Claffy and Amin Vahdat. 'The internet AS-level topology'. *ACM SIGCOMM Computer Communication Review* 36.1 (2006), pp. 17–26.

[80] Ronald Meester and Rahul Roy. *Continuum percolation*. Vol. 119. Cambridge Tracts in Mathematics. (1996), pp. x+238.

[81] Denis Michel. 'Graph distances in Yukich's scale-free geometric network model'. MA thesis. University of Cologne, 2021.

[82] Stanley Milgram. 'The small world problem'. *Psychology today* 2.1 (1967), pp. 60–67.

[83] Michael Molloy and Bruce Reed. 'A critical point for random graphs with a given degree sequence'. *Proceedings of the Sixth International Seminar on Random Graphs and Probabilistic Methods in Combinatorics and Computer Science, "Random Graphs '93" (Poznań, 1993)*. Vol. 6. 2-3. (1995), pp. 161–179.

[84] Christian Mönch. 'Distances in Preferential Attachment Networks'. PhD thesis. University of Bath, 2013.

[85] T. F. Móri. 'On random trees'. *Studia Scientiarum Mathematicarum Hungarica. Combinatorics, Geometry and Topology (CoGeTo)* 39.1-2 (2002), pp. 143–155.

[86] Thomas Mountford, Jean-Christophe Mourrat, Daniel Valesin and Qiang Yao. 'Exponential extinction time of the contact process on finite graphs'. *Stochastic Processes and their Applications* 126.7 (2016), pp. 1974–2013.

[87] Thomas Mountford, Daniel Valesin and Qiang Yao. 'Metastable densities for the contact process on power law random graphs'. *Electronic Journal of Probability* 18 (2013), pp. 1–36.

[88] Jean-Christophe Mourrat and Daniel Valesin. 'Phase transition of the contact process on random regular graphs'. *Electronic Journal of Probability* 21 (2016), pp. 1–17.

[89] M. E. J. Newman. *Networks: An Introduction*. (2010), pp. xii+772.

[90] M. E. J. Newman, S. H. Strogatz and D. J. Watts. 'Random graphs with arbitrary degree distributions and their applications'. *Physical Review E* 64.2 (2001), p. 026118.

[91] Ilkka Norros and Hannu Reittu. 'On a conditionally Poissonian graph process'. *Advances in Applied Probability* 38.1 (2006), pp. 59–75.

[92] Mathew D. Penrose and J. E. Yukich. 'Weak laws of large numbers in geometric probability'. *The Annals of Applied Probability* 13.1 (2003), pp. 277–303.

[93] Bruno Schapira and Daniel Valesin. 'Exponential rate for the contact process extinction time'. *Annales de la Faculté des Sciences de Toulouse. Mathématiques. Série 6* 30.3 (2021), pp. 503–526.

[94] Alan Stacey. 'The contact process on finite homogeneous trees'. *Probability Theory and Related Fields* 121.4 (2001), pp. 551–576.

[95] Augusto Teixeira and Daniel Ungaretti. 'Ellipses percolation'. *Journal of Statistical Physics* 168.2 (2017), pp. 369–393.

[96] Jeffrey Travers and Stanley Milgram. 'An experimental study of the small world problem'. *The Structure and Dynamics of Networks*. Vol. 32. 4. Princeton University Press, (2011), pp. 130–148.

[97] Duncan J. Watts and Steven H. Strogatz. 'Collective dynamics of 'small-world' networks'. *Nature* 393.6684 (1998), pp. 440–442.

[98] Chang-Long Yao, Ge Chen and Tian-De Guo. 'Large deviations for the graph distance in supercritical continuum percolation'. *Journal of Applied Probability* 48.1 (2011), pp. 154–172.

[99] J. E. Yukich. 'Ultra-small scale-free geometric networks'. *Journal of Applied Probability* 43.3 (2006), pp. 665–677.

Erklärung zur Dissertation
gemäß der Promotionsordnung vom 12. März 2020

Diese Erklärung muss in der Dissertation enthalten sein.
(*This version must be included in the doctoral thesis*)

„Hiermit versichere ich an Eides statt, dass ich die vorliegende Dissertation selbstständig und ohne die Benutzung anderer als der angegebenen Hilfsmittel und Literatur angefertigt habe. Alle Stellen, die wörtlich oder sinngemäß aus veröffentlichten und nicht veröffentlichten Werken dem Wortlaut oder dem Sinn nach entnommen wurden, sind als solche kenntlich gemacht. Ich versichere an Eides statt, dass diese Dissertation noch keiner anderen Fakultät oder Universität zur Prüfung vorgelegen hat; dass sie - abgesehen von unten angegebenen Teilpublikationen und eingebundenen Artikeln und Manuskripten - noch nicht veröffentlicht worden ist sowie, dass ich eine Veröffentlichung der Dissertation vor Abschluss der Promotion nicht ohne Genehmigung des Promotionsausschusses vornehmen werde. Die Bestimmungen dieser Ordnung sind mir bekannt. Darüber hinaus erkläre ich hiermit, dass ich die Ordnung zur Sicherung guter wissenschaftlicher Praxis und zum Umgang mit wissenschaftlichem Fehlverhalten der Universität zu Köln gelesen und sie bei der Durchführung der Dissertation zugrundeliegenden Arbeiten und der schriftlich verfassten Dissertation beachtet habe und verpflichte mich hiermit, die dort genannten Vorgaben bei allen wissenschaftlichen Tätigkeiten zu beachten und umzusetzen. Ich versichere, dass die eingereichte elektronische Fassung der eingereichten Druckfassung vollständig entspricht."

Teilpublikationen:

Chemical distance in geometric random graphs with long edges and scale-free degree distribution mit Peter Gracar und Peter Mörters, *Communications in Mathematical Physics (2022)*, DOI: 10.1007/s00220-022-04445-3

The age-dependent random connection model mit Peter Gracar, Lukas Lüchtrath und Peter Mörters, *Queueing Systems: Theory and Applications (2019)*, DOI: 10.1007/s11134-019-09625-y

The contact process on scale-free geometric random graphs mit Peter Gracar *ArXiv Preprint:* 2208.08346

Datum, Name und Unterschrift

18.08.2022, Arne Andreas Grauer